HAL
open science

The effect of pathogens on the water and carbon economy of grapevines : implications for the grapevine dieback crisis

Giovanni Bortolami

To cite this version:

Giovanni Bortolami. The effect of pathogens on the water and carbon economy of grapevines : implications for the grapevine dieback crisis. Vegetal Biology. Université de Bordeaux, 2021. English. NNT : 2021BORD0114 . tel-03218191

HAL Id: tel-03218191

https://theses.hal.science/tel-03218191v1

Submitted on 5 May 2021

HAL is a multi-disciplinary open access archive for the deposit and dissemination of scientific research documents, whether they are published or not. The documents may come from teaching and research institutions in France or abroad, or from public or private research centers.

L'archive ouverte pluridisciplinaire **HAL**, est destinée au dépôt et à la diffusion de documents scientifiques de niveau recherche, publiés ou non, émanant des établissements d'enseignement et de recherche français ou étrangers, des laboratoires publics ou privés.

THÈSE PRÉSENTÉE
POUR OBTENIR LE GRADE DE

DOCTEUR DE L'UNIVERSITÉ DE BORDEAUX

Ecole doctorale 304 Sciences et Environnements

Spécialité Ecologie évolutive, fonctionnelle et des communautés

Par Giovanni Bortolami

The effect of pathogens on the water and carbon economy of grapevines: implications for the grapevine dieback crisis

Sous la direction de : Chloé Delmas et Gregory Gambetta

Soutenue le 31 Mars 2021

Membres du jury :

Mme. Florence Fontaine, Professeure, Université de Reims Champagne-Ardenne	Presidente
M. Hans Reiner Schultz, Professeur, University of Geisenheim	Rapporteur
Mme. Christelle Lacroix, Chargée de recherche, INRAE	Examinatrice
Mme. Aude Tixier, Chargée de recherche, INRAE	Examinatrice
M. Cornelis van Leeuwen, Professeur, Bordeaux Sciences Agro	Examinateur
Mme. Chloé Delmas, Chargée de recherche, INRAE	Directrice
M. Gregory Gambetta, Professeur, Bordeaux Sciences Agro	Co-directeur

Je dédie cette thèse à Guido Fidora,
Scientifique, pionnier de l'agriculture biologique,
Inoubliable grand-père.

Remerciements, Acknowledgments, Ringraziamenti

Tout d'abord je remercie Florence Fontaine et Hans Schultz pour avoir accepté d'être les rapporteurs de cette thèse. Je remercie aussi Christelle Lacroix, Aude Tixier et Kees van Leeuven qui ont acceptés de composer mon jury en tant que examinateurs.

Mes premiers remerciements vont à Chloé et Greg, qui ont su, hors pair, me guider pendant ces trois ans (et demi). Chloé, je te remercie pour ton enthousiasme et ta passion scientifique qui ont abouties à des excellents résultats pour tout le groupe physiopath. Au-delà de te remercier pour tout ce que tu m'as appris pendant ce parcours (et comment poser les questions de recherche), c'était un immense plaisir commencer à gratter à tes cotés la couche de mystère autour des maladies du bois de la vigne. C'est en fait un remerciement très scientifique celui que je veux te faire, car c'est avec la remise en question de chaque phrase dans chaque article que l'on a pu stimuler notre intérêt jour par jour (qui connait déjà toute les réponses, enfin, il s'ennuie non ?). Enfin, je n'oublie pas tes appel presque journaliers pendant les premières manips de l'été 2018 que plusieurs fois ont sauvé l'aboutissement des expériences et mon intégrité psychique. Pour ça et tout ce que je n'ai bien exprimé ici, merci. Greg, it is now more than four years since we met. I want to thank you because you are a great mentor, you know what to say to support the people around you, and you know how to extract the best scientific quality from messy datasets. I thank you because you were always enthusiast about my results, also when the error bars were huge and I thought to throw away months of work. I thank you A LOT because you teach me how to write in English, and that was not easy (and I guess there are many mistakes in these acknowledgments). Enfin, je vous remercie beaucoup à tous les deux pour nos longues conversations scientifiques, pour avoir regardé et analysé tous les piles de graphiques que j'ai sortis pendant les analyses de données, et pour votre patience en mes égards ; vous êtes des bons scientifiques ! Je suis sûr que notre collaboration n'est pas encore terminée !

Je remercie infiniment Sylvain, sans lequel cette thèse aurait bien moins de données et de qualité scientifique. Merci pour ta disponibilité à l'écoute, l'aide dans la planification des manips, et les échanges (parfois intenses !) sur l'interprétations des résultats. T'avoir dans l'équipe de travail et pouvoir signer des articles avec toi était une grande chance et un immense plaisir.

Je remercie Nathalie Ferrer, qui m'a accompagné depuis 2019 dans les manips. Ton savoir-faire, ta parlantine, et ta bonne humeur nous ont sauvés plusieurs fois. On a réussi à bien travailler en serre à 40 °C, ce qui n'est pas donné. Merci pour avoir exécuté parfaitement les manips en biomol, vu que j'arrive à peine à tenir une pipette en main. Et toutes les centaines de coupes de feuilles que tu as faites ! Merci pour toutes les fois où tu m'as amené du chocolat pendant la rédaction, ça a aidé vraiment.

Je remercie Jérôme Jolivet, sans toi cette thèse aurait été toute une autre histoire ! C'est grâce à ton expertise qu'on a pu arracher les vignes et les mettre en pot. Et ça c'est une pierre angulaire

de la thèse. Merci pour m'avoir accompagné pendant les manips, c'était un grand plaisir. Je suis encore désolé pour les noms des flacons pendant les pesées, je t'assure que maintenant j'ai bien compris comment nommer les échantillons.

Je remercie Elena et Marie, sans vous il y aurait un chapitre en moins. Elena, grazie per aver passato un'estate in serra con me ad attaccare tubi e insacchettare piante. La tua tesi di laurea è stata un gran successo, e ora ti auguro un gran dottorato, ma son già sicuro che tra qualche anno ci sarà una gran tesi da leggere. Marie, c'était un grand plaisir de travailler avec toi et de t'aider dans le beau mémoire qui est sorti de ton stage.

Je remercie les trois collègues avec qui j'ai partagé plein de moments : Silvina, Pim et Jérôme Pouzoulet. Silvina, merci pour avoir été là pendant le premier été en serre, pour avoir partagé les potentiels de nuit et m'avoir empêché de jeter le Waltz par la fenêtre. Ton travail est de la plus haute qualité et je suis sûr que notre collaboration est loin d'être terminée. Pim, tu as été pour moi une de plus chère collaboration pendant cette thèse, on était tristes quand tu es parti (il n'est pas mort ne vous inquiétez pas), j'ai hâte de venir chez vous au Canada. Jérôme, merci pour tes longues discussions, pour nous avoir aidés avec les qPCR (ce qu'elles ont changées les discussions des articles après tes détections !), ta participation à la thèse va bien au-delà d'un simple remerciement.

Je remercie Nathalie Ollat, une des personnes qu'ils m'ont plus inspirées scientifiquement pendant ces années. Merci pour m'avoir accepté comme stagiaire il y a quelques années, c'était une grande chance, et tous les échanges (à parole et au champ) qu'on continue à avoir sont entre les plus chers et intéressants.

Je remercie Pascal, qui m'a appris à connaitre l'évolution du symptôme d'esca. Ton expertise c'était fondamentale dans cette thèse. Merci pour ta sympathie et ton énergie toujours présente. Tu mérites bien qu'on donne ton nom à au moins un champignon des GTD.

Je remercie Yves et Cédric, qui m'ont accompagné et aidé dans la quantification des métabolites. Sans vous dans le titre de cette thèse « carbon economy » ne serait pas là. Je vous remercie pour votre expertise et gentillesse, je sais que je ne suis pas le plus ordonné au labo, mais au moins j'ai fait rire tout le monde quand j'ai fait tomber une plaque (100 échantillon) par terre. Les résultats sortis sont de grande qualité, et c'est grâce à vous !

Je remercie Hervé et Marie-Laure qui m'ont suivi au cours de ces trois ans. Vos conseils et remarques ont été fondamentales dans l'avancement de la thèse. Merci encore pour m'avoir écouté et guidé pendant ce parcours.

Je remercie Jessica pour l'aide dans la méta-génomique, franchement là j'aurais juste la poudre des échantillons broyés.

Je remercie toute la team soleil pour avoir collaboré à la réalisation de deux chapitre de la thèse : Sylvain, Greg, Laurent, Deborah, Silvina, Eric, Hervé, Régis, Guillaume, Steven, Andrew, Fre-

deric, José, Elena et Santiago. C'était magnifique de collaborer et discuter avec vous entre un scan et l'autre. Merci surtout à Andrew qui est le chef du PSICHE et sans lui on aurait 0 scans. Merci à l'équipe de feu Laurent, Eric, Silvina et Deborah avec lesquels j'ai passé les nuits les plus productives de ma vie.

Je remercie l'équipe Régis, Anne-Isabelle et Camille pour avoir partagé des moments inoubliables pendant notre saison en serre.

Je remercie les équipes de tous les labos où je suis passé : SAVE, BIOGECO, EGFV, BFP, ISPA. Chacun d'entre vous a une place particulière dans cette thèse. Un merci spécial à Isabelle, Sylvie et Seb de SAVE qui m'ont aidé beaucoup beaucoup, à Guillaume, Nabil et Nabil de l'EGFV pour avoir géré la serre balance quand elle n'avait pas envie de travailler.

Je remercie Christian pour son aide précieuse, ses conseils, et les longs appels pour m'expliquer comment organiser les expériences pour la détection de l'éthylène.

Je remercie chaleureusement mes collègues de thèse Lionel, Enora et Noémie pour être là et ne pas avoir abandonné le bureau. J'augure un excellent parcours à ceux qui vont rester dans ce bureau et utiliser mon fauteuil. Je tiens aussi à remercier Fréderic (qui m'amène le Saint Nectaire) et Adrien parce que ensemble dans leur bureau sont très mignons et ça mérite d'être reconnu plus souvent.

I thanks David Gramaje, Kendra Baumgartner, and Gianfranco Romanazzi for their samples.

Je remercie toutes les personnes (du stagiaire au professeur) qui sont venu au moins une fois à mesurer les feuilles de mes plantes. Merci pour votre patience et bonne volonté. Votre travail a été déterminent pour faire du *Chapitre 5* un vrai article scientifique (regardez Fig. 2 et Supplemental Fig. 2, 3, 5, vous êtes là).

Je tiens à remercier le group dégustation Oenochoé et la dégustation décontractée de Carlos et Soizic, qu'ils m'ont fait déguster des excellents vins et ont donné aussi lieux à des soirées très drôles.

Je remercie mes voisins Juliette, Laurette, Céline et Charles, sans lesquels la dernière année aurait été insoutenable.

Je remercie tous mes amis, ceux que j'ai rencontré pendant le travail, ceux que j'avais déjà, et ceux que j'ai rencontré ailleurs. Sans vous j'aurais que ma thèse et ça ne serait rien sans vous.

Ovviamente ringrazio tutta la mia famiglia, per il loro supporto e presenza (anche se troppo lontana). Li ringrazio per avermi sopportato guardar scrivere sotto le palme in Sicilia e cominciar la festa solo la sera. Ringrazio le mie nonne che mi danno le mancette quando torno a casa. Ringrazio Giulia, Silvia, Alessandro e Marco per farmi stare a casa loro quando torno a Venezia e i nipoti Ettore, Nico e Agata che mi fanno sempre molto ridere. Complimenti a Ettore che ha appena finito tutta la saga di guerre stellari. Ringrazio la mia mamma e il mio papà che conti-

nuano a sostenermi anche se sono andato lontano.

Je remercie Mahaut qui est toujours là même si je suis comme je suis et toute la famille de Beg Nod pour m'avoir accueilli.

Enfin, ces remerciements sont bien trop long et si vous êtes arrivés là j'espère qu'il vous reste de l'énergie parce que il y encore toute la thèse à lire.

Giovanni (Nanne)

C'era una volta....
— Un re! — diranno subito i miei piccoli lettori.
— No, ragazzi, avete sbagliato. C'era una volta un pezzo di legno.

Il était une fois....
- Un roi ! - diront immédiatement mes petits lecteurs.
- Non, les enfants, vous vous trompez. Il était une fois un morceau de bois.

Once upon a time, there was....
- A king! - my little readers will immediately say.
- No, kids, you are mistaken. Once upon a time, there was a piece of wood.

Carlo Collodi, le avventure di Pinocchio

Abstract

Perennial plant dieback is an increasing and complex phenomenon. Perennial plants experience many interacting stressing events leading to final plant mortality. These interactions, and how they may change regarding climatic conditions and plant physiological status, are key in understanding the dieback process. Although dieback events are increasing worldwide, the knowledge on the dieback mechanisms are scarce, given the many technical challenges in studying complex interactions. In this thesis, we studied the interaction between two stresses frequently experienced by grapevines, one of the most important perennial crops: drought and esca (a vascular disease). Esca is a disease in which there are many competing hypotheses regarding its pathogenesis. One of the main hypothesis is that leaf symptoms and plant death are caused by hydraulic failure in xylem vessels. For this reason, drought is thought to contribute synergistically with esca to grapevine dieback. In this context, this thesis has primarily explored the hydraulic failure hypothesis during esca pathogenesis. We found that during leaf symptom expression both leaves and stems suffer from hydraulic failure causing (on average) 69% loss of hydraulic conductance in midribs, 55% in petioles, and 30% in stems. Differing from classical air embolism during drought, we observed that hydraulic failure during esca was caused by the presence of plant-derived vascular occlusions (i.e. tyloses and gels) produced at a distance from the pathogen niche in the trunk. After this discovering, we explored the interaction between esca and drought, subjecting naturally infected plants to drought. We found that drought totally inhibits esca leaf symptoms, as none of the plants under water deficit (at $\Psi_{PD} \approx$ -1MPa for three months) expressed leaf symptoms in two consecutive seasons. At the same time, in order to understand the interaction between esca and drought, we recorded the whole-plant water relations and carbon economy of grapevine under both stresses. We highlight the distinct physiology behind these two stresses, indicating that esca and drought present different underlying mechanisms, and induce different plant responses and physiological consequences. Esca (and subsequent stomatal conductance decline) does not result from decreases in water potential, and generates different gas exchange and non-structural carbohydrate seasonal dynamics compared to drought. Finally, we observed that esca affected the recorded plant physiology only seasonally, and not over the long-term. This thesis highlights the importance in finding the physiological thresholds triggering the different interactions during plant dieback. Together, the results open new scientific and agronomical perspectives on plant-pathogen-environment interactions and vineyard sustainability.

Résumé

Au cours de leur vie les plantes pérennes sont confrontées à plusieurs stress en interaction qui les entrainent dans un processus de dépérissement. Ces interactions, et leurs changements par rapport aux conditions climatiques et à l'état physiologique de la plante, sont fondamentales pour la compréhension du processus de dépérissement. Malgré l'augmentation des évènements de dépérissement à l'échelle mondiale, les connaissances sur ces mécanismes restent limitées, étant données les difficultés techniques rencontrées dans l'étude des interactions complexes. Dans cette thèse nous avons étudié l'interaction entre deux stress fréquemment vécus par la vigne : la sècheresse et une maladie vasculaire, le mal d'esca. L'esca est une maladie qui soulève plusieurs hypothèses sur sa pathogénèse. Une des principales hypothèses est que les symptômes foliaires et la mort de ceps de vigne soient causés par un dysfonctionnement hydraulique dans les vaisseaux du xylème. Pour cette raison, la sècheresse pourrait contribuer en synergie avec l'esca au dépérissement de la vigne. Compte tenu de ce contexte, nous avons tout d'abord exploré l'hypothèse de dysfonctionnement hydraulique pendant la pathogenèse de l'esca. Nous avons mis en évidence que pendant l'expression des symptômes foliaires plusieurs organes sont atteints par un dysfonctionnement hydraulique qui cause en moyenne une perte de conductivité hydraulique de 69% sur les nervures centrales des feuilles, 55% sur les pétioles et 30% sur les tiges. Contrairement à l'embolie gazeuse classiquement observée pendant la sècheresse, le dysfonctionnement hydraulique pendant l'esca est causé par la présence d'occlusions vasculaires (thylloses et gels) produites par la plante. Après cette découverte, nous avons exploré l'interaction entre l'esca et la sècheresse, en imposant une contrainte hydrique aux plantes naturellement infectées. Nous avons découvert que la sécheresse inhibait complètement l'expression des symptômes d'esca, étant donné qu'aucune plante en stress hydrique (à $\Psi_{PD} \approx$ -1MPa pour trois mois) n'a montré de symptômes foliaires pendant deux saisons consécutives. Nous avons également étudié les relations hydriques et carbonées, à l'échelle de la plante entière au cours de ces expérimentations. Nos résultats soulignent un fonctionnement physiologique distinct lorsque la vigne est soumise à une sécheresse ou exprime des symptômes d'esca. L'esca (et la baisse de la conductance stomatique associée) n'est pas causé par une chute de potentiel hydrique, et génère des dynamiques saisonnières différentes de la sécheresse au regard des échanges gazeux et des teneurs en carbohydrates non-structuraux. Cette thèse souligne l'importance d'identifier les seuils physiologiques sous-jacents aux différentes interactions entre facteurs pendant le processus de dépérissement des plantes. Dans l'ensemble, ces résultats ouvrent des nouvelles perspectives scientifiques et agronomiques pour les interactions plante-pathogène-environnement et pour la durabilité des vignobles.

Cette these a été finance par le ministère Français de l'agriculture et de l'alimentation (FranceAgriMer et CNIV) dans le cadre du projet PHYSIOPATH (program Plan national Dépérissement du Vignoble).

Cette thèse a été préparé à UMR 1065 SAVE

Centre INRAE Bordeaux Nouvelle-Aquitaine, Villenave d'Ornon

Summary

ABBREVIATIONS **14**

CHAPTER 1
Research Context, Hypotheses, and Study Framework **15**

CHAPTER 2
Exploring the Hydraulic failure hypothesis of Esca Leaf Symptom Formation **54**
Results summary - Chapter 2 **75**

CHAPTER 3
Similar Symptoms Do Not Induce Similar Changes in Grapevine Leaf Xylem Anatomy, Comparisons between Senescing Processes and Climatic Regions **77**
Results summary - Chapter 3 **95**

CHAPTER 4
Seasonal and Long-Term Consequences of Esca on Grapevine Stem Xylem Integrity **97**
Results summary - Chapter 4 **127**

CHAPTER 5
Grapevines under Drought Do Not Express Esca Leaf Symptoms: the Physiology behind Drought and Vascular Pathogen Antagonism **129**
Results summary - Chapter 5 **163**

CHAPTER 6
Discussions, Conclusions, and Perspectives **165**

Annex 1
Preliminary Results on Necrosis Extension and Ascomycota Communities in Plants under Water Deficit and Esca **182**

Cited Literature **193**

ABBREVIATIONS

A, CO_2 assimilation

ABA, abscisic acid

C, carbon

CODIT, compartmentalization of decay in trees

gs, stomatal conductance

Gs, whole-plant stomatal conductance

Gs_{MAX}, maximum whole-plant stomatal conductance of the day

GTD, grapevine trunk disease

E, transpiration

FM, fresh matter

Fom, *Fomitiporia* spp.

INRAE, institut national de recherche pour l'agriculture, l'alimentation et l'environnement

k, hydraulic conductance

k_h, hydraulic conductivity

k_s, specific hydraulic conductivity

k_{th}, specific theoretical hydraulic conductivity

MRI, Magnetic resonance imaging

NSC, non-structural carbohydrates

OIV, organisation internationale de la vigne et du vin

OV, Optical vulnerability technique

pA, previously asymptomatic plants

pS, previously symptomatic plants

P_{50}, xylem pressure inducing 50% loss of hydraulic conductance

P_{88}, xylem pressure inducing 88% loss of hydraulic conductance

Pch, *Phaeomoniella chlamydospora*

PLC, percentage loss of hydraulic conductance

Pmin, *Phaeoacremonium minimum*

PPFD, photosynthetic photon flux density

PSII, quantum yield of photosystem II

SPAC, soil-plant-atmosphere continuum

VPD, vapor pressure deficit

WUE, water use efficiency

WW, well-watered (plants)

WD, water-deficit (plants)

X-ray microCT, X-ray microcomputed tomography

Ψ, water potential

Ψ_{MD}, midday water potential

$\Psi_{osmotic}$, osmotic water potential

Ψ_{PD}, predawn water potential

Ψ_{Stem}, stem water potential

Ψ_{TLP}, turgor loss point

CHAPTER 1

Research Context, Hypotheses, and Study Framework

Résumé: Le dépérissement des plantes pérennes est une problématique très importante aujourd'hui. On observe une augmentation de la mortalité des plantes pérennes que ce soit dans des écosystèmes naturels ou agricoles. Le dépérissement est un processus complexe, car une plante pérenne passe par différents stress avant la mort. Même lorsque celle-ci est rapide (en cas de feu ou de tempête), les facteurs visibles de mortalité sont seulement les dernières d'une longue liste d'évènement stressants. L'interaction entre plusieurs stress pourrait donc être la clé de la compréhension du dépérissement de plantes pérennes. Cependant, le phénomène est bien plus difficile à étudier lorsque l'on prend en compte le fait que les interactions entre stress sont conditionnées par la réponse physiologique des plantes, et les conditions environnementales ; et d'autant plus lorsque le changement climatique continue à modifier le cadre d'étude. Dans cette thèse, nous avons étudié deux stress qui sont fréquemment rencontrés au champ : la sécheresse et les maladies vasculaires. Différentes hypothèses, expliquant la mortalité des plantes, voient ces stress en synergie pendant le dépérissement, soit par des mécanismes liés au transport de l'eau (les deux pouvant entrainer un dysfonctionnement hydraulique), soit par des mécanismes liés au métabolisme carboné (les deux pouvant entrainer un appauvrissement en carbohydrates). Dans les vignobles européens, il est observé depuis une vingtaine d'années, une baisse de production liée à une augmentation d'évènements de mortalité des pieds de vigne. Nous nous sommes intéressés ici au dépérissement du vignoble, en regardant de près les relations entre le fonctionnement hydraulique, l'anatomie du xylème, et la pathogenèse de l'esca (une maladie vasculaire). Dans un premier temps (*Chapitres 2* à *4*) nous avons testé l'hypothèse de la présence d'un dysfonctionnement hydraulique pendant l'expression des symptômes foliaires liés à l'esca. Cette hypothèse, proposant que la mortalité des vignes pendant l'esca soit due à un déséquilibre entre la demande et l'offre de l'eau transportée, n'a jamais été testée pendant la formation des symptômes foliaires. Dans un second temps (*Chapitre 5*) nous avons soumis à une contrainte hydrique (moyenne-intense) des plantes naturellement infectées par l'esca en notant, pendant deux saisons consécutives, l'incidence de la maladie, les relations hydriques des plantes (potentiels hydriques et échanges gazeuses) et le métabolisme carboné (quantification des chlorophylles et des carbohydrates non-structuraux).

Table of contents - Chapter 1

1. Research context: perennial plant dieback 17

1.1. Evidences and definition 17

1.2. Mechanisms and causal factors of perennial plant dieback 17

1.3. A complex and difficult phenomenon to study 19

1.4. Drought and vascular diseases during dieback 20

2. The hypotheses behind perennial plant dieback 20

2.1. The hypothetical mechanisms of mortality during drought 20

2.2. The hypothetical mechanisms of plant mortality during vascular disease 22

2.3. The hypothetical interactions between drought and vascular diseases, synergism or antagonism? 24

2.4. Xylem anatomy, a crucial trait in plant resistance to drought and vascular diseases 25

3. Grapevine, the European dieback crisis 26

3.1. Evidences, definition, and mechanisms 26

3.2. Esca, a complex disease 29

3.3. The hypotheses behind esca leaf symptoms, and the possible interaction with drought 32

4. Thesis objectives 33

5. Theoretical framework 35

5.1. Plant-water relations and xylem tissue 35

5.2. Carbon balance and non-structural carbohydrates 38

5.3. Drought and its consequences on plant physiology 39

5.4. Vascular diseases and their consequences on plant physiology 43

5.5. X-ray microcomputed tomography, in *vivo* visualizations of hydraulic integrity 48

6. Experimental framework 49

6.1. Plant material: designing a new experimental setup to study esca 49

6.2. Esca leaf symptom notation 50

6.3. Experiment timetable 50

1. Research context: perennial plant dieback

1.1. Evidences and definition

Perennial plants are one of the most important component in natural and agricultural ecosystems, both from ecological and economical aspects (Attiwill and Adams, 1993, Costanza *et al*., 1997). Perennial plant mortality events could unbalance natural and agricultural equilibrium as they help maintaining soil fertility, guarding against erosion (Ewel, 1999), as well as sustaining biodiversity richness and abundance (Malézieux *et al*., 2009). Moreover, perennial plants are one of the main agents in atmospheric carbon sequestration (Montagnini and Nair, 2004). In the context of climate change, perennial plant mortality events are increasing worldwide (Allen *et al*., 2010, Anderegg *et al*., 2016), and affect a large spectrum of perennial species (see examples in Table 1). Moreover, the causes (from biotic to abiotic) can be various, sometimes acting in sequence or in combination (Table 1). In this context, many studies have documented the existence of dieback events, resulting in yield decreases and in mortality of perennial plants (or just a part of them, such as leaves and stems, Table 1). In the plant pathology manual written by George Agrios (2004), the term "dieback" is found in the list of disease symptoms, and defined as the "extensive necrosis of twigs beginning at their tips and advancing toward their basis". More generally, the term "dieback" is used to describe crown defoliation and mortality of twigs, branches and trunks in perennial plants (as done in the studies in Table 1). Moreover, dieback can also be seen as a synonym of tree decline, implying a long-term physiological weakening (e.g. Facelli *et al*., 2009, Pellizzari *et al*., 2016), closely associated with the term die-off (Anderegg *et al*., 2012) and plant death (O'Brien *et al*., 2017).

1.2. Mechanisms and causal factors of perennial plant dieback

When perennial plants die, the causal factors are frequently numerous and interacting. Even during sudden and spectacular events (e.g. wildfires and hurricanes), the detectable causal factors of plant mortality represent just the last of a long list (Franklin *et al*., 1987, McDowell *et al*., 2008). The interaction between these factors, and in which order they cause disorders are fundamental in the understanding and prediction of perennial plant mortality. These interactions have been conceptualized in the "decline disease spiral diagram" (Manion, 1991). This framework organized the factors in different categories: (i) predisposing factors, such as poor soil conditions, or air and water pollution which can reduce the trees ability to respond to attacks; (ii) inciting factors such as seasonal drought, chronic pathogen infestations, or competition with other plants, which start the visible tree decline; and (iii) contributing factors, such as acute pathogen attacks, frost, intense drought or secondary pathogen colonization, which finally lead to plant death. Manion visually represented his theory as a spiral because trees fall from vigor to death passing through many different stressing events and because the stressing fac-

Table 1. Examples of studies on dieback events affecting perennial plant species (forest or crop) in different part of the world. The list is non-exhaustive and only one example per species and geographical repartition was chosen

Reference	Plant	forest/ crop	Causal factor	Country
Miller and Hiemstra, 1987	*Fraxinus excelsior*	forest	unknown	Nederland
Renaud and Mauffette, 1991	*Acer saccharum*	crop	unknown	Canada
Aleemullah and Walsh, 1996	*Carica papaya*	crop	unknown	Australia
Facelli *et al*., 2009	*Pistacio vera*	crop	vascular disease	Australia
Raimondo *et al*., 2010	*Citrus aurantium*	crop	vascular disease	Italy
Worrall, 2010	*Alnus incana*	forest	non-identified biotic	U.S.
Safrankova *et al*., 2013	*Bruxus spp.*	forest	fungi	Czech Republic
Jacobsen *et al*., 2012	*Brunia noduliflora*	forest	unknown	South Africa
Bertsch *et al*., 2013	*Vitis vinifera*	crop	trunk disease	Europe
Eskalen *et al*., 2013	many species	forest	vascular disease	U.S.
Urbez-Torres *et al*., 2013	*Olea europaea*	crop	fungi complex	U.S.
Elmer *et al*., 2013	many species	forest	multi-stress	U.S.
Kreuzwieser and Rennenberg, 2014	many species	forest	waterlogging	worldwide
Davison, 2014	*Banksia*	forest	vascular disease and abiotic stress	Australia
Goberville *et al*., 2016	*Fraxinus excelsior*	forest	fungi and environment	Europe
Pellizzari *et al*., 2016	*Abies alba*	forest	long-term drought events	Spain
Alvindia and Gallema, 2017	*Theobroma cacao*	crop	vascular disease	Philippines
Roseli Correa *et al*., 2017	*Eucalyptus*	forest	multi-stress	Australia
Tulik *et al*., 2017	*Fraxinus excelsior*	forest	multi-stress	Poland
Schulz *et al*., 2018	*Pinus strobus*	forest	bacterial cankers	U.S.
Pandey *et al*., 2018	*Aquilaria malaccensis*	crop	vascular disease	India
Savi *et al*., 2019a	*Pinus nigra*	forest	drought	Italy
Lachenbruch and Zhao, 2019	*Corylus avellana*	crop	bacterial cankers	U.S.
Lopez-Moral *et al*., 2020	*Pistacio vera*	crop	trunk disease	Spain
Rossi *et al*., 2020	*Rhizophora mangle*	forest	multi-stress	Bahamas

tors can move on the spiral (from predisposing to inciting and contributing factors) depending on their chronic or acute form, on their intensity, and on which moment they affect the plant. Moreover, in recent times, by the use of genomic technologies we learned that the distinction between pathogenic and non-pathogenic microorganisms is questionable (Méthot and Alizon, 2014), as the virulence of microorganisms is given by the interaction between host and parasite genotypes and phenotypes under varying environment. In view of this, perennial species are preferably considered as holobiont (i.e. sum of different species) in which the microbiome equilibrium, altogether with plant physiological status and environmental conditions, dictate the general plant decline or survival (Bettenfeld *et al*., 2020). For example, it has been observed that in some cases drought conditions predispose plants to pathogen attack, and, in other cases, pathogen and drought combine their effect during plant decline (Desprez-Loustau *et al*., 2006). Finally, the underlying physiological mechanisms are numerous and interconnected with the stressing factors, and their role during plant decline is not fully understood (McDowell *et al*., 2008, Oliva *et al*., 2014, Pellizzari *et al*., 2016). If this background could already seems complicated, climate change is constantly modifying the impacts of the environment on pathogens, plants, and their interactions, resulting in accelerated plant mortality (Allen *et al*., 2010).

1.3. A complex and difficult phenomenon to study

When plant pathologists study perennial plant dieback, they frequently refer to field notations (such as disease incidence or insect presence) coupled to climatic record datasets (e.g. Souza *et al*., 2013, Li *et al*., 2017). This approach seems to be the only one to precisely quantify the contribution of each different predisposing, inciting and contributing factors to plant decline. However, the plant physiological state is rarely measured during these surveys, impeding a clear interpretation on how climatic and environmental conditions affect plants, pathogens, and more generally, the dieback progression. Indeed, the key in the understanding in some (if not all) abiotic-biotic stress interactions could be the detection of the plant physiological thresholds at which the different interactions take place. Just because are the physiological turnovers that impose the different plant responses to stresses (such as production of defense compounds or organ abscission), and it is only through physiological measures that we can establish the different steps before plant death. This lack of information on dieback phenomena is probably given because many measures are impracticable in the field, or need destructive methodologies. Finally, field surveys needs long-term studies (often more than 10 or 20 years) in many different sampling sites. Oppositely, controlled conditions (greenhouses and laboratories) offer many advantages (e.g. availability of plant material and controlled climatic conditions), but they will never fully represent field conditions.

In this context, there is a need to realize integrative studies to understand, and hopefully contrast, the different causes and mechanisms inducing plant death. As integrative studies, we intend the measurement of plant physiological status, the different environmental and climatic

conditions, and the biotic agents that participate to perennial plant dieback. We also intend the detection of plant physiological thresholds triggering the different responses that will help understand when the plant life is irreparably compromised, and when climatic parameters effectively affect plants *in natura*. In this thesis we will focus our attention on two recurrent stresses during perennial plant dieback (drought and vascular disease), researching the physiological mechanisms that result in their synergistic (or antagonistic) interaction.

1.4. Drought and vascular diseases during dieback

Plant dieback is visually observed in nature as the loss of leaves of the entire crown or just a part of it. Intuitively, we can identify a central role of plant water transport in dieback events, as the result is the crown desiccation. Indeed, the plant hydraulic system is at the core of the hypothetical processes leading to plant mortality during two main factors often encountered in plant dieback: drought and vascular disease. Drought is one of the main environmental stresses threatening perennial plants worldwide (Choat *et al*., 2012). Moreover, current climate change is increasing the frequency and intensity of drought events (Brodribb *et al*., 2020). At the same time, vascular diseases are one of the major biotic stresses menacing perennial plant vitality (Pearce, 1996). During perennial plant dieback, many authors found both drought (e.g. Allen *et al*., 2010, Rodriguez-Calcerrada *et al*., 2016, Savi *et al*., 2019a) and vascular diseases (e.g. Facelli *et al*., 2009, Raimondo *et al*., 2010, Eskalen *et al*., 2013) as recurrent causal factors. Moreover, many studies suggest a synergistic interaction (Yadeta and Thomma, 2013, Oliva *et al*., 2014) between these stresses, because they affect the same plant tissue, the xylem, enhancing the interest in their coupled consequences.

2. The hypotheses behind perennial plant dieback

2.1. The hypothetical mechanisms of mortality during drought

Drought might cause plant mortality by intervening in two major physiological processes, plant-water relations and carbon balance (Fig. 1). Plant-water relations are primarily affected when the difference in water potential between air and soil is so high that the water column inside the plant breaks, producing cavitation events, air embolism spreading, and final plant desiccation. The carbon balance is affected by the reduced photosynthetic activity (mostly by stomatal closure and leaf shedding), and by the changes in source-sink relations (mostly by reserve consumption for root growth). These mechanisms (described in details in the *Theoretical framework* paragraph *5.3*) are the theoretical basis behind the two main hypotheses of plant death during drought: hydraulic failure and carbon starvation (McDowell *et al*., 2008, Fig. 1).

On one side, hydraulic failure is defined as the disruption of water flow inside the plant by air during cavitation events (Tyree and Sperry, 1989). Hydraulic failure is measurable (as a loss

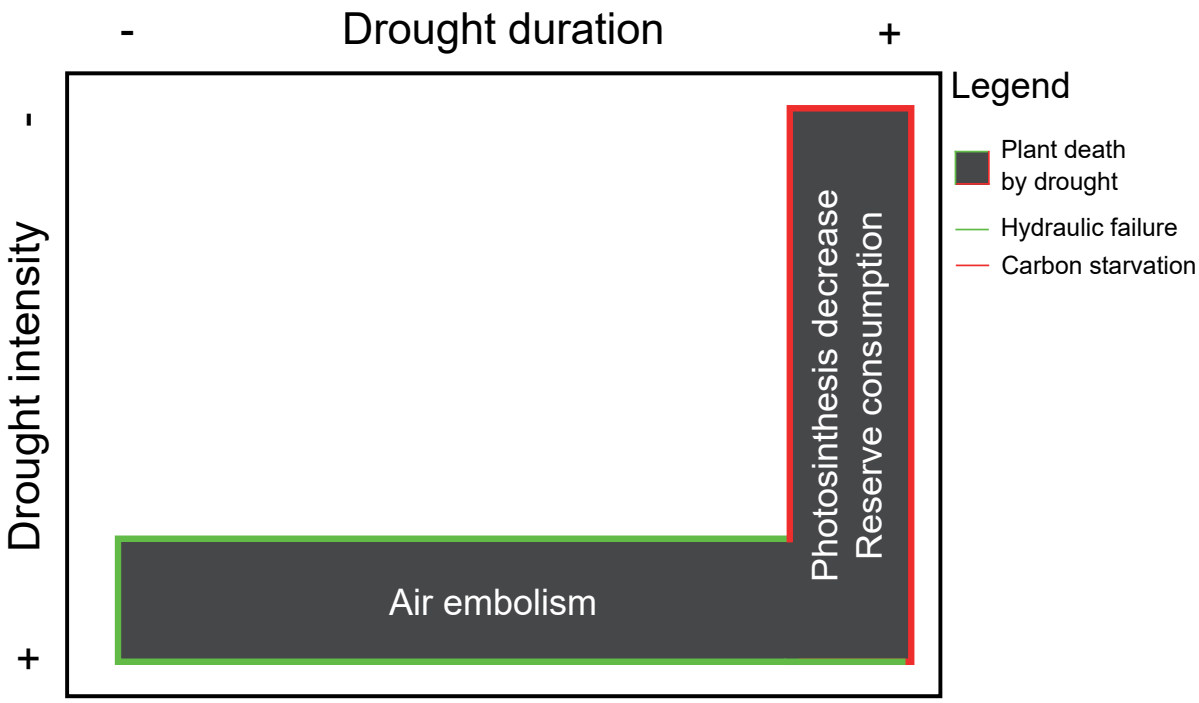

Figure 1. Major hypotheses explaining death (grey area) during drought. Carbon starvation (red borders) is hypothesized to occur when drought duration is long enough to curtail photosynthesis longer than the equivalent storage of carbon reserves for maintenance of metabolism. Hydraulic failure (green borders) is hypothesized to occur if drought intensity is sufficient to push a plant past its threshold for irreversible desiccation before carbon starvation occurs Adapted from McDowell *et al*. (2008).

of hydraulic conductivity) and gives clear indicators in plant survival to drought. In particular, authors identified the highest water potential at which we do not observe stem recovering, corresponding to a loss of 50% of stem hydraulic conductance in conifers (P_{50}, Brodribb *et al*., 2010) and 88% in angiosperms (P_{88}, Urli *et al*., 2013).

On the other side, the carbon starvation hypothesis states that during drought plants could die by insufficient non-structural carbohydrates (NSC, Hartmann, 2015). This theory is based on the main evidence that leaf assimilation is reduced during drought (see Fig. 10C in the *Theoretical framework* paragraph *5.3*), and the assumption that without transpiration, phloem transport should be reduced (Sala *et al*., 2010). Oppositely to hydraulic failure, carbon starvation might be a myth as it has never been measured. Some authors observed a decrease in total NSC in plants under drought (Tommasella *et al*., 2017, Savi *et al*., 2019a), and a significantly lower NSC content compared to controls is present in 60% of drought studies (in the meta-analysis of Adams *et al*., 2017). However, a total absence of NSC in woody organs will unlikely be observed as starch has also a structural function (Taiz and Zeiger, 2003). Therefore, how many NSC reserves are truly available for plants and how they are consumed during drought is still an open question.

Finally, in the case of perennial species, some questions remain on their long-term survival. Especially because authors determine if plants are able to recover after drought right after

the end of the stressing period (Adams *et al*., 2017). Consequently, even in case of extensive hydraulic failure during drought, doubts remain on the fact that some species could generate new xylem and regrow the following season. At the same time, studies are missing on repeated drought events (over several years); in order to understand if perennial plants could really die from carbon starvation over the long-term.

2.2. The hypothetical mechanisms of plant mortality during vascular disease

The mechanisms behind plant death during vascular diseases are less understood compared to drought. Vascular pathogens (see the *Theoretical framework* paragraph *5.4* for more details), once inside the host, physically spread and develop inside the xylem vessels, and they could theoretically cause plant death by hydraulic failure or by the action of toxic metabolites (i.e. hydraulic failure and toxin hypotheses, Fig. 2).

The hydraulic failure hypothesis state that during vascular pathogenesis, plant death is given by impairment between water demand and supply. Xylem hydraulic failure has been associated with pathogen development inside the vessels (Yadeta and Thomma, 2013). However, during vascular diseases, the nature of hydraulic failure is not fully understood, as not only air (as during drought) could cause xylem dysfunctions. The physical presence of pathogens could reduce the water flow; pathogens could cause air entrance inside the xylem vessels, leading to cavitation events (as observed by Perez-Donoso *et al*., 2016, during Pierce's disease); or the presence of plant-derived vascular occlusions, produced to compartmentalize the pathogens (CODIT model, Shigo, 1984), could cause non-gaseous embolism (Sun *et al*., 2013, Venturas *et al*., 2014). Even if during vascular diseases the nature of hydraulic failure is not fully qualitatively appreciated, some studies tried to quantify it, finding that following pathogen inoculations the stem hydraulic conductivity was reduced (Parke *et al*., 2007, Beier *et al*., 2017, Lachenbruch and Zhao, 2019, Mensah *et al*., 2020).

The toxin hypothesis state that plant death is mainly caused by the production of toxic me-

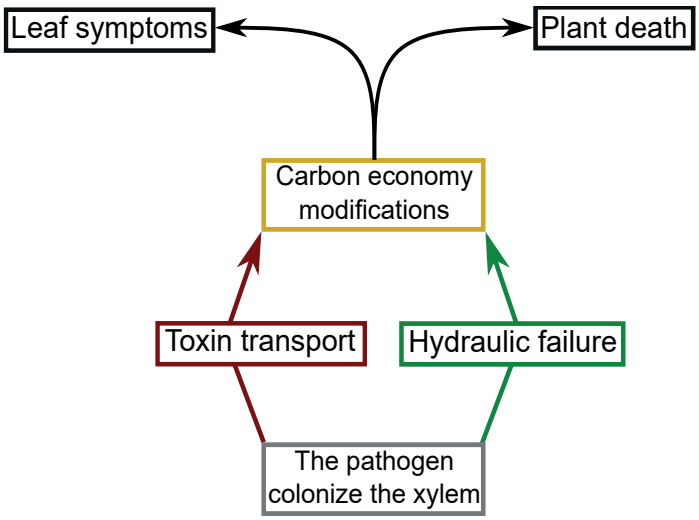

Figure 2. Major hypotheses explaining death during vascular diseases. Once the pathogen has colonized the xylem vessels, it could provoke: (1) a transport of toxins (or other elicitors) through the transpiration stream (red arrow); or by (2) hydraulic failure (by any combination of air embolism, physical presence, or stimulation of plant-derived vascular occlusions) leading to an impairment in water demand and supply (green arrow). Both mechanisms could cause (3) changes in the plant carbon economy, possibly accelerating plant death. Finally, altogether or exclusively, these hypothetical mechanisms could cause leaf symptom expression and plant death (black arrows).

tabolites by the pathogen, that imply a general destruction of tissues. Indeed, other than the structural consequences in the vessels, vascular pathogens also produce toxic metabolites that interfere with plant physiological functioning (Van Alfen, 1989). These toxins are delivered by the pathogens to destroy the physical barriers (i.e. tyloses and gels) produced by the plant and the neighbor-vessel parenchyma cells (Pearce, 1996); if released in functional xylem vessels, toxins could become systemic and cause symptoms at a distance from pathogens. Consequently, it has been hypothesized that the major symptoms related to vascular pathogens (i.e. wood necrosis and leaf wilting or scorching) and ultimately plant death are caused by the production of toxins.

These two hypothetical mechanisms have been suggested to explain leaf symptoms during vascular disease. Prior to leaf symptom appearance, many authors recorded a decrease in stomatal conductance, carbon assimilation, and quantum yield of photosystem II (Magnin-Robert *et al*., 2011, Castillo-Argaez *et al*., 2020). However, it is not clear whether hydraulic failure decrease *gs* mechanistically by a decrease in the transported water volume (Bowden *et al*., 1990, Castillo-Argaez *et al*., 2020), or by pathogen-derived toxins that could interfere with leaf functioning (Sun *et al*., 2017, Fallon *et al*., 2020).

Vascular pathogens also interfere with the carbon economy, consuming NSC reserves, and theoretically accelerate plant death, other than by toxins or hydraulic failure, by carbon starvation (McDowell *et al*., 2008, Yadeta & Thomma, 2013, Oliva *et al*, 2014). Directly, pathogen consume carbon metabolites for their survival, and could cause reduced phloem transport (in case of hydraulic failure); indirectly, pathogens cause a shift in plant carbon metabolism to defense compounds production and a reduced photosynthetic activity during leaf symptom expression.

The demonstration of these different hypotheses need to overcome several practical problematics: (i) The evident necessity of long-term study, or at least the use of naturally infected plants, which should test the physiological response in models as close as possible to field conditions. (ii) The practical problem to quantify hydraulic failure. Actually, X-ray microCT is the only technique to visualize and quantify hydraulic failure *in vivo*, avoiding experimental bias (Brodersen *et al*., 2013, Torres-Ruiz *et al*., 2015). However, it is an expensive technique (usually Synchrotron-based) and it is space limited as (nowadays) to obtain a sufficient resolution to quantify the effective functionality of single vessels we can scan only a restrict volume (~1cm^3). (iii) The chemical challenge of detecting pathogen-derived molecules; as they could be present in very small amounts and/or be effective in a very short period (for example, they could be already metabolized after the visualization of leaf symptoms).

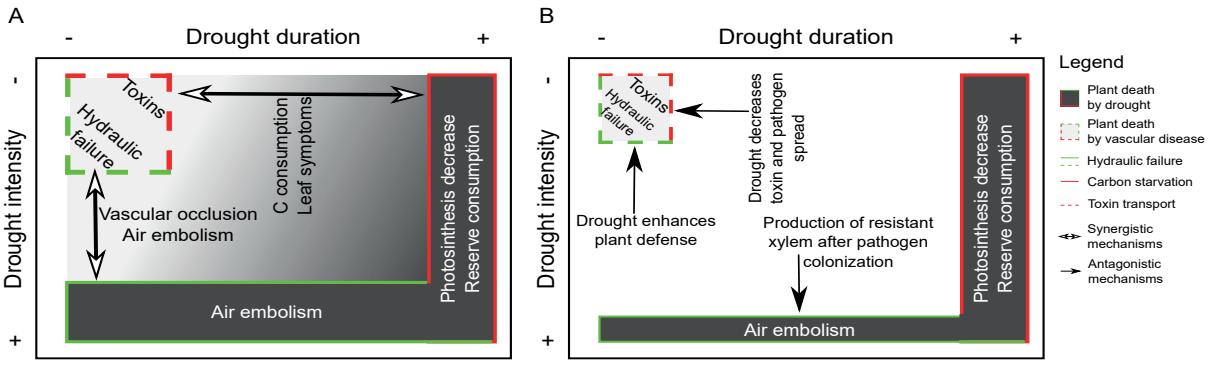

Figure 3. Possible interactions between drought and vascular diseases. The grey area represent the zone of plant death (from light grey and dashed borders for vascular disease, to dark grey and solid borders for drought). Colors correspond to different mechanisms inducing plant death by hydraulic failure (solid and dashed green lines), carbon starvation (solid red lines), or toxin transport (red dashed lines). The double-headed arrows represent synergystic interactions between stresses, while sing-headed arrows antagonistic interactions. (**A**) Synergistic interaction hypotheses. Drought and vascular diseases could interact by enhancing the incidence of hydraulic failure (vertical arrow) by coupling vascular occlusions to air embolism. Otherwise, they could increase plant death (horizontal arrow) by coupling the C decrease during drought to pathogen toxic activities. (**B**) Antagonistic interaction hypotheses. Drought could negatively affects pathogen development by decrease toxin and pathogen spread by a decrease in transpiration, or by enhancing the plant defenses by stimulating antioxidant compound synthesis. At the same time, pathogen could stimulate the formation of new xylem tissue more resistant to air embolism spreading. Adapted from McDowell *et al*. (2008).

2.3. The hypothetical interactions between drought and vascular diseases, synergism or antagonism?

It has been hypothesized that drought and vascular pathogens could interact during perennial plant dieback (Fig. 3); this hypothesis is based on the experimental evidence that they primarily affect the same plant tissue, the xylem.

Both stresses induce many similar physiological changes: decrease in leaf gas exchange, NSC consumption, a decrease in hydraulic conductivity (by hydraulic failure), and wilting of leaves. Therefore, drought and vascular pathogens could hypothetically contribute to plant death in synergy (Fig. 3A), for example by inducing xylem hydraulic failure, coupling drought-induced air embolism to pathogen-induced hydraulic failure, as proposed by Yadeta and Thomma (2013). In addition, drought and vascular disease could contribute together to plant death by coupling the decreased photosynthetic activity and carbon reserve mobilization during drought to phytotoxic activities, direct carbon consumption by pathogens, and leaf symptoms during vascular diseases, as proposed by Oliva *et al*. (2014).

Oppositely, it has been hypothesized that drought and vascular diseases could antagonistically interact (Fig. 3B). In this case, drought could decrease or contain vascular pathogenesis; otherwise, vascular pathogens could increase plant resistance to drought. Consequently, the resulted plant mortality would be attributed at only drought or vascular pathogen, as the impact of one of the two stresses would be drastically reduced (if not suppressed). Decreasing the transpiration rates, drought could induce a subsequent decrease in toxin transport by the transpiration stream. Moreover, drought could directly have a negative impact on pathogen development that

are not able to survive at very low water potentials. Drought could also enhance the synthesis of antioxidant compounds inducing a faster plant defense against pathogens (as in Arango-Velez *et al*., 2016). Finally, vascular pathogens could stimulate the synthesis of new xylem vessels resulting in enhanced resistance to xylem embolism (as in Reusche *et al*., 2012).

Studies conducted with simultaneous drought and vascular pathogens contrast in their results, indicating (in different plant-pathogen-drought intensity combinations) that they could interact synergistically (Croisé *et al*., 2001, Silva-Lima *et al*., 2019), antagonistically (Pennypacker *et al*., 1991, Reusche *et al*., 2012, Arango-Velez *et al*., 2016), or neutrally (Lopisso *et al*., 2017). In different plant-pathogen associations, authors found that mild drought enhanced the host resistance (resulting in drought-vascular pathogen antagonism, e.g. Salle *et al*., 2008, Pennypacker *et al*., 1991), while severe drought for several weeks increased pathogen development after inoculation (resulting in drought-vascular pathogen synergy, Croisé *et al*., 2001, Gao *et al*., 2017). In this last case, we could hypothesize that when drought is intense enough to induce cavitation events could facilitate pathogen development; otherwise, mild drought conditions could reduce disease incidence maybe by slowing down the toxins spread by reducing the transpiration rates, or by inducing the synthesis of antioxidant compounds. In view of this, the physiological thresholds revealing different phases in pathogen-drought interactions needs to be deeply investigated to fully understand perennial plant dieback.

Suggesting another central role for plant physiological status during drought-pathogen interactions, Arango-Velez *et al*. (2016) added a new variable to their study, the tree age, finding that drought reduced pathogen lesion length in pine seedlings, while it increased the lesion in mature trees. This finding enhance the importance of the model choice when we want to apply our results in in the field. The plant physiological state could also be important when the order of the stressing events applied is varying. In the "decline disease spiral diagram" (Manion, 1991) we could hypothesize that pathogens could predispose plants to drought sensibility, or drought incite the pathogen aggressiveness accelerating the disease process. Finally, studying the long-term physiological status in perennial plants could help us to detect the thresholds in which successive and repeated diseases and drought events aimed to plant death.

2.4. Xylem anatomy, a crucial trait in plant resistance to drought and vascular diseases

As just reviewed, plant hydraulic functioning is at the core of the main hypotheses of plant mortality both during drought and vascular diseases. Therefore, xylem anatomy could strongly influence the plant susceptibility (or resistance) to one or both stresses and play a key role during the dieback process. For a detailed description of the main anatomical traits distinguishing xylem vessels in angiosperms see Fig. 9 in the *Theoretical framework* (Paragraph 5.1.).

During drought, perforation plates and pit membranes in and around xylem vessels can maintain (after a cavitation event) the air inside a single vessel element. However when the water

potential is reaching critical thresholds, gas will eventually be able to pass through the pit membranes and let the air spread into the neighbor xylem vessels (Choat *et al*., 2008). The breaking of just one pit membrane should be sufficient to air to spread in neighbor vessels, and larger pits are more sensible to rupture than thinner pits. Consequently, the maximum pit membrane size determine the xylem sensibility to air seeding (Choat et al., 2008).

During vascular diseases, the main anatomical traits influencing the resistance to vascular pathogen are the xylem vessel diameter (more precisely the density of wide vessels, Venturas *et al*., 2014, Pouzoulet *et al*., 2017, 2020), and pit size and distribution (Martín *et al*., 2009). Theoretically if a vessel has a bigger diameter, pathogens would have more chances to escape vascular occlusion (by tyloses) and continue their progression in the vasculature, if a vessel presents small diameter, plants could occlude it faster and compartmentalize the pathogens in a restricted zone (see *Theoretical framework 5.4*). Moreover, vessel width and length are positively correlated (Tyree and Zimmermann, 2002); consequently, in wider vessels pathogens should encounter less perforation plates along their path, facilitating their movement. Likewise, a higher pit size and density could increase fungal spore dispersion within neighbor vessels (Martín *et al*., 2009).

Finally, the xylem anatomy could also influence vascular pathogens-drought interactions. Theoretically, we could imagine that because during drought plant growth is reduced, the new xylem is exclusively formed by small vessels, more resistant to pathogen development. Likewise, pathogen growth could induce xylem hyperplasia (production of numerous small vessels), and subsequent resistance to drought-induced embolism. In this context, there is a need in characterize the effective role of xylem anatomy under the combined action of drought and vascular pathogen.

3. Grapevine, the European dieback crisis

3.1. Evidences, definition, and mechanisms

Grapevine (*Vitis vinifera*) is one of the most economically important perennial crops worldwide, especially in Europe (OIV report, 2020). Since the early 2000s, European vineyards are experiencing a decrease in grape yield (Riou *et al*., 2016). This yield loss, closely related to vine age, has not been ascribed to specific stressing factors. Consequently, in recent times the term dieback has been associated with the yield loss and plant mortality and ascribed to multiple stresses acting simultaneously or in sequence (Riou *et al*., 2016). In the picture of grapevine dieback (Fig. 4), we can observe that, multiple factors may act in concert: the environmental conditions at the base, the biotic agents and the cultural practices that, side-by-side, reduce plant vitality, and finally, the plant physiological response in the background. Climate change can influence all the factors contributing to plant dieback, and it represents the frame of the picture (Fig. 4). Since 30 years, winegrowers are observing a shift in many phenological phases

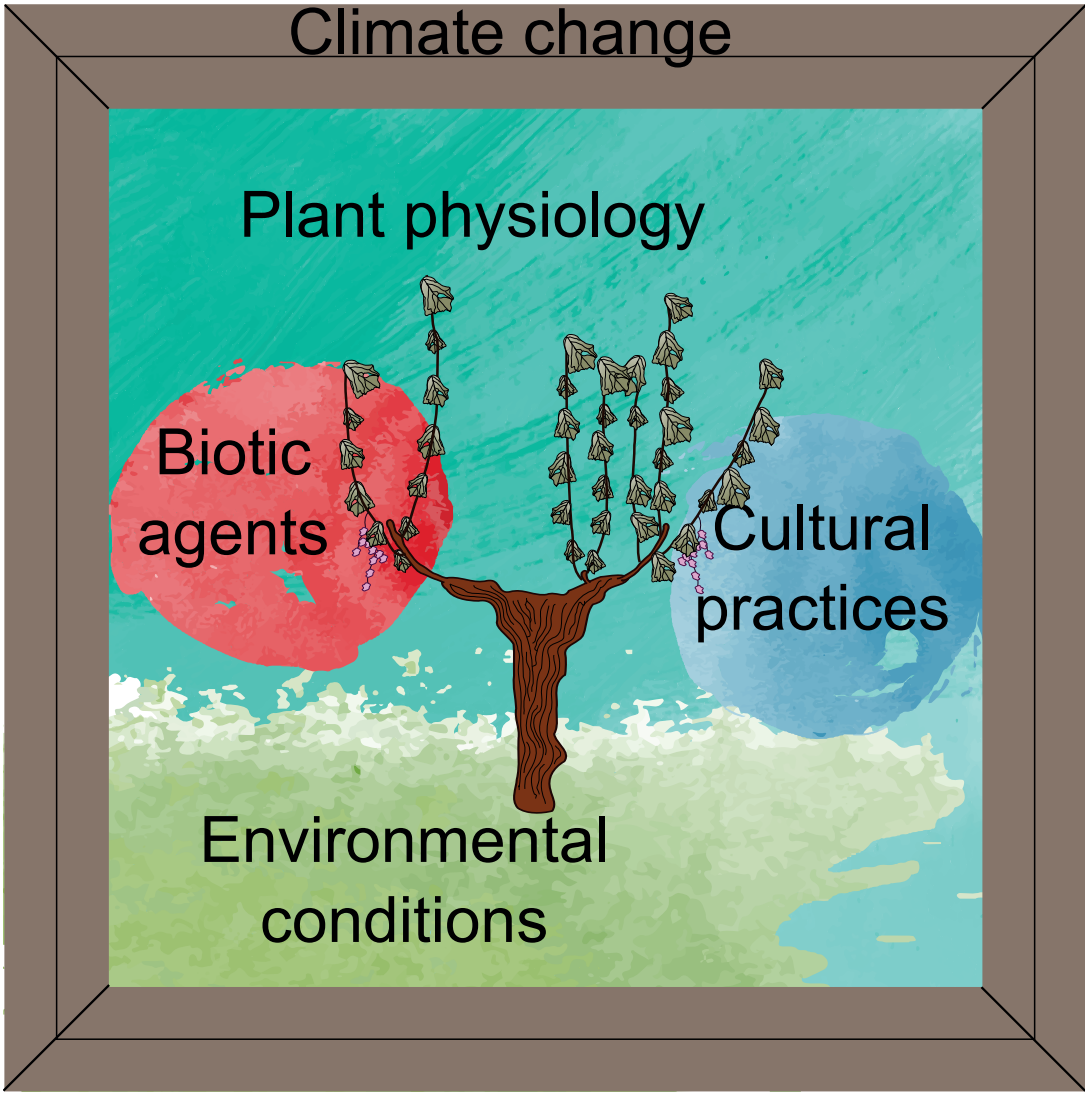

Figure 4. Grapevine dieback picture. The dead/unproductive vine is surrounded by multiple interacting factors. Inside the frame of climate change, the environmental conditions are drawn at the base of the picture. The cultural practices and the biotic agents, side-by-side, play a major role in the decreasing of plant vitality. Finally, the plant physiology, cover the whole background interacting with the different factors.

(including bud-break, veraison, and fruit maturity, van Leeuwen and Darriet, 2016). Even if drought will unlikely attain grapevine lethal thresholds in the short term (confirmed by 20 years monitoring of Ψ_{stem} in California and Bordeaux, Charrier *et al*., 2018); changes in climatic conditions are modifying yield quality and quantity (e.g. increasing wine pH and alcohol degree, van Leeuwen and Darriet, 2016). Consequently, it has been predicted, even with a "low" global warming scenario (+ 2 °C), that current winegrowing regions could lose from 20 to 60% of surface, depending on the cultivar diversity (Morales-Castilla *et al*., 2020).

At the bottom of the picture, we observe the environmental conditions (especially climate and soil conditions, and geographical position Fig. 4). Other than changes related to the global warming, we also need to consider that grapevines are frequently cultivated in hostiles environments: draining (and frequently dry) soils, hot summers (e.g. southern Europe), sometimes

in altitudes (e.g. in northern Italy, or Alsace). These conditions are strictly related to the notion of "terroir" (i.e. the ensemble of variety, soil, climate and practices that differentiate a wine region from another, van Leeuwen and Seguin, 2006). Moreover, frequent and mild water deficit conditions are related to higher wine quality (especially for red cultivars, van Leeuwen and Darriet, 2016). Finally, we can notice that the most rentable vines are frequently planted where there are sufficient resources (especially water and minerals) to maintain plant life and fruit productions, but not enough to have a well vigorous liana.

On the left-hand side of the picture, there are the biotic agents (Fig. 4). Grapevines are constantly submitted to continuous attacks from different biotic agents. The biotic pressure in European vineyards has seen a drastic increase concomitantly with the second industrial revolution (XIX century), when the progression of world trade market has caused the importation (from the U.S.) of powdery and downy mildews, and Phylloxera. In France, it has been estimated that vineyards are one of the cultures that receive the most abundant phytosanitary treatments, despite their relative low surface (Butault *et al*., 2011). Indeed, powdery and downy mildews, together with *Botrytis cinerea* (and other grape molds), numerous viruses, and the insects *Eupoecilia ambiguella*, *Lobesia botrana*, and *Scaphoideus titanus* (vector of flavescence dorée), and other secondary agents, oblige winegrowers to a strict and continue health control to assure grape production. Among the biotic agents that still do not have an efficient sanitary control, we found the grapevine trunk diseases (GTD), caused by a complex microbiome in the woody organs. GTD can affect young plants (e.g. Petri and black foot diseases), which are frequently related to contaminations during grafting, and bad soil management in nurseries (Gramaje *et al*., 2018). GTD can also affect mature plants (more than 7 years-old): mainly esca and eutypiose diseases (Bertsch *et al*., 2013). While a rigorous chemical control during plant vegetative reproduction can reduce the GTD impact on young plants, it is not the case in old vines (even if chemical treatments after winter pruning can reduce Eutypiose incidence, Gramaje *et al*., 2018). This is probably due to the fact that pathogens develop deep in the woody organs (where chemical products can hardly penetrate), and that pathogens employ several years before the plants express visual symptoms, and when this happens is frequently too late to organize any safety strategy (Gramaje *et al*., 2018). GTD impact is increasing in the last 20 years in Europe, and this might be partly due to prohibition of the only chemical product used against esca (sodium arsenite, Songy *et al*., 2019), and to the increased vineyard mechanization, which increased the winter pruning damage (Gramaje *et al*., 2018).

Indeed, in the picture of grapevine dieback we observe, on the right-hand side of the vine, the cultural practices (Fig. 4). It has been demonstrated that the winter pruning (necessary to obtain high and regular yields), can affect negatively the plant physiology, and positively the GTD development (Gramaje *et al*., 2018, Lecomte *et al*., 2018). Moreover, the increase in vineyard mechanization and industrialization is related to an accelerated grapevine dieback. For example, an excessive fruit production (especially during the first years after plantation), reduce the

plant lifetime (Carbonneau, 2015).

In the background of grapevine dieback, we observe plant physiology (Fig. 4). Indeed, if many studies have focused on how singular stresses influence plant physiology (e.g. reviews in Fontaine *et al*., 2016 for GTD and Gambetta *et al*., 2020 for drought), few tried to understand the physiological response to combined stresses (e.g. Savi *et al*., 2019b, Songy *et al*., 2019), and none studied the underlying physiological mechanisms behind the complex process of grapevine dieback. The field monitoring usually implemented to correlate the disease incidence to climatic conditions (e.g. Marchi *et al*., 2006, Serra *et al*., 2018, Kraus *et al*., 2019, for esca) are rarely (or never) associated with measurements of the physiological status of the plants (for example, transpiration rates and water potential) impeding the understanding on how climatic conditions effectively influence the plant functioning and mortality processes. We know that these kind of integrated studies are extremely challenging and demand long-term monitoring in the fields of many different factors and parameters. However, if we are to understand the sequence of events that lead to grapevine dieback, the picture has to be looked into its entirety, because one single stressing factor would unlikely be the only responsible to grapevine (or perennial plants in general) dieback. In this thesis, we focused our attention on two factors contributing to grapevine dieback: esca (a vascular GTD) and drought, because their presence is frequently recorded in the field and because they could synergistically interact during the dieback process.

3.2. Esca, a complex disease

Esca is a grapevine trunk disease; its presence is endemic in Europe, and probably it has always existed together with *Vitis vinifera* (Mugnai *et al*., 1999). From the first scientific description of esca (Viala, 1926) to the recent fungal characterization (Morales-Cruz *et al*., 2018, Brown *et al*., 2020), esca definition (and even its name) has changed (Mondello *et al*., 2018), creating long debates in the scientific community. However, at present time, the major traits that define esca disease are broadly recognized. Esca (we will simply name it "esca" in this thesis) is characterized by internal necrosis in the perennial trunk (Lecomte *et al*., 2012, Bruez *et al*., 2014, Morales-Cruz *et al*., 2018). A black necrosis, where the vascular fungi *Phaeomoniella chlamydospora* (*Pch*) and *Phaeoacremonium minimum* (*Pmin*) are detected in high abundance (Fig. 5G, Morales-Cruz *et al*., 2018), a white necrosis where the Basidiomycota *Fomitiporia* spp. are isolated (*Fom*, Fig. 5C, Fischer, 2002), and a brown stripe on the external vasculature which causing mechanisms and agents are still uncertain (Fig. 5F, Lecomte *et al*., 2012). The role played by the fungi of the Botryosphaeriaceae family is still uncertain (many authors distinguish esca from Botryosphaeriaceae dieback, or BDA, Bertsch *et al*., 2013, Bruez *et al*., 2014, even if the observed symptoms are very similar, if not equal, Lecomte *et al*., 2012), so does the role played by bacteria (Bruez *et al*., 2015, 2020; Haidar *et al*., 2015). Given the mode of action of the three more recurrent fungi in in trunk necrosis (*Pch*, *Pmin*, and *Fom*), it

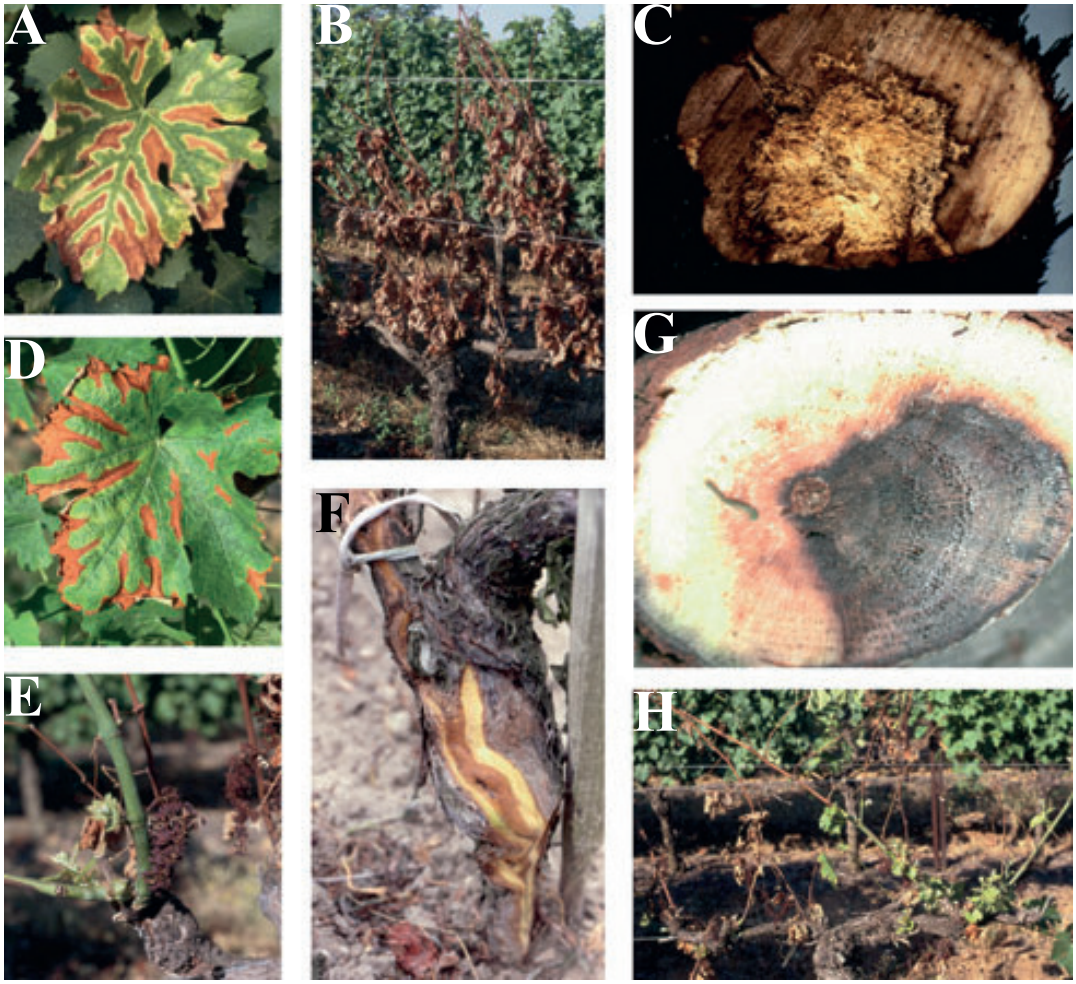

Figure 5. External and internal symptoms related to esca or Botryosphaeriaceae dieback. (**A**) Tiger-stripe symptoms with scorched and yellow area. (**B**) Apoplectic (severe) form characterized by dieback of one or more shoots and leaf drop. (**C**) Trunk-cross section with white rot (**D**) Tiger-stripe symptoms with scorched area only. (**E**) Cluster desiccation. (**F**) Brown stripe in the external vasculature of trunk. (**G**) Sectorial black necrosis. (**H**) Final plant desiccation. From Bertsch *et al*. (2013).

is assumed that the vascular pathogens (*Pch* and *Pmin*) firstly colonize the functional healthy wood (they are also detected in non-necrotized tissue, Bruez *et al*., 2014, 2020, and in young vines, Gramaje *et al*., 2015). *Fom* species (among other Basidiomycota) colonize tissues already dead (they are detected in white rot tissue only, Bruez *et al*., 2020). Esca also presents two distinct foliar symptoms: a tiger-stripe symptom, characterized by a yellowing or scorching (depending on symptom intensity) between the main ribs that remain green (Fig. 5A, D and 6), and apoplexy, when the crown desiccates in one to three days (Fig. 5B, H). Esca leaf symptoms (both tiger-stripe and apoplexy), as well as the brown stripe along the vasculature, cannot be reproduced under controlled conditions (i.e. after pathogen inoculations), they are only observed in vineyards. Consequently, the underlying mechanisms behind these symptoms are still unknown. Moreover, leaf symptom presence has been shown to be randomly distributed in space and time. In space, because esca leaf symptoms are usually dispatched all over the vineyard (suggesting limited esca transmission from neighbor plants, Surico *et al*., 2000, Li *et*

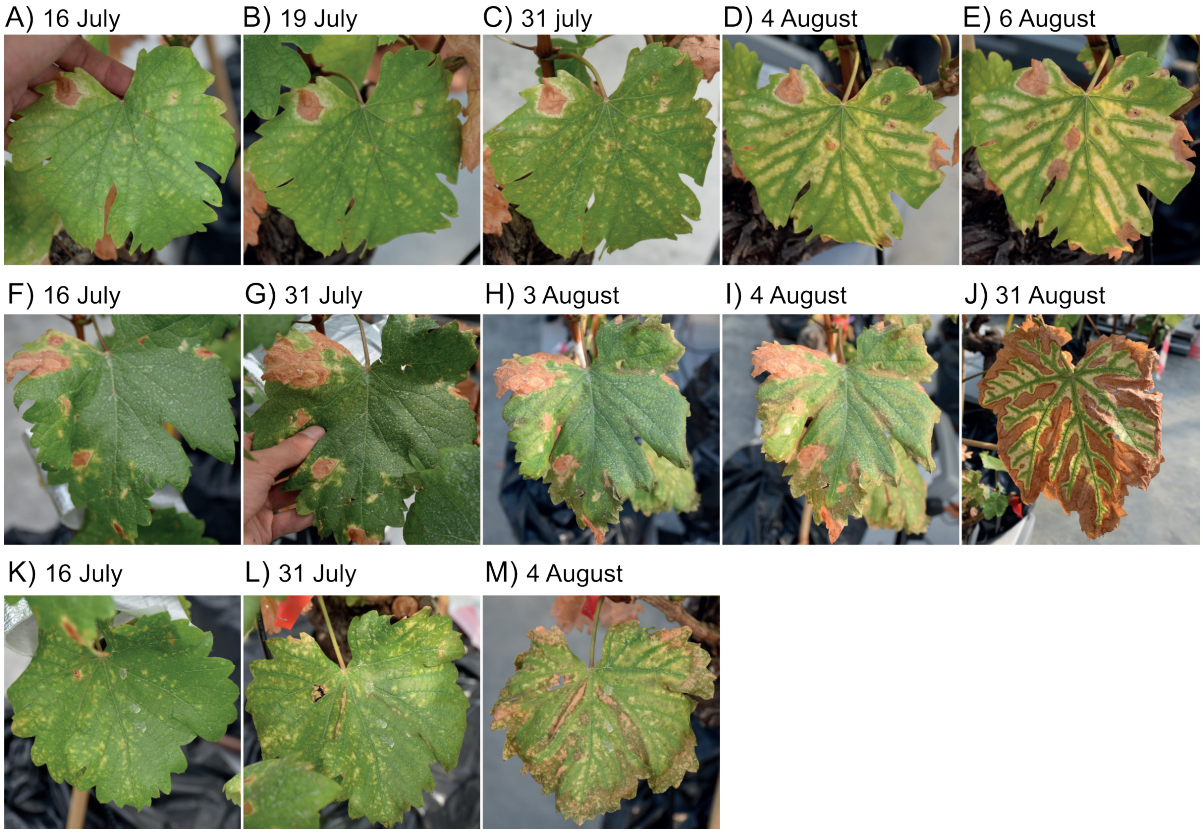

Figure 6. Esca leaf symptom evolution in three different leaves of one single *V. vinifera* cv Sauvignon blanc plant. (**A**-**E**) We can observe that small yellow dots are already present soon in the season (**A**, mid-July), and that progressively expand, occupying more and more space, the scorched area arrive later (**D**, 4 August) and then progress inside the yellow area (**E**, 6 August). (**F**-**J**) In this leaf (n.b. from the same plant and season), the yellowing is less present, and the scorched area occupy directly the interveinal space since the beginning of August. (**K**-**M**) In this third leaf, the yellow and scorched areas share different zone of the interveinal space. These pictures, illustrating the diversity in esca leaf symptoms within one plant, were taken during our 2018 greenhouse experiment.

al., 2017). In time, because its sudden appearance is not regular over different seasons, even if hot and rainy conditions seems to increase esca incidence (Marchi *et al*., 2006, Serra *et al*., 2018, Kraus *et al*., 2019), and because symptomatic plants can appear asymptomatic the following seasons (Li *et al*., 2017). In this uncertainty, some patterns and characteristics have led scientists to state different hypotheses on esca leaf symptom formation (reviewed in Claverie *et al*., 2020). It is assumed (without any published evidence of the absence of the esca-related pathogens in leaves) that leaf symptoms appear at a distance from the pathogens (that have been detected on >1-year-old perennial organs). In symptomatic leaves, different studies have observed a decrease in transpiration, CO_2 assimilation, and chlorophyll fluorescence (Petit *et al*., 2006, Magnin-Robert *et al*., 2011). In addition, a defense response prior (or during) symptom expression in leaves is supported by transcriptomic (Magnin-Robert *et al*., 2011, Martín *et al*., 2019), proteomic (Valtaud *et al*., 2009, Calzarano *et al*., 2016, Goufo *et al*., 2019), and lipidomic (Goufo and Cortez, 2020) approaches, and NSC quantifications, which detect a decrease in starch content and an accumulation in soluble monomers (Petit *et al*., 2006, Valtaud

et al., 2011). Finally, esca leaf symptoms are associated with the development of tyloses in stems (Fleurat-Lessard *et al*., 2013). Since (i) *Pch* and *Pmin* (the two recurrent pathogens in trunk necrosis from esca symptomatic plants, Morales-Cruz *et al*., 2018, Brown *et al*., 2020) develop in xylem vessels (Pouzoulet *et al*., 2014); (ii) the visual symptoms are strikingly similar to vascular diseases (compare Fig. 5 and 6 to Fig. 13 and 14, in *Theoretical framework*); and (iii) the impact on the plant physiology is similar between esca and other vascular diseases, we treated esca as a vascular disease in this thesis. However, we are well aware that some technical impediments (especially the reproduction of leaf symptoms and the possible role of other pathogens such as the Botryosphaeriaceae), leave our assumption as still hypothetical, and not totally demonstrated.

3.3. The hypotheses behind esca leaf symptoms, and the possible interaction with drought

The two different hypotheses on vascular pathogenesis described above (paragraph 2.2.) has been transposed for esca (Claverie *et al*., 2020). (i) The "toxin" hypothesis states that the pathogens (living in the woody perennial organs) can produce toxic metabolites inside the xylem vessels. The water flow then transport these metabolites up to the leaves, where they accumulate and generate leaf cellular death. (ii) The "hydraulic failure" hypothesis state that a decrease in xylem hydraulic conductivity (generated by air or nongaseous embolism) can generate leaf cell death by an impairment between water demand and supply. Hydraulic failure is still a hypothetical mechanism during esca as no studies have directly tested it so far. Some studies (reviewed in Fontaine *et al*., 2016) discarded its intervention on the main observation that in symptomatic leaves the genes classically related to drought are not overly expressed. This point of view closely associates hydraulic failure to a drought-like event, but in general, when hydraulic failure is observed during vascular pathogenesis, the underlying mechanisms are different from drought. We should acknowledge here that some technical impediments have delayed the test of the hydraulic failure hypothesis in the esca pathogenesis: the impossibility to reproduce esca leaf symptoms under controlled conditions (leaving us with the only option of using mature vines from the field), and the obligation to use *in vivo* observations (by X-ray or IMR technologies) to quantify xylem functionality that are still impossible in the field.

If esca affects grapevine hydraulic functioning, by any mechanisms, it could decrease xylem functionality and/or efficiency, possibly increasing plant susceptibility to drought. Alternatively, we could hypothesize that vascular pathogens need nonfunctional vessels to develop and necrotize the tissues, benefiting from drought-induced cavitation. Finally, we could imagine that esca and drought-related embolism could synergistically contribute in reducing xylem hydraulic conductivity, desiccating organs, and accelerating plant death. These hypothetical consequences in esca-related hydraulic failure, give us the suspicion that drought and esca could synergistically participate to grapevine dieback (as during vascular diseases in general, Fig. 3A). Moreover, we are also missing a clear study on how esca is affecting the plant hydraulic

functioning seasonally and over the long-term, and on how the different hydraulic properties of the plant could accelerate or slow the disease process. Indeed, even if esca is considered a vascular disease, its effects on the vascular system remain largely unknown: both on functional and anatomical features.

Drought and esca could also synergistically deteriorate grapevine carbon economy. Indeed, if carbon starvation has still not been observed during drought, the possible intervention of pathogens could accelerate decrease in non-structural carbohydrates. Moreover, even if vascular pathogens and drought could not result in synergy when applied together; both stresses should end in reduced photosynthetic activity and reserve accumulation. In this case, repeated events of esca leaf symptom and drought over the plant lifetime, could cause plant death by carbon starvation over the long-term.

Consequently, this thesis will first focus on exploring the hydraulic failure hypothesis during esca in leaves and stems of naturally infected plants. More specifically, we will test whether (and to what extent) esca induces a loss of hydraulic conductivity in symptomatic leaves and stems, and whether esca modifies the xylem anatomy over the long term. Second, this thesis will focus on whether esca and drought synergistically participate to grapevine dieback, and whether they induce similar or different plant water relations and carbon economy.

4. Thesis objectives

As just reviewed, the understanding of perennial plant dieback is still impeded by many knowledge gaps. Dieback is a long-term process that involve many interacting factors and the extent and directions of these interactions are probably at the core of the major scientific issues of plant mortality. Moreover, we evidenced the central role of the hydraulic functioning and carbon economy during perennial plant dieback, especially when drought and vascular diseases are studied. In this thesis, we characterized the role of hydraulic failure in esca pathogenesis, and the interaction between vascular pathogens and drought during grapevine dieback. The readers should consider all the reported results as the interaction of given (and quantified) symptom severity, drought intensity, and timing (meant as length and moment) of events.

The general objective of this thesis is to characterize the relationships between grapevine hydraulic functioning, xylem anatomy, and esca pathogenesis. In this context, we explored the hydraulic integrity in leaves during esca leaf symptom expression (*Chapter 2*) and compared the leaf xylem anatomy between multiple induced-senescing process and varieties (*Chapter 3*). We then characterized stem hydraulic integrity during esca seasonally and over the long-term (*Chapter 4*). Finally, we observed the plant physiological response to the simultaneous effect of drought and esca, focusing on plant-water relations and carbon balance (*Chapter 5*).

We overcame to the esca-related technical problem by uprooting old (~30 years-old) vines from a vineyard identified by a plant-by-plant disease notation since 2012 (the experiments took place from 2017 to 2020) and characterized by a high esca incidence (44% of symptomatic plants yearly on average, Table 2 in *Experimental framework*, paragraph 6.2.). These plants were transplanted into pots and they naturally expressed leaf symptoms in the greenhouse. Consequently, we were able to manipulate and transport these plants to different laboratories and study leaf symptom development in a controlled environment.

The *Chapters 2* to *4* of this thesis focused on the impact of esca (i.e. leaf symptom presence) on the hydraulic integrity of leaves and stems. We then submitted half of the plants to drought during two consecutive seasons (from June to October) to study the effect of drought on leaf symptom expression. At the same time, we characterized the whole-plant physiology (as plant-water relations and carbon economy) during esca and drought, in order to understand the physiological mechanisms behind their interaction.

The main scientific question addressed in the second chapter is: to what extent esca symptomatic leaves suffer from hydraulic failure? We hypothesized that, as well as during other vascular diseases, leaf hydraulic integrity would be compromised. In this chapter, we quantified and characterized hydraulic failure in control and symptomatic midribs and petioles through X-ray microCT and light microscopy; we quantified the presence of esca-related vascular pathogens in different organs.

The main scientific question addressed in the third chapter is: are vascular occlusions in grapevine leaves a general response during different induced-senescence processes? We hypothesized that in senescing leaves with visual symptoms similar to esca, the xylem anatomy would be similar. We compared the xylem anatomy in midribs collected from leaves presenting various symptoms (winter senescence, magnesium deficiency, esca symptomatic and control leaves). We further studied esca by comparing xylem anatomy of midribs collected from different varieties and countries. Moreover, we tested the impact of esca on the functionality of the leaf lamina by embolism optical visualization.

The main scientific question addressed in the fourth chapter is: what are the seasonal and long-term consequences of esca on stem hydraulic integrity? We hypothesized that esca would induce hydraulic failure in stems presenting symptomatic leaves and that, over the long term, it would affect the xylem anatomy. To answer this question we quantified and characterized hydraulic failure in control and symptomatic stems through X-ray microCT. Then we quantified specific and theoretical hydraulic conductivity all along one season (in order to detect the moment of hydraulic failure appearance relative to the onset of leaf symptoms) and comparing stems with different long-term disease record.

The main scientific questions addressed in the fifth chapter are: are drought and esca synergistic or antagonistic during grapevine dieback? To what extent plants submitted to drought or

esca present different physiological responses? We hypothesized that esca and drought would synergistically interact, amplifying esca leaf symptom development and plant susceptibility to drought. Moreover, we also expected that drought and esca induce similar physiological responses at leaf (by similar water potential regulation and leaf gas exchange) and at whole-plant (by similar whole-plant stomatal conductance and carbon balance) scales. In order to explore drought-esca interaction we submitted half of the plants to three months of water deficit (moderate to severe) in two consecutive years.

5. Theoretical framework

5.1. Plant-water relations and xylem tissue

To begin the photosynthetic process, leaves must open their stomata and let CO_2 enter in the mesophyll. Unfortunately, the high difference in relative humidity between the atmosphere and the leaf, let huge amount of water directly flow into the atmosphere (this water loss is called transpiration, *E*). It has been estimated that for every gram of organic matter synthetized, the plant consume 500g of water (Taiz and Zeiger, 2003). In our physiological survey, we found that healthy well-watered leaves in grapevine release (on average) 167 mol of H_2O every mol of absorbed CO_2 (*Chapter 5*). Consequently, to maintain an active photosynthesis, plants need to sustain a constant water flow up to the leaves. The cohesion-tension theory (Steudle, 2001) explains how plants are able to maintain a constant water flow through the stomata, even at height of more than 100m. The air water potential create a surface tension in the capillary menisci inside the intercellular space in leaves. Thanks to the cohesion among water molecules, the tension is transmitted to the connected (adjacent) water molecules. Plants maintain a continuous water column that connect directly the water in the soil to the leaves (i.e. forming the soil-plant-atmosphere continuum, SPAC), that move acropetally thanks to the difference in water potential between the soil and the air (i.e. creating a tension). As the water flows through

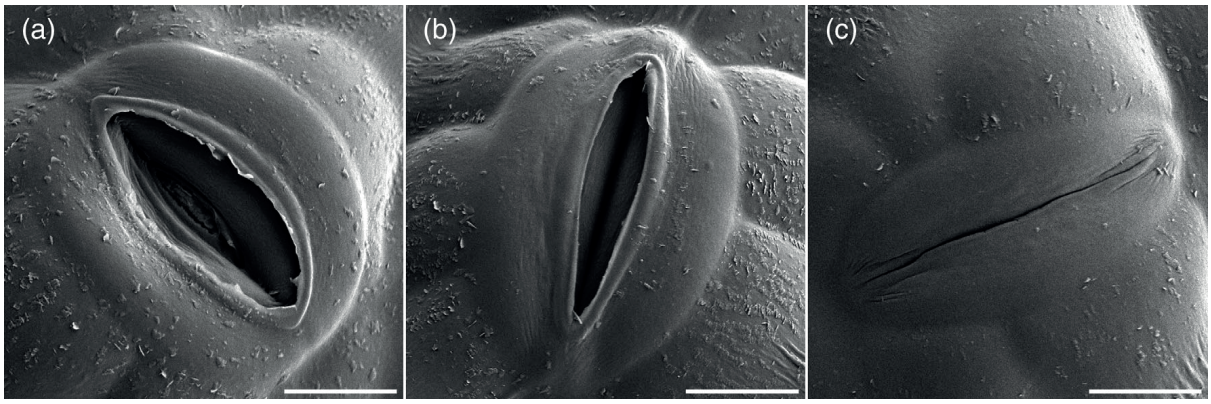

Figure 7. Cryo-SEM microscopy images of stomata on the abaxial side of Vitis vinifera leaves. (**a**) Slightly open stomata; H_2O and CO_2 molecules can flow in and out the leaf. (**b**) Closed stomata with cuticles open; H_2O and CO_2 flow is strongly reduced. (**c**) Completely closed stomata; H_2O and CO_2 flow is negligible. From Dayer *et al.* (2020a).

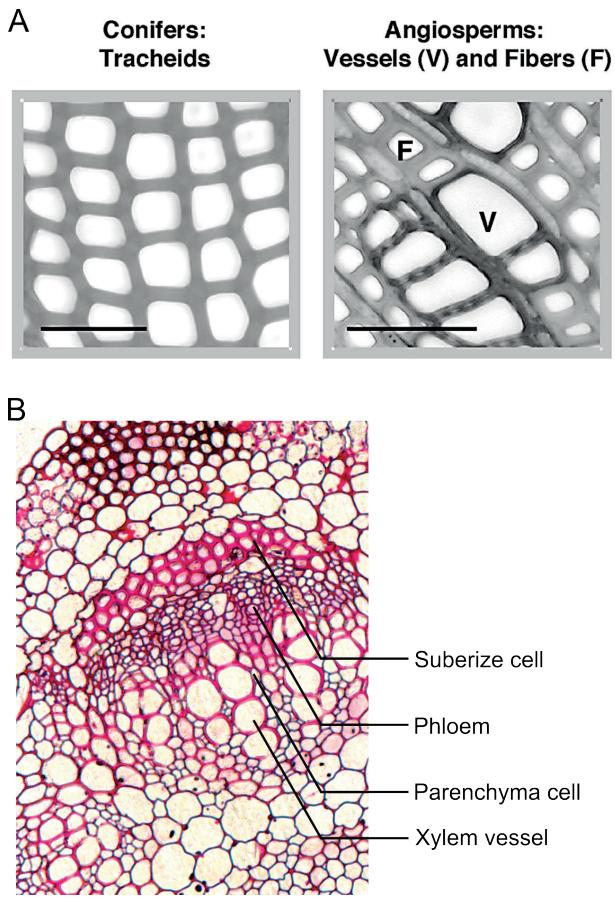

Figure 8. (**A**) Transverse sections of conifer vs angiosperm xylem tissue. Conifer tracheids (here *Pinus nigra*) provide both transport and structural support. Angiosperm xylem (here *Acer negundo*) is more specialized. Water transport occurs in vessels (stained darker, V), whereas structural support is often provided by fibers (F). Scale bars are 50 µm. From Hacke and Sperry (2001). (**B**) Photomicrograph of a vascular bundle from a *Vitis vinifera* midrib. The different anatomical elements are indicated. Personal production.

the plant by a difference in water potential, we can apply the Ohm's law for electric circuits, and estimate the hydraulic conductivity of the plant or just a part of it (i.e. its hydraulic properties, Box 1). Transpiration is controlled by stomata (Fig. 7), which are small apertures located on the green organs where the photosynthesis is active (especially leaves). Stomata respond continuously to different environmental stimuli to regulate plant transpiration. The main environmental factors that induce stomatal closure (or aperture) are light conditions, vapor pressure deficit (VPD, an indicator of air humidity and temperature), and soil water content. When air temperature increase and/or relative humidity decrease, VPD become more intense, and air attracts water with higher tension. While in absence of light stomata simply close because photosynthesis is impossible, during VPD increase or soil water content decrease, stomatal closure intervene to impede the water column to reach too negative tensions and therefore, to produce a cavitation event, leading to xylem embolism and plant desiccation (Martin-StPaul *et al.*, 2017). Xylem is the vascular tissue that transport water and mineral elements from the soil up to the roots, and its specialization help plants to avoid cavitation events. Xylem is formed by empty tubes (transporting water), which type and morphology depend on the genotype, arranged in vascular bundles with parenchyma cells and phloem (Fig. 8). Xylem anatomy can be highly diverse depending on the species (Tyree and Zimmermann, 2002). Conifers are known to present thin and short tracheids, while angiosperms usually present larger and longer vessels to ensure water transport and fibers to ensure structural support (Fig. 8A). In angiosperms, a reticulate network of many interconnected vessels composes the xylem tissue (one example in Fig. 9). These vessels are formed by different vessel elements (Fig. 9A), that can reach, in some species, meters in length (Tyree and Zimmermann, 2002). Vessels always end by a perforation plate (Fig. 9B), and contoured by vessel walls (Fig. 9C) which primary role is to prevent the spreading of air, in case a cavitation event embolize a vessel (Tyree and Sperry, 1989). Vessels are connected with other vessels or

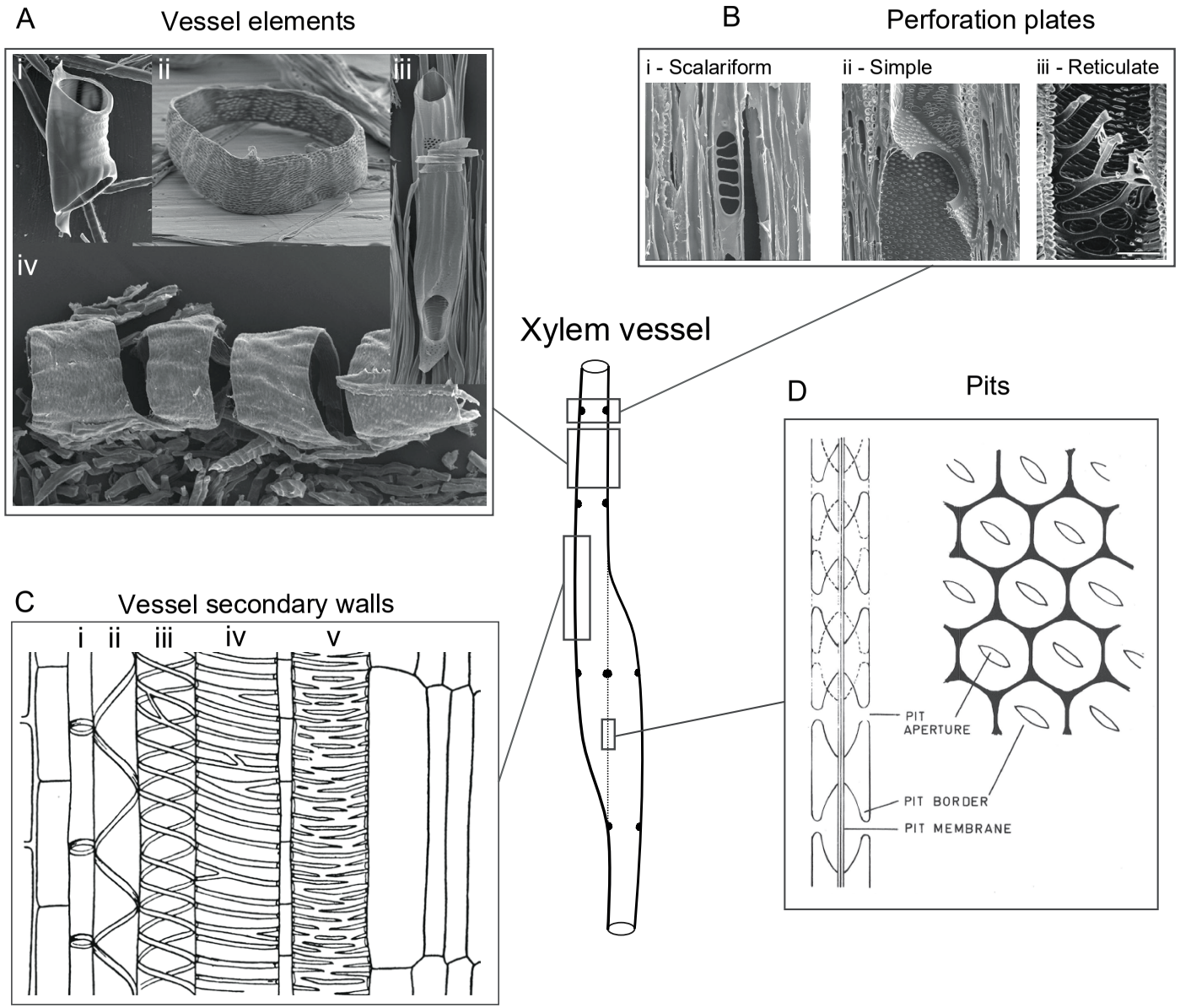

Figure 9. Anatomical diversity and complexity of xylem vessels in angiosperms. (**A**) Representative vessel elements from Crang *et al*. (2018). (**Ai**) Vessel element from red oak (*Quercus rubra*) (**Aii**) A honey locust (*Gleditsia triacanthos*) vessel element is larger in diameter than height. The side walls contain numerous scalariform pits. (**Aiii**) and (**Aiv**) Red maple (*Acer rubrum*) vessel elements. Note the lateral pit field and associated ray parenchyma at the top of the vessel element in Aiii. The four vessel elements in Aiv were once interconnected to form part of a vessel. All of these vessel elements shown here have simple perforation plates. (**B**) Representative perforation plates from Crang *et al*. (2018). (**Bi**) Scalariform perforation plate from tulip tree (*Liriodendron tulipifera*). (**Bii**) Simple perforation plate form Black walnut (*Juglans nigra*). (**Biii**) Reticulate perforation plate from the feather duster palm (*Rhopalostylis sapida*). (**C**) Patterns of secondary cell wall deposition in vessel elements from Crang *et al*. (2018). (**Ci**) Annular. (**Cii**, **Ciii**) Spiral or helical. (**Civ**) Scalariform. (**Cv**) Reticulate. (**D**) Diagrammatic representation of vessel-to-vessel pit apertures from Tyree and Zimmermann (2002). In longitudinal sections, we can observe the pit membrane that delimitate two xylem vessels. In transversal sections the honeycomb distributions of pits. Note that pits can also be found in perforation plates and in vessel walls (i.e. between xylem vessels and parenchyma cells).

with parenchyma cells by pits (Fig. 9D).

Box 1. Ohm's law application for plant water movement and the concept of hydraulic conductivity.

Ohm's law analogy for plant transpiration correspond to:

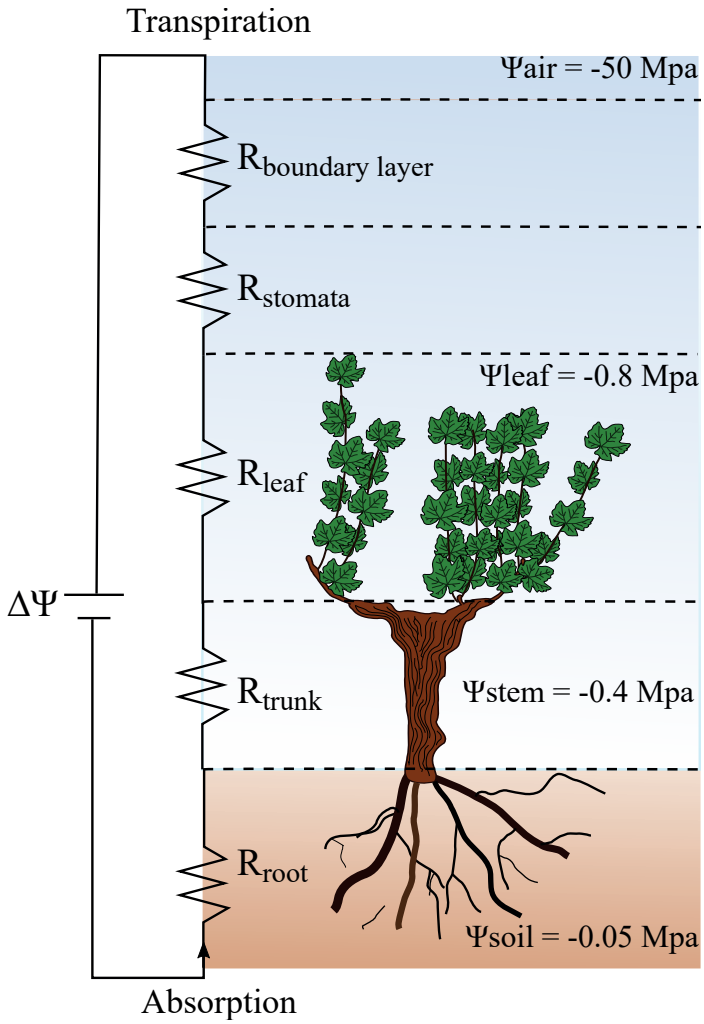

$$[1]\ F = \Delta\Psi / R$$

Where: F is the water flow that pass through the plant [g s^{-1}], $\Delta\Psi$ is the difference in water potential between air and soil [Mpa], R is the hydraulic resistance, dependent of physical and chemical properties of the flow pathway [Mpa s g^{-1}], and corresponds to the inverse of the hydraulic conductance k. We can consider the soil-plant-atmosphere continuum (SPAC) as a series of hydraulic resistances (as in the figure on the left), and calculate the contribution of each to the total hydraulic resistance as:

$$[2]\ R = R_{root} + R_{trunk} + R_{leaf} + R_{stomata} + R_{boundary\ level}$$

If R is high, the water will flow with difficulty, if R is low, the water will flow easily (i.e. faster). The comparison of hydraulic resistances (or their inverse, k), is used in the literature to understand which part of the plant results in bottleneck for the water flow (Sperry *et al*., 1988). Commonly, studies compare different hydraulic conductivities k_h [g m Mpa^{-1} s^{-1}], calculated as:

$$[3]\ k_h = k \times l$$

Where: k is the hydraulic conductance ($1/R$), and l the length of the segment (e.g. stem or root) analyzed. Authors also use the specific hydraulic conductivity k_s [g Mpa^{-1} s^{-1} m^{-1}]:

$$[4]\ k_s = k_h / A$$

Where A correspond to the sapwood cross-sectional area [m^2] of the segment analyzed.

5.2. Carbon balance and non-structural carbohydrates

Carbon (C) is the primary element that characterized life forms. Plants are able to transform the inorganic carbon (CO_2) into organic carbon (sugars) through an elegant process called photosynthesis. Many studies focusing on the plant carbon balance, and on plant physiological status, analyze the non-structural carbohydrates (NSC, Hoch *et al*., 2003, Sala *et al*., 2012). These compounds can give a nice overview on the activities of the tissue (from one cell to whole plant) analyzed, even if the information will never be complete as the metabolic pathway is complex, and sometimes other C forms strongly participate to the carbon balance. Classically, NSC include glucose, fructose, sucrose, and starch. Glucose and fructose are the two monosaccharides at the base of (almost) any metabolic pathway, they are the final C form after photosynthesis, and their concentration is used to interpret the cellular activity. If one tissue (or cell) present higher content of glucose and fructose that usually means that the cells are stimulated to enhance the production of other metabolites (e.g. for growth or defense response, Roitsch and Gonzalez, 2004).

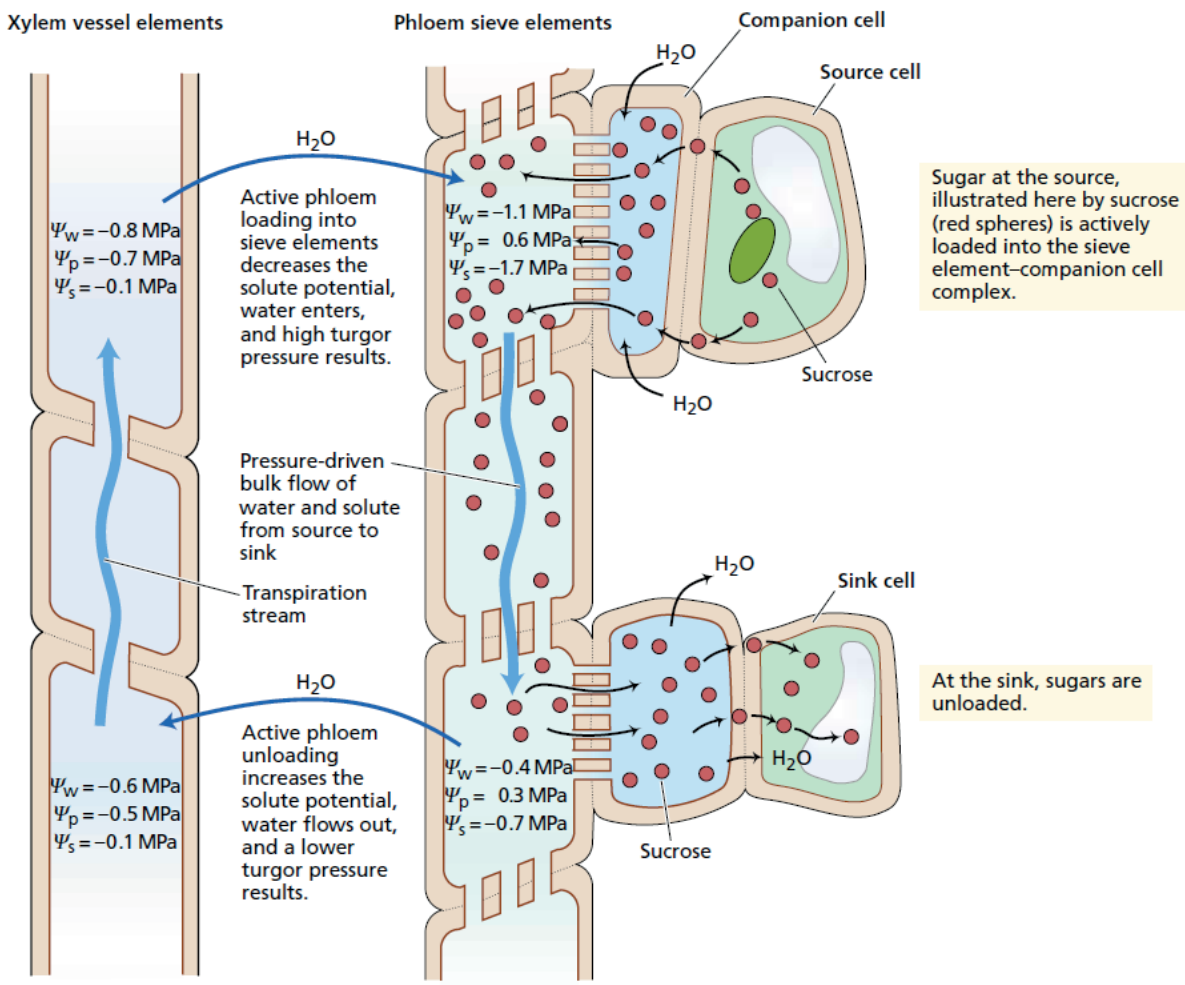

Figure 10. Pressure-flow model. The source cell actively (ATP-dependent) load sucrose into the phloem sieve element (top-right), the decreased solute potential (Ψs) in the sieve element attract water from the neighbors xylem vessels. The water entrance (top blue arrow) increase the turgor pressure (Ψp) in the phloem element, and the solutes can move to the sink cell, which actively unload sucrose and restore a higher solute water potential. From Taiz and Zeiger (2003).

The sucrose is the mobile C form; the plant uses sucrose to move C from C-source (especially leaves) to C-sink (fruits and perennial organs). In vascular plants, sucrose is transported through the phloem, the vascular tissue parallel to xylem. Following photosynthesis, glucose and fructose are combined together in sucrose molecules and loaded into the phloem tissue. The pressure-flow model theorizes how sugars can move from sources to sinks through the phloem tissue (Taiz and Zeiger, 2003, Fig. 10). It has been shown that phloem anatomy play an important role in sugar flow (Savage *et al*., 2017). Sieve elements can adapt their morphology in function of tree height, reducing sieve element hydraulic resistance when the distance represent a problem (Savage *et al*., 2017). Finally, starch is the reserve C form, it is found inside the vacuole and it is composed by long chain of glucose molecules. Consequently, quantifying glucose, fructose, sucrose, and starch, we can, with a good approximation, estimate the carbon cycles and balance inside the plants. Many authors used these analysis to explore the day/night cycles within organs (Dayer *et al*., 2016, Tixier *et al*., 2018, Gersony *et al*., 2020), or the C repartition among different organs (Tixier *et al*., 2018, 2020, Savi *et al*., 2019a), and theorized the response to multiple stresses (McDowell *et al*., 2008, Oliva *et al*., 2014).

5.3. Drought and its consequences on plant physiology

One of the best indicator to understand how plants perceive drought is the measure of the water potential (Ψ). Indeed, drought denote that less amount of water is available for the plant; the first direct implication is the increased difference in water potential between air and soil. Supposing that all vascular plants transport water mostly by the hydrostatic difference in water potential, give us the opportunity to compare different drought events at different intensities by one single measure: Ψ.

Ψ is not uniform at different height of the SPAC (or different height of the plant, Box 1), and the Ψ gradient changes in function of soil and air conditions (Fig. 11, 12). Among other studies, Knipfer *et al*. (2020) evidenced that the relationship between PreDawn water potential (Ψ_{PD}) and MidDay water potential (Ψ_{MD}) changed as drought increased (Fig. 11A). Ψ_{PD} corresponds to Ψ in the soil: it is measured in leaves at night when the stomata are closed and the Ψ gradient between soil and leaves is close to zero (Améglio *et al*., 1999). Ψ_{MD} corresponds to the lowest Ψ that leaves are experiencing during the day, when the transpiration is at its maximum. We observe that when the plant is at well-watered conditions (Ψ_{PD} > -0.5 MPa, *period I* in Fig. 11A) Ψ_{MD} is highly variable (from 0 down to -1.5 MPa), this variation is exclusively driven by the VPD of the air. As the VPD increase, the Ψ_{MD} decrease (the leaf is experiencing lower water potentials), and the transpiration (*E*) rate increase (as in Fig. 12 for well-watered grapevines). As drought continue, Ψ_{PD} become more negative, and we observe (*period II*, Fig. 11A) that Ψ_{MD} remains constant. This phenomenon is given by the stomatal closure that reduces the gas exchange and impede the water column to reach too negative values. Indeed, the authors observed that in *period II*, both stomatal conductance and CO_2 assimilation are strongly reduced

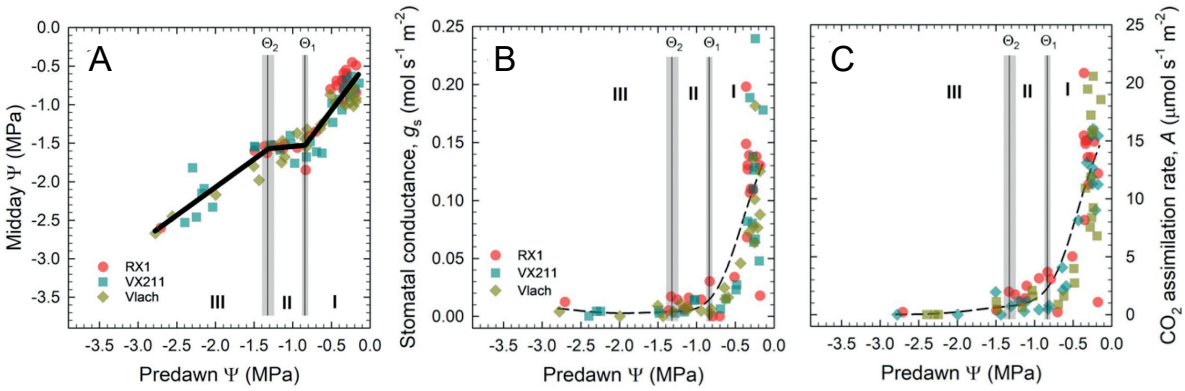

Figure 11. Water potential and gas exchange during a slow dry down experiment in *Juglans* spp. (**A**) Relationship between Predawn Ψ (Ψ_{PD}) and Midday Ψ (Ψ_{MD}) [MPa], the black thick line indicate a model describing the different phases of relationship, the vertical solid lines separate the three different phases. (**B**) Relationship between Ψ_{PD} and the stomatal conductance, *gs* [mol s^{-1} m^{-2}]. (**C**) Relationship between Ψ_{PD} and the CO_2 assimilation, *A* [µmol s^{-1} m^{-2}]. From Knipfer *et al*. (2020).

(Fig. 11B, C). The stomatal closure, chemically imposed by the phytohormone abscisic acid (ABA, Assmann, 2003), is concomitant with (or caused by?) an accentuate sensibility to VPD in leaves (Charrier *et al*., 2018, Dayer *et al*., 2020b) and a decrease in root-soil interface conductance (Carminati and Javaux, 2020). The slope in the regression curve between Ψ_{PD} and Ψ_{MD} can define the plant response to a moderate level of drought (Martínez-Vilalta *et al*., 2014). Authors have defined plants behavior as isohydric and anisohydric: an isohydric behavior will close the stomata as soon as drought starts (with a slope close to zero), an anisohydric behavior will let the transpiration continue even at low Ψ_{PD} (with a slope close to one, Martínez-Vilalta *et al*., 2014). Recent studies have now demonstrated that some species can adapt their behavior from anisohydric to isohydric in function of different drought level (Charrier *et al*., 2018, Knipfer *et al*., 2020). This is what characterize *period I* and *II* in Fig. 11A: a first anisohydric behavior (the plant continue to transpire as Ψ_{PD} decreases), then an isohydric behavior (the plant close its stomata). Consequently, it has been hypothesized that the observed differences in aniso- and iso-hydric behavior between different cultivars of the same species (as observed by Schultz, 2003 in grapevine), is given by a different shift between *period I* and *II*, not by a constant behavior over all drought intensities (Charrier *et al*., 2018).

As drought continues, Ψ_{PD} decreases and plants enter in *period III* (Fig. 11A), here Ψ_{PD} is perfectly correlated with Ψ_{MD} (i.e. the stomata are completely closed and the increase in xylem tension is driven by the decrease in soil water content). In this phase, the plant is in a critical state, at these tensions the water column inside the xylem vessels could broke (by a cavitation event) and irreparably decrease the xylem hydraulic conductivity (inducing xylem hydraulic failure, Delzon and Cochard, 2014). Once a xylem vessel embolize by the rupture of water column, the air can rapidly spread and desiccate the plant. If generalized, this phenomenon could lead to plant death by hydraulic failure (see paragraph 2.1). When the level of embolism in stems reach critical level, plants are not able to recover. This threshold has been evaluate to the

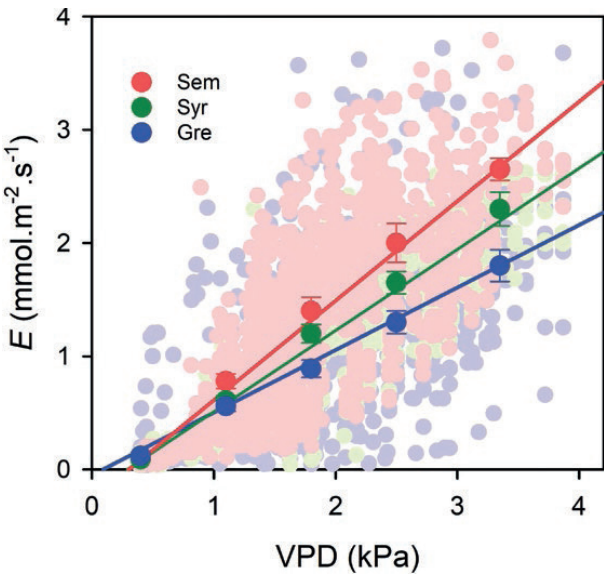

Figure 12. Daytime (08.00–20.00) whole-plant transpiration rates (E, mmol m^{-2} s^{-1}) depending on vapor pressure deficit (VPD, kPa) in three grapevine cultivars (Grenache, Semillon, and Syrah) under well-watered conditions (Ψ_{PD}>-0.5 MPa). Light colored dots are single values registered across 15 days and dark colored dots represent the mean of 0.5 kPa ranges of VPD ± SE. From Dayer *et al*., 2020b.

loss of 50% of stem hydraulic conductivity for conifers (P_{50}, Brodribb *et al*., 2010), and 88% of stem hydraulic conductivity for angiosperms (P_{88}, Urli *et al*., 2013).

Some plants have also another mechanism (other than pit size, see paragraph 2.4) to avoid the air spreading during intense drought: the hydraulic segmentation (Tyree and Ewers, 1991). In those plants, the annual organs (i.e. leaves) are more sensible than perennial organs (i.e. stems or roots) to xylem embolism, thus the leaves would shed protecting the perennial organs from air embolism (Hochberg *et al*., 2015, Charrier *et al*., 2016). However, the anatomical characteristics that could explain hydraulic segmentation are still unclear. Charrier *et al*. (2018) showed that grapevine stems in spring are more vulnerable to xylem embolism than stems in late summer, suggesting that the summer lignification could increase the embolism resistance. Interestingly, a seasonal change in embolism vulnerability exists also in grapevine leaves (Sorek *et al*., 2020). Sorek *et al*. (2020) demonstrated that "even mature xylem elements are 'only mostly dead'", and they can modify the thickness of pit membranes over the season, influencing their vulnerability to embolism. Finally, it is also known that embolism in stems begin in the middle of stems, and expand towards the bark (Brodersen *et al*., 2013), suggesting that primary xylem (i.e. the same found in petioles) is more sensible to embolism. Another indicator that is correlated with the leaf tolerance to drought is the turgor loss point (Ψ_{TLP}, Bartlett *et al*., 2016). Ψ_{TLP} correspond to the leaf Ψ at which the leaf wilt and it is reached when the Ψ_{leaf} is equal to $\Psi_{osmotic}$ inside the leaf cells (Brodribb and Holbrook, 2003). Before reaching Ψ_{TLP}, the outside-xylem hydraulic conductivity decrease (Scoffoni *et al*., 2017), and the stomata start to close (Brodribb and Holbrook, 2003). Ψ_{TLP} also indicate the starting point in leaf xylem hydraulic failure (Bartlett *et al*., 2016, Brodribb *et al*., 2016, Dayer *et al*., 2020b). Consequently, if plants are able to delay Ψ_{TLP}, they can also increase their sustainability. The only technique plants have to decrease Ψ_{TLP} is to decrease $\Psi_{osmotic}$ by accumulating small compounds (also called osmolytes) inside leaf cells (comprehending fructose, Rodrigues *et al*., 1993).

Other than hydraulic integrity, drought modifies the carbon balance in the plant. Indeed, when

stomata close the photosynthetic activity is reduced (CO_2 assimilation is reduced together with *gs*, Fig. 5C), and the carbon reserves are mobilized toward roots, mostly in order to explore other soil portions (Hagedorn *et al*., 2016). These observations were the starting point of the carbon starvation theory (described in the paragraph 2.1.of the *Research context*).

5.4. Vascular diseases and their consequences on plant physiology

Either fungi or bacteria can cause vascular diseases. The different vascular pathologies are often described together by two main aspects: all the pathogens live, spread, and develop (mostly) inside the xylem vasculature and the pathologies result in similar symptoms.

Fungal vascular diseases can be distinguished from other plant disorders by their particular visual symptoms. Leaves can present characteristic tiger-stripe symptoms (as for hop-*Verticillium* pathosystem, Fig. 13 0-5), where the main veins remains green and the interveinal space first become yellow and then scorched. Leaves can just yellow in part (Fig. 13A, B), uniformly (Fig. 13c), or present different deformations (Fig. 13C). Finally, leaves can also totally wilt, and the crown defoliate. Inside the stems, the xylem vasculature appears dark (Fig. 13D) or brown (Fig. 13a, b). In woody species, wood necrosis is easily recognizable (Fig. 14). Inside xylem vessel lumina, we found tyloses and gels (Fig. 15A, C). When the vessel is completely occluded, thick tyloses occupy the whole lumen (Fig. 15B).

The most popular fungal genera associated with vascular diseases are *Ceratocystis*, *Ophiostoma*, *Fusarium*, and *Verticillium* (Agrios 2004), and we can add two commonly encountered in grapevine: *Phaeomoniella* and *Phaeoacremonium*. These pathogens can overwinter in soils and in plant debris, frequently they enter into the host directly from the roots: this is the case for *Fusarium* (Di Pietro *et al*., 2003) and *Verticillium* (Klosterman *et al*., 2009) pathologies. Fungi can also infect the host by insect vectors: for example, *Coleoptera* beetles transport *Ophiostoma novo-ulmi* during Dutch elm disease (Webber, 2004), *Ceratocystis fagacearum* during oak wilt (Hayslett *et al*., 2008), *Ceratocystis fimbriata* during mango wilt (Souza *et al*., 2013). One study suggest the intervention of different arthropods in grapevine trunk diseases dispersal (Moyo *et al*., 2014). Otherwise, pathogens can directly colonize natural wounds in the aerial part of the plants: for example, *Phaeomoniella* and *Phaeoacremonium* in grapevine pruning wounds (Larignon and Gramaje, 2015). Once the host has been penetrated (by any mechanism), the fungi need to rapidly reach the xylem vessels, and successively develop. Vascular pathogens have a cohort of enzymes specialized in cell wall degradation (Van Alfen, 1989), in order to move radially until reaching the xylem vessels. However, vascular pathogens are not able to digest lignin and suberin, and one successful strategy from the host could be to “lignified” the cells surrounding the pathogens (Beckman and Roberts, 1995). It has been documented that the majority of *Verticillium* penetrations fail at this step in the root endodermis, which is rich in phenolic and anti-oxidant compounds (Beckman and Roberts, 1995). Consequently, it is broadly assumed that vascular pathogens prefer enter passively (by wounds

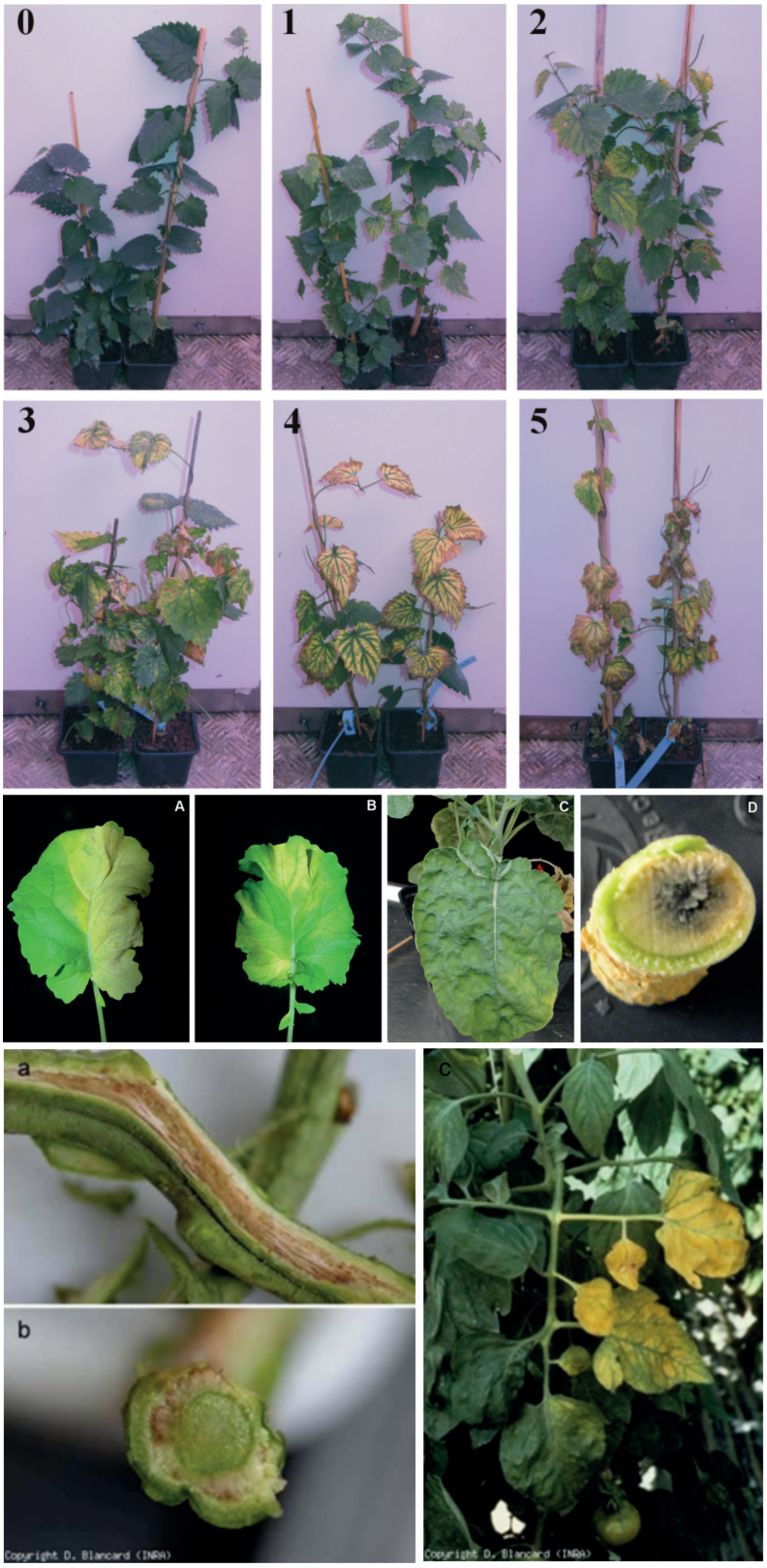

Figure 13. Examples of leaf symptoms during vascular pathogenesis. (**0**-**5**). *Verticillium* symptom evolution in *Humulus lupulus* (from Flajšman *et al*., 2017), from green (**0**) to almost complete defoliation (**5**). **0** corresponds to the inoculation day, and each picture was taken at a 7 days interval. (**A**-**D**) *Verticillium* symptoms in *Brassica napus* (from Lopisso *et al*., 2017). (**A**) One-sided leaf chlorosis at 28 days post-inoculation (DPI). (**B**) Interveinal chlorosis at 28 DPI. (**C**) Leaf deformation at 49 DPI. (**D**) Hypocotyl cross-section showing vascular discoloration at 49 DPI. (**a**-**c**) *Fusarium* symptoms in *Solanum lycopersicum* (from Ephytia, Blancard, INRAE) (**a**,**b**) Brown discoloration in xylem vasculature. (**c**) Leaf chlorosis.

Figure 14. Trunk discolorations caused by *Fusarium* with galleries from the fungi-associated beetles in (**A**) *Quercus agrifolia*. (**B**) *Persea Americana*. (**C**) *Quercus robur*. (**D**) *Ricinus communis*. From Eskalen *et al*. (2013).

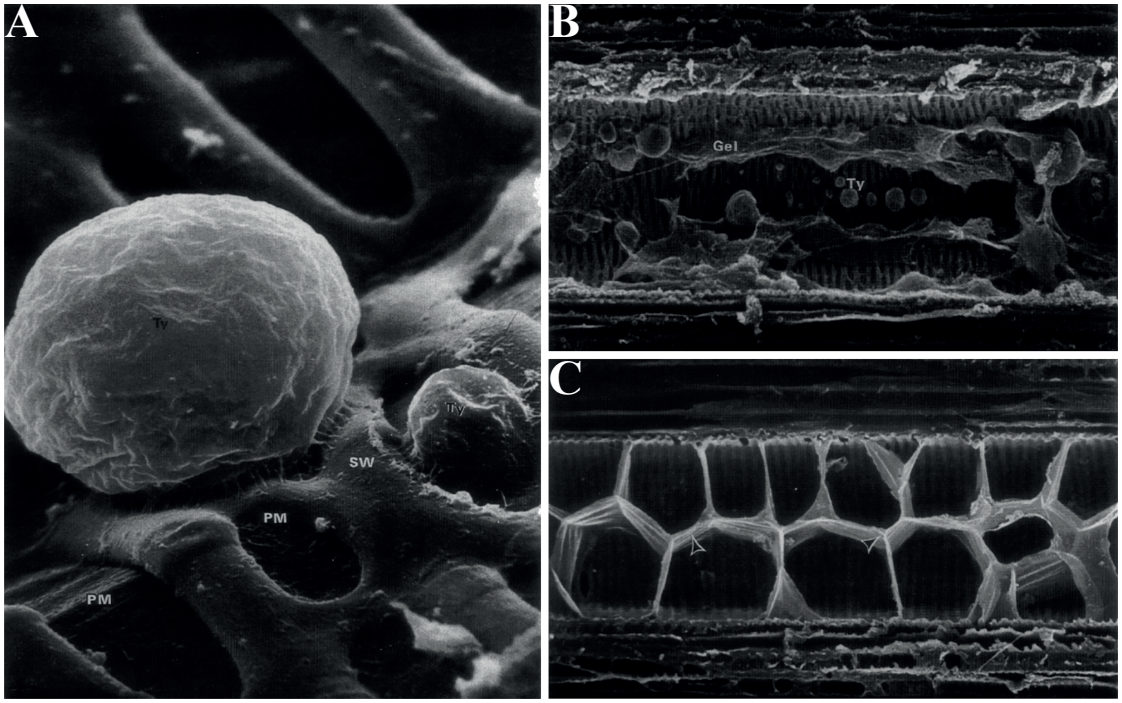

Figure 15. Plant-derived vascular occlusions at SEM microscopy following *Fusarium oxysporum* inoculation in banana. (**A**) Tyloses (Ty) expanding from pit membranes (PM); vessel secondary wall (SW) is indicated. (**B**) Complete occlusion of a vessel lumen by the adherence of adjacent tyloses walls (arrowheads) 8 days after inoculation. (**C**) Presence of small tyloses (Ty) and gels within a vessel lumen 4 days after inoculation. From VanderMolen *et al*., 1987).

in roots and stems or by insect-vector mediated transmission) inside the plants, in order to be in direct contact with the xylem.

Once inside the vessels, vascular fungi can move axially and colonize systemically the plant, in opposition, the plant try to slow and stop pathogen progression in the xylem (Fig. 16). Once the plant recognize a vascular pathogen inside the xylem vessel lumen, it might use different defense mechanisms (Fig. 16, left side). Around colonized parenchyma cells, a callose deposition can impede the pathogen to move into neighbor healthy cells; the secretion of antioxidant compounds (e.g. phenols) can help the destruction of pathogen mycelium. Finally, the strongest and microscopically visible response that is the production of tyloses (expansions of parenchyma cells) and gels inside the xylem vessel lumen that are produced in order to physically restrict pathogens in a certain area. If the defense mechanisms against pathogen fail (Fig. 16, right side), the pathogen will be able to colonize the successive vessel element and continue

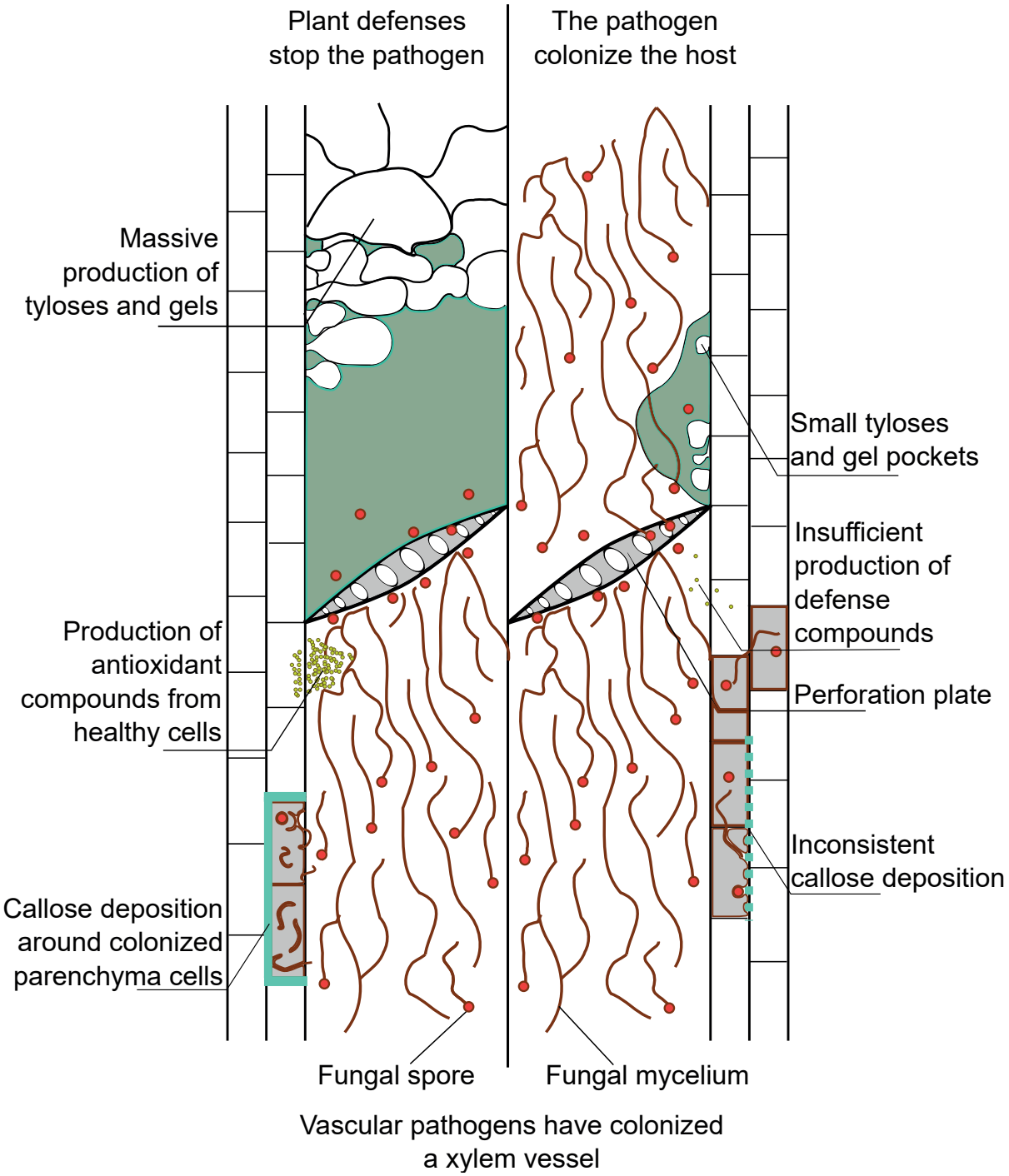

Figure 16. Theoretical model of vascular pathogen development. On the left side of the figure is schematized the different steps of plant-pathogen interaction when the plant efficiently stops the pathogen spread. On the right side of the figure is schematized the vessel colonization by vascular pathogens. Simplified from Beckmann and Roberts (1995), see text for details.

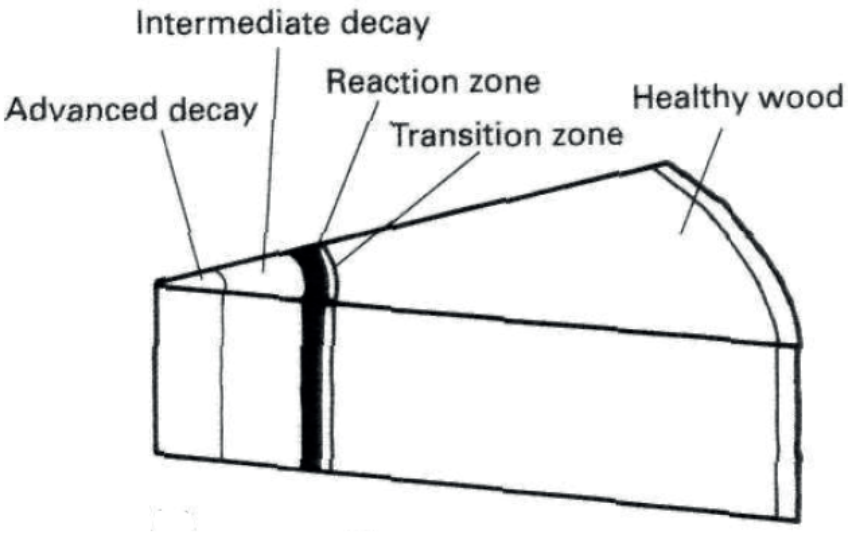

Figure 17. Conceptual model of "compartmentalization of decay in trees" (CODIT). Originally conceptualized by Shigo 1984. Wood decay pathogens have colonized the center of the trunk (i.e. in advanced and intermediate decay). The plant enhance its chemical and physical defenses in the reaction zone and in the transition zone in order to maintain the pathogens compartmentalized and physically distant from the healthy wood. From Pearce (1990).

its progression. Because the pathogens always move slower than the water flow (even in the most susceptible hosts), it has been hypothesized that fungi need to create spores and germinate every time they reach a perforation plate (Fig. 16, Beckman and Roberts, 1995), this could also explain the high resistance of conifers to vascular diseases (Van Alfen, 1989). Conifers present short tracheids, instead of long and large vessels (Fig. 8A), the high frequency of perforation plates should therefore reduce pathogen progression rate and help the plant to have an efficient response.

The hypothesis of the physical restriction (or compartmentalization) of vascular pathogens is reminiscent of plant resistance model for wood decay pathogens (Shigo, 1984, Pearce, 1996, Fig. 17). In the compartmentalization of decay in trees (CODIT) model, the wood decay fungi are physically separated from the healthy wood by different layers of response zones (Fig. 17). Similarly, tyloses and gels during vascular diseases would physically restrict pathogens in dead tissues. Consequently, the amount of xylem vessels filled with tyloses and gels is often correlated with the plant resistance to pathogen infections (Jacobi and MacDonald, 1980, Ouellette *et al*., 1999, Clérivet *et al.,* 2000, Et-Touil *et al*., 2005, Venturas *et al*., 2014, Park and Juzwik 2014, Rioux *et al*., 2018). However, other studies have theorized that an excessive amount of tyloses and gels inside the xylem vessels could interfere with the water movement and cause plant death by hydraulic failure (detailed in *Research context 2.2*).

5.5. X-ray microcomputed tomography, in *vivo* visualizations of hydraulic integrity

Since the first publication of the cohesion-tension theory (Dixon and Joly, 1894), many studies tried to discover how and at which moment cavitation events lead to irreversible loss of hydraulic conductivity. Nowadays, plant sensibility to hydraulic failure is mostly measured by the *Cavitron* technique (Cochard, 2002), or by k_s / k_{sMAX} comparisons (Sperry and Tyree, 1988). These techniques are prone to different artifacts; especially the open vessel artifacts, for which long vessel species such as grapevine are extremely sensible (Wheeler *et al*., 2013), and plant response to wound, as both methodologies require to cut the plant at certain moments. Three techniques are now able to visualize the embolism spreading *in vivo* (i.e. without cutting the plant and avoiding at maximum experimental artifacts): X-ray microtomography (X-ray microCT, Brodersen *et al*., 2013), magnetic resonance imaging (MRI, Holbrook *et al*., 2001), and optical vulnerability (OV, Brodribb *et al*., 2016). Among the three, X-ray microCT present the advantages to visualize woody organs and to quantify with high resolution and in 3D the functionality vessel-by-vessel (which is impossible by OV), and to distinguish between air and non-gaseous embolism (as MRI evidence the functional vessels only). However, in other context MRI and OV can offer different advantages compared to X-ray microCT. In this thesis, we mostly used X-ray microCT to explore the *in vivo* hydraulic integrity of grapevines during esca leaf symptom expression.

All measures were done at beamline PSICHE (King *et al*., 2016), at Synchrotron (cyclic particle accelerator) SOLEIL (Paris-Saclay). The goal of our experiments was to quantitatively differentiate functional vessels filled with water and non-functional vessels filled with gaseous or nongaseous embolism in different organs. Entire stems were cut under water and immersed in an iohexol solution. Iohexol appears bright when excited with X-ray; in the final 3D volumes, we were then able to distinguish functional, occluded and air-filled vessels (Fig. 19). As detailed in *Chapter 2* and *4*, we were able to quantify the loss of hydraulic conductivity given by native air embolism and by occlusion.

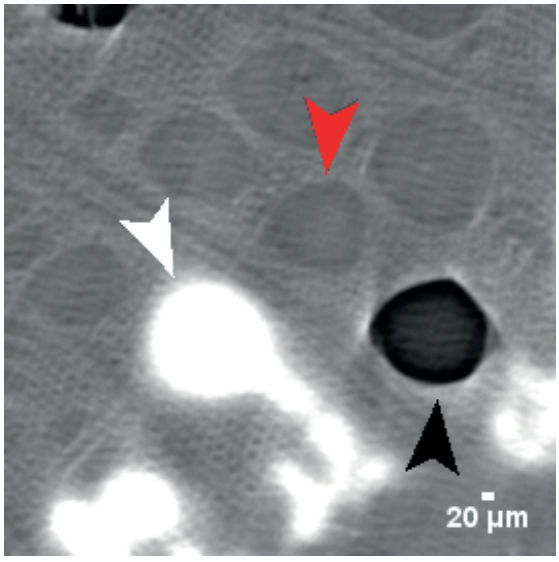

Figure 18. Detail from an X-ray microCT scan. The iohexol appear bright and the functional vessels are easily visible (white arrow). Air-filled vessels (black arrow) and occluded vessels (red arrow) are indicated. Personal production.

6. Experimental framework

6.1. Plant material: designing a new experimental setup to study esca

As presented in the introduction, esca leaf symptoms cannot be reproduced under controlled conditions. This technical impediment is one of the main lock restricting the researches on esca. In this thesis, we overcame to this technical problem by uprooting 30 years-old plants from a vineyard and transplanting them into pots. Thus, we were able to control the water regime of each single plant and transport symptomatic plants at pleasure. The protocol (detailed in *Chapter 2*) includes: plant excavation in late winter, a water immersion overnight of the root system, and one month resting on heating tables. Finally, plants were inserted in 20-L pots in fine clay medium. During the whole experiment (excepted for short periods with only water), plants were watered with nutritive solution (0.1 mM $NH_4H_2PO_4$, 0.187 mM NH_4NO_3, 0.255 mM KNO_3, 0.025 mM $MgSO_4$, 0.002 mM Fe, and oligo-elements [B, Zn, Mn, Cu, and Mo]). In the greenhouse, plants were exposed to natural light conditions. All the vines used in this experiment came from the same experimental plot ("la parcelle Météo"), located at INRAE Nouvelle Aquitaine (44°47'24.8"N, 0°34'35.1"W). *Vitis vinifera* cv Sauvignon blanc, grafted onto 101-14 MGt, were planted in 1992 in 8 rows of 42 plants each at a density of 0.57 plants

Table 2. Esca incidence on *V. vinifera* cv Sauvignon blanc plot before the experiment. The plants are subdivided in previously asymptomatic (pA, plants that have never express esca leaf symptoms before the considered year), previously symptomatic (pS, plants that have express esca leaf symptoms at least once before the considered year). In 2012 there is no subdivision in pA/pS because there were no informations on which plants have already express esca leaf symptoms

Year	Esca incidence (symptomatic plants/total plants)			Mortality (plants)*
	pA	pS	TOT	
2012	-	-	64.8 % (193/298)	38
2013	23.8 % (25/105)	79.2 % (137/173)	58.3 % (162/278)	20
2014	13.7 % (11/80)	72 % (108/150)	51.7 % (119/230)	48
2015	8.7 % (6/69)	28.1 % (34/121)	21.1 % (40/190)	40
2016	3.4 % (2/59)	38.5 % (47/122)	27.1 % (49/181)	9
2017	12.3 % (7/57)	53.2 % (58/109)	39.2 % (65/166)	15
Mean ± SE	12.4 ± 3.4 %	54.2 ± 9.7 %	43.7 ± 7.1 %	

*Comprehending non-sprouted plants, plant substitution, and plant sampling for other experiments

m^{-2} (3 m between rows, 1 m between plants in a row). This plot was surveyed each year since 2012 for esca leaf symptom development (following Lecomte *et al*., 2012 notation, Table 2). We were able, during the experiments, to divide plants by their disease historical record and evaluate the long-term impact of esca leaf symptoms on plant physiology. We separated pA plants (plants that never expressed leaf symptoms since 2012, previously asymptomatic) from pS plants (plants that expressed leaf symptoms at least once from 2012, previously symptomatic). Plants were uprooted in 2017 (n=4), 2018 (n=51) and 2019 (n=50).

6.2. Esca leaf symptom notation

The apparition and evolution of esca leaf symptoms was surveyed twice a week from June 2018 to October 2019 on every plant. Single leaves could be noted as asymptomatic (green and apparently healthy), pre-symptomatic (presenting yellowing or small yellow spots between the veins, as in Fig. 6A, B, C, F, G, H, K, L), tiger-stripe (with the main veins green and the interveinal space from yellow to scorch, as in Fig. 6 D, E, I, J, M), or apoplectic (wilted leaves). Entire plants were noted as pre-symptomatic, tiger-stripe symptomatic or apoplectic when at least 25% of the canopy were presenting these symptoms. For specific and accurate analysis (i.e. plants placed on scales for whole-plant transpiration estimates) a leaf-by-leaf count of symptoms were done every week in 2018 and every-other week in 2019. Some plants (n=5 in 2018 and n=16 in 2019) were presenting pre-symptomatic leaves at the end of the season (i.e. without a clear distinction between green and tiger-stripe). Samples from these plants (note that they were always on well-watered conditions) were removed from the analysis. However, we considered these plants as asymptomatic for the disease historical record (i.e. a pA plant presenting intermediate symptoms was still considered pA for the following season).

6.3. Experiment timetable

The different experiments took place from September 2017 (with a synchrotron SOLEIL campaign before the starting of the PhD thesis) to October 2019 as presented in Fig. 20. The experiments, detailed in each different chapter, comprehend:

- X-ray microCT: at synchrotron SOLEIL, beamline PSICHE. To quantify *in vivo* the loss of hydraulic conductivity in midribs and stems (*Chapters 2-4*).
- Uprooting and transplanting the plants: at UMR SAVE, INRAE. To obtain naturally infected plants under controlled conditions (*Chapters 2-5*).
- qPCR vascular pathogen detection: at UMR EGFV and SAVE, INRAE. Using primers set already developed. To detect and quantify *Pch* and *Pmin* in different grapevine tissues (*Chapters 2-5*).
- Symptom notation: at UMR SAVE, INRAE. Necessary to conduct study on esca. (*Chapters 2-5*).
- Water deficit maintenance: at UMR EGFV (platform Bord'ô) and SAVE, INRAE. Using pressure chambers, stem psychrometers and scales. To understand the interaction between

esca and drought (*Chapter 5*).

- Leaf anatomy sampling: at UMR SAVE, INRAE. Samples prepared at SAVE, cross-sections obtained using the Ultra-microtome Reichert Ultracut S at the Bordeaux Imaging Center (BIC "Imagerie végétale"). To understand the nature of hydraulic failure during esca, and compare it with other induced-senescing processes (*Chapter 2, 3*).
- Transpiration record: at UMR EGFV (platform Bord'ô) and SAVE, INRAE. At the whole-plant and continuously (platform Bord'ô) and leaf scale (using a TARGAS). (*Chapter 5*).
- Leaf and stem NSC sampling: sampled at UMR EGFV (platform Bord'ô) and SAVE, INRAE. Quantified at hit-me platform (UMR BFP, INRAE). To understand the carbon balance during stressing conditions (*Chapter 5*).
- Stem hydraulic conductivity measurements: at UMR SAVE, INRAE. Stem specific hydraulic conductivity (k_s) and theoretical specific hydraulic conductivity (k_{th}). To understand the effect of esca and drought on stem hydraulic integrity (*Chapter 4, 5*).
- Ethylene quantification essay: sampled at UMR EGFV (platform Bord'ô) and SAVE, INRAE. Quantified at ENSAT, Toulouse. To understand the role of ethylene during leaf symptom expression (Box 1 *Chapter 6, Discussion*).
- Optical vulnerability technique: stems sampled at UMR SAVE, INRAE. Leaves analyzed at UMR BIOGECO, INRAE. To quantify the functionality of esca symptomatic leaf lamina (*Chapter 3*).
- Sampling for Ascomycota metagenomics: DNA extracted and purified at UMR SAVE, INRAE. PCRs realized at SAVE. Sequenced at PGTB sequencing facility. To understand the changes in Ascomycota population in different organs in different stressing conditions (*Annex 1*).

My personal participation at each different measure is detailed in the corresponded chapter.

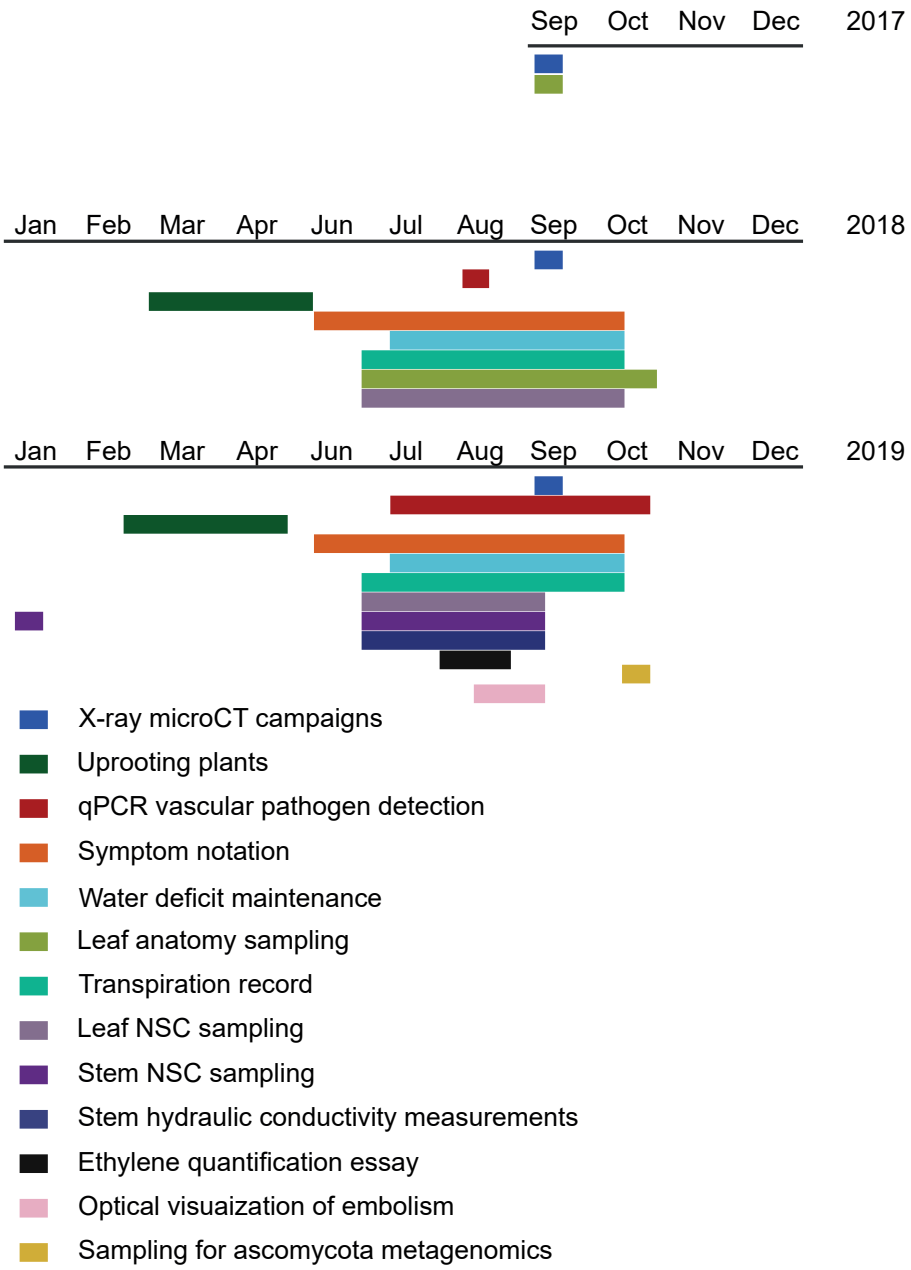

Figure 19. Experimental timetable of the thesis from 2017 to 2019.

CHAPTER 2

Exploring the Hydraulic failure hypothesis of Esca Leaf Symptom Formation

Published in: *Plant Physiology*, November 2019, Volume 181, pages 1163–1174.

Résumé : Les pathogènes vasculaires sont à l'origine de plusieurs maladies chez les plantes pérennes et c'est sur feuilles que nous retrouvons un des symptômes les plus remarquables. L'esca est une maladie vasculaire qui entraine des impacts fortement négatifs sur la production de raisin et l'industrie du vin. Même si les mécanismes sous-jacents à la formation des symptômes foliaires restent méconnus, deux hypothèses sont souvent citées par les scientifiques. La première hypothèse propose qu'une production des toxines par les pathogènes soit à l'origine de ces symptômes. La seconde propose que les symptômes soient dus à un dysfonctionnement hydraulique qui pourrait être causé par des embolies gazeuses, par la présence physique des pathogènes dans les vaisseaux de xylème, et/ou par la production par la plante de thylloses et de gels. Lors de cette étude, nous avons transplanté en pot des ceps de Sauvignon blanc âgés d'environ 30 ans, naturellement infectés par l'esca. Ce système nous a permis d'explorer l'intégrité hydraulique des feuilles (dans les nervures centrales et les pétioles) par microtomographie à rayon-X et par microscopie optique. Nos résultats ont montré que les feuilles symptomatiques n'étaient pas associées à la présence d'embolie gazeuse dans les vaisseaux. Cependant, les feuilles symptomatiques présentaient des niveaux significativement importants des vaisseaux non-fonctionnels, obstrués par des embolies non-gazeuses (i.e. thylloses et gels), entrainant une perte de conductivité hydraulique de 69% sur nervures centrales et 55% sur pétioles en moyenne. Présente en pourcentages variables, cette perte de conductivité hydraulique n'était pas corrélée à la sévérité de la maladie sur les feuilles. Grâce à la PCR quantitative, nous avons quantifié la présence des deux pathogènes vasculaires associés à l'esca, sans en trouver dans les feuilles. Dans l'ensemble, ces résultats démontrent que le développement des symptômes est associé à une forte perturbation de l'intégrité vasculaire, stimulée à distance par les pathogènes, qui prolifèrent dans le tronc. Cette recherche ouvre de nouvelles perspectives sur l'expression des symptômes d'esca où les hypothèses du dysfonctionnement hydraulique et des toxines ne sont pas nécessairement en opposition.

Check for updates

Exploring the Hydraulic Failure Hypothesis of Esca Leaf Symptom Formation[1[OPEN]]

Giovanni Bortolami,[a] Gregory A. Gambetta,[b] Sylvain Delzon,[c] Laurent J. Lamarque,[c] Jérôme Pouzoulet,[b] Eric Badel,[d] Régis Burlett,[c] Guillaume Charrier,[d] Hervé Cochard,[d] Silvina Dayer,[b] Steven Jansen,[e] Andrew King,[f] Pascal Lecomte,[a] Frederic Lens,[g] José M. Torres-Ruiz,[d] and Chloé E.L. Delmas[a,2,3]

[a]SAVE, INRA, BSA, ISVV, 33882 Villenave d'Ornon, France
[b]EGFV, Bordeaux-Sciences Agro, INRA, Université Bordeaux, ISVV, 33882 Villenave d'Ornon, France
[c]BIOGECO, INRA, Université Bordeaux, 33610 Cestas, France
[d]Université Clermont Auvergne, INRA, PIAF, F-63000 Clermont-Ferrand, France
[e]Institute of Systematic Botany and Ecology, Ulm University, D-89081 Ulm, Germany
[f]Synchrotron SOLEIL, L'Orme de Merisiers, Saint Aubin-BP48, 91192 Gif-sur-Yvette cedex, France
[g]Naturalis Biodiversity Center, Leiden University, 2300RA Leiden, The Netherlands

ORCID IDs: 0000-0001-7528-9644 (G.B.); 0000-0002-8838-5050 (G.A.G.); 0000-0003-3442-1711 (S.D.); 0000-0002-1430-5193 (L.J.L.); 0000-0001-8589-3474 (J.P.); 0000-0003-2282-7554 (E.B.); 0000-0001-8289-5757 (R.B.); 0000-0001-8722-8822 (G.C.); 0000-0002-2727-7072 (H.C.); 0000-0002-4476-5334 (S.J.); 0000-0002-0479-0295 (P.L.); 0000-0002-5001-0149 (F.L.); 0000-0003-1367-7056 (J.M.T.-R.); 0000-0003-3568-605X (C.E.L.D.).

Vascular pathogens cause disease in a large spectrum of perennial plants, with leaf scorch being one of the most conspicuous symptoms. Esca in grapevine (*Vitis vinifera*) is a vascular disease with huge negative effects on grape yield and the wine industry. One prominent hypothesis suggests that vascular disease leaf scorch is caused by fungal pathogen-derived elicitors and toxins. Another hypothesis suggests that leaf scorch is caused by hydraulic failure due to air embolism, the pathogen itself, and/or plant-derived tyloses and gels. In this study, we transplanted mature, naturally infected esca symptomatic vines from the field into pots, allowing us to explore xylem integrity in leaves (i.e. leaf midveins and petioles) using synchrotron-based in vivo x-ray microcomputed tomography and light microscopy. Our results demonstrated that symptomatic leaves are not associated with air embolism. In contrast, symptomatic leaves presented significantly more nonfunctional vessels resulting from the presence of nongaseous embolisms (i.e. tyloses and gels) than control leaves, but there was no significant correlation with disease severity. Using quantitative PCR, we determined that two vascular pathogen species associated with esca necrosis in the trunk were not found in leaves where occlusions were observed. Together, these results demonstrate that symptom development is associated with the disruption of vessel integrity and suggest that symptoms are elicited at a distance from the trunk where fungal infections occur. These findings open new perspectives on esca symptom expression where the hydraulic failure and elicitor/toxin hypotheses are not necessarily mutually exclusive.

Maintaining the integrity of the plant vascular system is crucial for plant health and productivity. Xylem tissue transports water and mineral nutrients and forms a complex reticulate network of many interconnected vessels (Zimmermann, 1983). This complex network of vessels hosts a large breadth of endophytic microorganisms, most of which live harmlessly within the plant (Fisher et al., 1993; Oses et al., 2008; Qi et al., 2012). However, some organisms in the vessel lumina can be (or become) pathogenic, and this class of pathogens is referred to as vascular pathogens (Pearce, 1996). Vascular pathogens are highly diverse, and their pathologies depend on the specific pathogen-host interaction. They cause diseases in a wide taxonomic range of plant species.

Plant vascular disorders are sometimes identified by conspicuous leaf scorch symptoms, which are strikingly similar and typically begin with necrosis at the leaf margin. The exact mechanisms driving these leaf symptoms remain largely unknown, and there are two long-standing and unresolved working hypotheses (Fradin and Thomma, 2006; Surico et al., 2006; McElrone et al., 2010; Sun et al., 2013; Yadeta and Thomma, 2013; Oliva et al., 2014; Pouzoulet et al., 2014). The first hypothesis proposes that symptoms result from the transport of pathogen-derived elicitors or toxins through the transpiration stream. The second proposes that symptoms result from hydraulic failure resulting from any combination of air embolism, occlusion of xylem vessels from the pathogen itself, and/or occlusion of xylem vessels by plant-derived tyloses and gels.

Esca disease in grapevine (*Vitis vinifera*) is one case where the conflict between these two hypotheses of leaf symptom formation remains unresolved (Surico et al., 2006; Pouzoulet et al., 2014). Esca is characterized by three main symptoms: leaf scorch, trunk necrosis, and a colored stripe along the vasculature (Lecomte et al., 2012). Esca belongs to a complex of diseases referred to as grapevine trunk diseases, which cause defoliation,

 © 2019 American Society of Plant Biologists. All Rights Reserved.

berry loss, and vine death (Bertsch et al., 2013; Mondello et al., 2018; Gramaje et al., 2018). This disease has been recognized for thousands of years and has been increasingly the focus of research over the past two decades, as it is believed to be one of the main causes of grape production decline, especially in Europe, the United States (California), and South Africa (Cloete et al., 2015; Guerin-Dubrana et al., 2019). The fungi most strongly associated with esca wood necrosis in the trunk have been identified (Larignon and Dubos, 1997; Mugnai et al., 1999; Fischer 2006; White et al., 2011; Bruez et al., 2014; Morales-Cruz et al., 2018). While the disease was formerly associated with the presence of soft rot (caused by basidiomycetes such as *Fomitiporia mediterranea*), studies have identified two vascular pathogens, *Phaeomoniella chlamydospora* and *Phaeoacremonium minimum*, which are detected in trunk necrotic tissues of esca symptomatic vines (Feliciano et al., 2004; Massonnet et al., 2018; Morales-Cruz et al., 2018). Esca leaf symptoms are only observed on mature vines (more than 7 years old) in the field (Mondello et al., 2018) and cannot be reliably reproduced by inoculating vines with the causal fungi (Surico et al., 2006; Bruno et al., 2007), despite testing various methodologies (Reis et al., 2019). This suggests that leaf scorch symptoms are the result of complex host-pathogen-environment interactions (Fischer and Peighami-Ashnaei, 2019). Neither the elicitor/toxin nor the hydraulic failure hypothesis of esca pathogenesis has been experimentally confirmed. It is generally accepted that the fungi responsible for esca wood necrosis are not present in leaves and that leaf symptoms are a consequence of fungal activities in the perennial organs (i.e. trunk). However, to our knowledge, leaves and current-year stems have never been investigated in detail to see if the key pathogens detected in necrotic regions of the perennial wood also occur in these organs.

In this study, we created an experimental system for the study of esca disease by transplanting mature, naturally infected esca symptomatic vines from the field into large pots. This allowed us to test the hydraulic failure hypothesis by exploring vessel integrity (presence of air embolism, occlusion, and the pathogens themselves) in leaves using noninvasive, in vivo imaging via x-ray microcomputed tomography (microCT), light microscopy, and quantitative PCR (qPCR). MicroCT avoids artifacts caused by traditional invasive techniques (Torres-Ruiz et al., 2015) and allows for the visualization of vessel content and functionality in esca symptomatic leaf petioles and midribs. We assessed the presence of two of the main pathogens associated with esca, *P. chlamydospora* and *P. minimum*, using qPCR in annual stems, leaves, and multiyear branches. These two species are tracheomycotic agents and could thus, in theory, disperse systemically via the sap flow from the trunk (Pouzoulet et al., 2014). This study provides new perspectives regarding the pathogenesis of esca leaf symptom formation.

RESULTS

Vessel Occlusion and the Percentage Loss of Conductivity in Symptomatic and Asymptomatic Leaves

Midrib and petiole vascular bundles of symptomatic and asymptomatic leaves were imaged in three dimensions using microCT (Fig. 1; Supplemental Figs. S1 and S2). These analyses allowed for the identification of embolized and occluded xylem vessels and the quantification of the percentage loss of theoretical hydraulic conductivity (PLC). The level of native air embolism was very low, ranging from 2.8% to 9.7%, for both asymptomatic and symptomatic midribs (Fig. 1, A and C) and petioles (Supplemental Fig. S1, A and D). There were no significant differences in the levels of native air embolism between symptomatic and asymptomatic leaves in petioles or midribs (Table 1; Fig. 2).

After exposing the xylem vessels to air by cutting the leaf or petiole just above (<2 mm) the scanned area, some proportion of vessels did not embolize immediately and apparently remained water filled (Fig. 1, B and D; Supplemental Figs. S1, B and E, red arrows, S2, C and D). These vessels were considered occluded. The average PLC in asymptomatic midribs due to occluded vessels was 12.4% ± 3.2%, while symptomatic midribs showed significantly higher values, 68.8% ± 6.4% (Table 1; Fig. 3). This is also the case for petioles, where asymptomatic leaves exhibited a PLC of only 1.9% ± 1.8%, while PLC in symptomatic leaves was 55.3% ± 9% (Table 1; Fig. 3). Detailed information on the contributions of different kinds of vessels to the theoretical hydraulic conductivity is presented in Supplemental Table S1.

[1]This work was supported by the French Ministry of Agriculture, Agrifood, and Forestry (FranceAgriMer and CNIV) within the PHYSIOPATH project (program Plan National Dépérissement du Vignoble, 22001150-1506), the Agence Nationale de la Recherche Cluster of Excellence COTE (ANR-10-LABX-45, within the VIVALDI and DEFI projects) and program Investments for the Future (ANR-10-EQPX-16, XYLOFOREST), and the AgreenSkills Fellowship program, which received funding from the European Union's Seventh Framework Program (FP7 26719-688 to G.C.).

[2]Author for contact: chloe.delmas@inra.fr.

[3]Senior author.

The author responsible for distribution of materials integral to the findings presented in this article in accordance with the policy described in the Instructions for Authors (www.plantphysiol.org) is: Chloé E.L. Delmas (chloe.delmas@inra.fr).

C.E.L.D., G.A.G., G.B., and S.De. designed experiments and analyzed the data; A.K., E.B., F.L., G.A.G., G.B., G.C., H.C., J.M.T.-R., L.J.L., R.B., S.Da., S.De., and S.J. participated in synchrotron campaigns; C.E.L.D. and G.B. conducted the histological observation; P.L. provided data on disease history of the plants used in this study; J.P. conducted the pathogen detection; G.B. analyzed the microCT images; C.E.L.D., G.A.G., and G.B. wrote the article; all authors edited and agreed on the last version of the article.

[OPEN]Articles can be viewed without a subscription.
www.plantphysiol.org/cgi/doi/10.1104/pp.19.00591

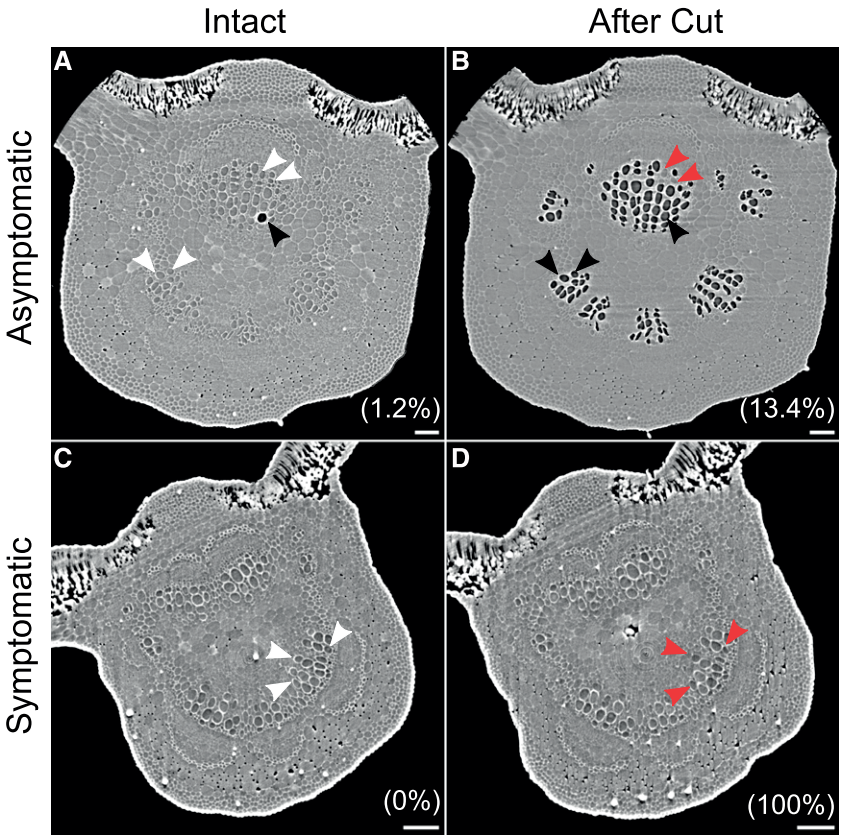

Figure 1. Two-dimensional reconstructions of cross sections from microCT volumes of grapevine leaves. Esca asymptomatic (A and B) and esca symptomatic (C and D) leaf midribs of grapevine plants are shown. After a first scan on intact leaves (A and C), the samples were cut (B and D) just above the scanned area to embolize the vessels and then scanned again. Air-filled (e.g. black arrowheads), water-filled (e.g. white arrowheads), and occluded (e.g. red arrowheads) vessels were counted and their cross-sectional diameters quantified to determine the PLC. The PLC represented by either native embolism (A and C) or occluded vessels (B and D) is given in parentheses. Bars = 100 μm.

The Nature of the Xylem Vessel Occlusions

We investigated the nature of the vessel occlusions causing the high percentage of nonfunctional vessels in esca symptomatic leaves using microCT and light microscopy. MicroCT was conducted both with and without the contrasting agent iohexol, which has been utilized previously to track the transpiration pathway and determine vessel functionality (as described by Pratt and Jacobsen [2018]). The subsequent robust (examining more than 200 cross sections per microCT volume) and detailed (examining both cross and longitudinal sections) examinations of the microCT volumes in symptomatic leaves revealed that the nature of the vessel occlusions is complex (Fig. 4). Occlusions can be larger, spanning the entire diameter of the vessel (Fig. 4A, red arrowheads), or smaller, occupying only a portion of the vessel (Fig. 4A, yellow arrowheads). Longitudinal sections of iohexol-fed symptomatic leaves revealed that the transpiration pathway can pass in between occlusions and through vessel connections (Fig. 4A, white arrowhead) but never diffuse in surrounding tissues. In asymptomatic samples fed with iohexol, occlusions expanding in iohexol-filled vessels were not observed (Supplemental Fig. S3). Some partially occluded vessels did not become air filled upon cutting (Fig. 4, B and C), and occlusions were also visible (although they were more obscure) in entirely occluded, nonfunctional vessels that did not fill with air after cutting (Fig. 4D, red arrowheads). When partially occluded vessels embolized after cutting, occlusions were easily visualized (Fig. 4E, red arrowheads). In these cases, the contact angle between these occlusions and the vessel wall was quantified and was always higher than 100°, with the highest frequency between 120° and 150° (Fig. 4F). Partially occluded vessels made up a small percentage of the total calculated PLC, representing 8.1% ± 3.7% for symptomatic midribs and 1.3% ± 0.6% for symptomatic petioles, while in asymptomatic leaves, partially occluded vessels were never observed (Supplemental Table S1). A negligible percentage of partially occluded vessels was observed within the native embolized vessels (i.e. air filled prior to cutting the samples), corresponding to 0.3% ± 0.2%

Table 1. *Effects of esca leaf symptom (asymptomatic or symptomatic), organ (midrib or petiole), and their interaction on the calculated PLC due to native embolism (Native PLC) and on the calculated PLC due to occlusions (Occlusion PLC)*

The plant was entered as a random effect in the models. Statistically significant results ($P < 0.05$) are shown in boldface. See the text for the model specificity for each trait.

Response Variable	Explanatory Variables	*F*	*P*
Native PLC (n = 35)	Leaf symptom	1.06	0.36
	Organ	0.37	0.61
	Interaction	2.53	0.25
Occlusion PLC (n = 35)	Leaf symptom	**14.32**	**0.02**
	Organ	1.99	0.29
	Interaction	0.61	0.52

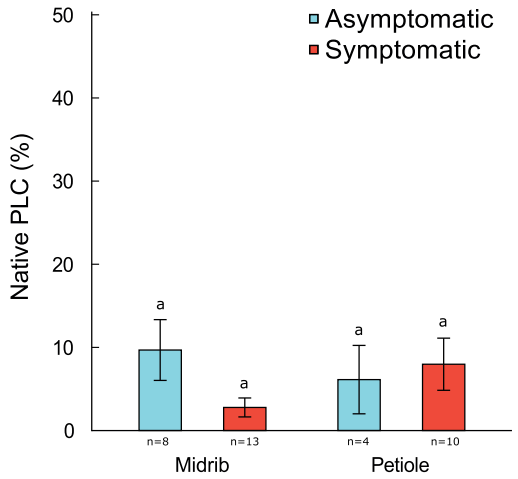

Figure 2. Mean native PLC in midribs and petioles of esca asymptomatic (blue) and esca symptomatic (red) leaves of grapevine plants using microCT imaging. PLC was calculated from the diameter of air-filled vessels in intact leaves, based on the total theoretical hydraulic conductivity of each sample. Error bars represent SE, and different letters represent statistically significant differences (least-squares mean differences of fixed effects, $P < 0.05$; n = sample size).

in symptomatic midribs and 0.4% ± 0.2% in symptomatic petioles (Supplemental Table S1).

The presence of these occlusions was likewise identified by light microscopy observations on symptomatic leaves (Fig. 5). To identify the chemical nature of the occlusions, cross sections were stained with four different dyes: Toluidine Blue O (Fig. 5A) in blue and periodic acid-Schiff reaction (Fig. 5B) in red indicate the presence of polysaccharides and polyphenols; Ruthenium Red (Fig. 5C) staining in pink for non-methyl-esterified pectins and Lacmoid Blue (Fig. 5D) showing the presence of callose in gray-pink shades. Quantifying the number of occluded vessels in histology cross sections of midribs, we found an average of 19.7% ± 11.6% of vessels with occlusions in symptomatic leaves, while just 0.4% ± 0.1% of vessels contained occlusions in asymptomatic leaves (Supplemental Table S2; Supplemental Fig. S4).

Relationship between Leaf Symptoms and Occlusion

Leaf symptom severity, quantified by the percentage of green tissue (in pixels) of each leaf, ranged from 6.1% to 93.9% for symptomatic leaves. In asymptomatic leaves, green tissue always accounted for 100%. We found no significant relationship between the percentage of green tissue (i.e. symptom severity) and PLC due to occluded vessels in symptomatic leaves ($F_{1,17}$ = 1.43, P = 0.25; Fig. 6). Additionally, there was no significant relationship between the percentage of green tissue and PLC when analyzed by plant or by organ ($F_{3,17}$ = 0.31, P = 0.81; $F_{1,17}$ = 0.80, P = 0.38, respectively).

Fungi Detection

The two vascular pathogens, *P. chlamydospora* and *P. minimum*, were not detected in leaves or lignified shoots. In 2-year-old cordons, their presence was detected in some samples but not others, regardless of whether the vines were symptomatic or asymptomatic (Table 2). However, *P. chlamydospora* and *P. minimum* DNA was detected in 100% of trunks (from 23 vines) sampled in the same field plot. The average quantity of *P. chlamydospora* and *P. minimum* DNA in the trunks was 3.6 ± 0.7 and 3.7 ± 0.9 log fg ng^{-1} dry tissue, respectively.

DISCUSSION

To date, no study has investigated leaf xylem water transport and vessel integrity during vascular pathogenesis using real-time, noninvasive visualizations. Transplanting esca symptomatic vines (identified from years of survey) from the field to pots allowed the transport of the plants, enabling the use of synchrotron-based microCT to explore the relationship between vessel integrity and esca leaf symptom formation in intact vines at high resolution and in three dimensions. We demonstrate that gaseous embolism was not associated with esca leaf symptoms. Instead, most of the vessels in symptomatic leaves contained nongaseous embolisms formed by gels and/or tyloses, hindering water transport and possibly leading to hydraulic failure. Nevertheless, there was no positive correlation between the severity of esca leaf symptoms and the loss of theoretical hydraulic conductivity resulting from these vascular occlusions. The two common vascular

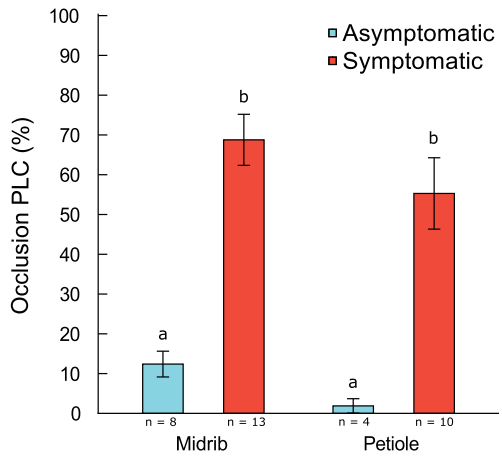

Figure 3. Mean occlusion PLC in midribs and petioles of esca asymptomatic (blue) and esca symptomatic (red) leaves of grapevine plants using microCT imaging. PLC was calculated from the diameter of occluded vessels, based on the total theoretical hydraulic conductivity of each sample. Error bars represent SE, and different letters represent statistically significant differences (least-squares mean differences of fixed effects, $P < 0.05$; n = sample size).

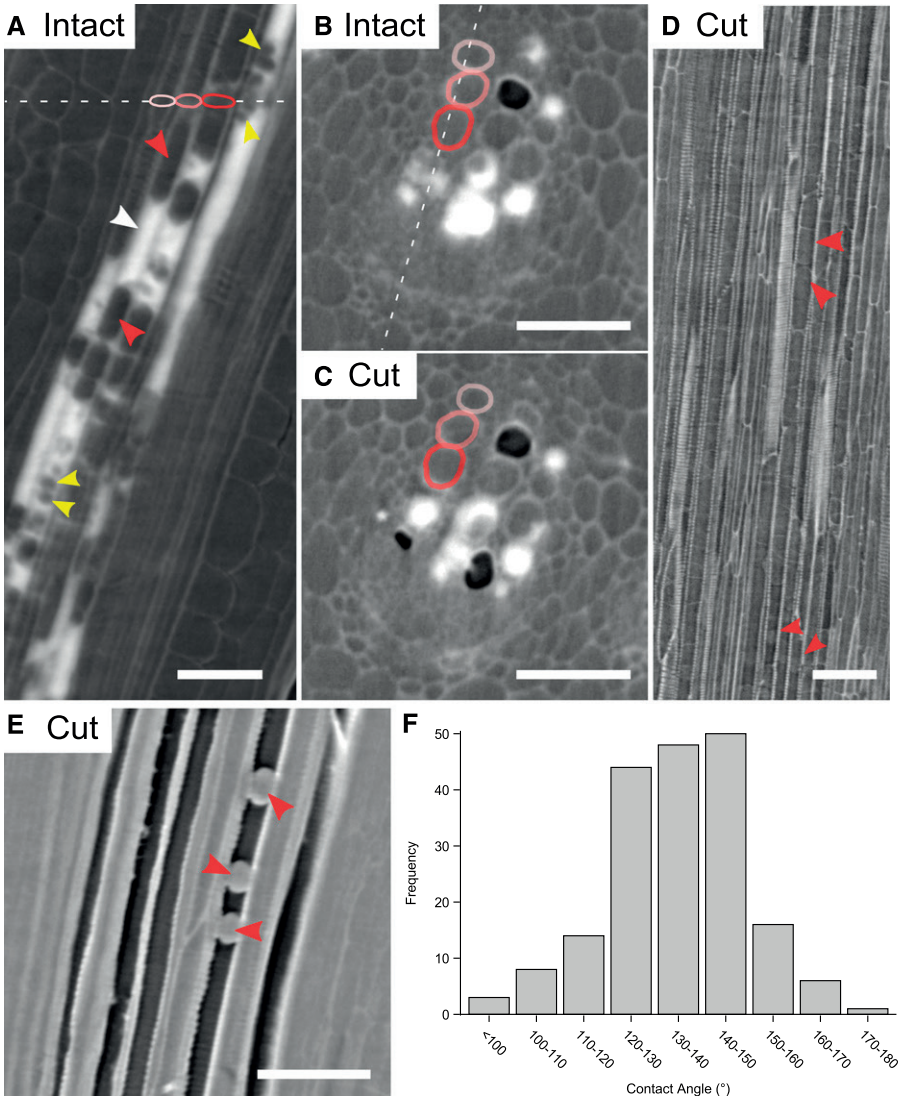

Figure 4. Two-dimensional reconstructions from microCT volumes of esca symptomatic leaves of grapevine. A to C, Iohexol-fed midrib viewed in a longitudinal section (A) and cross sections (B and C). For clarity and orientation, the same three vessels are color coded, and dotted lines represent the locations of the sections relative to each other. The contrasting agent iohexol appears bright white and allows for the identification of the water-transport pathway. The iohexol signal can even be seen in partially occluded vessels (e.g. white arrowhead). Occlusions (i.e. gels or tyloses) can span the entire diameter of the vessel (red arrowheads) or only a portion (yellow arrowheads). After a first scan on intact leaves (A and B), the sample was cut (C) just above the scanned area and scanned again. D, Longitudinal section of a midrib with completely occluded vessels. The presence of occlusions is visible (although obscure) inside the vessel lumen (red arrowheads). E, Longitudinal section of an air-filled midrib (after cutting) with clearly visible occlusions (red arrowheads). F, Frequency distribution of the contact angles between the occlusions and the vessel wall (sample size = 190). Bars = 100 μm.

pathogens related to esca were undetected in the vine's distal organs (i.e. annual stems and leaves), confirming that the symptoms and vascular occlusions occur at a distance from the pathogen niche localized in the trunk. Overall, these observations generate new perspectives regarding the nature and cause of esca leaf symptoms.

Native Embolism in Leaves

Vascular wilt diseases have been associated with significant levels of air embolism at the leaf level during oak (*Quercus* spp.) bacterial leaf scorch (McElrone et al., 2008) and at the stem level during pine (*Pinus* spp.) wilt and Pierce's disease (Umebayashi et al., 2011; Kuroda, 2012; Pérez-Donoso et al., 2016). In these cases, the formation of air embolism was speculated to result from the cell wall-degrading enzymatic activity of the pathogens (presumably to facilitate pathogen colonization through the vascular network). In our study, there were extremely low levels of native gaseous embolism in both esca symptomatic and asymptomatic leaves (petioles and midribs), demonstrating that symptom formation was not associated with the presence of air-filled vessels.

Leaf Xylem Occlusion: The Presence of Tyloses and Gels in Symptomatic Leaves

Under certain circumstances, xylem vessels can be occluded by tyloses (outgrowths from adjacent parenchyma cells through vessel pits; Zimmermann, 1979; De Micco et al., 2016) and/or gels (i.e. gums) composed of polysaccharides and pectins, which are secreted by parenchyma cells or directly by tyloses (Rioux et al., 1998). Tylose and/or gel formation is a general defense response of the plant against different biotic or abiotic stresses (Bonsen and Kučera, 1990; Beckman and Roberts, 1995; Sun et al., 2008). In this study, microCT imaging of leaf xylem vessels (both in petioles and midribs) revealed that all symptomatic leaves had

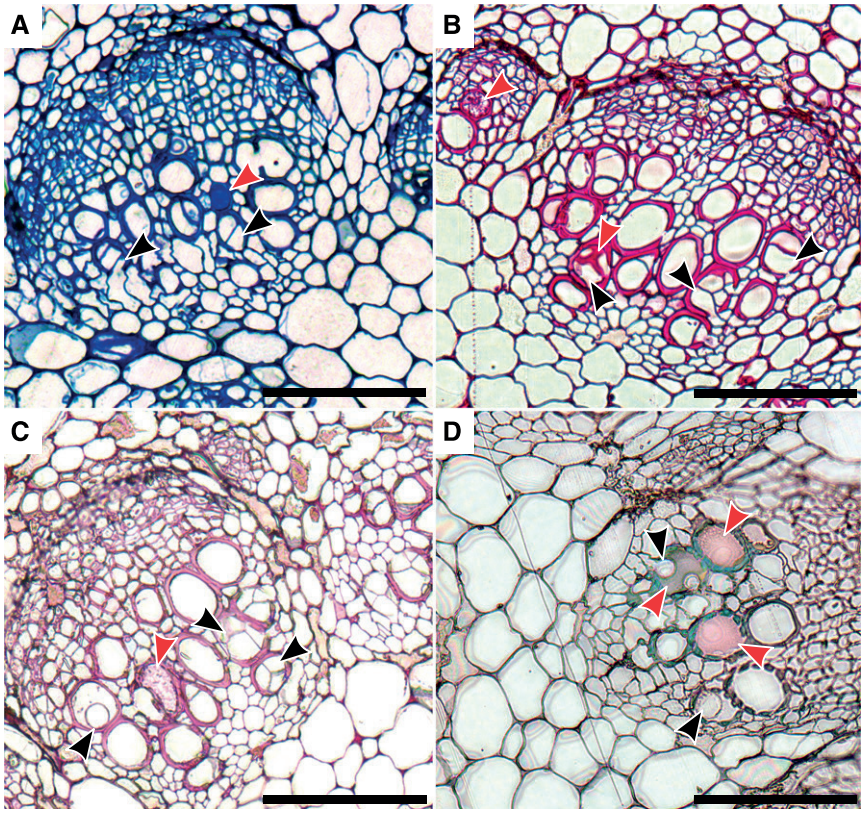

Figure 5. Light microscopy images of cross sections of esca symptomatic midribs of grapevine. Cross sections were stained with Toluidine Blue O (A), periodic acid-Schiff reaction (B), Ruthenium Red (C), and Lacmoid Blue (D). Red arrowheads indicate the presence of gels filling entirely the vessel lumen, while black arrowheads indicate the presence of tyloses in vessel lumina. Bars = 100 μm.

occluded vessels, although the loss of theoretical hydraulic conductance resulting from these occlusions was highly variable between leaves. Using reconstructions of 3D microCT volumes (Fig. 4) and light microscopy (Fig. 5), we determined that the occlusions in esca symptomatic leaves were due to both tyloses and gels. Numerous studies investigating vascular diseases have utilized artificial inoculation of the causal pathogen and observed the presence of vessel occlusions associated with decreases in hydraulic conductivity in either leaves or stems (Newbanks, 1983; Choat et al., 2009; Collins et al., 2009; Pouzoulet et al., 2017). The artificial inoculation in these studies resulted in high levels of the pathogen at the same location as the observed vascular occlusions. During esca pathogenesis in naturally infected vines, xylem occlusions were observed in 2-year-old symptomatic branches and in roots, and the pathogens were detected at the same locations (Gómez et al., 2016). In this study, the two vascular pathogen species associated with esca trunk necroses, *P. chlamydospora* and *P. minimum*, were not detected in current-year stems and leaves by a highly sensitive qPCR assay. This result was expected but had never been formally tested in the past according to the published literature. Thus, the vascular occlusions observed in leaves appeared to occur at some distance from the trunk, where the necroses are usually observed and both of the fungal species were detected (Bruez et al., 2014, 2016; Massonnet et al., 2018; Morales-Cruz et al., 2018), suggesting that vascular occlusions are caused by something other than the fungi themselves.

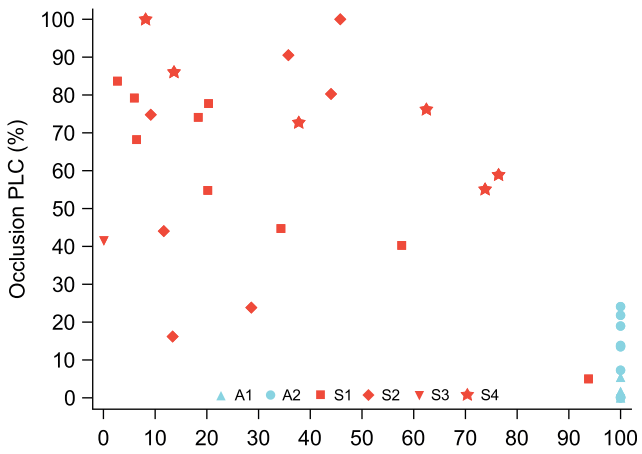

Figure 6. Relationship between the esca symptom severity (expressed as percentage of green tissue per leaf) and the theoretical loss of hydraulic conductivity due to occluded vessels (occlusion PLC) in midribs and petioles of grapevine. Points are grouped by plant: A1 and A2 (blue, asymptomatic) and S1 to S4 (red, symptomatic). The relationship between PLC and green tissue is not significant among symptomatic samples (red points, $P = 0.25$).

Light microscopy and histochemical analyses showed that occlusions are associated with the production of different compounds in symptomatic

Table 2. *Quantification by qPCR of* P. chlamydospora *and* P. minimum *(log fg ng^{-1} dry tissue)*

A high quantity of the DNA of the two pathogens was confirmed in 100% of the trunks of symptomatic plants sampled from the same vineyard (n = 23; see text for details). Values represent means ± SE in different organs; n = sample size. For esca leaf symptom, S = symptomatic and A = asymptomatic.

Pathogen	n	Esca	Petiole	First Internode	Fifth Internode	Multiyear Branches
P. chlamydospora	6	S	0	0	0	1.05 ± 0.58 (3/6)[a]
P. chlamydospora	6	A	0	0	0	1.13 ± 0.38 (4/6)[a]
P. minimum	6	S	0	0	0	1.48 ± 0.75 (3/6)[a]
P. minimum	6	A	0	0	0	0.59 ± 0.37 (2/6)[a]

[a]Number of samples positive for the pathogen.

leaves: polysaccharides, including pectins and callose. Grapevine is known to accumulate polyphenolic compounds during *P. chlamydospora* and *Phaeoacremonium* spp. infections (Del Rio et al., 2001; Martin et al., 2009) and in esca symptomatic leaves (Valtaud et al., 2009, 2011; Martín et al., 2019). Also, it is well documented that gels are composed of pectins (Rioux et al., 1998) and that parenchyma cells and tyloses accumulate pectin during vessel occlusion (Clérivet et al., 2000). In their review, Beckman and Roberts (1995) proposed a strong role of callose in tomato (*Solanum lycopersicum*) resistance to *Verticillium* spp., whereby callose xylem occlusions limit the spread of the pathogen. In this study, the presence of tyloses and gels (of any chemical nature) not colocalized with pathogens suggests that parenchyma cells play an important and active role during esca pathogenesis, expanding into the vessel lumen, secreting extracellular compounds, and eventually occluding the vessel.

Occlusions were clearly visible in partially occluded vessels that embolized after cutting, and the contact angle between the outside wall of occlusions and the inner vessel wall ranged mostly from 120° to 150° (Fig. 4, E and F). This result suggests that these occlusions are tyloses, as water droplets expanding into the vessels present lower contact angles (McCully et al., 2014).

Leaf Xylem Occlusion Occurs in Water-Filled Vessels

There are two main theories regarding the underlying mechanisms triggering vascular occlusion. Some studies have hypothesized the occlusions are always initiated by gaseous embolism and require the presence of air inside the vessel to stimulate the expansion of tyloses and/or the synthesis of gels (Zimmermann, 1978; Canny, 1997). Other studies suggest that gaseous embolism is not required and instead occlusion formation is stimulated by the plant hormone ethylene (Pérez-Donoso et al., 2007; Sun et al., 2007). Observations of samples fed with iohexol (Fig. 4A) demonstrated that occlusions were formed in water-filled vessels, suggesting that gaseous embolism is not necessary to induce occlusion formation in esca symptomatic leaves. In grapevine, similar occlusions in water-filled vessels were identified via microCT in grape berry pedicels associated with the onset of ripening (Knipfer et al., 2015).

The reconstruction of longitudinal sections of these vessels also demonstrated that the flow pathway can be extremely reticulate, moving between adjacent vessels and around occluded portions. Complex flow pathways such as these have been suggested previously by microCT-based flow modeling in grape (Lee et al., 2013), but this is the first direct empirical evidence supporting these models. In grape berry pedicels, partial occlusions are formed at the onset of ripening, yet despite a loss of conduit functionality, the pedicel hydraulic conductivity remained significantly high, suggesting a similar reticulate flow pathway in that context (Knipfer et al., 2015). The presence of partially occluded vessels that still conduct water around occluded portions confirms that occlusions were formed in functional water-filled vessels but creates difficulties with regard to interpreting images in cross section to determine vessel functionality. However, partially occluded vessels were found in very low percentage (1% in petioles and 8% in midribs; Supplemental Table S1), so they would not affect the loss of hydraulic conductivity estimated using microCT. In this study, we show examples of vessels that, when observed in a single cross section, appeared to be fully functional because of the clear iohexol signal (Fig. 4, B and C). However, when more comprehensive analyses of the volume are made (e.g. here with more than 200 cross sections per microCT volume), it became apparent that the iohexol signal was sometimes found in between occlusions (Fig. 4A). Therefore, quantifying occlusions from a limited number of cross sectional images could lead to an underestimation of the number of occluded vessels (Pérez-Donoso et al., 2016). This is well illustrated in our study, where the percentage of occluded vessels in midribs of symptomatic leaves was underestimated (only 19.7%) when examining a limited number of light microscopy images compared with microCT image analyses. Even more problematic for magnetic resonance imaging and microCT studies without the use of a mobile contrasting agent like iohexol, neither imaging technology appears capable of clearly distinguishing between functional, water-filled vessels and nonfunctional vessels filled by tyloses and/or gels. Only the use of robust volume analyses, in conjunction with contrasting agents, such as iohexol, can identify occlusions

in apparently water-filled vessels. The presence of visible occlusions after cutting the sample (Fig. 4E) complicates the interpretation regarding the effective functionality of the vessels. These partially occluded vessels represented only a maximum of 8% of the total conductivity (Supplemental Table S1) and should not significantly impact the overall PLC calculation. However, we can speculate that embolisms form even in these partially occluded vessels because (1) the vessel was still partially functional with space between the visible occlusion and the vessel wall (Fig. 4E) yet the resolution of the scan was not sufficient enough to visualize this space, (2) the water flow can avoid occlusions by passing through pits between vessels, or (3) grapevine leaves are able to secrete gels and tyloses in a very short period (i.e. during the few minutes between the cut and the end of the scan). Since we never observed occlusions remaining in air-filled vessels in asymptomatic samples, this third possibility also implies that symptomatic leaves are significantly more susceptible to occlusion than asymptomatic ones.

Leaf Symptoms, Occlusion, and Hypotheses on the Pathogenesis of Esca

Our results showed that there was no significant correlation between the level of leaf necrosis and the level of occluded vessels in symptomatic leaf midribs and petioles. Similarly, it has been shown that during Pierce's disease in grapevine, leaf symptoms are not correlated with the presence of the bacterial pathogen (Gambetta et al., 2007). Although many symptomatic leaves exhibited high levels of occlusion, many did not, and even leaves with high levels of scorched area can exhibit low levels of occlusion. The absence of any relationship between these variables could suggest that there is no causal relationship between xylem occlusions and esca leaf symptoms. However, it could have equally resulted because of the positions of our observations in relation to the way leaf necrosis proceeds. This study may have missed even more significant levels of vascular occlusion localized just at the front of the leaf necrosis (secondary order veins). In addition, we demonstrated that *P. chlamydospora* and *P. minimum* were not detected in the tissues of current-year petioles and stems but only in some of the 2-year-old branches sampled and always in the trunks of symptomatic plants. Altogether, these results demonstrate that symptom development was associated with vascular occlusions that are likely elicited at a distance from the pathogen niche localized in the trunk.

Hypotheses on the pathogenesis of esca largely fall into two broad categories: (1) the hydraulic failure hypothesis, where air embolism or vessel occlusion would disrupt the flow of sap in the xylem and lead to leaf desiccation; and (2) the elicitor-toxin hypothesis, where elicitors/toxins produced by the pathogenic fungi or plant-derived signals move into the vine's transpiration stream, inducing symptoms at a distance. The hydraulic failure hypothesis has never been properly tested, but observed decreases in stomatal conductance and photosynthesis in esca symptomatic leaves have been interpreted as supporting this hypothesis (Petit et al., 2006; Andreini et al., 2009; Magnin-Robert et al., 2011). Some studies call this into question because water stress-related genes are not overexpressed during esca symptom formation (Letousey et al., 2010; Fontaine et al., 2016). The elicitor/toxin hypothesis is supported by numerous works that aimed to identify phytotoxins and effectors secreted by fungal pathogens associated with esca and their potential contributions in disease etiology (Abou-Mansour et al., 2004; Bruno and Sparapano, 2006; Bruno et al., 2007; Luini et al., 2010; Masi et al., 2018). Other evidence is provided by the accumulation of antioxidant compounds prior to symptom expression in leaves (Valtaud et al., 2009; Magnin-Robert et al., 2011, 2016). Esca pathogenesis could also involve plant-derived signals (e.g. hormones, defense molecules, etc.) triggering and/or accelerating leaf senescence (Häffner et al., 2015). Although esca leaf symptoms often take a form that differs from natural senescence, the role of the senescence program in esca pathogenesis should be more thoroughly studied in the future. Natural leaf senescence includes many of the same changes (Salleo et al., 2002; Brodribb and Holbrook, 2003) that occur in esca symptomatic leaves: xylem vessel occlusion, decreases in stomatal conductance and photosynthesis, chlorosis, and eventually shedding. Some authors have also suggested a role for the senescence program in Pierce's disease pathogenesis (Choat et al., 2009).

The results presented here are consistent with the hypothesis that esca pathogens are restricted to the

Table 3. *Disease history of the grapevine 'Sauvignon blanc' plants used in this study*

Symptom frequency over time indicates the number of years with symptoms over the 6 or 5 years before transplantation.

Plant	Year of Transplantation	Symptom Frequency over Time (No. of Years)	Duration of Leaf Symptoms (Weeks) prior to the Moment of the Experiment
A1	2018	0/6	0
A2	2018	0/6	0
S1	2018	4/6	2
S2	2018	6/6	4
S3	2018	5/6	6
S4	2017	5/5	5

trunk and/or multiyear branches and that elicitors and/or toxins (for review, see Andolfi et al., 2011) become systematic in the plant via the transpiration stream, accumulate in the canopy, and trigger a cascade of events that lead to visual symptoms. These events include the production of tyloses and gels by the plant that occlude vessels, suggesting that the elicitor/toxin and hydraulic failure hypotheses are not necessarily mutually exclusive. This is also congruent with the observation of necrosis/oxidation along the vasculature that is spatially associated with leaf symptoms (Lecomte et al., 2012). The precise timing and direct impact of vessel occlusion relative to symptom formation remains unclear, so this study cannot determine whether occlusions lead to hydraulic failure and symptom formation or whether the observed vessel occlusion is simply a result of an early induced senescence process. Future research should be aimed at exploring this sequence of events leading to leaf scorch symptoms in naturally infected esca symptomatic vines in the field.

MATERIALS AND METHODS

Plant Material

Grapevine (*Vitis vinifera* 'Sauvignon blanc') plants aged 27 years old were transplanted from the field into pots from a vineyard at Institut National de la Recherche Agronomique (INRA) Aquitaine (44°47′24.8′′N, 0°34′35.1′′W). The transplantation was the only method allowing the study of natural esca symptom development on mature plants outside the field (greenhouse and synchrotron) and to bring the plants from Bordeaux (INRA) to Paris (synchrotron SOLEIL). The experimental plot included 343 plants organized in eight rows surveyed each season before transplantation for esca leaf symptom expression during the previous 5 to 6 years following Lecomte et al. (2012) leaf scorch symptom description. Esca incidence in this vineyard was very high, as 77% of the plants (n = 343 plants) presented trunk and/or leaf symptoms the summer before the plants were uprooted. The presence of two vascular fungi associated with esca (*Phaeomoniella chlamydospora* and *Phaeoacremonium minimum*) in this plot was confirmed by using qPCR on the trunk of 23 symptomatic vines randomly sampled (methodology described below). To reduce stressful events, the plants were excavated during dormancy before bud burst in late winter from the field by digging around the woody root system and attempting to preserve as many of the large woody roots as possible. Following excavation, the root system was immersed under water overnight, and then powdered with indole-3-butyric acid to promote rooting. To equilibrate the vigor of the plants and their leaf-root ratio, three to five buds per arm (one per side) were left. The plants were potted in 20-L pots in fine clay medium (Klasmann Deilmann substrate 4:264) and placed indoors for 2 months on heating plates (30°C) to encourage root development before they were transferred to a greenhouse and irrigated to capacity every other day under natural light. Plants were irrigated with nutritive solution (0.1 mM $NH_4H_2PO_4$, 0.187 mM NH_4NO_3, 0.255 mM KNO_3, 0.025 mM $MgSO_4$, 0.002 mM Fe, and oligo-elements [B, Zn, Mn, Cu, and Mo]) to prevent mineral deficiencies.

Plants were grown in a greenhouse and exposed to natural light. Temperature and air relative humidity were monitored every 30 min: average daily values corresponded to 26°C ± 4°C (SE) and 64% ± 13% (SE), respectively. Leaf predawn water potential was monitored regularly to ensure that the plants were never water stressed (leaf predawn water potential close to 0 MPa). The plants were surveyed weekly for esca leaf symptom development from May to September. The plants were noted as symptomatic when at least 50% of the canopy was presenting the tiger-stripe leaf symptom, characteristic for esca (see examples of leaf symptoms in Supplemental Fig. S5A and entire plants in Supplemental Fig. S5B). Six plants were selected (Table 3) and transferred to the microCT PSICHE (Pressure Structure Imaging by Contrast at High Energy) beamline (SOLEIL synchrotron facility, Saclay, France): two control asymptomatic plants that had never expressed symptoms either during the year of the experiment or the past 5 years, and four symptomatic plants with differences in the timing of the first leaf symptom expression (6, 5, 4, and 2 weeks before the experiment). Leaf symptoms (Supplemental Fig. S5) were typical esca leaf symptoms for cv Sauvignon blanc and were similar to the symptoms we observed in the experimental vineyard from which the plants came. All symptomatic plants had expressed esca symptoms for at least three different seasons in the past (Table 3). Asymptomatic leaves were always sampled only from the control plants A1 and A2.

MicroCT

Synchrotron-based microCT was used to visualize the contents of vessels in the esca symptomatic and asymptomatic leaf midribs and petioles. The PSICHE beamline at the SOLEIL synchrotron facility that is dedicated to x-ray diffraction under extreme conditions (pressure-temperature) and to high energy absorption contrast tomography (20–50 keV) was used (King et al., 2016). During the first campaign, in September 2017, one 26-year-old plant presenting characteristic tiger-stripe leaf symptoms was scanned with the microCT PSICHE beamline (King et al., 2016). In the second campaign, in September 2018, five different plants of the same age (two asymptomatic and three symptomatic) were brought to the same facility. Intact shoots (>1.5 m in length) were cut at the base under water at least 1 m away from the scanned leaves. Leaves were scanned using a high-flux (3×10^{11} photons mm^{-2}) 25-keV monochromatic x-ray beam. Midribs (n = 21) and petioles (n = 15) were scanned in symptomatic and asymptomatic leaves (from one to five leaves per plant), then cut just above the scanned area and scanned again. The projections were recorded with a Hamamatsu Orca Flash sCMOS camera equipped with a 250-μm-thick LuAG scintillator for petioles and with a 90-μm-thick LuAG scintillator for midribs. The complete tomographic scan included 1500 projections, and each projection lasted 50 ms for petioles and 200 ms for midribs. Thus, the total exposure time was 75 s for petioles and 300 s for midribs. Tomographic reconstructions were performed using PyHST2 software (Mirone et al., 2014) using the Paganin method (Paganin et al., 2002), resulting in 32-bit volume reconstructions of 2,048 × 2,048 × 1,024 voxels for petioles and 2,048 × 2,048 × 2,048 voxels for midribs. The final spatial resolution was 2.8769^3 μm^3 per voxel for petioles and 0.8601^3 μm^3 for midribs.

Iohexol Contrasting Agent

A subset of 10 shoots were fed with the contrasting agent iohexol. Five symptomatic shoots (from two plants: S1 and S2 described in Table 3) and five asymptomatic shoots (from two plants: A1 and A2 described in Table 3) were cut at the base under water and immediately transferred to a solution containing the contrasting agent iohexol (150 mM) to visualize functionality (i.e. vessels that were effectively transporting sap; Pratt and Jacobsen, 2018). In asymptomatic plants, five midribs (from three different shoots) and three petioles (from two different shoots), and in symptomatic plants, five midribs (from three different shoots) and four petioles (from three different shoots), were scanned. These shoots were exposed to sunlight outdoors for at least half a day to permit the contrasting agent to reach the leaves through transpiration. The capacity and rapidity of iohexol to move was first checked by cutting leaves under water, submerging them directly in iohexol solution, and scanning several times each 10 min. Its capacity to move up to the shoots was then checked by scanning leaves at the top. These results were not coupled with the ones from intact leaf scans. In this case, scans were performed at two different energies, just below and just above the iodine K-edge of 33.2 keV. At 33.1 keV, the contrasting agent presents little contrast, while it presents strong contrast at 33.3 keV. The leaves (17 of 35 total samples) were then analyzed in the beamline as described for the other samples above.

Image Analysis

Leaf Symptoms

Scanned leaves were photographed, and the green area was calculated using the G. Landini plug-in threshold_color v1.15 (http://www.mecourse.com/landinig/software/software.html) in ImageJ software (http://rsb.info.nih.gov/ij), differentiating four color regions: red, yellow, pale green, and green. The number of pixels for each region was summed to determine the leaf area corresponding to each color region. To obtain a scale of symptom severity, the percentage of green leaf area (relative to total leaf area) was calculated for each leaf.

Analysis of MicroCT Images

All samples (including those stained with iohexol) were analyzed in the following manner. The geometrical diameter of air-filled and non-air-filled vessels was measured on cross sections taken from the central slice of the microCT scanned volume using ImageJ software. For iohexol-fed samples, an example of vessel identification is included in Supplemental Figure S6. The theoretical hydraulic conductivity of each vessel was calculated using the Hagen-Poiseuille equation:

$$\mathrm{Kh} = \frac{(\pi \times \varnothing^4 \times \rho)}{(128 \times \eta)} \quad (1)$$

where *Kh* is the theoretical hydraulic conductivity ($m^4\ MPa^{-1}\ s^{-1}$), ø is the geometrical diameter of the vessel (m), ρ is the density of water ($kg\ m^{-3}$), and η the viscosity of water (1.002 mPa s^{-1} at 20°C). The percentage of native embolism was calculated in the first scan, before cutting the leaf, using the following equation:

$$\text{Native PLC } (\%) = 100 \times \frac{(\Sigma\ \mathrm{Kh}_{\text{air filled vessels}})}{(\Sigma\ \mathrm{Kh}_{\text{all vessels}})} \quad (2)$$

After a first scan, the samples were cut with a clean razor blade just above the scanned area and scanned again. Cut open vessels will embolize because the xylem sap is under negative pressure. Leaf water potential (Ψ_L) measured on an adjacent leaf just after the scan indicated sufficient tension in the xylem sap to embolize in all leaves measured (n = 17 leaves, $\Psi_L = -0.46$ MPa on average). Under control conditions, nearly all the xylem vessels became air filled upon cutting (e.g. black vessels in Fig. 1B; Supplemental Fig. S1B). To estimate the loss of conductivity caused by occluded vessels (Eq. 3 below), the *Kh* of apparent water-filled vessels was calculated in the central cross section of the entire microCT volume after cutting. Vessels that did not become completely air filled after cutting were considered occluded (i.e. having the same gray level after cutting as water-filled conduits before cutting). To adjust PLC (Eq. 3 presented below) by those vessels that appeared water filled or air filled only at specific points along the length of the vessel, the presence of apparent water-filled vessels and droplets was checked in at least 200 cross sectional slices in each volume, corresponding to 160 μm for midribs and 570 μm for petioles. If a particular vessel appeared water filled in any of the 200 slices examined, this vessel was classified as partially occluded and added to the PLC given by occlusions:

$$\text{Occlusion PLC } (\%) = 100 \times \frac{(\Sigma\ \mathrm{Kh}_{\text{occluded vessels}} + \Sigma\ \mathrm{Kh}_{\text{partially occluded vessels}})}{(\Sigma\ \mathrm{Kh}_{\text{all vessels}})} \quad (3)$$

Contact Angles

To gain insight into the nature of occlusion, the contact angle between each droplet and the inner vessel wall was measured using ImageJ following McCully et al. (2014). First longitudinal slices were reconstructed from each microCT volume. Then the contact angles between each observed droplet and the vessel wall were measured in partially occluded, air-filled vessels (n = 190 droplets from 65 partially occluded vessels in two different samples).

Light Microscopy

Ten-millimeter sections from midribs and petioles of three esca symptomatic and three asymptomatic leaves were cut and fixed in a solution containing 0.64% (v/v) paraformaldehyde, 50% (v/v) ethanol, 5% (v/v) acetic acid, and 44.36% (v/v) water. Samples were then dehydrated using a graded series of ethanol (50%, 70%, 85%, 95%, 100%, 100%, and 100% [v/v] for 30 min each) and embedded using a graded series of LR White resin (Agar Scientific; 33%, 50%, and 66% [v/v] LR White in ethanol solutions for 120 min each and 100% [v/v] LR White three times overnight). Two- to 2.5-μm-thick transverse sections were cut using an Ultracut S microtome (Reichert) equipped with a glass knife. As described by Neghliz et al. (2016), the cross section was stained with different dyes. To investigate anatomical features, lignin, phenolic compound, and polysaccharide cross sections were stained with 0.05% (w/v) Toluidine Blue O. Sections to be examined for polysaccharides were stained with periodic acid-Schiff reagent. Pectins were detected by staining sections overnight with 1% (w/v) Ruthenium Red. Callose was revealed by staining sections overnight with 1% (w/v) Lacmoid Blue in 3% (v/v) acetic acid. Stained sections were dried and photographed with a RTKE camera (Spot) mounted on an Axiophot microscope (Zeiss) at the Bordeaux Imaging Center, a member of the France Bio Imaging national infrastructure (ANR-10-INBS-04). In midribs, the image of the entire cross section was analyzed to quantify the percentage of occluded vessels (by tyloses, gels, or both) in 55 sections for symptomatic and 56 sections for asymptomatic midribs obtained from six different leaves (three symptomatic and three asymptomatic). Occlusions were classified as tyloses if tylose cell walls (formed during tylosis development) were visualized within the vessel lumen (Fig. 5B) or as gels if cell walls were not visualized and the vessel lumen appeared totally filled (Fig. 5A, red arrowheads). Tyloses and gels can also be observed within the same vessel (Fig. 5D). In some cases, tyloses and gels can be difficult to distinguish if tyloses filled the entire vessel lumen with a wall closely attached to the inner vessel wall, or if the tylose wall was lignified. However, this uncertainty would not change the total number of occluded vessels observed in this study.

Fungal Detection

The presence of *P. chlamydospora* and *P. minimum* was assessed in different parts of asymptomatic and symptomatic plants. Plants were sampled directly from the same field plot as described above. In mid-August 2018, a survey of leaf esca symptoms was conducted, and six asymptomatic and six symptomatic vines were selected at random. Four different samples were collected for each plant: (1) petioles of three leaves located in the first 50 cm of the shoot; sections of the (2) first and (3) fifth internodes of the third shoot on the 2-year-old cane; and (4) a section of the 2-year-old branch just basal to the third shoot (i.e. canes trained across in the Guyot system). These organs were focused on as they are typically not used to detect esca pathogens, which have mainly been observed in the trunk. However, to control the presence of these fungi in the trunk, 23 symptomatic plants were randomly sampled from the same plot by drilling 1 cm at the same height in each trunk. All samples were collected using ethyl alcohol-sterilized pruning shears and placed immediately in liquid nitrogen. DNA extraction and qPCR analysis were conducted as previously described by Pouzoulet et al. (2013, 2017) using the primer sets PchQF/R and PalQF/R. Briefly, samples were lyophilized for 48 h. After the bark and pith were removed from the samples (except for petioles) using a sterile scalpel, samples were ground and DNA was extracted as described by Pouzoulet et al. (2013). Quantification of *P. chlamydospora* and *P. minimum* DNA by qPCR (SYBR Green assays) was conducted as described by Pouzoulet et al. (2017). Pathogen DNA quantity was normalized by the amount of total DNA used as template, and the mean of three technical replicates was used for further analysis.

Statistical Analysis

The effects of leaf symptom (asymptomatic or symptomatic), organ (midrib or petiole), and their interaction on the calculated native PLC and on the PLC due to occluded vessels were tested using PROC GLIMMIX in SAS software (SAS 9.4; SAS Institute). The plant was entered into models as a random effect, since different leaves were sometimes scanned from the same plant (from one to five per plant). Proportional data (ranging from 0 to 1, dividing all PLC data by 100) was analyzed to fit a logit link function and binomial distribution as appropriate. We computed pairwise least-squares mean differences of fixed effects. The effect of symptom severity (expressed as the percentage of green tissue) among symptomatic leaves on PLC was tested as described above including the plant and organ as covariables (fixed effects) in the model.

Supplemental Data

The following supplemental materials are available.

Supplemental Figure S1. Two-dimensional reconstructions of cross sections from microCT volumes and optical microscopy cross sections of grapevine leaf petioles.

Supplemental Figure S2. Two-dimensional reconstructions of longitudinal and cross sections from microCT volumes of grapevine leaf midribs.

Supplemental Figure S3. Two-dimensional reconstructions of longitudinal and cross sections from microCT volumes for esca asymptomatic leaf midribs scanned on iohexol-fed grapevine shoots.

Supplemental Figure S4. Light microscopy images of cross sections of esca asymptomatic midribs of grapevine.

Supplemental Figure S5. Images of asymptomatic control and esca symptomatic plants of grapevine cv Sauvignon blanc.

Supplemental Figure S6. Method used for vessel segmentation in iohexol-fed grapevine petioles.

Supplemental Table S1. Calculated theoretical conductivity from microCT volumes.

Supplemental Table S2. Quantification of not-filled and occluded vessels in a histological photomicrograph of grapevine midribs.

ACKNOWLEDGMENTS

We thank the experimental teams of UMR SAVE and UMR EGFV (Bord'O platform, INRA, Bordeaux, France) and the SOLEIL synchrotron facility (HRCT beamline PSICHE) for providing the materials and logistics. We thank Jérôme Jolivet (UMR SAVE) for providing technical knowledge and support for plant transplantation and Brigitte Batailler (Bordeaux Imaging Center) for providing technical support for the light microscopy sample preparation.

Received June 24, 2019; accepted August 9, 2019; published August 27, 2019.

LITERATURE CITED

Abou-Mansour E, Couché E, Tabacchi R (2004) Do fungal naphthalenones have a role in the development of esca symptoms? Phytopathol Mediterr **43:** 75–82

Andolfi A, Mugnai L, Luque J, Surico G, Cimmino A, Evidente A (2011) Phytotoxins produced by fungi associated with grapevine trunk diseases. Toxins (Basel) **3:** 1569–1605

Andreini L, Caruso G, Bertolla C, Scalabrelli G, Viti R, Gucci R (2009) Gas exchange, stem water potential and xylem flux on some grapevine cultivars affected by esca disease. S Afr J Enol Vitic **30:** 2

Beckman CH, Roberts EM (1995) On the nature and genetic basis for resistance and tolerance to fungal wilt diseases of plants. In Adv Bot Res, Vol **21**. pp 35–77

Bertsch C, Ramírez-Suero M, Magnin-Robert M, Larignon P, Chong J, Abou-Mansour E, Spagnolo A, Clément C, Fontaine F (2013) Grapevine trunk diseases: Complex and still poorly understood. Plant Pathol **62:** 243–265

Bonsen KJM, Kučera LJ (1990) Vessel occlusions in plants: Morphological, functional and evolutionary aspects. IAWA J **11:** 393–399

Brodribb TJ, Holbrook NM (2003) Stomatal closure during leaf dehydration, correlation with other leaf physiological traits. Plant Physiol **132:** 2166–2173

Bruez E, Baumgartner K, Bastien S, Travadon R, Guérin-Dubrana L, Rey P (2016) Various fungal communities colonise the functional wood tissues of old grapevines externally free from grapevine trunk disease symptoms. Aust J Grape Wine Res **22:** 288–295

Bruez E, Vallance J, Gerbore J, Lecomte P, Da Costa JP, Guerin-Dubrana L, Rey P (2014) Analyses of the temporal dynamics of fungal communities colonizing the healthy wood tissues of esca leaf-symptomatic and asymptomatic vines. PLoS ONE **9:** e95928

Bruno G, Sparapano L (2006) Effects of three esca-associated fungi on *Vitis vinifera* L. III. Enzymes produced by the pathogens and their role in fungus-to-plant or in fungus-to-fungus interactions. Physiol Mol Plant Pathol **69:** 182–194

Bruno G, Sparapano L, Graniti A (2007) Effects of three esca-associated fungi on *Vitis vinifera* L. IV. diffusion through the xylem of metabolites produced by two tracheiphilous fungi in the woody tissue of grapevine leads to esca-like symptoms on leaves and berries. Physiol Mol Plant Pathol **71:** 106–124

Canny M (1997) Tyloses and the maintenance of transpiration. Ann Bot (Lond) **80:** 565–570

Choat B, Gambetta GA, Wada H, Shackel KA, Matthews MA (2009) The effects of Pierce's disease on leaf and petiole hydraulic conductance in *Vitis vinifera* cv. Chardonnay. Physiol Plant **136:** 384–394

Clérivet A, Déon V, Alami I, Lopez F, Geiger JP, Nicole M (2000) Tyloses and gels associated with cellulose accumulation in vessels are responses of plane tree seedlings (*Platanus* × *acerifolia*) to the vascular fungus *Ceratocystis fimbriata* f. sp *platani*. Trees (Berl) **15:** 25–31

Cloete M, Mostert L, Fischer M, Halleen F (2015) Pathogenicity of South African Hymenochaetales taxa isolated from esca-infected grapevines. Phytopathol Mediterr **54:** 368–379

Collins BR, Parke JL, Lachenbruch B, Hansen EM (2009) The effects of *Phytophthora ramorum* infection on hydraulic conductivity and tylosis formation in tanoak sapwood. Can J For Res **39:** 1766–1776

Del Rio JA, Gonzalez A, Fuster MD, Botia JM, Gomez P, Frias V, Ortuno A (2001) Tylose formation and changes in phenolic compounds of grape roots infected with *Phaeomoniella chlamydospora* and *Phaeoacremonium* species. Phytopathol Mediterr **40:** S394–S399

De Micco V, Balzano A, Wheeler EA, Baas P (2016) Tyloses and gums: A review of structure, function and occurrence of vessel occlusions. IAWA J **37:** 186–205

Feliciano AJ, Eskalen A, Gubler WD (2004) Differential susceptibility of three grapevine cultivars to the *Phaeoacremoium aleophilum* and *Phaeomoniella chlamydospora* in California. Phytopathol Mediterr **43:** 66–69

Fischer M (2006) Biodiversity and geographic distribution of basidiomycetes causing esca-associated white rot in grapevine: A worldwide perspective. Phytopathol Mediterr **45:** S30–S42

Fischer M, Peighami-Ashnaei S (2019) Grapevine, esca complex, and environment: The disease triangle. Phytopathol Mediterr **58:** 17–37

Fisher PJ, Petrini O, Sutton BC (1993) A comparative study of fungal endophytes in leaves, xylem and bark of Eucalyptus in Australia and England. Sydowia **45:** 338–345

Fontaine F, Pinto C, Vallet J, Clément C, Gomes AC, Spagnolo A (2016) The effects of grapevine trunk diseases (GTDs) on vine physiology. Eur J Plant Pathol **144:** 707–721

Fradin EF, Thomma BP (2006) Physiology and molecular aspects of *Verticillium* wilt diseases caused by *V. dahliae* and *V. albo-atrum*. Mol Plant Pathol **7:** 71–86

Gambetta GA, Fei J, Rost TL, Matthews MA (2007) Leaf scorch symptoms are not correlated with bacterial populations during Pierce's disease. J Exp Bot **58:** 4037–4046

Gómez P, Báidez AG, Ortuño A, Del Río JA (2016) Grapevine xylem response to fungi involved in trunk diseases: Grapevine vascular defence. Ann Appl Biol **169:** 116–124

Gramaje D, Úrbez-Torres JR, Sosnowski MR (2018) Managing grapevine trunk diseases with respect to etiology and epidemiology: Current strategies and future prospects. Plant Dis **102:** 12–39

Guerin-Dubrana L, Fontaine F, Mugnai L (2019) Grapevine trunk disease in European and Mediterranean vineyards: Occurrence, distribution and associated disease-affecting cultural factors. Phytopathol Mediterr **58:** 49–71

Häffner E, Konietzki S, Diederichsen E (2015) Keeping control: The role of senescence and development in plant pathogenesis and defense. Plants (Basel) **4:** 449–488

King A, Guignot N, Zerbino P, Boulard E, Desjardins K, Bordessoule M, Leclerq N, Le S, Renaud G, Cerato M, et al (2016) Tomography and imaging at the PSICHE beam line of the SOLEIL synchrotron. Rev Sci Instrum **87:** 93704

Knipfer T, Fei J, Gambetta GA, McElrone AJ, Shackel KA, Matthews MA (2015) Water transport properties of the grape pedicel during fruit development: Insights into xylem anatomy and function using microtomography. Plant Physiol **168:** 1590–1602

Kuroda K (2012) Monitoring of xylem embolism and dysfunction by the acoustic emission technique in *Pinus thunbergii* inoculated with the pine wood nematode *Bursaphelenchus xylophilus*. J For Res **17:** 58–64

Larignon P, Dubos B (1997) Fungi associated with esca disease in grapevine. Eur J Plant Pathol **10:** 147–157

Lecomte P, Darrieutort G, Liminana JM, Comont G, Muruamendiaraz A, Legorburu FJ, Choueiri E, Jreijiri F, El Amil R, Fermaud M (2012) New insights into esca of grapevine: The development of foliar symptoms and their association with xylem discoloration. Plant Dis **96:** 924–934

Lee EF, Matthews MA, McElrone AJ, Phillips RJ, Shackel KA, Brodersen CR (2013) Analysis of HRCT-derived xylem network reveals reverse flow in some vessels. J Theor Biol **333:** 146–155

Letousey P, Baillieul F, Perrot G, Rabenoelina F, Boulay M, Vaillant-Gaveau N, Clément C, Fontaine F (2010) Early events prior to visual symptoms in the apoplectic form of grapevine esca disease. Phytopathology **100:** 424–431

Luini E, Fleurat-Lessard P, Rousseau L, Roblin G, Berjeaud JM (2010) Inhibitory effects of polypeptides secreted by the grapevine pathogens Phaeomoniella chlamydospora and Phaeoacremonium aleophilum on plant cell activities. Physiol Mol Plant Pathol **74:** 403–411

Magnin-Robert M, Letousey P, Spagnolo A, Rabenoelina F, Jacquens L, Mercier L, Clément C, Fontaine F (2011) Leaf stripe form of esca induces alteration of photosynthesis and defence reactions in presymptomatic leaves. Funct Plant Biol **38:** 856–866

Magnin-Robert M, Spagnolo A, Boulanger A, Joyeux C, Clément C, Abou-Mansour E, Fontaine F (2016) Changes in plant metabolism and accumulation of fungal metabolites in response to esca proper and apoplexy expression in the whole grapevine. Phytopathology **106:** 541–553

Martín L, Fontaine F, Castaño FJ, Songy A, Roda R, Vallet J, Ferrer-Gallego R (2019) Specific profile of Tempranillo grapevines related to Esca-leaf symptoms and climate conditions. Plant Physiol Biochem **135:** 575–587

Martin N, Vesentini D, Rego C, Monteiro S, Oliveira H, Ferreira RB (2009) *Phaeomoniella chlamydospora* infection induces changes in phenolic compounds content in *Vitis vinifera*. Phytopathol Mediterr **48:** 101–116

Masi M, Cimmino A, Reveglia P, Mugnai L, Surico G, Evidente A (2018) Advances on fungal phytotoxins and their role in grapevine trunk diseases. J Agric Food Chem **66:** 5948–5958

Massonnet M, Morales-Cruz A, Minio A, Figueroa-Balderas R, Lawrence DP, Travadon R, Rolshausen PE, Baumgartner K, Cantu D (2018) Whole-genome resequencing and pan-transcriptome reconstruction highlight the impact of genomic structural variation on secondary metabolite gene clusters in the grapevine esca pathogen *Phaeoacremonium minimum*. Front Microbiol **9:** 1784

McCully M, Canny M, Baker A, Miller C (2014) Some properties of the walls of metaxylem vessels of maize roots, including tests of the wettability of their lumenal wall surfaces. Ann Bot **113:** 977–989

McElrone AJ, Grant JA, Kluepfel DA (2010) The role of tyloses in crown hydraulic failure of mature walnut trees afflicted by apoplexy disorder. Tree Physiol **30:** 761–772

McElrone AJ, Jackson S, Habdas P (2008) Hydraulic disruption and passive migration by a bacterial pathogen in oak tree xylem. J Exp Bot **59:** 2649–2657

Mirone A, Gouillart E, Brun E, Tafforeau P, Kieffer J (2014) PyHST2: An hybrid distributed code for high speed tomographic reconstruction with iterative reconstruction and a priori knowledge capabilities. Nucl Instrum Methods Phys Res B **324:** 41–48

Mondello V, Larignon P, Armengol J, Kortekamp A, Vaczy K, Prezman F, Serrano E, Rego C, Mugnai L, Fontaine F (2018) Management of grapevine trunk diseases: Knowledge transfer, current strategies and innovative strategies adopted in Europe. Phytopathol Mediterr **57:** 369–383

Morales-Cruz A, Allenbeck G, Figueroa-Balderas R, Ashworth VE, Lawrence DP, Travadon R, Smith RJ, Baumgartner K, Rolshausen PE, Cantu D (2018) Closed-reference metatranscriptomics enables in planta profiling of putative virulence activities in the grapevine trunk disease complex. Mol Plant Pathol **19:** 490–503

Mugnai L, Graniti A, Surico G (1999) Esca (black measles) and brown wood-streaking: Two old and elusive diseases of grapevines. Plant Dis **83:** 404–418

Neghliz H, Cochard H, Brunel N, Martre P (2016) Ear rachis xylem occlusion and associated loss in hydraulic conductance coincide with the end of grain filling for wheat. Front Plant Sci **7:** 920

Newbanks D (1983) Evidence for xylem dysfunction by embolization in Dutch elm disease. Phytopathology **73:** 1060

Oliva J, Stenlid J, Martínez-Vilalta J (2014) The effect of fungal pathogens on the water and carbon economy of trees: Implications for drought-induced mortality. New Phytol **203:** 1028–1035

Oses R, Valenzuela S, Freer J, Sanfuentes E, Rodriguez J (2008) Fungal endophytes in xylem of healthy Chilean trees and their possible role in early wood decay. Fungal Divers **33:** 77–86

Paganin D, Mayo SC, Gureyev TE, Miller PR, Wilkins SW (2002) Simultaneous phase and amplitude extraction from a single defocused image of a homogeneous object. J Microsc **206:** 33–40

Pearce RB (1996) Antimicrobial defences in the wood of living trees. New Phytol **132:** 203–233

Pérez-Donoso AG, Greve LC, Walton JH, Shackel KA, Labavitch JM (2007) *Xylella fastidiosa* infection and ethylene exposure result in xylem and water movement disruption in grapevine shoots. Plant Physiol **143:** 1024–1036

Pérez-Donoso AG, Lenhof JJ, Pinney K, Labavitch JM (2016) Vessel embolism and tyloses in early stages of Pierce's disease. Aust J Grape Wine Res **22:** 81–86

Petit AN, Vaillant N, Boulay M, Clément C, Fontaine F (2006) Alteration of photosynthesis in grapevines affected by esca. Phytopathology **96:** 1060–1066

Pouzoulet J, Mailhac N, Couderc C, Besson X, Daydé J, Lummerzheim M, Jacques A (2013) A method to detect and quantify *Phaeomoniella chlamydospora* and *Phaeoacremonium aleophilum* DNA in grapevine-wood samples. Appl Microbiol Biotechnol **97:** 10163–10175

Pouzoulet J, Pivovaroff AL, Santiago LS, Rolshausen PE (2014) Can vessel dimension explain tolerance toward fungal vascular wilt diseases in woody plants? Lessons from Dutch elm disease and esca disease in grapevine. Front Plant Sci **5:** 253

Pouzoulet J, Scudiero E, Schiavon M, Rolshausen PE (2017) Xylem vessel diameter affects the compartmentalization of the vascular pathogen *Phaeomoniella chlamydospora* in grapevine. Front Plant Sci **8:** 1442

Pratt RB, Jacobsen AL (2018) Identifying which conduits are moving water in woody plants: A new HRCT-based method. Tree Physiol **38:** 1200–1212

Qi F, Jing T, Zhan Y (2012) Characterization of endophytic fungi from *Acer ginnala* Maxim. in an artificial plantation: Media effect and tissue-dependent variation. PLoS ONE **7:** e46785

Reis P, Pierron R, Larignon P, Lecomte P, Abou-Mansour E, Farine S, Bertsch C, Jacques A, Trotel-Aziz P, Rego C, et al (2019) *Vitis* methods to understand and develop strategies for diagnosis and sustainable control of grapevine trunk diseases. Phytopathology **109:** 916–931

Rioux D, Nicole M, Simard M, Ouellette GB (1998) Immunocytochemical evidence that secretion of pectin occurs during gel (gum) and tylosis formation in trees. Phytopathology **88:** 494–505

Salleo S, Nardini A, Lo Gullo MA, Ghirardelli LA (2002) Changes in stem and leaf hydraulics preceding leaf shedding in *Castanea sativa* L. Biol Plant **45:** 227–234

Sun Q, Rost TL, Matthews MA (2008) Wound-induced vascular occlusions in Vitis vinifera (Vitaceae): Tyloses in summer and gels in winter. Am J Bot **95:** 1498–1505

Sun Q, Rost TL, Reid MS, Matthews MA (2007) Ethylene and not embolism is required for wound-induced tylose development in stems of grapevines. Plant Physiol **145:** 1629–1636

Sun Q, Sun Y, Walker MA, Labavitch JM (2013) Vascular occlusions in grapevines with Pierce's disease make disease symptom development worse. Plant Physiol **161:** 1529–1541

Surico G, Mugnai L, Marchi G (2006) Older and more recent observations on esca: A critical overview. Phytopathol Mediterr **45:** S68–S86

Torres-Ruiz JM, Jansen S, Choat B, McElrone AJ, Cochard H, Brodribb TJ, Badel E, Burlett R, Bouche PS, Brodersen CR, et al (2015) Direct x-ray microtomography observation confirms the induction of embolism upon xylem cutting under tension. Plant Physiol **167:** 40–43

Umebayashi T, Fukuda K, Haishi T, Sotooka R, Zuhair S, Otsuki K (2011) The developmental process of xylem embolisms in pine wilt disease monitored by multipoint imaging using compact magnetic resonance imaging. Plant Physiol **156:** 943–951

Valtaud C, Foyer CH, Fleurat-Lessard P, Bourbouloux A (2009) Systemic effects on leaf glutathione metabolism and defence protein expression caused by esca infection in grapevines. Funct Plant Biol **36:** 260

Valtaud C, Thibault F, Larignon P, Bertsch C, Fleurat-Lessard P, Bourbouloux A (2011) Systemic damage in leaf metabolism caused by esca infection in grapevines: Starch and soluble sugars in esca-infected *Vitis* leaves. Aust J Grape Wine Res **17:** 101–110

White C, Hallen F, Mostert L (2011) Symptoms and fungi associated with esca in South African vineyards. Phytopathol Mediterr **50:** 236–246

Yadeta KA, Thomma BPHJ (2013) The xylem as battleground for plant hosts and vascular wilt pathogens. Front Plant Sci **4:** 97

Zimmermann MH (1978) Vessel ends and the disruption of water flow in plants. Phytopathology **68:** 253–255

Zimmermann MH (1979) The discovery of tylose formation by a Viennese lady in 1845. IAWA Bull 51–56.

Zimmermann MH (1983) Xylem Structure and the Ascent of Sap. Springer-Verlag, Berlin

Supplemental Materials for

Exploring the Hydraulic Failure Hypothesis of Esca Leaf Symptom Formation

Giovanni Bortolami, Gregory A. Gambetta, Sylvain Delzon, Laurent J. Lamarque, Jérôme Pouzoulet, Eric Badel, Régis Burlett, Guillaume Charrier, Hervé Cochard, Silvina Dayer, Steven Jansen, Andrew King, Pascal Lecomte, Frederic Lens, José M. Torres-Ruiz, Chloé E. L. Delmas

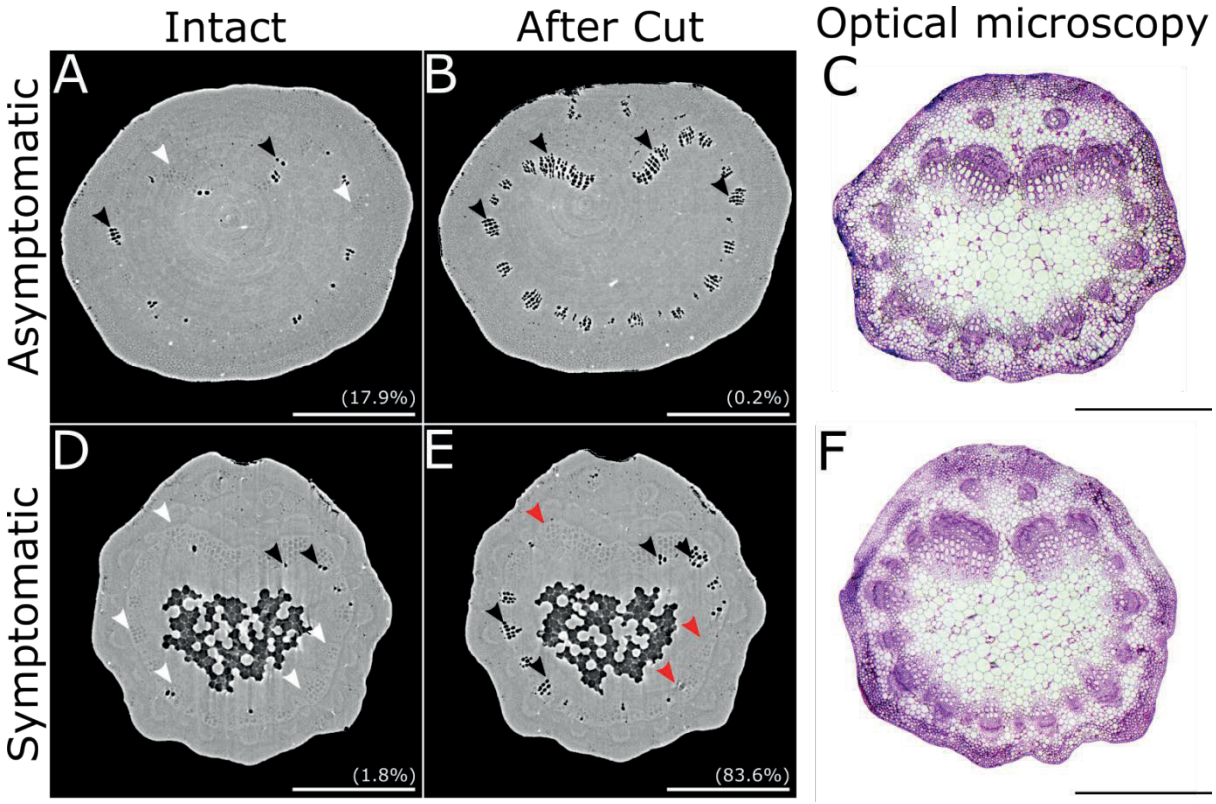

Supplemental Figure S1 (A-F). Two-dimensional reconstructions of cross sections from microCT volumes and optical microscopy cross sections. Esca asymptomatic (**A-C**) and esca symptomatic (**D-F**) leaf petioles of *V. vinifera*. After a first scan on intact leaves (**A**, **D**) the samples were cut (**B**, **E**) just above the scanned area to embolize the vessels and then scanned again. Air-filled (*e.g.* black arrows), water-filled (*e.g.* white arrows), and occluded (*e.g.* red arrows) vessels were counted and their cross-sectional diameters quantified to determine the percentage loss of conductivity (PLC). The PLC represented by either native embolism (**A**, **D**) or occluded vessels (**B**, **E**) is given in parentheses. Light microscopy cross sections (**C**, **F**) were stained with periodic-acid Schiff's reactive. Scale bar = 1mm.

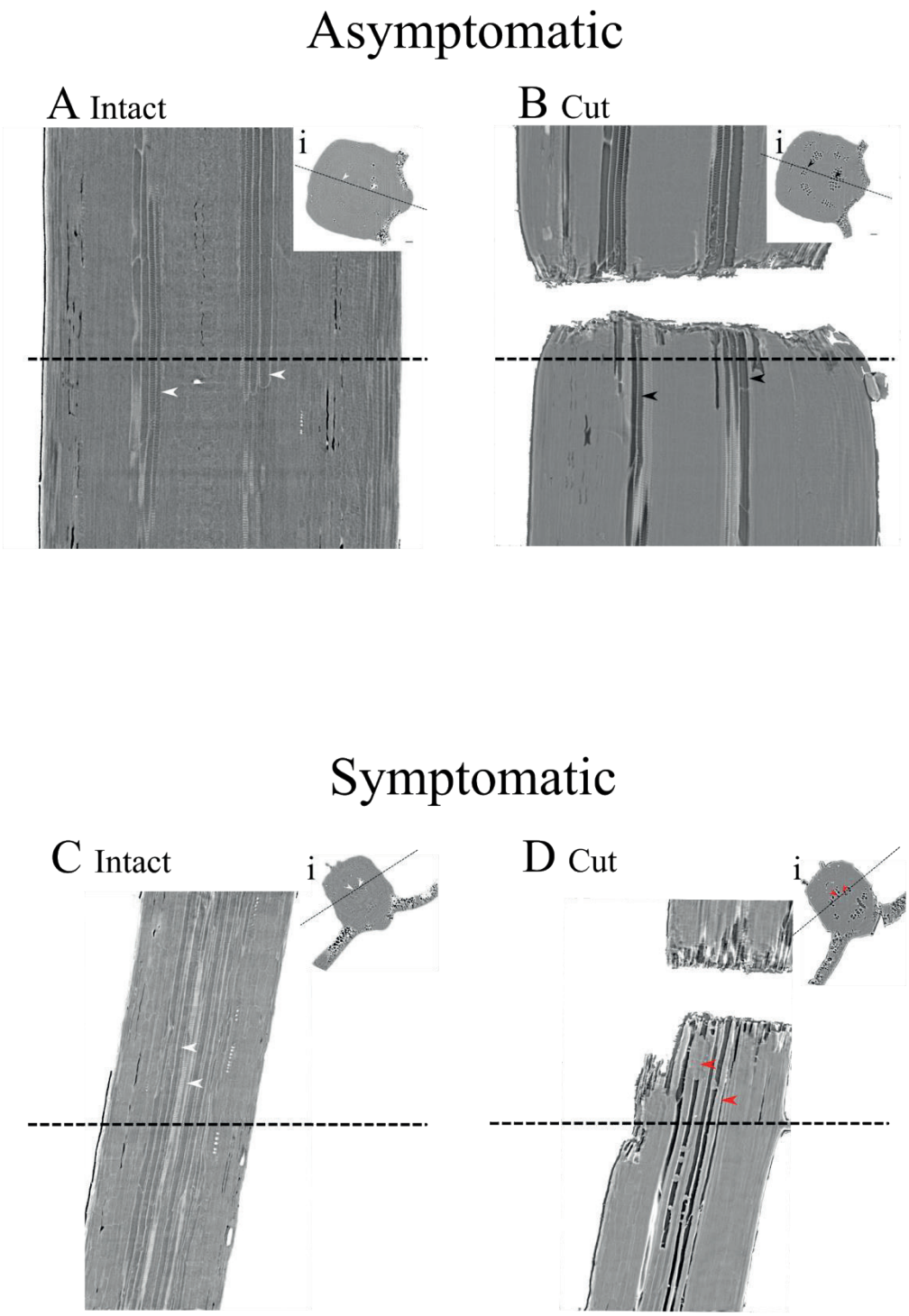

Supplemental Figure S2. Two-dimensional reconstructions of longitudinal (A-D) and cross (insets, i) sections from microCT volumes. Esca asymptomatic (A, B) and esca symptomatic (C, D) leaf midribs of *V. vinifera* plants. The scans were taken before (A, C) and after (B, D) cutting the sample. The dotted lines represent the location of the sections relative to each other. Water-filled (*e.g.* white arrows), air-filled (*e.g.* black arrows), occluded vessels (*e.g.* red-arrows) are evidenced.

Esca asymptomatic iohexol fed midrib

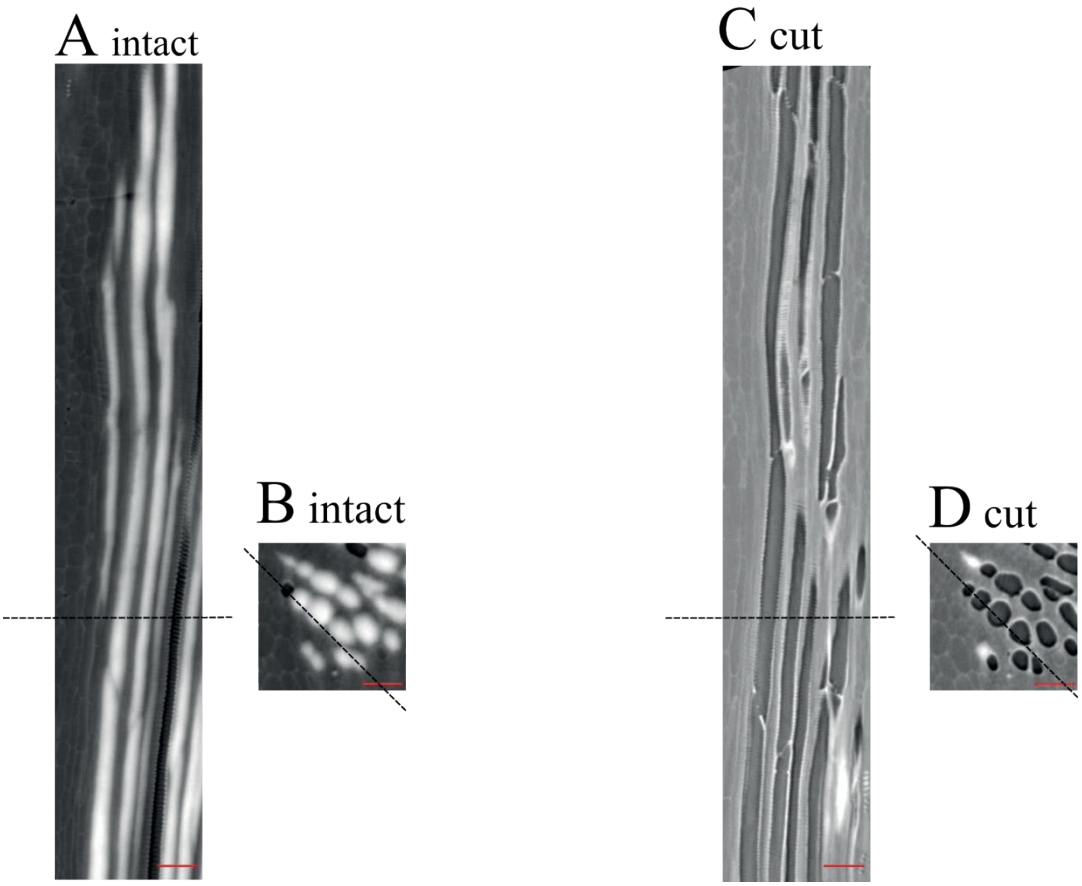

Supplemental Figure S3. Two-dimensional reconstructions of longitudinal (A, C) and cross (B, D) sections from microCT volumes for esca asymptomatic leaf midribs scanned on iohexol fed *V. vinifera* shoots. The dotted lines represent the location of the sections relative to each other. The scans were taken before (A, B) and after (C, D) cutting the sample. Iohexol evidences the functional vessels, in bright white, while air-filled vessels appear in black.

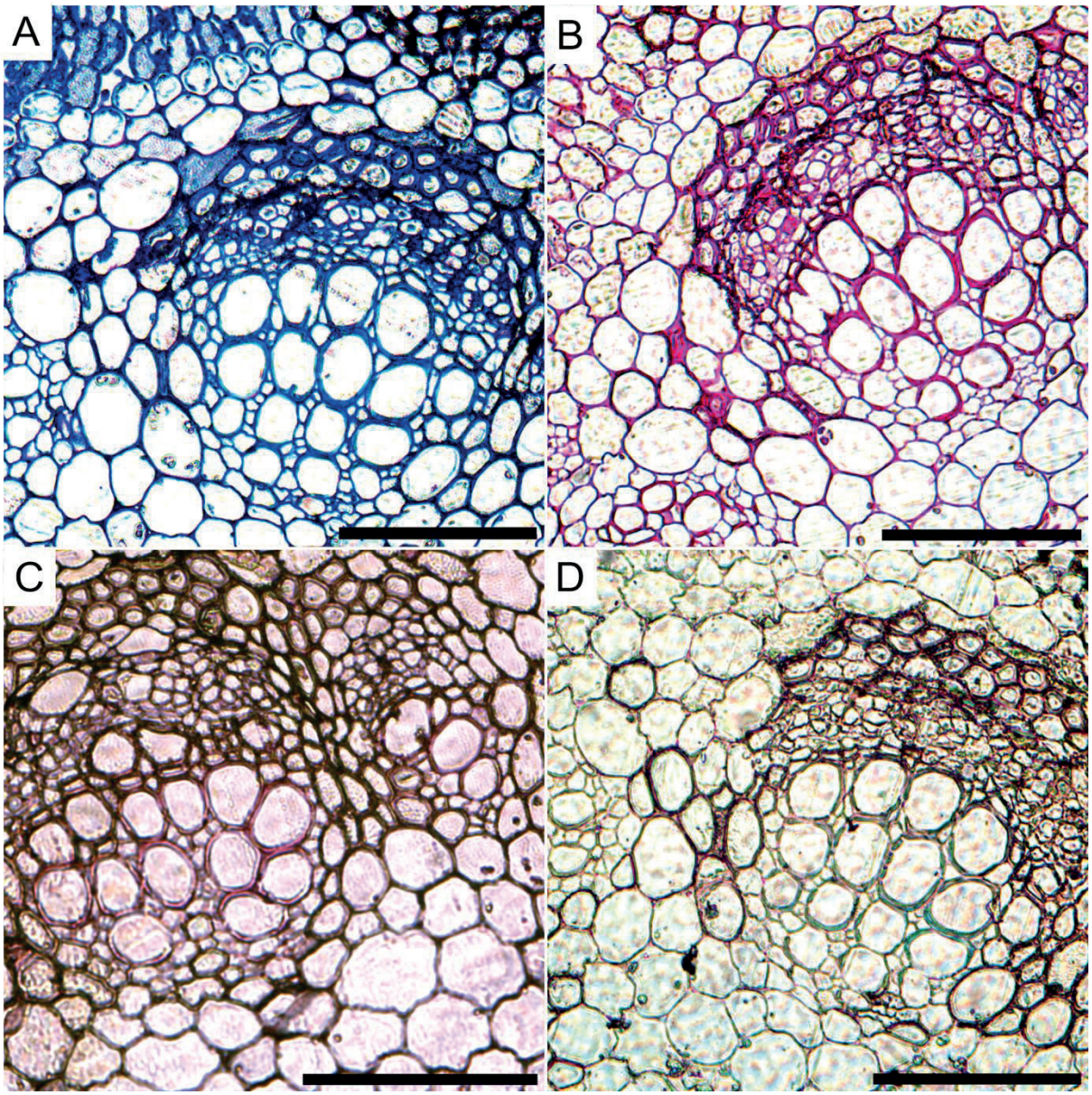

Supplemental Figure S4. Light microscopy images of cross sections of esca asymptomatic midribs of *V. vinifera*. Cross-sections were stained with toluidine blue O (**A**), periodic-acid Schiff's reactive (**B**), ruthenium red (**C**), and lacmoid blue (**D**). Scale bars = 100µm.

A. Examples of esca asymptomatic (A1, A2) and symptomatic (S1-S4) leaves

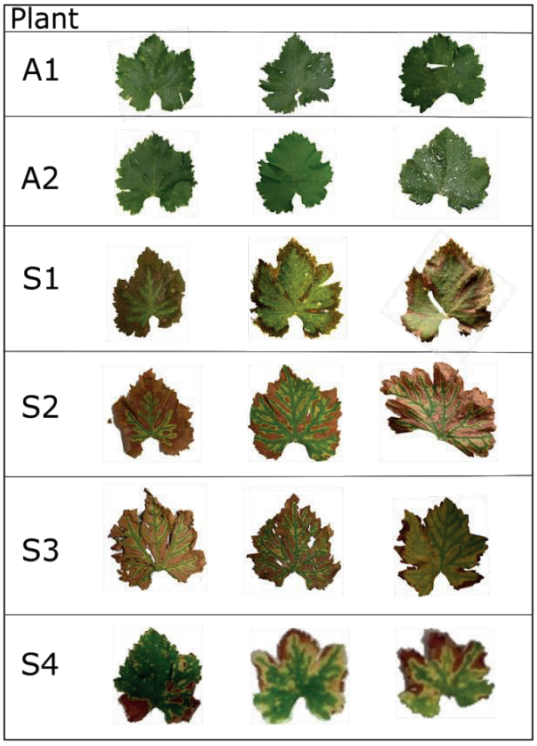

B. Examples of potted entire plants

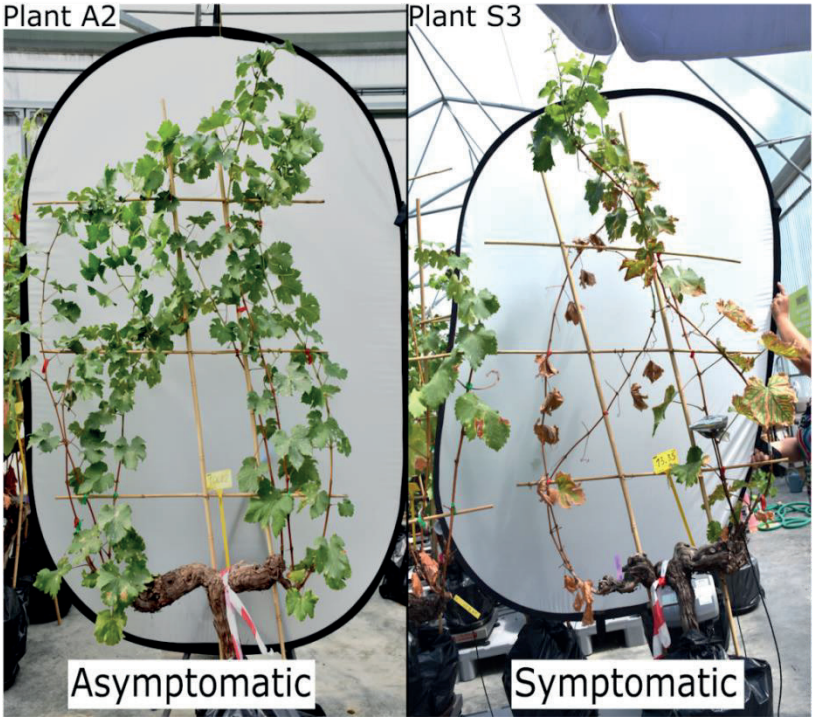

Supplemental Figure S5. Pictures of asymptomatic control and esca symptomatic plants of *V. vinifera* cv. Sauvignon blanc. **(A)** examples of leaves: A1, A2 asymptomatic plants, S1-S4 symptomatic plants. Details on disease history and duration of esca leaf symptom in weeks is given in Table 1. **(B)** Pictures of one asymptomatic (plant A2) and one symptomatic (plant S3) entire *V. vinifera* plants.

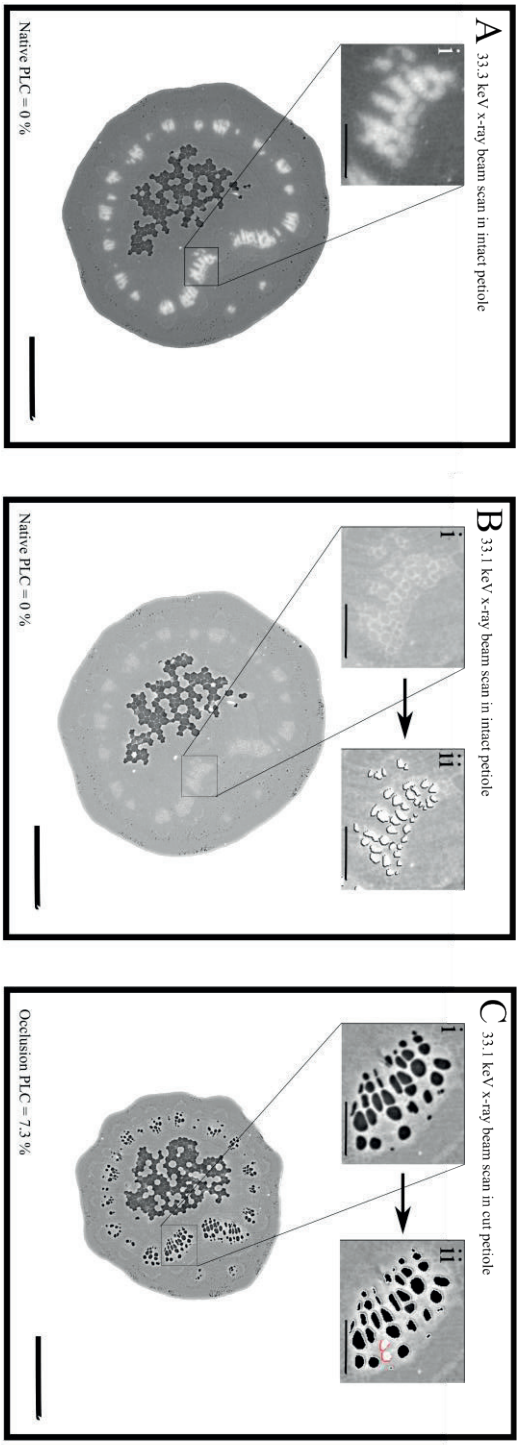

Supplemental Figure S6. Method used for vessel segmentation in iohexol fed petioles. The insets show a detail before (i) and after (ii) image segmentation (using imagej software) to measure the diameter of each single vessel. The high contrast given by iohexol at 33.3 keV can impede the clear differentiation of vessels ends (A, inset Ai), the samples was then re-scanned at 33.1 keV (B before cut, C after cut), to provide an optimal segmentation (insets Bi and Bii, Ci and Cii). Scale bars: A, B, and C = 1000µm; all insets i and ii = 100µm.

Supplemental Table S1 Calculated theoretical conductivity (% Kh) from microCT volumes. Intact *V. vinifera* leaves and after cutting the sample just above the scanned area. Values represent means ± standard error, n=sample size.

Esca	Organ	n	Intact			After cut		
			Air-filled (% Kh)[1]	Water-filled (% Kh)	Partially-occluded (% Kh)	Air-filled (% Kh)	Occluded (% Kh)[2]	Partially-occluded (% Kh)
Asymptomatic	Midrib	8	9.68 ± 3.66	90.32 ± 3.66	0	87.61 ± 3.24	12.39 ± 3.24	0
Asymptomatic	Petiole	4	6.12 ± 4.11	93.88 ± 4.11	0	98.12 ± 1.81	1.88 ± 1.81	0
Symptomatic	Midrib	13	2.77 ± 1.14	96.93 ± 1.14	0.29 ± 0.16	31.22 ± 6.42	60.7 ± 6.80	8.07 ± 3.65
Symptomatic	Petiole	10	7.97 ± 3.14	91.6 ± 3.1	0.42 ± 0.24	44.71 ± 8.97	54.02 ± 8.72	1.27 ± 0.61

[1] Values correspond to Native PLC, Figure 2
[2] Values correspond to Occlusion PLC, Figure 3

Supplemental Table S2 Quantification of not-filled and occluded vessels in histological photomicrograph of *V. vinifera* midribs. not-filled=% of vessels not presenting tyloses nor gels; tyloses=% of vessels presenting one or more tyloses; gel=% of vessels presenting gel filling the whole vessel section; tyloses & gel=% of vessels presenting tyloses and gel at the same time; occluded total=% of vessels presenting tyloses, gel, or both. Values represent means ± standard error, n=number of cross sections.

Esca	n	not-filled (%)	tyloses (%)	gel (%)	tyloses & gel (%)	occluded total (%)
Symptomatic	55	80.3 ± 1.6	17.1 ± 1.3	1.2 ± 0.2	1.4 ± 0.3	19.7 ± 1.6
Asymptomatic	56	99.6 ± 0.1	0.4 ± 0.1	0.04 ± 0.1	0.02 ± 0.02	0.4 ± 0.1

Results summary - Chapter 2

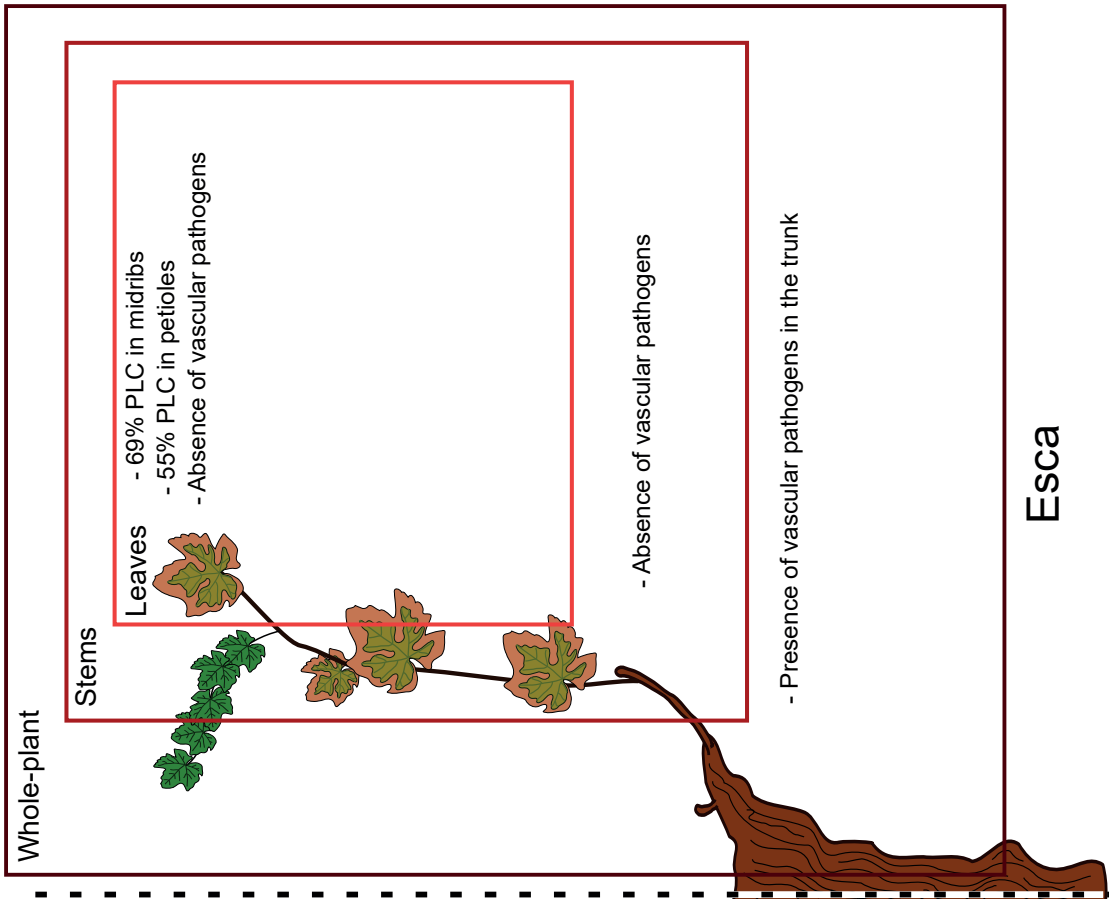

CHAPTER 3

Similar Symptoms Do Not Induce Similar Changes in Grapevine Leaf Xylem Anatomy, Comparisons between Senescing Processes and Climatic Regions

Résumé : L'anatomie du xylème peut apparaitre très différente si les plantes sont soumises à des contraintes biotiques ou abiotiques. Les occlusions vasculaires sont un des principaux traits anatomiques qui influencent la résistance ou la sensibilité des plantes aux différents stress. Ces occlusions ont été étudiées par le passé sur les organes pérennes de plusieurs espèces lors de différents processus de senescence induite. Cependant, leur présence et fonction au sein des feuilles restent méconnues. Chez la vigne, plusieurs processus de senescence présentent des symptômes visuellement similaires, mais nous ne savons pas encore si leurs mécanismes physiologiques le sont également, ni comment l'anatomie du xylème foliaire en est affectée. Dans cette étude, nous avons quantifié les occlusions vasculaires dans les nervures centrales de feuilles présentant différents symptômes (esca, déficience en magnésium, et senescence d'automne). Nous avons trouvé que l'esca entraine un processus de senescence unique, avec des occlusions présentes en moyenne dans 28% des vaisseaux, là où les autres feuilles symptomatiques (et les feuilles contrôles) n'en présentent que dans 3%. Par la suite, nous avons approfondi les connaissances sur la senescence induite par l'esca en comparant des feuilles issues de différents pays (Californie, France, Italie et Espagne) et variétés (Sauvignon blanc et Castet), et mis en évidence que les deux paramètres peuvent affecter le niveau d'occlusion dans les vaisseaux. Pour identifier le moment d'apparition des occlusions dans les vaisseaux, nous avons suivi des plantes (symptomatiques d'esca et contrôles) au cours d'une saison, trouvant que les occlusions peuvent (bien que rarement) apparaitre sans l'expression visuel des symptômes. Enfin, nous avons étudié la fonctionnalité des vaisseaux du xylème par une méthode optique sur des portions de limbe des feuilles, en trouvant que la propagation de l'embolie gazeuse dans les feuilles symptomatiques présente un comportement non-uniforme (comparé aux contrôles), probablement dû à la présence d'occlusions. Ces résultats ouvrent de nouvelles perspectives sur le rôle des occlusions vasculaires pendant la senescence sur feuilles, en suggérant que leur formation pourrait être stimulée seulement sous certaines conditions, avec des fonctions et conséquences très spécifiques pour la survie des plantes et des feuilles.

AUTHORS

Bortolami, G.[a], Ferrer, N.[a], Baumgartner, K.[b], Delzon S.[c], Gramaje, D.[d], Lamarque, L.J.[c,e], Romanazzi, G.[f], Gambetta G.A.[g], Delmas, C.E.L[a].

[a]INRAE, BSA, ISVV, SAVE, 33882 Villenave d'Ornon, France.
[b]United States Department of Agriculture-Agricultural Research Service, Crops Pathology and Genetics Research Unit, Davis, CA 95616, USA.
[c]Univ. Bordeaux, INRAE, BIOGECO, 33615 Pessac, France
[d]Institute of Grapevine and Wine Sciences (ICVV), National Research Council (CSIC), University of La Rioja and Government of La Rioja, Logroño 26007, Spain.
[e]Département des Sciences de l'Environnement, Université du Québec à Trois-Rivières, Trois-Rivières, Québec, G9A 5H7, Canada.
[f]Department of Agricultural, Food and Environmental Sciences, Marche, Polytechnic University, Ancona, Italy.
[g]EGFV, Bordeaux-Sciences Agro, INRAE, Université de Bordeaux, ISVV, 33882 Villenave d'Ornon, France.

AUTHOR CONTRIBUTIONS

G.B., C.E.L.D., G.A.G., designed the experiments;
G.B., K.B., D.G., G.R., conducted the leaf sampling;
N.F. conducted the histological observations;
L.J.L., S.D. conducted the non-invasive optical visualization of embolism, and analyzed the images;
G.B. analyzed the images from optical microscopy, and analyzed the data;
G.B., C.E.L.D., G.A.G. wrote the article;

ABSTRACT

Xylem anatomy can differently respond to environmental or biotic stresses. Vascular occlusion is one of the main functional anatomical traits, influencing plant resistance and susceptibility to different stresses. While occlusion presence has been studied in xylem from woody organs during different induced senescence processes, their presence and function in leaves remain obscure. In grapevine, many senescence processes present similar visual symptoms. However, we still do not know whether the underlying physiological mechanisms are similar as well, and whether leaf anatomy is affected in similar ways. In this study, we quantified vascular occlusions in midribs from different symptomatic leaves (i.e. esca, magnesium deficiency, and autumn senescence). We found that esca leaf symptom formation is a unique senescence process, presenting vascular occlusions in 28% of xylem vessels (on average), while the other senescing leaves (as well as the asymptomatic controls) presented occlusion in approximately 3% of vessels. Therefore, we extended our investigations of esca leaf senescence to different countries (California, France, Italy, and Spain) and varieties (Sauvignon blanc and Castet), finding that both parameters can affect occlusion level. We followed plants over the course of the season, finding that vascular occlusions can rarely appear without esca visual symptoms. Finally, we investigated the functionality of xylem vessels by optical visualization of embolism in intact leaf lamina, finding that air embolism spreading in symptomatic leaves has a different and non-uniform behavior, probably given by the presence of occlusions, compared to controls. These results open new perspectives on the role of vascular occlusions during leaf senescence, suggesting that they could be stimulated only during certain conditions with specific function and consequences in leaf (and plant) survival.

INTRODUCTION

Xylem vascular occlusions are considered as a functional anatomical trait responding to a broad range of environmental and biotic factors (De Micco *et al*., 2016). Their nature comprises gels (or gums), formed by amorphous extracellular materials (such as pectin, callose, or other polysaccharide chains, Rioux *et al*., 1998), and tyloses, which are expansions of parenchyma cells inside the vessel lumen (Zimmermann, 1979). Their presence has been detected during many different induced senescence processes, such as tissue ageing (Dute *et al*., 1999, Salleo *et al*., 2002), wound response (Sun *et al*., 2007, 2008), flooding (Davison and Tay, 1985), and vascular diseases (Pouzoulet *et al*., 2019, Mensah *et al*., 2020). In general, vascular occlusions are formed to hydraulically isolate some regions of the plant, contributing to wound or pathogen compartmentalization (Pearce, 1996), or help woody organs in decay resistance and

mechanical support during heartwood formation (De Micco *et al*., 2016). Their role is largely studied in woody perennial organs, where occlusions are associated with decrease in hydraulic conductivity under diverse induced senescence processes (e.g. McElrone *et al*., 2010, Deyett *et al*., 2019, Mensah *et al*., 2020). Vascular occlusions (especially tyloses) have been shown in a strict relationship with plant resistance to different vascular pathogens in stems (e.g. Venturas *et al*., 2014; Park and Juzwik 2014; Rioux *et al*., 2018). Moreover, many theoretical articles have hypothesized that an excessive production of vascular occlusions during disease would lead to lethal impairment in plant water transport (Fradin and Thomma, 2006, Yadeta and Thomma, 2013, Oliva *et al*., 2014).

In leaves xylem occlusions have been studied only during induced senescence by *Xylella spp.* infections (Fritschi *et al*., 2008, Choat *et al*., 2009) and winter (Salleo *et al*., 2002), and their functions and consequences on leaf physiology are not clear. Recently, we have associated vascular occlusions with *in vivo* quantification of xylem hydraulic failure in midribs and petioles during esca leaf symptoms (Bortolami *et al*., 2019), enhancing the interest in the physiological role of vascular occlusions during leaf senescence. Finally, probably because vascular occlusions are frequently observed late during the senescence process (Chaffey and Pearson, 1985), they were not even mentioned in reviews on leaf senescence (Lim *et al*. 2007, Schippers *et al*., 2015). In this context, there is a need in improving the knowledge on xylem vascular occlusions (especially in leaves), the consequences they have on plant physiology, and the underlying mechanisms of their formation.

In this study, we compared grapevine midrib vascular occlusion presence during different symptom development and induced senesce processes (esca, magnesium deficiency, and autumn senescence). We hypothesized that similar visual leaf symptoms observed following these environmental factors (i.e. discolorations between the major veins) would induce equal responses in the xylem anatomy. As *Vitis vinifera* cv Sauvignon blanc presented significant levels of vascular occlusions in midribs during esca leaf senescence (Bortolami *et al*., 2019), this model was taken as reference to compare occlusion production in different climatic regions and cultivars. We then followed esca leaf symptom appearance in specific plants, to follow the progression between vascular occlusions and esca leaf symptom development. Finally, by the use of non-invasive visualization of embolism, we quantified the residual xylem functionality in esca symptomatic leaf lamina.

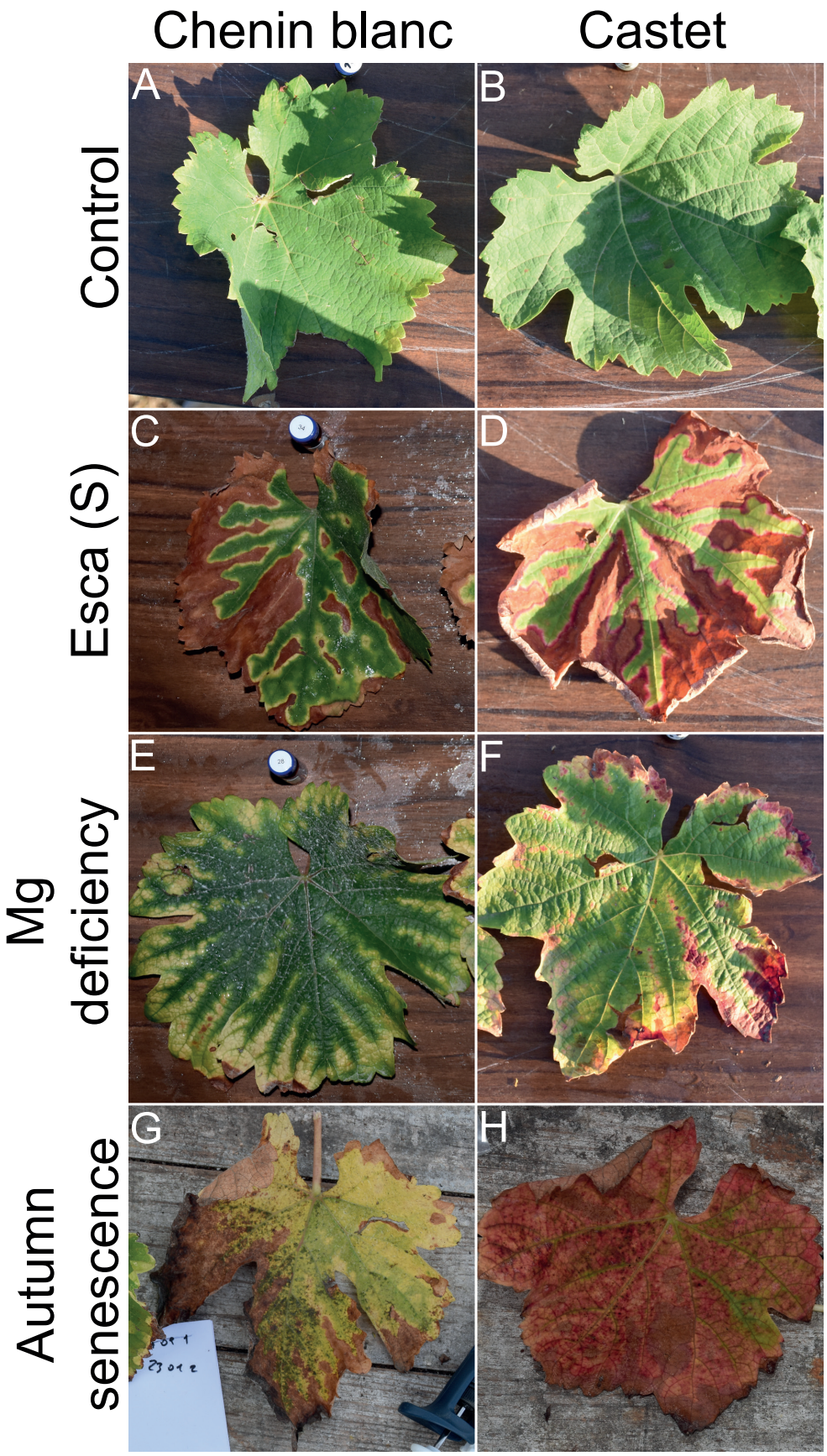

Figure 1. Pictures of different induced-senescence processes from a white (Chenin blanc, A, C, E, G) and a red (Castet, B, D, F, H) *V. vinifera* cultivar. **A**, **B**, control (asymptomatic) leaves in August. **C**, **D**, esca symptomatic leaves in August. **E**, **F**, magnesium deficient leaves in August. **G**, **H**, autumn senescent leaves in October.

MATERIALS AND METHODS

Plant material and sampling*

To quantify the occlusions during different stresses, we sampled plants in the Vitadapt experimental plot (van Leeuwen *et al*., 2019) planted in 2009 in the Bordeaux region (France, 44°47'23.8"N 0°34'39.7"W). Ten control leaves were sampled in August 2018 from eight different plants (*V. vinifera* grafted onto SO4 cv Castet n=5, Chenin blanc n=1, Sangiovese n=1, and Sauvignon blanc n=3). Thirteen esca symptomatic leaves were sampled from nine different plants (*V. vinifera* cv Castet n=5, Chenin blanc n=1, Mourvedre n=1, Sangiovese n=1, Sauvignon blanc n=5). Four magnesium deficient leaves were sampled in August and October 2018 from five different plants (*V. vinifera* cv Castet n=2, Mourvedre n=1, and Sauvignon blanc n=1). Twenty-three autumn senescent leaves were sampled in October 2018 from eleven different plants (*V. vinifera* cv Castet n=5, Chenin blanc n=4, Mourvedre n=8, Sangiovese n=1, and Sauvignon blanc n=5).

Esca leaf symptoms were identified by tiger-stripe scorched symptoms, as described in Lecomte *et al*. (2012). We identified magnesium deficiency symptoms in plants with tiger-stripe discolorations (yellow or red depending on grape color) in the lower part of the canopy and without the presence of scorched area. We identified autumn senescence in leaves with total or partial discoloration, sometimes with tiger-stripe patterns. Examples of the sampled induced senescence leaf symptoms are presented in Fig. 1 for a white (Chenin blanc) and a red (Castet) *V. vinifera* cultivar.

To further explore leaf xylem anatomy during esca, symptomatic and control leaves were sampled from different countries (France, Italy, Spain, and California in the United States). In France, eighteen leaves were sampled in august 2018 from twelve different plants (six control and six esca symptomatic) *V. vinifera* cv Castet and Sauvignon blanc, planted in 2006, grafted onto SO4 at Vitadapt experimental plot. In Italy, seven leaves were sampled in June 2019 from five different plants (three control and two esca symptomatic) *V. vinifera* cv Sauvignon blanc (Carassai, Ascoli Piceno, central-eastern Italy, 43°02'18.07''N 13°39'39.41''E). In Spain (42°26'07.4"N 2°30'48.5"W), eight leaves were sampled in late August 2019 from six different plants (three control and three esca symptomatic) *V. vinifera* cv Castet, grafted onto 110R, planted in 2013. In California (39°00'15.1"N 122°51'08.3"W), sixteen leaves were sampled in August 2020 from six different plants (three control and three esca symptomatic) *V. vinifera* cv Sauvignon blanc, planted in 2000, grafted onto 5C.

To explore the evolution of occlusion formation over time during esca pathogenesis, we sampled leaves from a unique experimental setup described in Bortolami *et al*. (2019). Briefly, 30 years-old *V. vinifera* cv Sauvignon blanc vines, grafted onto 101-14 MGt, were uprooted from the field in February 2018 and transferred into 20L pots. We sampled, over the experimen-

*The presented results are only preliminary. More samples will complete the dataset; in particular, the comparisons for esca leaf symptoms will include more varieties from the presented geographic regions.

tal season 2018, twenty-eight leaves (eight control leaves, eight asymptomatic leaves before symptom expression, six asymptomatic leaves in symptomatic plants, and six symptomatic leaves showing typical esca tiger stripe symptoms) from ten different plants (three control, and four esca symptomatic). In September 2017 and 2018 we brought control and symptomatic plants to synchrotron SOLEIL (PSICHE beamline), and scanned leaf midribs with X-ray microCT as described in Bortolami *et al*. (2019). The same midribs analyzed in Bortolami *et al*. (2019) are reported here, with the only difference that in this study we quantified the percentage of occluded vessels (in number) not the theoretical loss of hydraulic conductivity.

Light microscopy and occlusion quantification

Prior to resin embedding, samples had a slightly different treatment if sampled in France, or in California, Italy, and Spain. In France, one-centimeter sections of midribs were cut at one centimeter from the petiole point and directly put in FAA solution, 0.64% paraformaldehyde, 50% ethanol, 5% acetic acid, and 44.36% water (v/v). After one to three days in the FAA solution on the shaker at 90rpm, samples were dehydrated using a graded series of alcohol (80%, 100%, 100% for 30' each) and stocked at 4 °C until analysis. In California, Italy, and Spain, one-centimeter sections were cut at one centimeter from the petiole point, directly put in 80% alcohol, mailed to France and stored at 4 °C until analysis. After one night in the FAA solution, samples were dehydrated using the same graded series (80%, 100%, 100% v/v for 30' each). All samples (from any country) were then embedded using a graded series of LR White resin (Agar scientific, 33%, 50%, and 66% LR White v/v in ethanol solution for 120' each, and 100% three times for 7 hours each). Finally, samples were polymerized in capsules at 60 °C for 24-48 hours. Transverse sections of 1.8 to 2 µm thickness were cut using an Ultracut S microtome (Reichert) equipped with a glass knife at the Bordeaux Imaging Center, a member of the France Bio Imaging national infrastructure (ANR-10-INBS-04). Cross sections were stained with 0.05% (w/v) Toluidine Blue O, able to marker vascular occlusions (Bortolami *et al*., 2019). Stained sections were dried and photographed with a DS-Fi3 camera (Nikon, France) mounted on a stereo microscope SMZ1270 (Nikon, France).

Xylem vessels were identified in each entire cross-section using imagej (Schneider *et al*., 2012) and categorized as empty vessels or occluded vessels (presenting gel or tyloses) as presented in Fig. 2. In addition, we observed a deposition of crystals in vessels of 93% of the samples and thus quantified their presence. For each sample, one cross-section was analyzed for vessel occlusion quantification. To confirm that vascular occlusion were equally distributed within the same sample (i.e. in the one-centimeter segment), we quantified vascular occlusions in three cross-sections from twenty-nine midribs, finding that there were no significant differences within samples ($F_{55,12498}$=0.97, P=0.54, treating repetition, samples, and their interaction as fixed effects in independent linear models with binomial distribution for absence or presence

of occlusion in each vessel in SAS proc GLIMMIX).

Non-invasive optical determination of xylem functionality

Leaf embolism formation and propagation were evaluated in four leaves from three different control (asymptomatic) plants and in eleven leaves from four different esca symptomatic plants using the optical vulnerability (OV) technique (Brodribb *et al*., 2016). The analysis took place in two weeks (from September 3rd to September 16th, 2019) plants (*V. vinifera* cv Sauvignon blanc) uprooted in February 2019 from the same plot for the leaf midrib analysis (INRAE, Bordeaux). To quantify embolism propagation in leaf lamina, we monitored changes in light transmission through the xylem (Brodribb *et al*., 2016). In the early morning, stems were cut under water, put inside dark plastic bags with humid paper and rapidly transported to the lab. Once at the lab, the abaxial side of intact leaves was fixed on a scanner (Perfection V800 Photo, EPSON, Suna, Japan) using a transparent glass and adhesive tape. Brightness and contrast as well as leaf scanned area were adjusted to optimize visualization of embolisms. 991 ± 90 mm^2 (average ± SE) of each leaf was automatically scanned every 5 min throughout plant dehydration using a computer automation software (AutoIt 3). Simultaneous measurements of stem water potential (Ψ_{stem}) were made every 30' using psychrometers (ICT Internationale, Armidale, NSW, Australia) properly installed on the stem. The stack of images captured at the end of the experiment comprised between 1800 and 2000 scans per leaf and they were analyzed using ImageJ software and following instructions from http://www.opensourceov.org. Briefly, total embolism was quantified by subtracting pixel differences between consecutive images (i.e. pixel values that did not change resulted in a value of zero). In these series, white pixels represented leaf embolism. Noise was removed using the Imagej outlier removal, and pixel threshold was used to extract embolism from any background noise remaining. The embolism area per image was calculated as the sum of non-zero pixels on the total scanned surface (mm^2) or on green leaf surface only (mm^2, excluding the symptomatic tissue). We considered the veins that embolized as functional (i.e. containing water under tension), while the remaining veins were considered as non-functional (i.e. containing any combination of air, occlusion, or static water). On each leaf used for OV measurements, we determined the percentage of green on the scanned area with ImageJ software. On RGB pictures, we detected the HUE green ranges (in color threshold) in control-asymptomatic leaves. We used these ranges to select and quantify the green pixels in each scanned area. The percentage of green pixels on the green area was then used to calculate the green surface (mm^2) on each scanned area.

Statistical analysis

We investigated whether induced senescence processes are affecting the probability of occlusions production in xylem vessels using different chi-square tests of independence. We investi-

gated whether esca symptomatic and control leaves presented different response in embolized surface during decreasing Ψ_{Stem} using generalized linear mixed model with the plant treated as random effect of the interaction between symptom presence and Ψ_{Stem}. All statistical tests were done using SAS software (SAS 9.4; SAS Institute).

RESULTS

Anatomical diversity of vascular occlusions and presence of crystals

In each sample, we quantified different types of vessels (Fig. 2). By the use of Toluidine blue O dye, we identified the nature of vascular occlusions, which comprehends gels (i.e. amorphous extracellular material, mainly composed by pectins and polysaccharides, Neghliz *et al*., 2016,

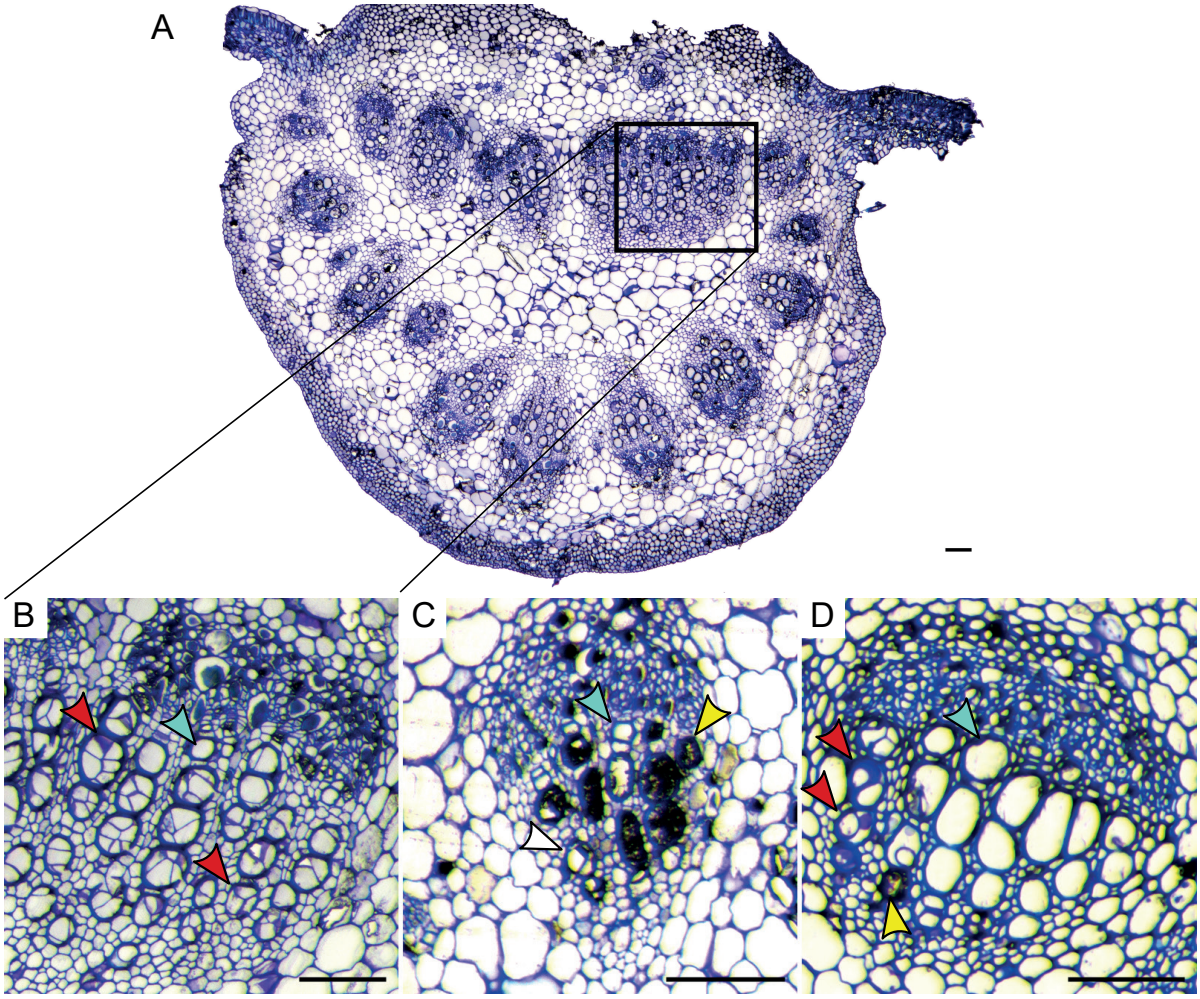

Figure 2. Different types of xylem vessels in *V. vinifera* midribs. (**A**) Entire cross-section of midrib from an esca symptomatic leaf containing occluded vessels. (**B-D**) Detail of vascular bundles. Vessels were classified as empty (i.e. apparently functional) if no structures were detected in their lumen (blue arrowheads, B-D). Vessels with crystal depositions were noted when druse crystals were covering the vessel surface (yellow arrowheads, C, D), or when prismatic crystals were identified (white arrowhead, C). Vessels were noted as occluded when we identified gel pockets and tyloses (red arrowhead, B, D. Scale bars = 100µm.

Bortolami *et al*., 2019) and tyloses (i.e. expansions of the neighbour-vessels parenchyma cells, Zimmermann, 1979, Zhao *et al*., 2019). The presence of crystals (both druse and prismatic) inside some vessel lumen was surprising (Fig. 2). The fact that crystals are more associated with occlusion-free samples (Fig. S1) and that xylem vessels in control asymptomatic midribs were almost totally functional under X-ray scans (data from Bortolami *et al*., 2019) and optical visualizations (Fig. 6), let us suppose that crystals are associated with functional vessels (i.e. transporting water), not with occluded ones (see discussion for details). Consequently, to evaluate the impact of different stresses on xylem anatomy, we reported here only the percentages of occlusions, and not of crystals, in different experiments and comparisons.

Vascular occlusions in presence of different induced senescence processes

To explore how different induced senescence processes affected leaf xylem vasculature, we compared midribs from controls, esca symptomatic, magnesium deficient, and autumn senescent leaves (Fig. 3). We found that midribs form control leaves presented 3.9 ± 1% of occluded vessels (average ± SE, Fig. 3). Esca symptomatic leaves presented the highest level with 28.5 ± 5% of occluded vessels. Magnesium deficient leaves presented the lowest content of occluded vessels (0.53 ± 0.5%), while autumn senescent leaves presented contents similar to controls (3.4 ± 1%). However, two autumn senescent midribs presented a percentage of occluded vessels over 15% (outliers in Fig. 3).

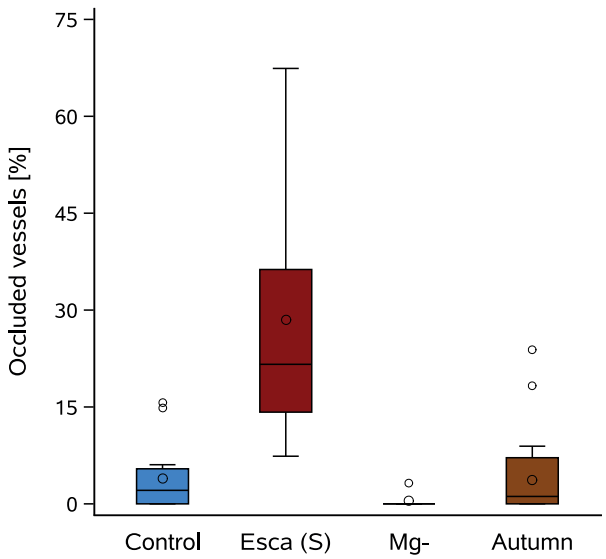

Figure 3. Occluded vessels in *V. vinifera* midribs during different senescence processes. Colors correspond to midribs from: control (blue, n=14), esca symptomatic (red, n=13), magnesium deficiency (grey, n=4) and autumn senescence (brown, n=23) leaves. Boxes and bars show the median, quartiles and extreme values, circles within boxes correspond to means, and circles outside boxes to outlier values. The probability in found occluded vessels among the induced senescence categories were significantly different (X^2=1186.01, P<0.0001).

Vascular occlusions in esca symptomatic leaves from different cultivars and countries*

We quantified the percentage of occluded vessels in esca symptomatic and control (asymptomatic) leaf midribs from four different countries (France, Italy, California, and Spain) in two varieties: Castet (CT, red) and Sauvignon blanc (SB, white). Our results show that, in general, symptomatic leaves presented a significantly higher presence of occlusions compared to controls in every country and variety (Table 1). Comparing esca leaf symptoms between varieties (all countries combined), we observed a difference between CT and SB (X^2=72.9

*The presented results are only preliminary. More samples will complete the dataset; in particular, the comparisons for esca leaf symptoms will include more varieties from the presented geographic regions.

Table 1. Effect of esca leaf symptoms on the probability to present occluded vessels. Different chi-square tests of independence were done between control and esca symptomatic leaves for each different country and variety.

Country – Variety	Sample size (Control - Esca)	X^2	P
France – Sauvignon blanc	(3 - 5)	223.97	<0.0001
France – Castet	(5 - 5)	55.90	<0.0001
Italy – Sauvignon blanc	(3 - 4)	217.20	<0.0001
California – Sauvignon blanc	(8 - 8)	136.11	<0.0001
Spain – Castet	(3 - 5)	101.95	<0.0001

P<0.0001, Fig. 4). Midribs from control plants presented low percentages of occluded vessels (2.2 ± 1%, average ± SE Fig. 4). CT esca symptomatic leaves presented an intermediate level of occluded vessels (14.4 ± 3%, Fig. 4), while SB esca symptomatic leaves presented the highest average percentage of occluded vessels (25.9 ± 5%, Fig. 4). For CT esca symptomatic midribs, we quantified similar percentage of occluded vessels in France and Spain (X^2=0.27 *P*=0.6, Fig 4i), while a significant effect of the geographical provenience (France, Italy, and California) was found in SB esca symptomatic midribs (X^2=176.4 *P*<0.0001, Fig 4ii).

Vascular occlusion evolution during esca symptom appearance

During one experimental season, we followed ten plants from July (doy=186) to September 2018 (doy=262, Fig. 5). Four of these plants expressed esca leaf symptoms, and three without symptoms were used as control. We found that, using optical microscopy, control plants always presented low levels of occlusions inside their midribs, as well as the majority of asymptomatic leaves both before and after symptom appearance (<10% of vessels, Fig. 5). Four out of six symptomatic leaves presented high content of occlusions (>20%), as well as one leaf before symptom appearance, and one asymptomatic leaf in symptomatic plants (Fig. 5). Scanning midribs with X-ray microCT, we found higher average occluded vessels (compared to optical microscopy) both in control and symptomatic midribs (15.2 ± 4% and 62.7 ± 7%, average ± SE for control and symptomatic leaves respectively, Fig.5).

Using a non-invasive optical vulnerability technique, we were able to test the vulnerability to embolism in control and esca symptomatic leaf lamina (Fig. 6, 7). At the end of dehydration, at -6 MPa, when no supplemental embolism was detected, we sum all the embolism formation events in each different sample (red vessels, Fig. 6). As expected, almost all the veins embolized in control leaves (Fig. 6 A-D), while esca symptomatic leaves presented wide portions of lamina where the veins did not embolize (Fig. 6 E-M), and two symptomatic leaves did not show any embolism (Fig. 6 N, O). We can observe that in most symptomatic leaves the primary veins readily embolize. Moreover, embolism is observed in correspondence of darker (i.e. green) zones (Fig. 6 E-M). Plotting the embolism expansion versus the decrease in stem

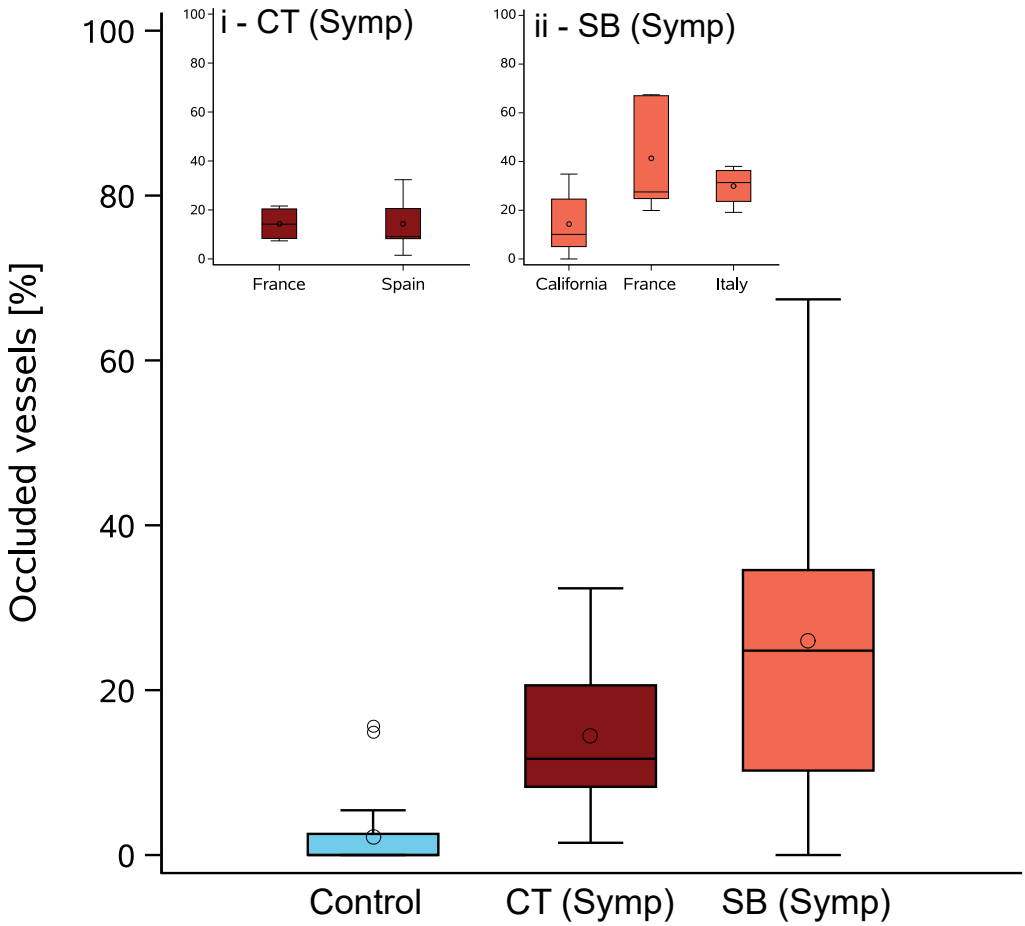

Figure 4*. Occluded vessels [%] in different varieties and countries in *V. vinifera* midribs in presence and absence of esca leaf symptoms. In the main figure boxes represent the percentage of occluded vessels in control (blue, all varieties and countries combined), Castet esca symptomatic (dark red, all countries combined), and Sauvignon blanc esca symptomatic (light red, all countries combined) leaves. (i) Occluded vessel comparison between countries in Castet esca symptomatic leaves. (ii) Occluded vessel comparison among countries in Sauvignon blanc esca symptomatic leaves. Boxes and bars show the median, quartiles and extreme values, circles within boxes correspond to means, and circles outside boxes to outlier values. Sample sizes and statistical differences between control and esca symptomatic for each different country and variety are presented in Table 1.

water potential, we found that control leaves presented a final embolized surface of 25.1 ± 7 x 100 pixels mm^{-2} (average ± SE, Fig. 7A) on the entire scanned surface. In symptomatic leaves only 5.2 ± 2 x 100 pixels mm^{-2} (Fig. 7A) presented embolism on the entire scanned surface. When only the green surface of the leaves was considered (Fig. 7B), control leaves presented the same embolized surface evolution (they were completely green), while symptomatic leaves presented a final embolized surface of 13.0 ± 4 x 100 pixels mm^{-2} (Fig. 7B). In control leaves, embolism events were detected between -1.9 and -3.3 MPa (Fig. 7A, B), while in symptomatic leaves these events appeared in a larger spectrum of Ψ_{Stem} (i.e. between -1.3 and -4.9 MPa, Fig. 7A, B). Finally, it is worth noting that in 82% (nine out of eleven) symptomatic leaves, when the whole scanned surface is considered, and in 54% (six out of eleven) symptomatic leaves, when only the green scanned surface is considered, the final embolized surface did not reach the half of the embolized surface of control leaves (Fig. 7).

*The presented results are only preliminary. More samples will complete the dataset; in particular, the comparisons for esca leaf symptoms will include more varieties from the presented geographic regions.

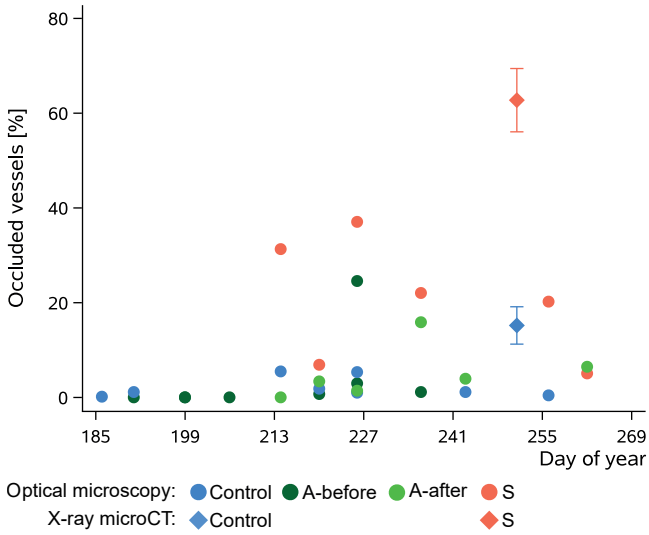

Figure 5. Evolution of occluded vessels [%] over the season (July to September) in *V. vinifera* cv Sauvignon blanc midribs. Symbols correspond to single leaves from well-watered control plants (blue, n=7), asymptomatic leaves before esca symptom appearance (dark green, n=7), asymptomatic leaves (light green, n=6) and esca symptomatic (red, n=6) leaves from well-watered esca plants. Circles correspond to measures by optical microscopy, diamond to X-ray microCT scans (data from Bortolami *et al*., 2019). In X-ray microCT quantification, symbols correspond to means and bars to ± SE (n=8 in control and n=13 in esca leaves). A significant effect of symptom was observed on the probability to present occluded vessels: X^2=217.20, P<0.0001, including points from optical microscopy only.

DISCUSSION*

In this study, we underlie the uniqueness of esca leaf symptoms compared to other induced senescence processes. We demonstrated that only esca symptomatic leaves presented significant percentages of occluded vessels in their midribs compared to leaves under magnesium deficiency or autumn senescence. We investigated esca leaf symptoms in detail and demonstrated that the percentage of occlusion: (i) could vary among varieties and geographic distribution within varieties; and (ii) did not evolve over the season in symptomatic leaves. Finally, by the optical vulnerability (OV) technique, we observed that the non-functional vessels covered large portions of symptomatic leaf lamina, suggesting higher percentages of vascular occlusions in secondary and most peripheral veins, as the mid veins presented the highest concentration of xylem functionality .

Crystals in xylem vessels, reality or artifact?

We regularly observed crystals inside xylem vessels. In the literature, when crystals are observed in leaves, authors usually refer to oxalate calcium, which is formed to regulate calcium bulk pressure, defense to herbivores, or metal detoxification (Franceschi and Nakata, 2005). Oxalate calcium crystals are found in leaves from different species (Somavilla *et al*., 2014) and this is also the case for grapevine (Jáuregui-Zúñiga *et al*., 2003, Şeker *et al*., 2016). However, to our knowledge, calcium oxalate was observed in parenchyma cells, never inside xylem vessels. One study found crystals in xylem vessels contaminated by fungi (Chattaway, 1952, in different woody species). More recently, Sun *et al*. (2013) found prismatic crystals in grapevine stems (in ~3% of vessels) following *Xylella* inoculations. In our case, we found crystals (both prismatic and druse) in 15% of vessels (on average) in midribs independently from leaf health

*The presented results are only preliminary. More samples will complete the dataset; in particular, the comparisons for esca leaf symptoms will include more varieties from the presented geographic regions.

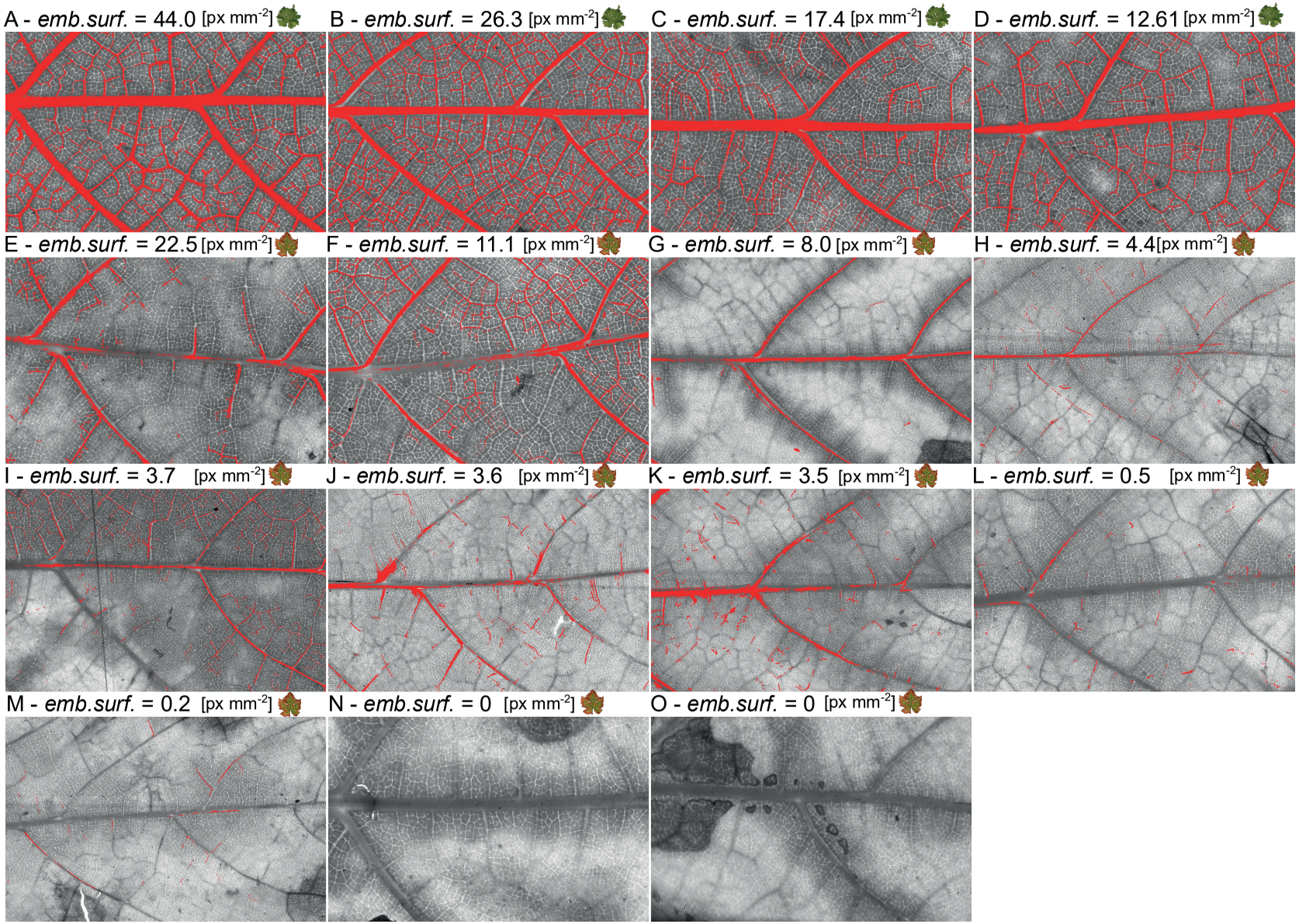

Figure 6. Visualization of embolism formation during dehydration of *V. vinifera* cv Sauvignon blanc leaves from control and esca symptomatic leaves. Each panel corresponds to leaf lamina from control leaves collected on asymptomatic control plants (A-D) and esca symptomatic leaves (E-O). Red veins correspond to veins that embolized during dehydration. The final embolized surface on the total surface of 100 pixels mm^{-2} is indicated for each sample.

status, thus we considered them as non-influential to xylem water transport. Moreover, druse oxalate calcium crystals were present asymptomatic leaves, while were absent in presence of esca leaf symptoms (Clazarano *et al*., 2014). However, other studies should investigate the chemical nature of these crystals, to identify their role in plant physiology and conclusively exclude that we (and other authors) are not observing artifacts resulting from sample manipulations (e.g. fixation, impregnation, or inclusion protocols).

Esca, a unique induced senescence process

Comparing different induced senescence processes, we observed the uniqueness of esca leaf symptoms. Both magnesium deficiency and autumn senescence present many similarities with esca (including the visual symptom of leaf chlorosis and a decrease in stomatal conductance and carbon assimilation, Salleo *et al*., 2002, Brodribb and Holbrook, 2003 for autumn, and Tränkner *et al*., 2016, Rogiers *et al*., 2020 for Mg deficiency). The absence of occlusions during magnesium deficiency suggests that the observed reduction in leaf gas exchange is related to a dysfunction in photosynthetic process, not to a decrease in water supply. During autumn senescence, the absence of vascular occlusion was somehow unexpected, as occlusions are frequently detected during this process (Chattaway, 1949, Salleo *et al*., 2002, De Micco *et al*., 2016). Vascular occlusions may affect only the petioles (and maybe only the stem-petiole junction) which were not studied here, in correspondence of the abscission point during leaf

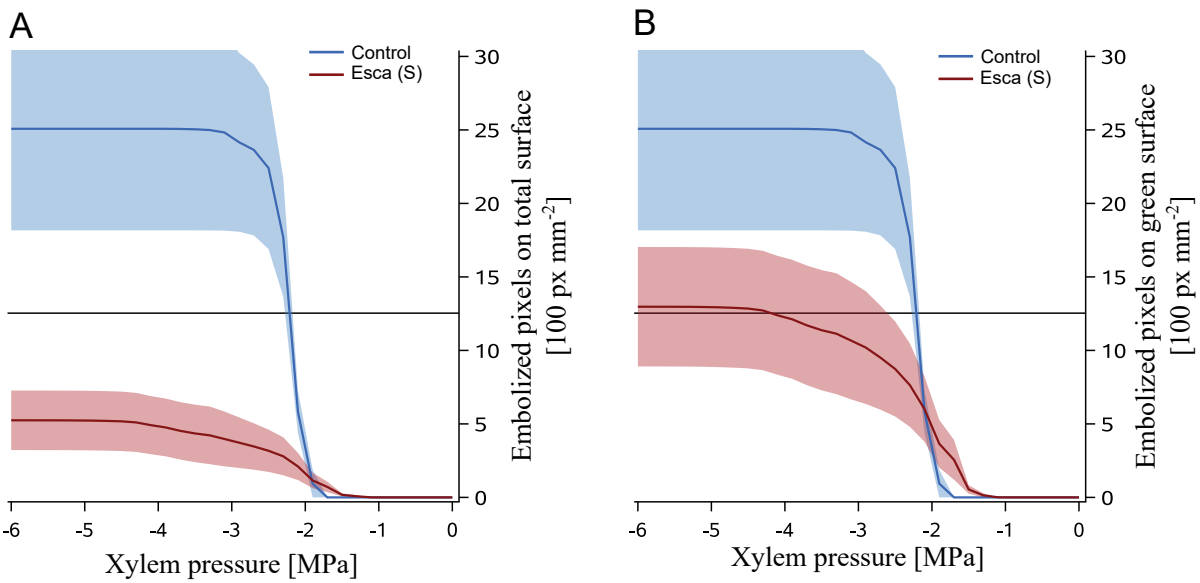

Figure 7. Embolism formation in leaf lamina from *V. vinifera* cv Sauvignon blanc from control (blue) and esca symptomatic (red) leaves during dehydration. (**A**) Sum of embolized pixels on the total (green and symptomatic) scanned surface over decreasing xylem pressure. A significant effect of symptom presence was found: $F_{2,456}$=219.05 P<0.0001. (**B**) Sum of embolized pixels on the green scanned surface over decreasing xylem pressure. A significant effect of symptom presence was found: $F_{2,456}$=128.80 P<0.0001. Lines represent the average evolution of embolized surface (100 pixels every mm²) during decreasing xylem pressure (MPa). The bands represent the SE for each group. The black horizontal line represent the level of embolized pixels corresponding to 50% the final embolized surface (on average) for control leaves.

shedding. Indeed, during autumn the hydraulic conductivity decreased in petioles, not in leaf lamina (Salleo *et al*., 2002). This difference in the spatial distribution of occlusions could suggest that the observed similarities are given by different underlying mechanisms. In the most prominent hypothesis of esca leaf symptom formation, toxins are transmitted from the pathogens (in the trunk) up to the leaves through the vascular system (Claverie *et al*., 2020). Thus, the presence of occlusions along the vasculature could be consistent with this hypothesis (i.e. when a pathogen-derived molecule enters in contact with a parenchyma cell, it could directly trigger the expansion of tyloses). In contrast, during autumn senescence the hormones triggering the senescence process are synthesized *in situ* (Schippers *et al*., 2015), suggesting a more local response in the vasculature (for example, only on the abscission point in petioles).

Exploring the vascular occlusions and functionality during esca leaf symptoms

Comparing esca symptomatic leaves among cultivars (Castet and Sauvignon blanc) and countries (France, Spain, Italy, California in the USA), we found tyloses and gels in the majority of the symptomatic leaves analyzed. It has been previously demonstrated that Sauvignon blanc vines (greenhouse grown) suffer from occlusion driven hydraulic failure during esca leaf symptom expression (Bortolami *et al*., 2019). Here, we demonstrated that occlusions (and subsequent hydraulic failure) can also be present in the field, and this phenomenon is not particular to one specific climate or cultivar. However, the higher percentage of occluded vessels in Sauvignon blanc compared with Castet is of note and suggests differences between genotypes regarding the extent of vascular occlusion. This is consistent with the fact that during other vascular diseases occlusions can be associated both with plant resistance and sensibility to disease symptoms. In the first case, occlusions efficiently compartmentalize pathogens in a restricted volume (Clérivet *et al.,* 2000, Rioux *et al*., 2018, Pouzoulet *et al*., 2020); in the second case, occlusions interfere with water movement, with detrimental consequences for the plant (Sun *et al*., 2013, Mensah *et al*., 2020). It is known that grapevine varieties present a different sensibility to esca (Romanazzi *et al*., 2009, Guerin-Dubrana *et al*., 2019). Consequently, are the occlusion quantification positively or negatively correlated with varietal sensibility? Should we consider these occlusions as beneficial or harmful for the plant? As vascular pathogens are detected far away from the leaves (i.e. in trunks, Bortolami *et al*., 2019), we are more inclined to hypothesize a harmful effect of occlusions for affected grapevines, and that hydraulic failure would exacerbate symptoms. However, we need more studies to confirm this hypothesis and relate the presence of occlusion with a direct measure of *in vivo* water flow.

Following symptomatic plants over the season, we observed that only two among twelve samples presented some occlusions without the visual symptom (light and dark green dots above 10% in Fig. 5). At the same time, we also observed that sometimes (two times on six samples) visual symptoms could also be accompanied with low presence of occlusions (red dots in Fig.

5). We could explain this variability by the fact that we analyzed 2µm thick cross-sections on midribs that can be 20cm long likely leading to an underestimation of the occlusion presence. The comparison with the optical embolism visualization supports this hypothesis, as the primary veins are not uniformly functional (or non-functional) along their length. From optical visualizations, we considered as functional each vein that presented embolism formation during dehydration (i.e. containing water under tension), and observed that the midribs are the most functional parts in symptomatic leaves (Fig. 6). We could then conclude that hydraulic failure given by occlusions may have a stronger impact on the total leaf hydraulic conductivity than what was previously estimated by X-ray scans in midribs (Bortolami *et al*., 2019). Moreover, even when only the remaining green asymptomatic part of the leaves was considered, we quantified that the relative embolized surface was lower in symptomatic leaves compared to controls, reinforcing the hypothesis that vascular occlusions strongly affect the leaf xylem functionality during esca. Finally, as in symptomatic leaves we also detected embolism events at very low Ψ_{Stem} (i.e. below -3 MPa), we could hypothesize that secondary veins are hydraulically disconnected from the rest of the plant even if they did not present vascular occlusions. We probably observed these late embolism events because occlusions isolated some water pockets in the most peripheral parts of the leaves.

CONCLUSION

In this study, we showed that esca leaf symptoms provoke anatomical changes that are unique to this induced senescence process. Indeed, no vascular occlusions were detected during magnesium deficiency or autumn senescence. This result reinforced the particularity of esca over other induced senescence, enhancing the scientific interest to understand the underlying physiological (and pathological) mechanisms that result in esca pathogenesis. This work confirms that vascular occlusions during esca are associated with hydraulic failure in the leaf lamina. Moreover, the different varietal susceptibility in presenting occlusions during esca, could open new perspectives on the role of these structures in varietal sensibility to the disease.

ACKNOWLEDGMENTS

We thank Mark Gowdy and Agnes Destrac-Irvine from UMR EGFV (INRAE) for providing technical help in the Vitadapt plot. We thank the team of UMR SAVE (INRAE) for the technical support in the greenhouse experimentations. We thank Patrick Leger and Regis Burlett from UMR BIOGECO (INRAE) for help with the optical vulnerability method implementation and the SOLEIL synchrotron facility (HRCT beamline PSICHE) for providing the materials and logistics. This work was supported by the French Ministry of Agriculture, Agrifood, and

Forestry (FranceAgriMer and CNIV) within the PHYSIOPATH project (program Plan National Dépérissement du Vignoble, 22001150-1506) and the LabEx COTE (ANR-10-LABX-45) “Projet Caviplace Platform”.

Supplemental Materials for

Similar Symptoms Do Not Induce Similar Changes in Grapevine Leaf Xylem Anatomy, Comparisons between Senescing Processes and Climatic Regions

Giovanni Bortolami, Nathalie Ferrer, Kendra Baumgartner, Sylvain Delzon, David Gramaje, Laurent J. Lamarque, Gianfranco Romanazzi, Gregory A. Gambetta, Chloé E.L. Delmas.

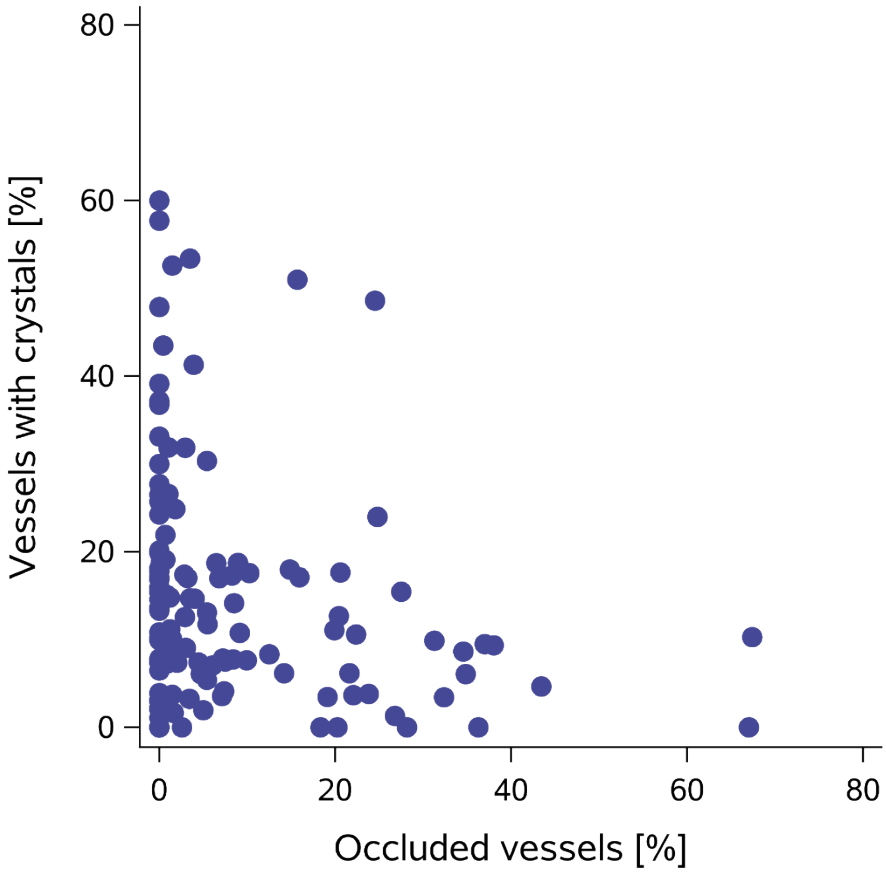

Fig. S1. Relationship between percentage of vessels presenting crystals and vessels presenting occlusion (examples in Fig. 1) for each sample. Symbols represent single samples (independently from their health status or geographical and varietal origin).

Results summary - Chapter 3

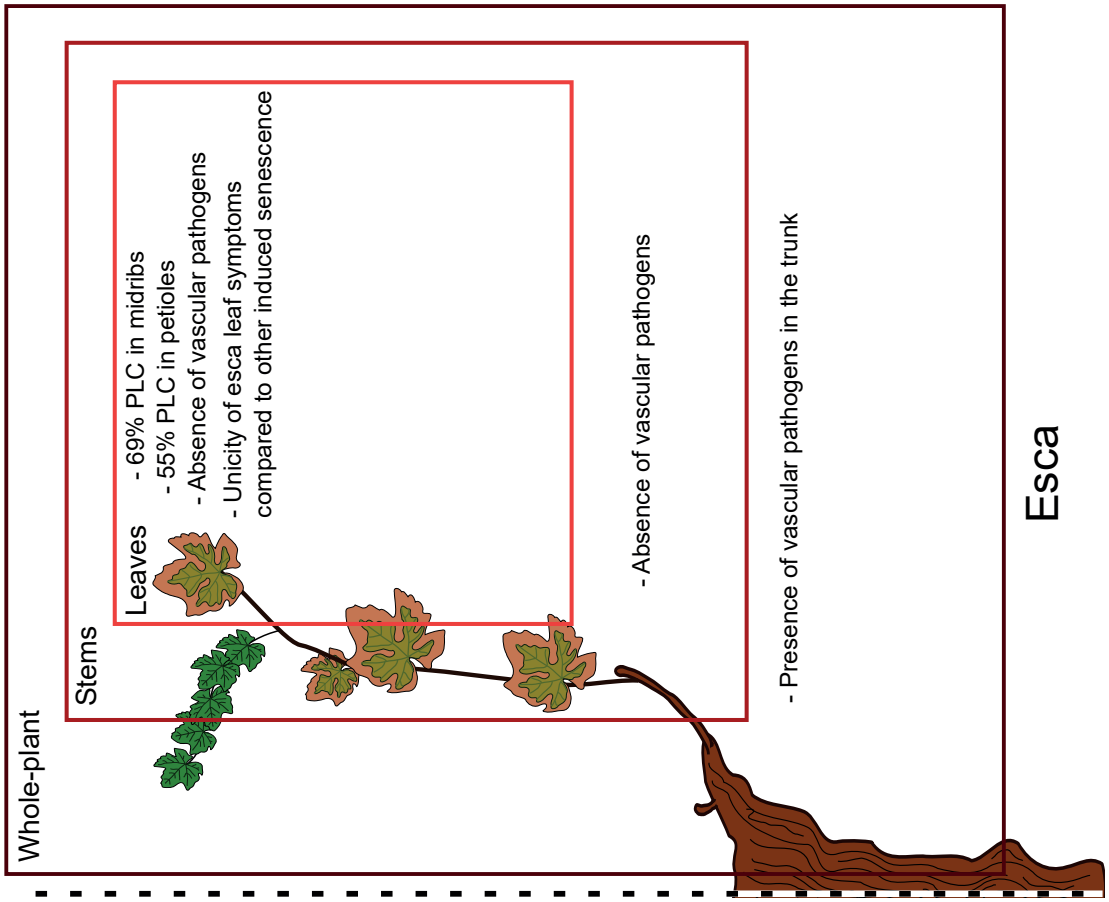

CHAPTER 4

Seasonal and Long-Term Consequences of Esca on Grapevine Stem Xylem Integrity

Published in BioRxiv in September 2020, https://doi.org/10.1101/2020.09.07.282582
Submitted to: Journal of Experimental Botany (revision submitted January, 27th 2021)

Résumé : Le dysfonctionnement hydraulique a été largement étudié dans le contexte du dépérissement des plantes en condition de sécheresse, mais son rôle durant les interactions avec les stress biotiques reste méconnu. L'esca, une maladie de la vigne, entraine chez les feuilles symptomatiques des niveaux significatifs de dysfonctionnement hydraulique irréversible, mais l'intégrité hydraulique des organes pérennes sur le long et le court terme reste méconnue. Nous avons étudié l'effet saisonnier et long-terme de l'esca sur l'intégrité hydraulique des tiges de plantes naturellement infectées. Nous avons couplé des mesures directes (k_s) et indirectes (k_{th}) de conductivité hydraulique, avec l'observation des occlusions vasculaires (thylloses), la détection de pathogènes, et des visualisations *in vivo* par rayons-X. Nous avons mis en évidence la présence de thylloses avec pour conséquence une perte de k_s dans toutes les tiges avec symptômes sévères (apoplexie) et dans plus de 60% des tiges présentant des symptômes modérés (tigrés). Cependant, aucune thyllose n'a été observée sur tiges asymptomatiques. Les observations *in vivo* ont démontré que les thylloses sont observées seulement avec l'apparition visible des symptômes, entrainant une perte au-delà de 50% de perte de conductance hydraulique (PLC) dans 40% des tiges symptomatiques, sans relation avec l'âge du symptôme. Enfin, l'impact de l'esca sur l'intégrité du xylème a été observé seulement au cours de la saison d'expression des symptômes, mais pas sur le long-terme. Cette étude démontre comment et à quel niveau une maladie vasculaire comme l'esca, qui affecte l'intégrité du xylème, pourrait amplifier la mortalité des plantes par dysfonctionnement hydraulique.

Running title: Impact of the trunk disease esca on stem hydraulic integrity

Highlight: Our study reveals that esca can critically affect xylem water movement in grapevine perennial organs, by the presence of plant-derived tyloses.

G. Bortolami[a], E. Farolfi[a], E. Badel[b], R. Burlett[c], H. Cochard[b], N. Ferrer[a], A. King[d], L.J. Lamarque[c,e], P. Lecomte[a], M. Marchesseau-Marchal[a], J. Pouzoulet[f], J.M. Torres-Ruiz[b], S. Trueba[c,g], S. Delzon[c], G.A. Gambetta[f], C.E.L. Delmas[a]

[a]INRAE, BSA, ISVV, SAVE, 33882 Villenave d'Ornon, France
[b]Université Clermont-Auvergne, INRAE, PIAF, 63000 Clermont-Ferrand, France
[c]Univ. Bordeaux, INRAE, BIOGECO, 33615 Pessac, France
[d]Synchrotron SOLEIL, L'Orme des Merisiers, Gif-sur-Yvette, 91192, France
[e]Département des Sciences de l'Environnement, Université du Québec à Trois-Rivières, Trois-Rivières, Québec, G9A 5H7, Canada
[f]EGFV, Bordeaux-Sciences Agro, INRAE, Université de Bordeaux, ISVV, 210 chemin de Leysotte, 33882 Villenave d'Ornon, France
[g]School of Forestry and Environmental Studies, Yale University, New Haven, CT 06511, USA

AUTHOR CONTRIBUTIONS

C.E.L.D., G.A.G., G.B., and S.D. designed the experiments;
E.F., G.A.G., S.D., E.B., R.B., H.C., A.K., L.J.L., J.M.T.-R., S.T. participated in synchrotron campaigns;
G.B., C.E.L.D., E.F., and N.F. conducted the esca symptom notations;
G.B., M.M.-M., and N.F. conducted the histological observations;
E.F. conducted the hydraulic conductivity measurements and participated to data analyses;
N.F., and J.P., conducted the pathogen detection;
G.B. analyzed the microCT, optical images, and analyzed the data;
P.L. provided data on disease history of the plants;
G.B., C.E.L.D., and G.A.G. wrote the article;
all authors edited and agreed on the last version of the article

ABSTRACT

Hydraulic failure has been extensively studied during drought-induced plant dieback, but its role in plant-pathogen interactions is under debate. During esca, a grapevine (*Vitis vinifera*) disease, symptomatic leaves are prone to irreversible hydraulic dysfunctions but little is known about the hydraulic integrity of perennial organs over the short- and long-term. We investigated the effects of esca on stem hydraulic integrity in naturally infected plants within a single season and across season(s). We coupled direct (k_s) and indirect (k_{th}) hydraulic conductivity measurements, and tylose and vascular pathogen detection with in vivo X-ray microtomography visualizations. We found xylem occlusions (tyloses), and subsequent loss of stem k_s, in all of the shoots with severe symptoms (apoplexy) and in more than 60% of the shoots with moderate symptoms (tiger-stripe), and no tyloses in shoots that were currently asymptomatic. *In vivo* stem observations demonstrated that tyloses were observed only when leaf symptoms appeared, and resulted in more than 50% PLC in 40% of symptomatic stems, unrelated to symptom age. The impact of esca on xylem integrity was only seasonal and no long-term impact of disease history was recorded. Our study demonstrated how and to what extent a vascular disease such as esca, affecting xylem integrity, could amplify plant mortality by hydraulic failure.

Key words: Esca, hydraulic failure, plant dieback, tyloses, vascular pathogens, *Vitis vinifera* L., X-ray microCT, xylem anatomy

INTRODUCTION

In agricultural and forest ecosystems, perennial plant dieback causes decreases in plant productivity and longevity (Aleemullah and Walsh, 1996, Eskalen *et al*., 2013, Urbez-Torres *et al*., 2013, Alvindia and Gallema, 2017). Plant dieback is a complex process where different biotic and/or abiotic stress factors interact and contribute to leaf and crown wilting and ultimately plant death (Desprez-Lostau *et al*., 2006, Anderegg *et al*., 2013, Cailleret *et al*., 2017, Bettenfeld *et al*., 2020). Drought-mediated plant dieback has been extensively studied, and in this case hydraulic failure has been identified as the primary cause of plant death (Anderegg *et al*., 2016). Hydraulic failure results from an interruption of the ascendant water flow by air embolism or xylem occlusion (Zimmermann, 1979, Tyree and Sperry, 1989). Vascular pathogens, which infect the xylem network (Yadeta and Thomma, 2013), are also important drivers of pathogen-mediated plant dieback (Goberville *et al.*, 2016, Pandey *et al*., 2018; Fallon *et al*., 2020).

Vascular pathogens induce wood necrosis, leaf symptoms, and crown defoliation (Beckmann and Roberts, 1995, Pearce, 1996). Their biology and toxic metabolite production has been well studied, in particular using controlled phytotoxicity assays (Andolfi *et al.*, 2011, Akpaninyang and Opara, 2017). However, the possible role of hydraulic failure during pathogen-mediated plant dieback has been poorly investigated, and the underlying physiological mechanisms inducing leaf symptoms are not clear yet (Fradin and Thomma, 2006, McDowell *et al*., 2008). Moreover, the long-term impact (over seasons) and relationships between pathogens, leaf symptom presence, and the hydraulic functioning of the plant are still unknown. During vascular pathogenesis, both air (Pérez-Donoso *et al*., 2016) and nongaseous (Sun *et al*., 2013, Czemmel *et al.,* 2015, Pouzoulet *et al*., 2019) embolism have been observed. For example, air embolism is thought to accelerate pathogen progression during Pierce's disease (Pérez-Donoso *et al*., 2016), and nongaseous embolism is associated with occlusion of the xylem conduits by the plant that could slow the disease process while interfering with xylem water transport (Sun *et al*., 2013, Pouzoulet *et al*., 2019).

Xylem occlusion, usually through the production of tyloses and gels, is one of the first plant defense mechanisms against vascular pathogens (Pearce, 1996). Xylem parenchyma cells secrete gels and expand into the vessel lumen, forming tyloses, physically blocking pathogen progression (Zimmermann, 1979). Xylem anatomy plays an important role, both for vascular pathogen development (Martin *et al*., 2009, Martín *et al*., 2013, Venturas *et al*., 2014, Pouzoulet *et al*., 2017, 2020) and for tylose formation (Bonsen and Kucera, 1990, De Micco *et al*., 2016, Pouzoulet *et al*., 2019). If effective, this occlusion mechanism allows the plant to compartmentalize the infected zone and to generate new tissue around it (CODIT model, Pearce, 1996). Because tyloses can potentially interfere with the hydraulic functioning of the plant, they could exacerbate disease symptoms (Talboys, 1972). Tyloses are usually observed in close proximity

to pathogens, as shown in artificial inoculation studies (Czemmel *et al*., 2015, Rioux *et al*., 2018, among others). However, pathogens frequently proliferate in perennial organs without physically reaching the leaves, thus leaf symptoms are often induced at a distance (Beckmann and Roberts, 1995). A recent study shows that tyloses can be present in symptomatic leaves at a distance from the pathogen niches resulting in decreased leaf hydraulic conductivity (Bortolami *et al*., 2019).

Over the last decades, grapevine (*Vitis vinifera* L.) mortality and yield loss have been reported in European, American, and South African vineyards due to esca trunk disease (Cloete *et al*., 2015, Guerin-Dubrana *et al*., 2019). Esca, a vascular disease caused by the infection of multiple fungal pathogens, affects mostly mature grapevines (more than seven-years-old), and symptoms include trunk necrosis and leaf symptoms, consisting of "tiger-stripe" necrosis and leaf wilting (Lecomte *et al*., 2012, Claverie *et al*., 2020), which are not regularly expressed season-to-season even within individual vines (Guerin-Dubrana *et al*., 2013, Li *et al*., 2017). While the pathogens responsible for esca-induced trunk necrosis have been identified (Morales-Cruz *et al*., 2018, Brown *et al*., 2020), the underlying mechanisms of leaf and fruit symptoms, and plant death are still poorly understood. Bortolami *et al*. (2019) demonstrated that the two vascular pathogens related to esca (*Phaeomoniella chlamydospora* and *Phaeoacremonium minimum*) were never detected in leaves or in stems of the current year, but always in the trunk (independently from leaf symptom presence). They further showed that esca symptomatic leaves presented significant losses in hydraulic conductivity due to the occlusion of the xylem conduits by tyloses. Together, these results reveal that esca impacts leaf hydraulic functioning, but whether or not there is a corresponding failure in perennial organs, and the exact timing of this phenomenon, are still unknown. As stems and branches are the direct connections between the pathogen niche in the trunk and the observed symptoms in the leaves, the study of stem xylem integrity is crucial in the understanding of esca impact on grapevine physiology in the current year and across seasons.

In this study, we investigated stem xylem integrity in grapevine during esca leaf symptom formation asking the following questions: (i) Can esca lead to hydraulic failure in perennial organs? (ii) Does stem hydraulic failure occur prior to or after leaf symptom expression, and does it depend on xylem anatomy? (iii) Do long-term symptomatic plants present different xylem anatomy and levels of hydraulic failure from long-term asymptomatic plants? To answer these questions, we transplanted 28-years-old grapevines (*Vitis vinifera* L. cv Sauvignon blanc) from the field into pots to transport, manipulate, and study naturally esca-infected vines. We coupled *in vivo* visualizations of stem xylem functionality (using synchrotron-based X-ray microcomputed tomography) with stem specific hydraulic conductivity measurements (k_s), theoretical hydraulic conductivity estimates (k_{th}), optical observations of vessel occlusions, and pathogen detection during symptom appearance, while comparing plants with different symptom history record.

MATERIALS AND METHODS

Plant material

Vitis vinifera cv. Sauvignon blanc grafted onto 101-14 MGt were uprooted in winter 2017, 2018, and 2019 from a vineyard planted in 1992 located at INRAE Bordeaux-Nouvelle Aquitaine (44°47'24.8"N, 0°34'35.1"W) and transferred into pots. Following plant excavation, the root system (around 0.125 m^3) was immersed under water overnight, and powered with indole-3-butyric acid. The plants were potted in 20l pots in fine clay medium (Klasmann Deilmann substrate 4:264) and placed on heating plates at 30 °C for two months. Plants were then moved to a greenhouse, under natural light conditions, and watered with nutritive solutions (0.1 mM $NH_4H_2PO_4$, 0.187 mM NH_4NO_3, 0.255 mM KNO_3, 0.025 mM $MgSO_4$, 0.002 mM Fe, and oligo-elements [B, Zn, Mn, Cu, and Mo]) until the end of experiment. Since the plantation these plants have been trained with a double Guyot system. This training system requires a permanent main trunk and one cane on each side of the trunk which is left every year to carry the buds that will produce the stems of the year. During the growing season, the stems of the current year were trimmed at 1.5-2m, the secondary stems and inflorescences were removed just after bud-break. Each of these plants has been surveyed each year in the field since 2012 for esca leaf symptom expression following Lecomte *et al*. (2012), and has been classified yearly as leaf-symptomatic or asymptomatic. Plants were then classified by their long-term symptomatology record: plants asymptomatic from 2012 to 2018 (pA, previously asymptomatic), and plants that have expressed symptoms at least once between 2012 and 2018 (pS, previously symptomatic).

Esca symptom notation

The evolution of esca leaf symptoms was surveyed twice a week from June to October 2019 on every plant (n=58, Fig. 1). As presented in Fig. 1A, esca symptoms were scored at the stem and whole plant scales. The stems of the current year collected for analyses (both hydraulic measurements or microCT observations) could be noted as: asymptomatic (green leaves and apparently healthy), pre-symptomatic (leaves presenting yellowing or small yellow spots between the veins), tiger-stripe (typical pattern of esca leaf symptoms), or apoplectic (leaves passing from green to wilted in a couple of days). Along the experimentation, entire plants could be noted as asymptomatic (control) or symptomatic (when at least 25% of the canopy was presenting tiger-stripe leaf symptoms). At the end of the experiment (week 40, October 2019) each plant was classified as symptomatic or asymptomatic (control). We were then able to group each stem measured into six different groups (Fig. 1A): one group of stems from

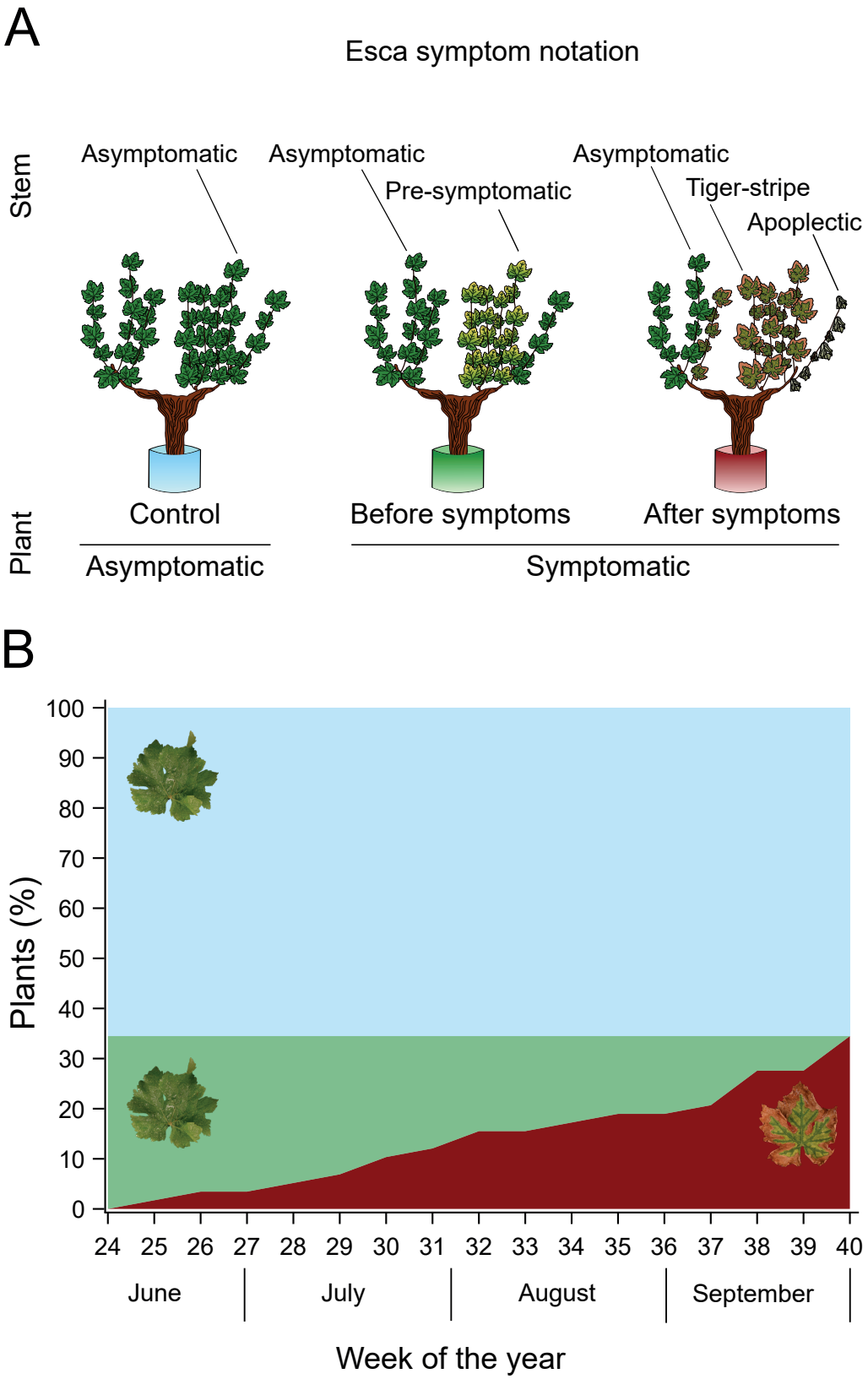

Figure 1. Representation of esca symptom notation during the experimental season. (**A**) Single stems could be noted as esca asymptomatic, pre-symptomatic, tiger-stripe, or apoplectic. Whole plants have been noted as control (asymptomatic from June to October) or symptomatic (with tiger-stripe symptoms at the end of the season). (**B**) Proportion of plants in each symptom category over the experimental season (n=58). The blue area corresponds to control plants, green area to esca symptomatic plants before symptom appearance, and red area to esca symptomatic plants.

control plants (asymptomatic from June to October) and five groups of stems from symptomatic plants: two before symptom appearance (asymptomatic and pre-symptomatic stems); and three after symptom appearance (asymptomatic, tiger-stripe, and apoplectic stems). To clearly differentiate asymptomatic stems collected from symptomatic plants and asymptomatic stems collected from asymptomatic plants, we considered plants (and their stems) that didn't show leaf symptoms during the experiment as control plants (or stems). We investigated whether symptom expression (final symptom notation in October 2019, see Fig. 1) differed between plants with contrasted long-term symptom history (previously asymptomatic vs previously symptomatic, Table 1) using a Chi-square test of independence.

X-ray microCT observation

Synchrotron-based microCT was used to visualize the content of vessels and their functionality in esca tiger-stripe and control stems. Three symptomatic plants (presenting tiger-stripe symptoms for 8, 7, and 3 weeks), and one asymptomatic-control plant were brought to the PSICHE beamline (King *et al*., 2016) at SOLEIL synchrotron facility in September 2019. Stems of the current year (ca. 2 m long) were cut under water and transferred into a solution containing 75mM of contrasting agent iohexol. The iohexol solution absorbs X-rays very strongly and appears bright white in X-ray scans above the iodine K-edge at 33.2 keV, and, once it has been taken up by the transpiration stream, the effective functionality of each vessel can be confirmed (Pratt and Jacobsen, 2018; Bortolami *et al.*, 2019). These stems were moved and left outdoor to transpire the solution for at least half a day. The stems were then transferred to the beamline stage and scanned twice in less than 5 minutes using two different energies of a high-flux (3 x 10^{11} photons mm^{-2}) monochromatic X-ray beam: 33.1 keV and 33.3 keV. The projections were recorded with a sCMOS camera equipped with a 250-mm-thick LuAG scintillator (Orca Flash, Hamamatsu, Japan). The complete tomographic scan included 1500 projections, and each projection lasted 50 ms. Tomographic reconstructions were performed using PyHST2 software (Mirone *et al*., 2014) using the Paganin method (Paganin *et al*., 2002), resulting in 32-bit volume reconstructions of 2048 x 2048 x 1024 voxels. The final spatial resolution was 2.8769 μm^3 $voxel^{-1}$.

Image analysis of microCT scans

The contrast agent iohexol allowed us to distinguish in intact scans the effective functionality of each vessel. In the absence of iohexol, X-ray microCT scans are used to distinguish air-filled vessels (appearing black, corresponding to native PLC) from sap-filled vessels (appearing grey). The addition of iohexol in the xylem sap allows to distinguish the functional vessels (they appear bright white when they transport the sap), from the non-functional ones (i.e. occluded vessels remaining grey, corresponding to occlusion PLC). We could also observe

partially occluded vessels (i.e. vessels with simultaneous presence of air and occlusions, or sap and occlusions). This specific case was observed by checking the presence of any occlusion in at least 200 slices in each volume. Partially occluded vessels were considered as occluded, some examples are presented in Fig. S1. The equivalent-circle diameter of air-filled, occluded, and functional (iohexol-filled) vessels was measured on the cross sections from the central slice of the microCT scanned volume using Imagej software (Schneider *et al*., 2012). In the high energy scans recorded at 33.3 keV X-ray beam, iohexol appears bright white but its contrast can sometimes impede the clear limit of the vessel lumen. Therefore, all vessel diameters were recorded on the scan recorded at low energy (33.1 keV X-ray beam), then the distinction of occluded from iohexol-filled vessels was done on the high energy scan (as done by Bortolami *et al*., 2019). The theoretical hydraulic conductivity of each vessel (k_{vessel}) [kg m MPa^{-1} s^{-1}] was calculated using the Hagen-Poiseuille equation [1]:

$$[1]\ k_{vessel} = \frac{(\pi \times Ø^4 \times \rho)}{(128 \times \eta)}$$

Where: Ø is the equivalent circle diameter [m], ρ the density of water [998.2 kg m^{-3} at 20°C], and η the viscosity of water [1.002 x 10^{-9} MPa s at 20°C]. The percentage loss of hydraulic conductivity given by native air embolism (native PLC) was calculated [2] by the ratio between the hydraulic conductivity of air-filled vessels and the whole-stem hydraulic conductivity:

$$[2]\ \text{Native PLC (\%)} = 100 \times \frac{(\sum k_{air-filled\ vessels})}{(\sum k_{\text{all vessels}})}$$

The percentage loss of hydraulic conductivity given by occlusions (occlusion PLC) was calculated [3] by the ratio between occluded (plus partially occluded) vessels and the whole-stem hydraulic conductivity:

$$[3]\ \text{Occlusion PLC (\%)} = 100 \times \frac{(\sum k_{\text{occluded vessels}} + \sum k_{\text{partially occluded vessels}})}{(\sum k_{\text{all vessels}})}$$

The total percentage loss of hydraulic conductivity (total PLC) was obtained by summing native PLC with occlusion PLC in each sample. As the first ring of xylem vessels (i.e. protoxylem) was always non-functional (>90% PLC), both in control and tiger-stripe stems, it was removed from the analysis.

We investigated whether native PLC, and occlusion PLC differed between control and esca tiger-stripe plants, using two independent generalized mixed linear models where plants were treated as a random effect. Proportional data (ranging from 0 to 1, dividing all PLC values by 100) was analyzed to fit a logit link function and binomial distribution as appropriate.

Monitoring stem hydraulic properties over time

Xylem integrity was monitored over time by measuring hydraulic properties in stems produced on the year of the experiment and collected on control and symptomatic plants along the season and during esca development. Specific hydraulic conductivity (k_s) was measured on internodes sampled in the center of the collected stem by the gravity method (Sperry *et al*., 1988), and compared to its theoretical analog (k_{th}) calculated from xylem anatomical observations on the same internode or on the one below (see the method described below). When there are observed differences in k_s among stems, comparisons with theoretical maximums (k_{th}) can show if lower k_s values result from anatomical differences (i.e. different vessel size distributions) or by hydraulic failure (in the case of similar vessel size and density). If k_s varies in unity with k_{th}, differences in k_s might result from anatomical differences (e.g. smaller k_s are related to smaller vessels), otherwise k_s variations are the consequence of hydraulic failure. Each method to measure k_s, k_{th}, and to observe tyloses is described below.

Sampling started on June 19th and finished on September 13th 2019 for a total of 10 sampling dates, 39 stems of the current year from 23 control-asymptomatic plants, and 49 stems of the current year from 17 symptomatic plants. We randomly sampled control plants and esca symptomatic plants all along the season through the evolution of esca symptoms, obtaining measurements from 14 weeks before until 10 weeks after symptom appearance. To explore the contribution of the experimental design to data analysis, we tested the effect of the year of uprooting (2018 and 2019), the position of the analyzed internode, and the week of the measurement (i.e. evolution during the season) on k_s and k_{th} in control plants using separate generalized linear mixed model with normal distributions and the plant treated as a random variable (Table S1). A significant impact of the year of uproot was found for k_s and k_{th} values in control plants (Table S1). This could have resulted from the more favorable conditions (i.e. climatic stability and nutrient availability) for the greenhouse grown vines (note that plants uprooted in 2017 were only esca symptomatic and were not included in this analysis). However, once k_s and k_{th} are plotted together (Fig. S2), all the values lie on the same regression line without generating outlier values (smaller k_s values correspond to smaller k_{th} values independently of the uprooting year).

Stem specific hydraulic conductivity (k_s)

k_s measurements were performed on one internode per stem, located in the center of the collected >1.5m long stem, following Torres-Ruiz *et al*. (2012) gravity method. In the early morning, each stem was cut at the base under water to avoid air entrance in the stem, maintained under water and brought to the laboratory. Hydraulic conductivity measurements were always done before noon, in order to minimize the delay (never more than four hours) from the cut to the measure. In the laboratory, a representative internode between the 4th to the 10th internode from the base (i.e. in the center of the stem) was cut underwater with a clean razor blade, the ends wrapped in tape, and the internode was connected to a pipe system. A flow of 20 mM KCl

solution passed through the sample from a reservoir to a precision electronic balance (AS220. R2, RADWAG, Radom, PL) recording the weight every 5 seconds using the WinWedge v3 5.0 software (TAL Technologies, Philadelphia, PA, USA). The solution was passed through the stem at four increasing pressures (ranging from 0.001 to 0.005 MPa), controlled by raising the source height. The average flow for each pressure step was determined after stabilization at a steady-state as the average of 10-15 measures. Hydraulic conductance, k [kg s^{-1} MPa^{-1}]

$$[4]\ k_S = \frac{(k \times l)}{A}$$

$$[5]\ A = (\left(\frac{d_1}{2}\right)^2 \times \pi) - (\left(\frac{d_2}{2}\right)^2 \times \pi)$$

was obtained by the slope generated by the flow and the corresponding pressure. The linear relationship between flow and pressure obtained were always characterized by R^2>0.97. Stem specific hydraulic conductivity, k_s [kg s^{-1} MPa^{-1} m^{-1}], was by the equations [4] and [5]:

Where: k is the hydraulic conductance, l is the length of the sample, A is the xylem area, d_1 is the external diameter of the debarked stem, and d_2 is the diameter of the central pith.

Stem theoretical hydraulic conductivity (k_{th}), vessel anatomy, and tylose observation

Just before hydraulic conductivity (k_s) measurements, the lower internode was stored at 4 °C in 80% ethanol for analysis of xylem anatomy. When possible, the same internode of k_s measurements was used for anatomical analysis and k_{th} estimations, otherwise the stored internode was used for the following protocol. 50 µm thick slices were obtained using a GSL-1 microtome (Gärtner *et al*., 2014). Slices were stained using a 0.5% safranin solution during 5 minutes, and then washed three to four times in ethanol (100%). They were quickly soaked in xylene and mounted on microscope slides with Permount Mounting Medium (Electron Microscopy Science, Hatfield, PA, USA). Images were captured with a stereo microscope SMZ1270 (Nikon,

$$[6]\ k_{th} = \frac{\sum k_{vessel}}{A}$$

France) mounted with a DS-Fi3 camera (Nikon, France). The theoretical conductivity of each vessel (k_{vessel}) [kg m MPa^{-1} s^{-1}] was calculated using the Hagen-Poiseuille equation [1]. k_{th} of the stem [kg s^{-1} m^{-1} MPa^{-1}] was then calculated, equation [6], by summing every k_{vessel} in the xylem area (A) [m^2]:

In the entire cross section of each sample, the physical presence (or absence) of tyloses in vessel lumina was visually assessed.

Regarding the statistical analysis, stems were grouped in six different categories following their esca symptomatology (as presented in Fig. 1A). We investigated whether k_s, k_{th}, and total vessel density differed among these different categories, and how k_s, k_{th}, and total vessel density

differed between stems with and without tyloses (independently from leaf symptom presence), using independent mixed linear general models. The symptom / tylose category and the year of uprooting (since it had a significant impact on k_s and k_{th} in control plants, Table S1) were entered as fixed effects, with the plant treated as a random effect since different stems were sometimes analyzed from the same plant (88 analyzed stems on 40 different plants). Total density and densities for each vessel diameter class were log-transformed prior to analysis to fit normality requirements. For the classes with no vessels (e.g. samples without vessel diameters above 160 µm), a minimal density of 0.0001 was assigned prior to log transformation. We investigated whether the frequency of symptomatic stems presenting tyloses changed with the symptom age (i.e. weeks between first symptom detection and k_s measurements on the same plant) with a Chi-square test. The relationships between stem k_s and k_{th} were tested using linear regression models. Finally, we investigated whether k_s and k_{th} in control stems differed between plants with different symptom history records using independent mixed linear general models with the plant treated as a random effect.

Fungal detection

Detection and quantification of *Phaeomoniella chlamydospora* and *Phaeoacremonium minimum* were performed using qPCR in a subsample of stems of the current year (n = 28) and perennial trunks (n = 20 plants) from the same symptomatic and control plants used for hydraulic and anatomical measurements. All along the season, basal internodes, from the same stems sampled for k_s and k_{th} measurements, were directly placed in liquid nitrogen and stored at -80 °C. At the end of the experiment, a subset of plants was cut at the base for trunk sampling. A 2 cm high section was cut with a sterilized hand saw. The bark was removed and the different tissues of each section (necrotic and apparently healthy wood) were separately collected using ethyl alcohol-sterilized shears in a sterile environment, and immediately placed in liquid nitrogen. All samples were ground in liquid nitrogen using a tissue lyser (Tissuelyser II, Qiagen, Germantown, MD, USA). DNA was extracted from 60mg of ground tissue using the Invisorb Spin Plant Mini Kit (Invitek GmbH, Berlin, Germany)according to the manufacturer's instructions. . Detection and quantification of *P. chlamydospora* and *P. minimum* (previously named *P. aleophilum*) DNA by qPCR (SYBR Green assays) was conducted using the primer sets PchQF (5'-CTCTGGTGTGTAAGTTCAATCGACTC-3')/PchQR (5'-CCATTGTAGCTGTTCCAGATCAG-3') and PalQF(5'-CCGGTGGGGTTTTTACGTCTACAG-3')/ PalQR(5'-CGTCATCCAAGATGCCGAATAAAG-3') (Pouzoulet *et al*. 2013). The qPCR reactions proceeded in a final volume of 25 µl, and the reaction mixtures containing 2 µL of DNA template, 12.5 µl of 2X SYBRGreen Quantitect Master Mix (Qiagen, Venlo, Netherlands), and each primer at a final concentration of 0.4 µM. Experiments were conducted with a Mx3005P Real-Time PCR cycler using MxPro qPCR software (Agilent Technologies). The cycling program, as described in Pouzoulet *et al*. (2017), consisted of an initial denaturation step at 95°C for 15 min,

and 40 cycles of 15 s at 95°C (for denaturation) followed by 45 s at 62°C (for both annealing and extension). A melting analysis of 40 min from 60 to 95° was performed to verify reaction's specificity and the absence of byproducts. Preparation and use of standard solutions for the absolute quantification of fungal DNA was realized following Pouzoulet *et al*. (2013) using ten-fold dilutions of fungal DNA extracts obtained from axenic cultures. Reaction efficiencies ranging from 90% and 95% with an $R^2 > 0.99$ (n=15) were obtained for both PchQF/R and PalQF/R primer sets. The average amount of DNA was determined based on three technical replicates (standards and plates) with a detection threshold superior to 95% (i.e. at least three positive amplification out of three replicates) or otherwise discarded (i.e. pathogen DNA was considered absent). Pathogen DNA quantity (average value of three technical replicates, fg/µl) was normalized by the amount of total DNA (ng/µl), measured using a Qubit fluorometer. The results from each trunk sample (i.e. necrotic or apparently healthy wood) were averaged together in order to obtain one quantification per plant. We investigated whether the amount of fungal DNA (both for *P. chlamydospora* and for *P. minimum*) in trunks differed between symptomatic and control plants, and between control plants with different symptom history records, using generalized linear mixed model with a poisson distribution and a log likelihood function.

Statistical analysis

All data management and statistical tests were done in SAS software (SAS 9.4; SAS Institute). We used PROC GLIMMIX for generalized linear mixed models, PROC GLM for generalized linear models, PROC REG for regression analyses and PROC FREQ for frequency analyses (Chi-square test of independence). The normality of the response variables was tested using a Kolmogorov-Smirnov test (PROC UNIVARIATE) prior to analyses. Data were log-transformed (total density) or appropriate distributions (binomial, poisson) were fitted when appropriate.

Table 1. Esca leaf symptom observations over the experimental season on *Vitis vinifera* cv Sauvignon blanc.

Symptom notation before 2019 / Symptom notation in 2019	All plants	Previously asymptomatic (pA)	Previously symptomatic (pS)
Esca-symptomatic	35 % (20/58)	30 % (6/20)	37 % (14/38)
Control-asymptomatic	65 % (38/58)	70 % (14/20)	63 % (24/38)

Plants are grouped by their symptom history: previously asymptomatic (pA, plants that have never expressed leaf symptoms between 2012 and 2018) and previously symptomatic (pS, plants that have expressed leaf symptoms at least once since 2012). Ratios present the number of plants in each symptom category (esca-symptomatic or control-asymptomatic) over the total number of plants of the category.

RESULTS

Esca leaf symptom expression within and across seasons

Esca leaf symptoms were recorded in 20 out of the 58 plants followed in this study (35%, Fig. 1, Table 1). The number of symptomatic plants increased gradually with time, from the first symptom appearance in early June to the last in late September (Fig. 1). There was no effect of the plant history (previously asymptomatic pA, or previously symptomatic pS) on 2019 symptom expression (n=58, X^2=0.27, P=0.60). On 20 pA plants, six (30%) expressed leaf symptoms in 2019 (Table 1). On 38 pS plants, fourteen (37%) showed symptoms in 2019 (Table 1). However, pS plants expressed symptoms from June to the end of September, while pA plants showed leaf symptoms only in September.

In vivo observations of esca symptomatic stems

Xylem vessels of control and tiger-stripe stems were observed using three dimensional X-ray microCT scans in iohexol-fed samples (Fig. 2, 3, Table S2). As shown in Fig. 2, functional and non-functional vessels can be discriminated through the use of iohexol (functional vessels appear bright white, non functional vessels appear either black if air-filled or grey if occluded). We observed almost totally functional stems in all asymptomatic stems (<20% total PLC, Fig. 2A-C), and 40% of tiger-stripe stems (e.g. Fig. 2D-G). Higher levels of PLC (>20% total PLC, Fig H-M) were observed in the remaining tiger-stripe stems, with 40% of tiger-stripe stems exhibiting over 50% total PLC (Fig. 2J-M). When the two components of PLC were disentangled, we observed that the level of native PLC remained low both in control (6.5 ± 2.6%) and in tiger-stripe (12.2 ± 2.9%) stems (Fig. 3A). Occlusion PLC values were virtually zero in control stems (0.7 ± 0.02%) while in tiger-stripe stems the mean occlusion PLC values was 27.5 ± 8.2% (Fig. 3B). Nevertheless, the variability of occlusion PLC across tiger-stripe stems was very high, the values ranging from 0.3% to 72.9% (Fig. 2D-M, and 3B), and occlusion

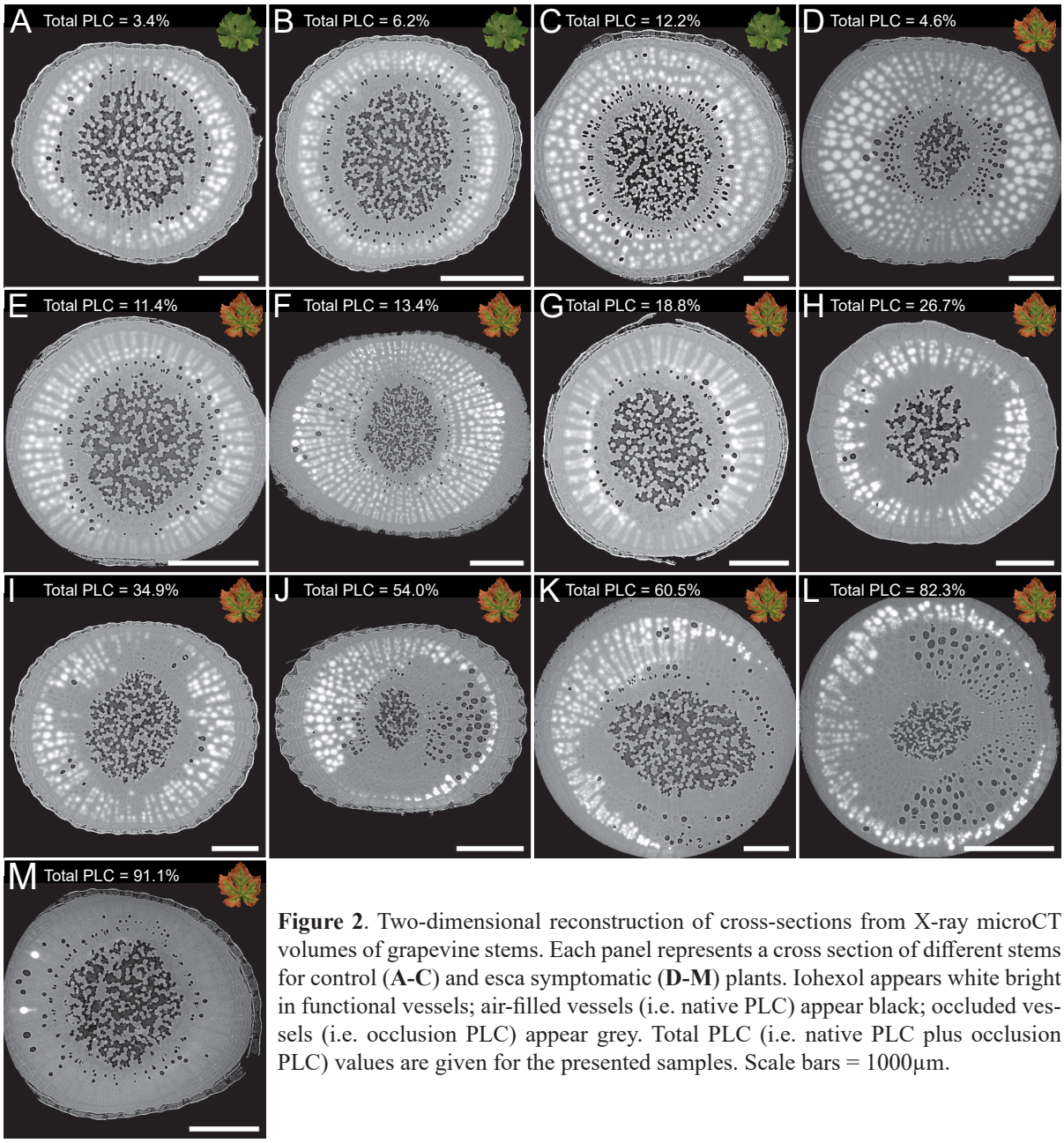

Figure 2. Two-dimensional reconstruction of cross-sections from X-ray microCT volumes of grapevine stems. Each panel represents a cross section of different stems for control (**A-C**) and esca symptomatic (**D-M**) plants. Iohexol appears white bright in functional vessels; air-filled vessels (i.e. native PLC) appear black; occluded vessels (i.e. occlusion PLC) appear grey. Total PLC (i.e. native PLC plus occlusion PLC) values are given for the presented samples. Scale bars = 1000µm.

PLC was not correlated to symptom age (n=10, $F_{2,7}$=0.19, P=0.83). Consequently, no statistical differences in native or occlusion PLC were found between control and tiger-stripe stems (Fig. 3). When higher occlusion PLC was measured (Fig. 2H-M), occluded vessels could be organized either on one side of the stem (Fig 2J-L) or randomly distributed across the section (Fig 2H, 2I, 2M). In 90% of symptomatic stems, we observed that the most external vessels were functional. Occlusions were present equally in all vessel diameter classes (Fig. S3).

Tylose development, stem specific (k_s) and theoretical (k_{th}) hydraulic conductivity during esca leaf symptom formation

Tyloses were identified in the xylem vessels of certain tiger-stripe stems and throughout the

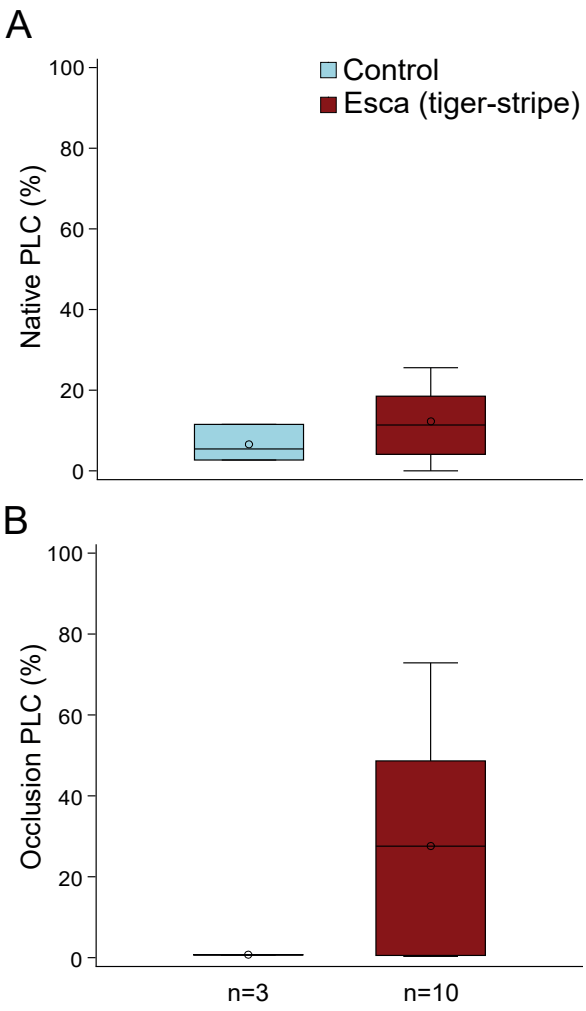

Figure 3. (**A**) Mean values of native PLC in control (blue) and esca tiger-stripe (red) stems of grapevine plants using X-ray microCT imaging. Differences were not significant (n=13, $F_{1,9}$=0.07, P=0.79). (**B**) Mean values of occlusion PLC in control (blue) and esca tiger-stripe (red) stems of grapevine plants using X-ray microCT imaging. Differences were not significant (n=13, $F_{1,9}$=0.33, P=0.58). Boxes and bars show the median, quartiles and extreme values, circles show mean values. N represents the sample size (number of analyzed stems) for each group.

temporal development of esca leaf symptoms, from the appearance of symptoms to 11 weeks after. All apoplectic stems and 62.5% (15 of 24 analyzed stems) of esca tiger-stripe stems presented tyloses, while all other stems (control, asymptomatic or pre-symptomatic) did not contain these occlusions, even until one week before symptom development. In esca tiger-stripe stems, tyloses were not related to specific plants, or to symptom age (i.e. on the same plant at the same moment, different symptomatic stems could present tyloses, or not, n=24, X^2=7.47, P=0.38).

Overall, no significant impact of esca symptoms was observed on k_s (Fig. 4A), even if tiger-stripe stems were divided between those with and without tyloses. Control stems presented a mean (± SE) k_s of 24.97 ± 1.72 kg s^{-1} MPa^{-1} m^{-1}; all the stems without tyloses measured on symptomatic plants showed the same range of values as control stems (Fig 4A, Table 2): 26.04 ± 4.71 for asymptomatic before symptoms appearance, 30.32 ± 4.26 for pre-symptomatic stems, 19.80 ± 5.18 for asymptomatic stems after symptom appearance on the plant, and 21.29 ± 5.40 for tiger-stripe stems without tyloses. Stems with tyloses (tiger-stripe and apoplectic stems) presented the lowest average k_s values (11.27 ± 2.86 and 2.47 ± 1.45 kg s^{-1} MPa^{-1} m^{-1} for tiger-stripe and apoplectic, respectively). Regarding k_{th}, no significant impact of esca symptoms was found (Fig. 4C, Table 2), all the values were in the same range, with average values ranging from 70.44 (for tiger-stripe stems with tyloses) to 87.88 (for pre-symptomatic stems) kg s^{-1} MPa^{-1} m^{-1}.

In order to further investigate the impact of esca on stem hydraulics, we explored the relationship between individual stem k_s and k_{th} in each symptom category (Fig. 4B, S4, Table 2). Significant relationships were found between k_s and k_{th} in all groups except in asymptomatic stems after symptom appearance and symptomatic stems with the physical presence of tyloses (Fig.

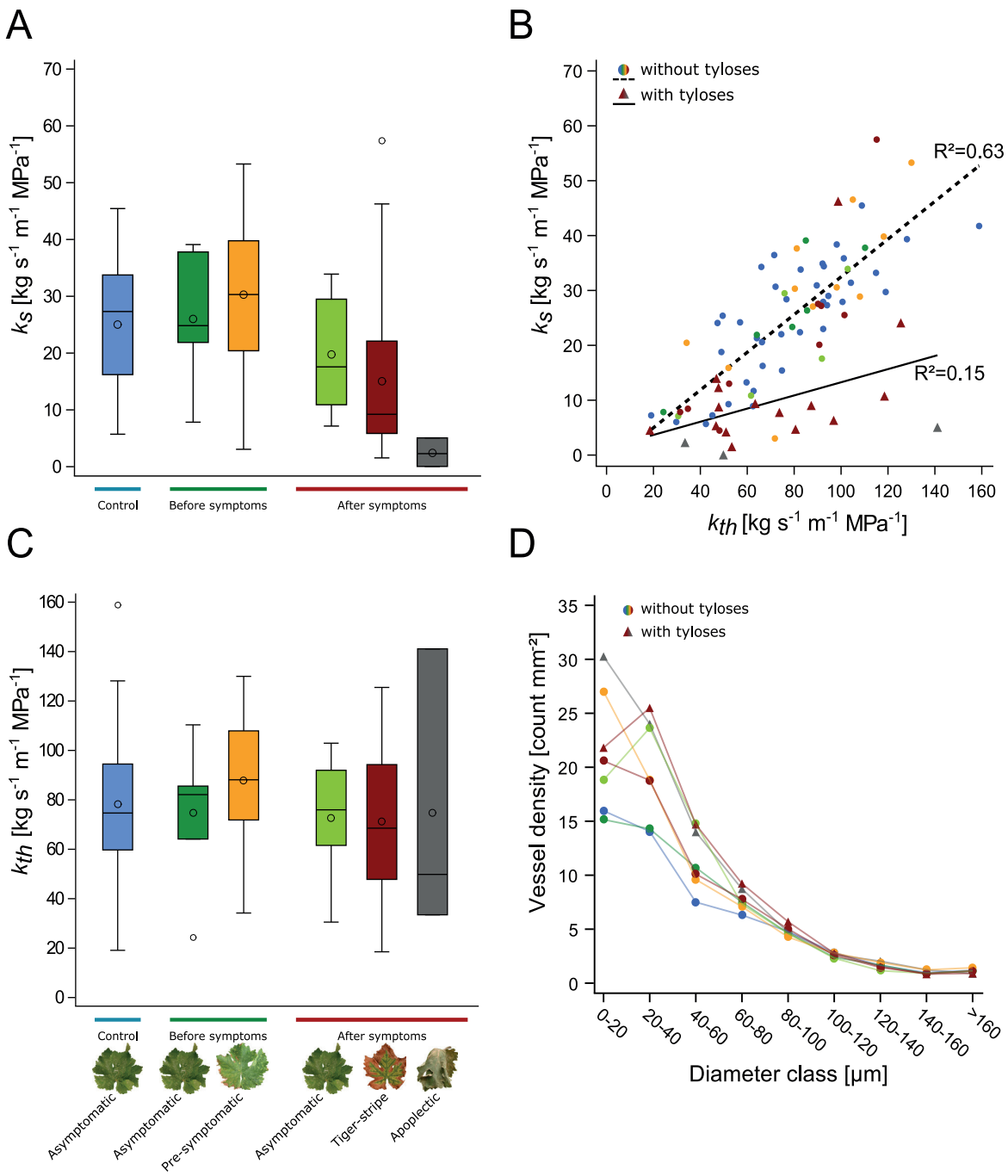

Figure 4. Relationships between specific stem hydraulic conductivity (k_s), theoretical stem hydraulic conductivity (k_{th}), and vessel density in control and esca symptomatic grapevine plants. (**A**) k_s values for control (blue); asymptomatic (dark green) and pre-symptomatic (yellow) stems in plants before symptom appearance; asymptomatic (light green), tiger-stripe (red), and apoplectic (grey) stems in plants after symptom appearance, differences were not significant (n=88, $F_{5,45}$=1.30 P=0.28). Boxes and bars show the median, quartiles and extreme values, circles within boxes correspond to means, and circles outside boxes to outlier values. (**B**) Relationships between k_s and k_{th}. Symbols represent the absence (circles) or presence (triangles) of tyloses in xylem vessels. Colors represent esca symptomatology (as in panel A). The dashed line represents the regression for stems in which no tyloses were observed in xylem vessels, and the solid line represents the regression for samples with tyloses. R² for the regression lines are indicated (see Table 2 and Fig. S4 for detailed analyses). (**C**) k_{th} values for the different stem categories as presented in panel a. Differences were not significant (n=88, $F_{5,45}$=0.58, P=0.71). (**D**) Relationships between mean values of xylem vessel density and their diameters. Differences in total vessel density and in vessel size distributions were not significant (n=88, $F_{6,45}$=0.77, P=0.60; n=792 (88 samples for 9 vessel classes), $F_{48,693}$=1.19, P=0.18). Colors and markers are the same as panel B.

Table 2. Values for specific stem hydraulic conductivity (k_s), theoretical stem hydraulic conductivity (k_{th}) and equations of regression lines between k_s and k_{th} for control and esca symptomatic stems.

Tyloses	Esca	k_s [kg s^{-1} m^{-1} MPa^{-1}]	k_{th} [kg s^{-1} m^{-1} MPa^{-1}]	n (stem - plant)	Regression
Absence	Control	24.97 ± 1.72	78.36 ± 4.51	39 - 23	$k_s = 0.3 \times k_{th} + 1.6$ R^2=0.61 P<0.0001
	Asymptomatic before symptoms	26.04 ± 4.71	74.75 ± 11.80	6 - 6	$k_s = 0.36 \times k_{th} - 0.94$ R^2=0.82 P=0.013
	Pre-symptomatic	30.32 ± 4.26	87.88 ± 8.54	11 - 7	$k_s = 0.37 \times k_{th} - 1.9$ R^2=0.54 P=0.010
	Asymptomatic after symptoms	19.80 ± 5.18	72.58 ± 12.64	5 - 2	$k_s = 0.33 \times k_{th} - 4$ R^2=0.64 P=0.104
	Esca (tiger-stripe)	21.29 ± 5.40	72.85 ± 10.41	9 - 5	$k_s = 0.45 \times k_{th} - 11.26$ R^2=0.74 P=0.003
Presence	Esca (tiger-stripe)	11.27 ± 2.86	70.44 ± 7.81	15 - 5	$k_s = 0.17 \times k_{th} -0.84$ R^2=0.22 P=0.077
	Esca (apoplectic)	2.47 ± 1.45	74.80 ± 33.48	3 - 2	$k_s = 0.04 \times k_{th} - 0.2$ R^2=0.68 P=0.385
Absence	All	25.06 ± 1.46	78.42 ± 3.37	70 - 37	$k_s = 0.34 \times k_{th} - 1.90$ R^2=0.63 P<0.0001
Presence	All	9.81 ± 2.51	71.16 ± 8.00	18 - 7	$k_s = 0.12 \times k_{th} - 1.28$ R^2=0.15 P=0.117

Values represent mean ± SE. n = sample size, (including the number of analyzed stems and- number of analyzed plants, respectively). See text and Fig. 4 for statistical analysis. A detailed esca symptom notation is provided in Fig. 1A. Bivariate plots of each regression are presented in Fig. S4.

S4, Table 2). The slopes of regression curves between k_s and k_{th} did not vary among groups in the absence of tyloses (slope values ranged between 0.3 and 0.4, Table 2) while it was close to 0 in the presence of tyloses (0.17 for tiger-stripe and 0.04 for apoplectic stems). When k_s and k_{th} are compared in the presence or absence of tyloses, we observed that k_s was significantly lower when tyloses were present (9.81 ± 2.51 kg s^{-1} MPa^{-1} m^{-1} in the presence of tyloses vs 25.06 ± 1.46 kg s^{-1} MPa^{-1} m^{-1} in the absence of tyloses, Table 2, n=88, $F_{1,49}$=7.11, P=0.01) while k_{th} did not significantly differ. Stems without tyloses presented a strong correlation between k_s and k_{th}, while in the presence of tyloses this relationship was not significant (Table 2, Fig. 4B).

Total vessel density did not significantly differ between stem symptomatology (comparing all the seven categories presented in Table 2), even when vessel density was partitioned by vessel diameter classes (Fig. 4D).

Finally, we tested the impact of disease history (comparing pA and pS plants) on the hydraulic conductivity and xylem anatomy in control plants. There were no differences between long-term symptomatic (pS) and long-term asymptomatic (pA) plants in stem k_s, stem k_{th}, or total

Table 3. Long-term impact of symptom presence (i.e. comparing plants with different disease history record) in control plants on specific stem hydraulic conductivity (k_s), theoretical stem hydraulic conductivity (k_{th}), stem total vessel density, and amount of *Phaeomoniella chlamydospora* and *Phaeoacremonium minimum* DNA in trunks of plants without foliar symptoms.

	Previously asymptomatic (pA)	**Previously asymptomatic (pS)**	**Type III Tests of Fixed Effects (pA vs pS)**
k_s [kg s^{-1} m^{-1} MPa^{-1}]	23.76 ± 2.30	26.54 ± 2.61	n=39, $F_{1,16}$=1.19, P=0.29
k_{th} [kg s^{-1} m^{-1} MPa^{-1}]	72.22 ± 4.85	86.30 ± 7.98	n=39, $F_{1,16}$=3.01, P=0.10
total vessel density [count mm^{-2}]	57.28 ± 4.03	52.61 ± 3.25	n=39, $F_{1,16}$=0.72, P=0.41
P. chlamydospora [pg ng^{-1}]	6.14 ± 1.90	10.15 ± 3.41	**n=13, $F_{1,11}$=5900.06, P<0.0001**
P. minimum [pg ng^{-1}]	9.27 ± 6.97	26.40 ± 13.83	**n=13, $F_{1,11}$=51014, P<0.0001**

Values represent means ± SE. Pathogen quantification was estimated as: pg fungal DNA ng^{-1} total DNA. Statistical tests used are individual generalized linear mixed models to compare pA vs pS plants (fixed effect) with the individual plants entered as a random effect in the models and the year of uprooting as a co-variable (fixed effect). Statistically significant results (P<0.05) are shown in bold.

vessel density (Table 3).

Fungal detection

The two vascular pathogens associated with esca (*Phaeomoniella chlamydospora* and *Phaeoacremonium minimum*) were never detected in stems of the current year while they were systematically detected in the perennial trunk of both control and symptomatic plants (Table 4). In trunks, a significantly higher quantity of fungal DNA was detected in tiger-stripe symptomatic plants than in controls (Table 4). We found 2.14- and 1.64-fold more of *P. chlamydospora* and *P. minimum* DNA in symptomatic trunks relative to controls. In control plants, different symptom history records impacted the quantity of fungal DNA detected by qPCR, for *Phaeomoniella chlamydospora*, and for *Phaeoacremonium minimum*. We found 1.65- and 2.84-fold more *P. chlamydospora* and *P. minimum* DNA in previously symptomatic trunks relative to previously asymptomatic trunks (Table 3).

DISCUSSION

Our results regarding the impact of esca on stem xylem integrity show that the presence of plant-derived tyloses induced hydraulic failure in 60% of symptomatic stems of the current year. Tyloses were only observed in symptomatic stems, and resulted in more than 50% PLC in 40% of the stems, unrelated to symptom age. We demonstrated that the presence of leaf symptoms during previous seasons had no impact on the likelihood of symptom appearance in the current year, or on stem hydraulic conductivity and xylem anatomy. Vascular fungi were

Table 4. Quantification by qPCR of *Phaeomoniella chlamydospora* and *Phaeoacremonium minimum* DNA in stems and trunks of different esca symptomatology.

Organ	Esca	n	*P. chlamydospora* [pg ng^{-1}]	*P. minimum* [pg ng^{-1}]
Stem	Control	8	0	0
	Pre-symptomatic	3	0	0
	Asymptomatic (after symptoms)	3	0	0
	Tiger-stripe (without tyloses)	4	0	0
	Tiger-stripe (with tyloses)	8	0	0
	Apoplectic	2	0	0
Trunk	Control	13	7.37 ± 1.67 (12/13)*	14.54 ± 6.51 (12/13)*
	Symptomatic	7	15.80 ± 3.12 (7/7)*	23.90 ± 8.82 (7/7)*

* Number of samples positive for the pathogen over the total number of analyzed samples.

Pathogen quantification was estimated as: pg fungal DNA per ng total DNA.Values represent means ± SE, n = sample size. Trunks of symptomatic plants presented higher amount of both *P. chlamydospora* and *P. minimum*, compared to control (n=20, $F_{1,18}$=29806.11.25, P<0.0001 and n=20, $F_{1,18}$=21925.4, P<0.0001, respectively). See text for statistical methods.

never detected in the same organs as the tyloses (stems of the current year), and although they were present in trunks of both tiger-stripe and control plants, tiger-stripe plants showed higher quantities of fungal DNA. Among control plants that did not express symptoms in the year of the study, we found higher quantities of fungal DNA in trunks of those plants with a long-term history of symptom formation. Albeit xylem occlusions were not observed in the totality of tiger-stripe stems, they could amplify yield loss plant mortality, especially in the context of climate change as they impair water transport in a majority of symptomatic stems.

In vivo xylem integrity observations and hydraulic vulnerability segmentation

Using direct X-ray microCT imaging in esca symptomatic stems, we found that hydraulic conductivity loss was almost entirely associated with the presence of tyloses. Different studies have investigated the link between vascular pathogen development and hydraulic conductivity in stems (Collins *et al*., 2009; Lachenbruch and Zhao, 2019; Mensah *et al*., 2020). During biotic stresses, air embolisms have been shown to decrease hydraulic conductivity during bacterial leaf scorch disease (McElrone *et al*., 2003; 2008), Pierce's disease (Pérez-Donoso *et al*., 2016), and Pine wilt disease (Yazaki *et al*., 2018). In the case of fungal wilt diseases, the hydraulic conductivity loss was associated with nongaseous embolism (i.e. tyloses) at the point of pathogen inoculation (Guerard *et al*., 2000; Sallé *et al*., 2008; Beier *et al*., 2017; Mensah *et*

al., 2020), or with canker presence in naturally infected stems (Lachenbruch and Zhao, 2019).

Using iohexol we were able to visually observe the exact spatial organization of functional vessels. Interestingly, in some symptomatic samples we found functional vessels surrounding the non-functional xylem (Fig. 2J-L), suggesting that the plant was able to preserve the more external vessels from occlusions or to form new functional vessels after the loss of conductivity. Moreover, the sectoriality of the occlusions observed in Fig. 2J-L was reminiscent of the sectoriality observed in the distributions of trunk necrosis, especially on the brown stripe necrosis appearing along the vasculature (Lecomte *et al*., 2012).

Comparing these results with our precedent study using the same technique in leaves, we showed that esca symptomatic leaves presented higher levels of occlusion PLC (61 ± 7% in midribs, and 54 ± 9% in petioles, data from Bortolami *et al*., 2019) compared to stems (27 ± 8 %, occlusion PLC), suggesting hydraulic vulnerability segmentation (although PLC in leaves and stems were measured in different plants and years). The hydraulic segmentation theory relies on the fact that annual organs (i.e. leaves) are more vulnerable than perennial organs (i.e. stems) to drought induced air embolism (Tyree and Ewers, 1991). Grapevine is well known for exhibiting strong hydraulic vulnerability segmentation (Charrier *et al*., 2016; Hochberg *et al*., 2016; 2017). This is thought to be adaptive, where the higher vulnerability in leaves and petioles favors embolism formation and leaf shedding prior to embolism formation in stems, thus protecting the perennial organs. Our observations during esca pathogenesis demonstrate that, analogous to the hydraulic vulnerability segmentation theory, leaves appear more vulnerable to the formation of nongaseous embolism as well, which could mitigate the risk of hydraulic failure in perennial organs. From another perspective, the difference may not be a direct effect of the specific organ's vulnerability to nongaseous embolism, but a consequence of a difference in the accumulation of putative toxins and/or elicitors. Indeed, we confirmed here that esca leaf symptoms occur at a distance from the pathogen niche because vascular pathogens were never detected in stems of the current year, suggesting that the plant may transport a signal (i.e. toxins or elicitors) from the infected trunk up to the leaves. If the signal accumulates in leaves in a higher amount than it does in the stems (water potentials are more negative in leaves compared to stems), and stimulates occlusion formation, stems would then be secondarily affected.

Hydraulic conductivity, tyloses, and vessel anatomy

Tyloses could have different impacts, both positive and negative, during wilt disease pathogenesis: (i) tyloses contribute to pathogen resistance as they aim to seal off vessel lumens and impede pathogens spread throughout the host (CODIT model, Shigo, 1984). This is the case regarding the susceptibility of different species or varieties to specific pathogens (Jacobi and MacDonald, 1980; Ouellette *et al*., 1999; Clérivet *et al.,* 2000; Et-Touil *et al*., 2005; Venturas *et al*., 2014; Park and Juzwik 2014; Rioux *et al*., 2018), in particular to *Phaeomoniella chlam-*

ydospora, one of the pathogen associated with esca (Pouzoulet *et al*., 2017; 2020). (ii) In other studies, it has been shown that tyloses can exacerbate symptoms (Talboys, 1972): they cause a reduction in stem hydraulic conductivity, sometimes associated with a reduction in stomatal conductance in leaves and, in the most severe cases, wilting (Parke *et al*., 2007; Beier *et al*., 2017; Lachenbruch and Zhao, 2019, Mensah *et al*., 2020 during fungi development; Sun *et al*., 2013; Deyett *et al*., 2019 during Pierce's disease). Our results suggest that during esca tyloses might lead to symptom exacerbation. Esca has also been suggested to lead to a general reduction in xylem water transport and stomatal conductance (Ouadi *et al*., 2019), and tyloses could be a major contributor to these phenomena as during winter senescence (Salleo *et al*., 2002; Sun *et al*., 2008). However, when symptomatic stems have no tyloses (~37% of the stems with tiger-stripe symptoms), esca leaf symptom formation seems to arise from within the leaf itself, and may not result from upstream hydraulic failure. Although tyloses were never detected in asymptomatic stems prior to the onset of leaf symptoms, the time sequence of tylose and leaf symptom development has still to be determined. Since both the microCT and anatomical observations visualize relatively narrow regions of the stems, tylose presence could have been underestimated (i.e. if there was additional tylose development up or downstream of the stem sections visualized). However, it should be pointed out that if significant underestimation were present we would expect some loss of conductivity even in internode sections from which we observed no tyloses in the sampled cross sections. At least when considering a single internode our direct hydraulic conductivity measurements do not support the hypothesis that tyloses were underestimated (Fig. 4B).

Xylem is the battleground between vascular pathogens and the plant's defense response (Yadeta and Thomma, 2013). Even if xylem vessel anatomy is less investigated, it could have a crucial role in plant resistance and response to vascular pathogens. For example, during Dutch elm wilt disease (due to *Ophiostoma spp.*) the most sensitive species and varieties present wider xylem vessels (Elgersma, 1970; Mcnabb *et al*., 1970; Solla and Gil 2002; Pita *et al*., 2018). Smaller vessels could occlude faster, sustaining a more efficient pathogen restriction (Venturas *et al*., 2014). Our results on xylem vessel anatomy suggest that stems with tyloses tend to present higher densities of small vessels, even if we did not observe any differences in total k_{th} values and microCT scans showed that occlusions appear randomly in every vessel size class (Fig. S3). It could be possible that tylose formation might be interfering with stem water relations reducing the carbohydrates available for plant growth, producing smaller vessels in stems of symptomatic plants. In contrast, artificial inoculations showed that xylem vessel diameter had a strong impact on esca-related vascular pathogen development (Pouzoulet *et al*., 2017; 2020), and in the kinetic of vessel occlusion in grapevine stems (Pouzoulet *et al*., 2019). The relationships between esca leaf symptoms, xylem anatomy, and tylose presence should be studied in detail in trunks, where vascular pathogens are present, and among different grapevine varieties

and rootstocks as they are known to show different susceptibility to symptom expression.

Long-term consequences of esca on leaf symptom expression and stem hydraulic integrity

In field surveys, esca leaf symptoms are often randomly distributed spatially throughout vineyards and are not consistent from season to season in individual vines (Mugnai *et al*., 1999; Surico *et al*., 2000; Marchi *et al*., 2006; Guerin-Dubrana *et al*., 2013; Li *et al*., 2017). However, esca-related vine death is strongly related to leaf symptoms as death is usually observed following a year with symptom expression (Guerin-Dubrana *et al*., 2013). In agreement with these field studies, we observed similar percentages of symptomatic plants between those that had already expressed esca symptoms in the past (from one to seven consecutive years, pS plants), and those that had never expressed symptoms over the past seven years (pA plants). However, we also found that pS plants expressed symptoms earlier in the season than pA plants, suggesting that symptoms might require more time to develop in pA plants. We did not find any significant differences in k_s and k_{th} values between plants with contrasted long-term symptom history. This result suggests that esca leaf symptoms may have xylem anatomical consequences within the year of expression by the production of tyloses, but not across seasons. Moreover, we showed that DNA pathogen amount (*Phaeoacremonium minimum* and *Phaeomoniella chlamydospora*) depends on the symptom expression in the season of sampling, and on the long-term symptom history. Altogether, these results suggest that a higher amount of vascular fungi in the trunk represents a higher risk in reproducing leaf symptoms, and consequently, a higher risk of plant death.

Hydraulic failure and esca leaf symptom pathogenesis

Our results showed that, even if esca-related stem occlusion was extremely variable, 40% of the microCT analyzed stems presented a total PLC greater than 50%. Under drought conditions alone, studies suggest that grapevines are not able to recover in the current season from PLC greater than 50% in stems (Charrier *et al*., 2018). Thus, to what extent these levels of esca-induced hydraulic failure compromise future vine performance, and/or increase the likelihood of developing esca leaf symptoms in the future remains an open question.

We showed that, similarly to visual leaf symptoms, tyloses in stems were generated at a distance from the pathogen niche in the trunk. Comparing our results with Bortolami *et al*. (2019), we show that the PLC due to the occlusions (hydraulic failure) observed using microCT in leaves was on average twice higher than the PLC observed in stems in the present work. We could hypothesize that, following pathogen activities in the trunk, a signal passing through the xylem network and stimulating tyloses, first accumulates in leaves and then affects the stems. However, the exact signal and action remain unknown, as we showed that the presence of ty-

loses depended upon given symptomatic stems rather than symptomatic plants (i.e. two stems in the same plant, with same tiger-stripe symptoms, sampled at the same moment, could or could not present tyloses).

We showed that there were no differences in symptom expression, nor in the stem hydraulic properties, regarding the long-term symptom history. We can conclude that the processes that generate tiger-stripe symptoms are largely restricted to the current year of the symptom expression. However, in plants expressing symptoms for the first time according to our disease record, these processes could require more time, as they showed symptoms only late in the season. The presence of occlusion, leading to hydraulic failure in stems, could exacerbate leaf symptom expression in the following seasons, possibly contributing to death. We could speculate that a stem expressing extensive hydraulic failure could be more prone to express symptoms in the following year or, in the worst cases, to die. If the level of hydraulic failure could affect the stem mortality in the following year, the choice of stems with a complete absence of failure during the winter pruning could reduce the impact of esca in vineyards. The pruning practices are known to impact the course of infection and leaf symptom development and it has been shown that trunk renewal could be an effective management practice to prevent grapevine trunk diseases in the vineyard (Travadon *et al*. 2016, Kaplan *et al*. 2016, Gramaje *et al*. 2018). In addition, the presence of occlusions could also amplify plant susceptibility to drought-induced hydraulic failure, enhancing the risk of plant mortality in the field as suggested by McDowell *et al*. (2008). It could be speculated that a decrease in soil water potential or a high evaporative demand, concomitant to esca-induced hydraulic failure, could embolize the remaining functional xylem vessels stopping the water flow and desiccating plant tissues (this could be the case in apoplectic plants for example). In perspective, future studies should in-

vestigate the link between pathogen activities and occlusion development, especially in trunks, and the subsequent hydraulic failure consequences on whole plant physiology.

SUPPORTING INFORMATION

The following Supporting Information is available for this article:

Figure S1. Two-dimensional reconstruction of longitudinal cross sections from X-ray microCT volumes of grapevine stems.

Figure S2. Relationship between k_s and k_{th} in control plants.

Figure S3. Vessel density and percentage of occluded vessels in tiger-stripe stems for different vessel diameter classes.

Figure S4. Relationships between k_s and k_{th} in each stem symptom category.

Table S1. Effect of year of uprooting, internode analyzed, and sampling date on k_s and k_{th} in control stems.

Table S2. Calculated theoretical hydraulic conductivity (k_{th} %), and hydraulic conductivity loss (PLC %) from X-ray microCT volumes of intact grapevine stems.

DATA AVAILABILITY STATEMENT

Raw datasets are available in the INRAE dataverse: Bortolami, Giovanni; Farolfi, Elena; Badel, Eric; Burlett, Regis; Cochard, Herve; Ferrer, Nathalie; King, Andrew; Lamarque, Laurent J.; Lecomte, pascal; Marchesseau-Marchal, Marie; Pouzoulet, Jerome; Torres-Ruiz, Jose M.; Trueba, Santiago; Delzon, Sylvain; Gambetta, Gregory A.; Delmas, Chloe E.L., 2021, "Raw data for the paper "Seasonal and long-term consequences of esca on grapevine stem xylem integrity"", https://doi.org/10.15454/U9KJEW, Portail Data INRAE, V1.

ACKNOWLEDGMENTS

We thank the experimental teams of UMR SAVE and UMR EGFV (Bord'O platform, INRAE, Bordeaux, France) and the SOLEIL synchrotron facility (beamline PSICHE) for providing the materials and logistics. Specifically, we thank Jérôme Jolivet and Sebastien Gambier (UMR SAVE) for providing technical knowledge and support for plant transplantation and maintenance. This work was supported by the French Ministry of Agriculture, Agrifood, and Forestry (FranceAgriMer and CNIV) within the PHYSIOPATH project (program Plan National Dépérissement du Vignoble, 22001150-1506) awarded to C.E.L.D., and program Investments for the Future (ANR-10-EQPX-16, XYLOFOREST).

Supporting information for:

Seasonal and long-term consequences of esca on grapevine stem xylem integrity.

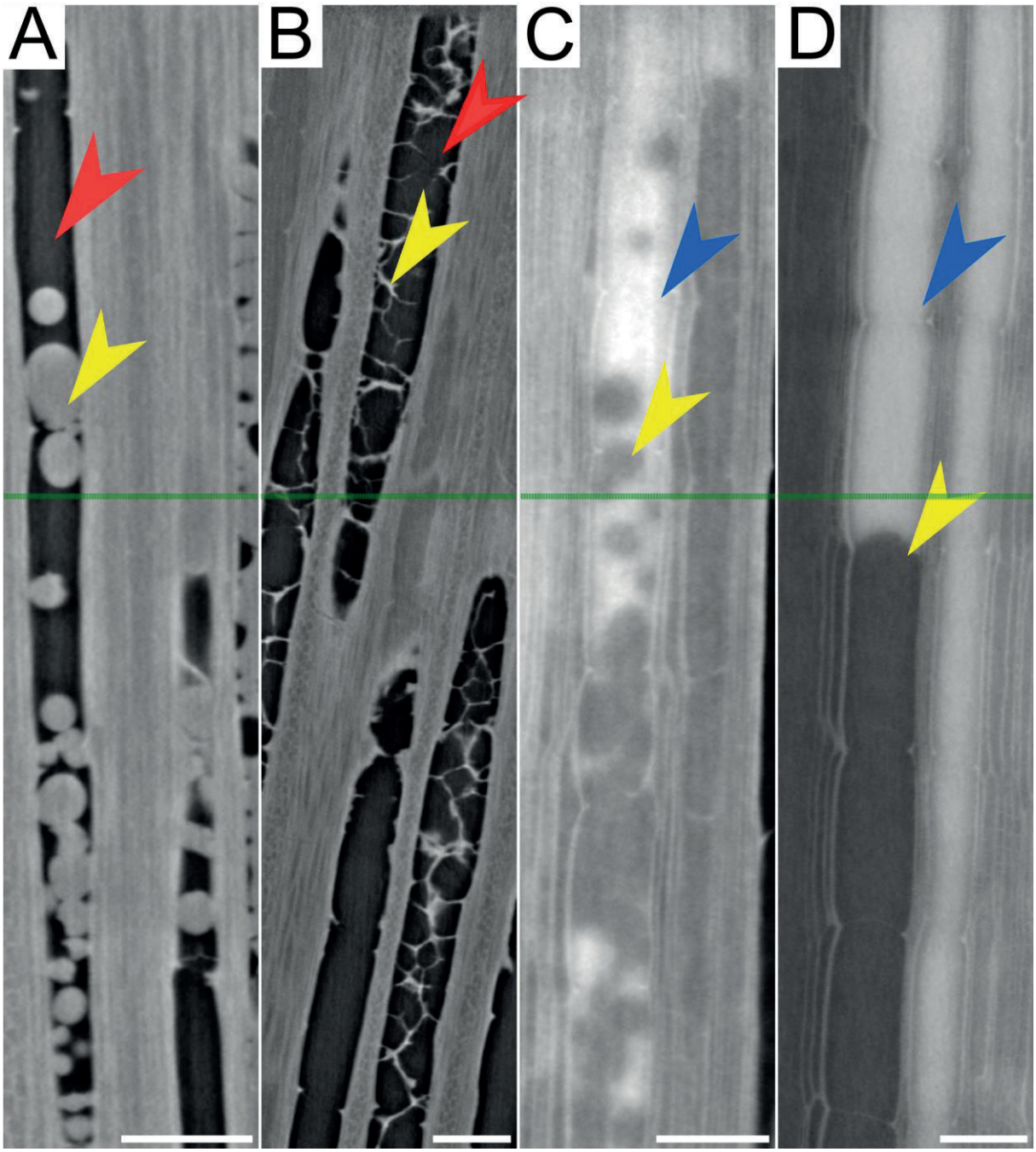

Fig. S1. Two-dimensional reconstruction of longitudinal cross sections from X-ray microCT volumes of grapevine stems, examples of apparently air-filled (A, B; red arrowheads), and apparently functional (C, D; blue arrowheads) vessels. Tyloses can only partially occlude the vessels (A, C, D, yellow arrowheads), or only the tylose walls are present without cellular content (B, yellow arrowheads). If only transversal cross sections (e.g. green lines) are analyzed, those vessels could be mistakenly considered as non-occluded. Scale bars = 200µm.

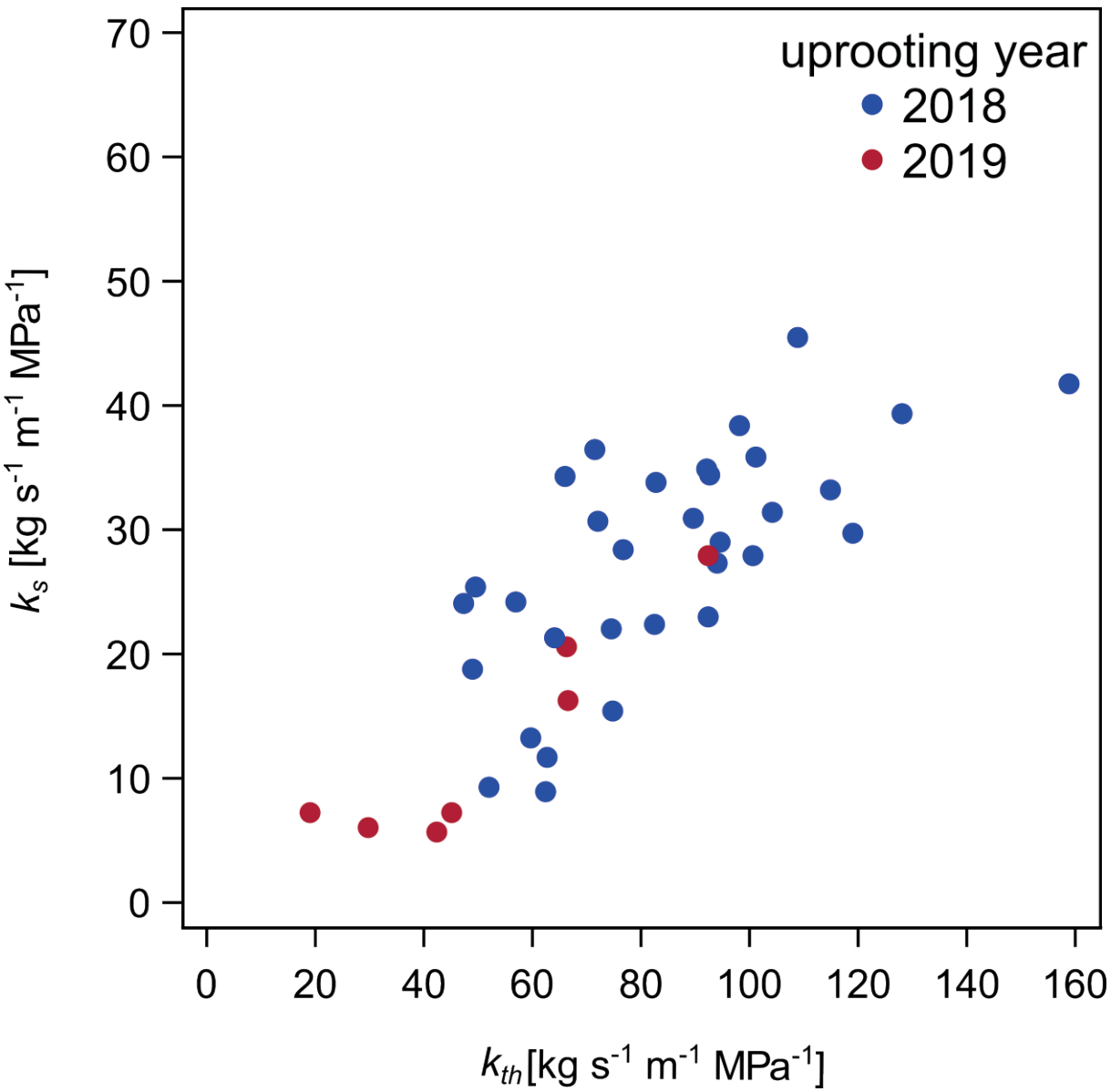

Fig. S2. Relationship between k_s and k_{th} in control plants. Blue dots represent plants uprooted in 2018 and red dots represent plants uprooted in 2019.

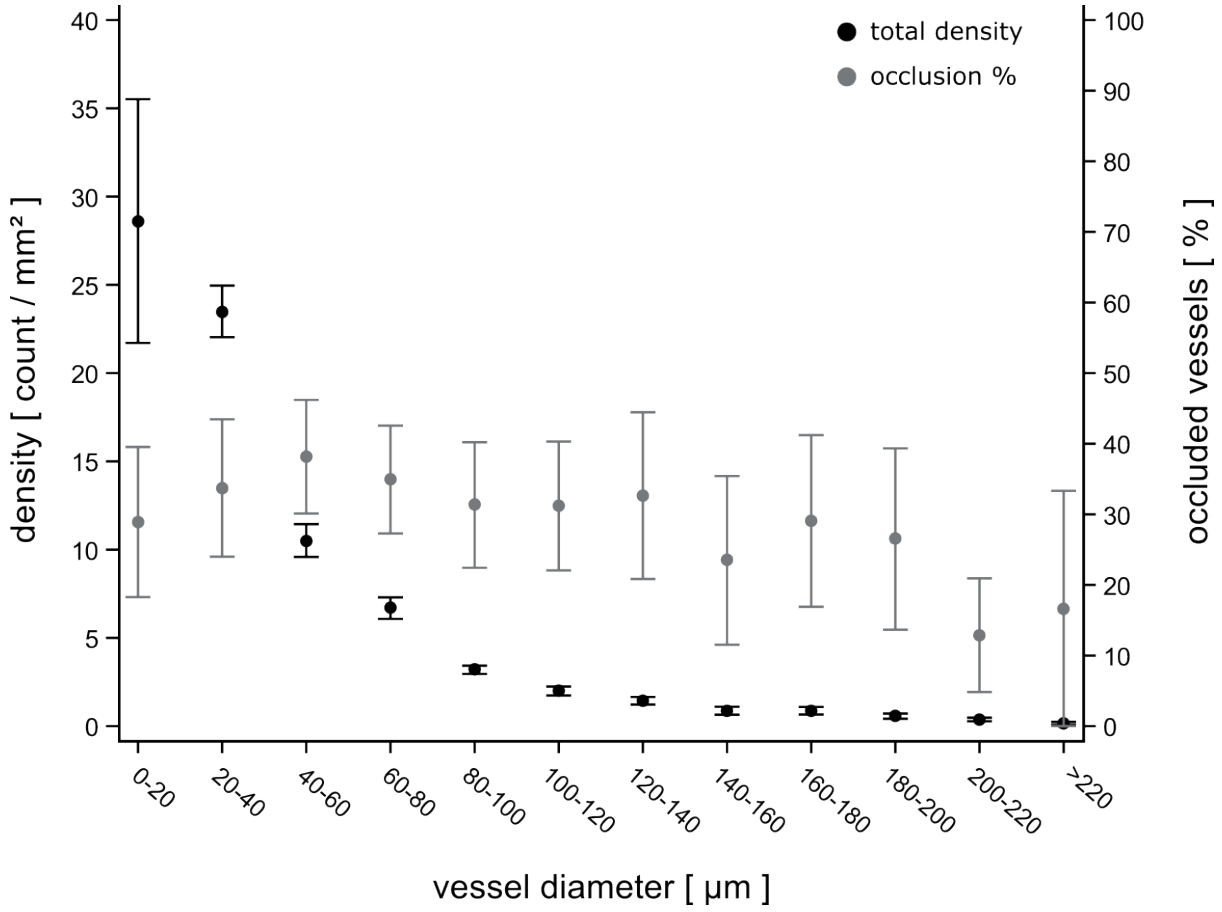

Fig. S3. Mean vessel density (black circles) in tiger-stripe stems for different vessel diameter classes and mean percentage of occluded vessels (grey circles) in each class from X-ray microCT imaging analysis. Error bars represent standard errors.

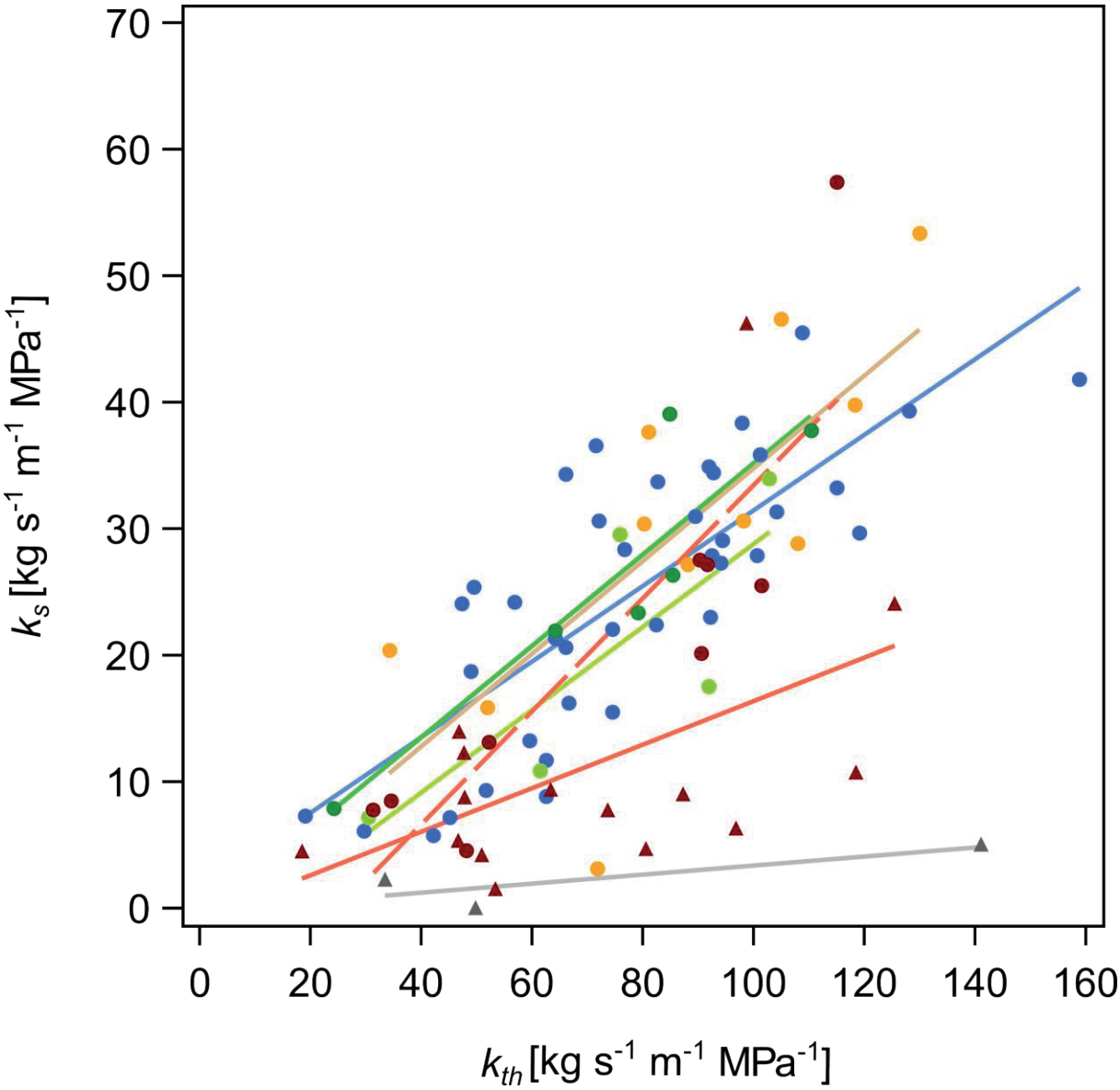

Fig. S4. Relationships between k_s and k_{th}. Blue symbols represent measurements in control stems; dark green symbols represent asymptomatic stems in plants before symptom appearance; yellow symbols represent pre-symptomatic stems in plants before symptom appearance; light green symbols represent asymptomatic stems in plants after symptom appearance; red circles and dashed red line tiger-stripe stems without tyloses; red triangles and solid red line tiger-stripe stems with tyloses; grey symbols represent apoplectic stems. Sample sizes, R^2 and equations of regression lines are presented in Table 2.

Table S1. Effect of year of uprooting, internode analyzed, and sampling date on k_s and k_{th} in control stems (n=39 stems from 23 plants) .

Fixed effects	**k_s (n=39)**	**k_{th} (n=39)**
Year of uprooting	**$F_{1,16}$ = 10.31** ***P* = 0.006**	**$F_{1,16}$ = 9.38** ***P* = 0.007**
Internode	$F_{4,12}$ = 2.15 *P* = 0.14	$F_{4,12}$ = 2.22 *P* = 0.13
Sampling date	$F_{7,9}$ = 1.77 *P* = 0.21	$F_{7,9}$ = 1.53 *P* = 0.27

Individual generalized linear mixed models with the individual plants entered as a random effect in the models. Statistically significant results (P<0.05) are shown in bold.

Table S2. Calculated theoretical hydraulic conductivity (k_{th} %), and hydraulic conductivity loss (PLC %) from X-ray microCT volumes of intact grapevine stems.

Stems	n	Functional k_{th}	Native PLC	Occlusion PLC
Control	3	92.75 ± 2.60	6.54 ± 2.61	0.71 ± 0.02
Esca (tiger-stripe)	10	60.22 ± 9.70	12.25 ± 2.87	27.53 ± 8.24

Values are means ± standard error, n = sample size (stems)

Results summary - Chapter 4

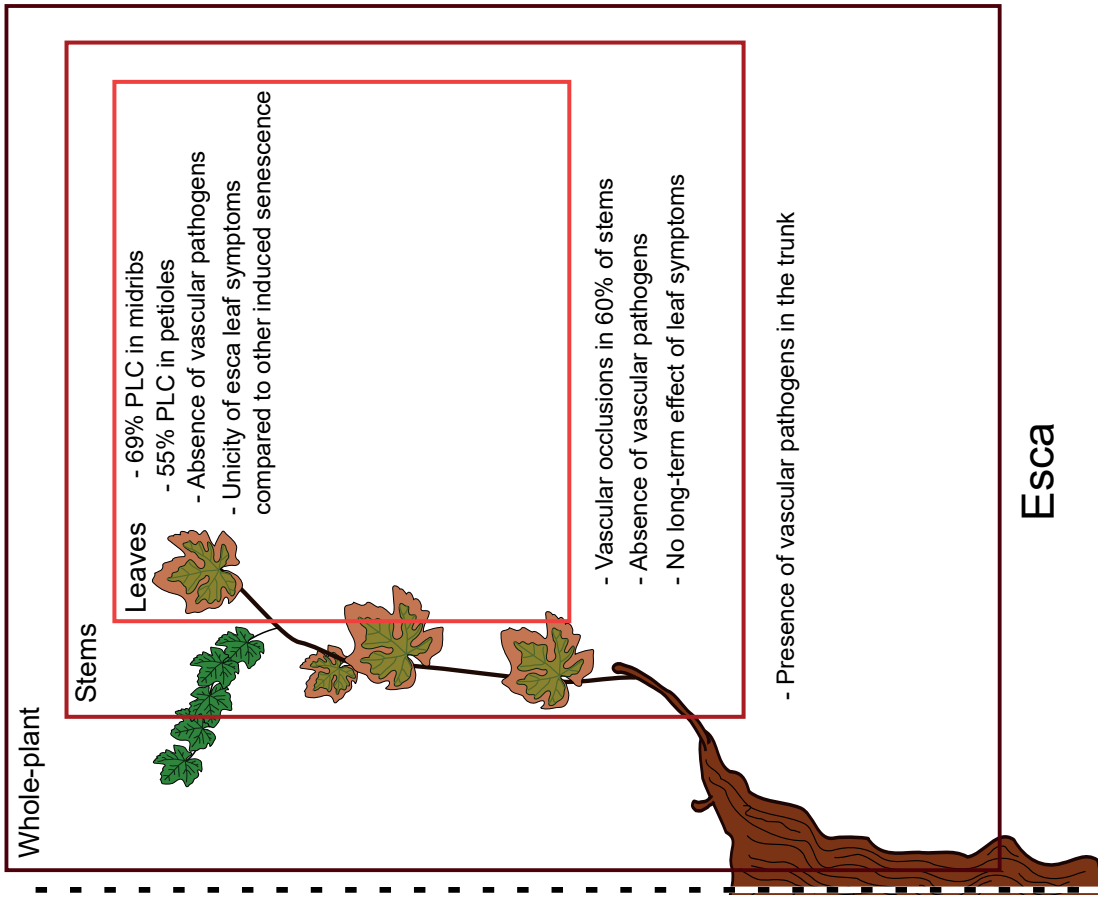

CHAPTER 5

Grapevines under Drought Do Not Express Esca Leaf Symptoms: the Physiology behind Drought and Vascular Pathogen Antagonism

Résumé : Dans le contexte du changement climatique, la mortalité des plantes pérennes est en train d'augmenter que ce soit dans les écosystèmes naturels ou agricoles. Cependant, la compréhension des mécanismes sous-jacents au processus de mortalité reste encore limitée, d'un côté par les interactions complexes entre facteurs biotiques et abiotiques, et de l'autre côté par les limites techniques imposées dans l'étude de ces interactions. Ici nous avons étudié l'interaction entre deux principaux facteurs qui causent le dépérissement des plantes pérennes, la sécheresse et les maladies vasculaires (plus spécifiquement, l'esca), dans le cas d'une des cultures les plus importantes économiquement au monde, la vigne. Nous avons mis en évidence que la sécheresse a complètement inhibé l'expression des symptômes foliaires d'esca. Pour mieux comprendre l'antagonisme observé entre sècheresse et esca, nous avons observé la réponse physiologique des plantes soumises à la sécheresse ou à l'esca, en quantifiant les relations hydriques des plantes (les potentiels hydriques et la conductance stomatique) et la balance carbonée (assimilation de CO_2, et quantification des chlorophylles et carbohydrates non-structuraux, NSC). Nos résultats soulignent la physiologie distincte derrière ces stress, en montrant que l'esca (et le déclin consécutif de la conductance stomatique) n'est pas lié à une baisse de potentiel hydrique, et qu'il génère différentes dynamiques saisonnières d'échanges gazeux et de NSC comparée à la sècheresse.

AUTHORS

G. Bortolami[a], G. A. Gambetta[b], C. Cassan[c,d], S. Dayer[b], E. Farolfi[a], N. Ferrer[a], Y. Gibon[c,d], P. Lecomte[a], J. Jolivet[a], C.E.L. Delmas[a]

[a]INRAE, BSA, ISVV, SAVE, 33882 Villenave d'Ornon, France

[b]EGFV, BSA, INRAE, Université de Bordeaux, ISVV, 33882 Villenave d'Ornon, France

[c]Univ. Bordeaux, INRAE, UMR1332 Biologie du fruit et Pathologie, Centre INRAE Nouvelle Aquitaine - Bordeaux, Villenave d'Ornon, France

[d]Bordeaux Metabolome Facility, INRAE, Univ. Bordeaux, doi:10.15454/1.5572412770331912E12, Centre INRAE Nouvelle Aquitaine - Bordeaux, F-33140 Villenave d'Ornon, France

AUTHOR CONTRIBUTIONS

G.B., G.A.G., C.E.L.D. designed the experiments;
G.B., C.E.L.D., N.F., J.J., S.D., E.F., conducted the measurements, sampling and drought maintenance in the greenhouse;
G.B., C.E.L.D., N.F., E.F., conducted the esca symptom notations;
G.B., C.C., Y.G., J.J. performed the NSC and chlorophyll quantification analysis;
E.F. conducted the hydraulic conductivity measurements;
J.J. assured the plant transplantation and maintenance;
P.L. provided data on disease history of the plants and shared expertise on esca symptoms;
G.B., C.E.L.D., G.A.G. wrote the article;
all authors edited and agreed on the last version of the article

ABSTRACT

In the context of climate change, plant mortality is increasing worldwide in both natural and agro-ecosystems. However, our understanding of the responsible underlying processes is limited by the complex interactions between abiotic and biotic factors and the technical challenges that limit investigations on these interactions. Here we studied the interaction between two main drivers of mortality, drought and vascular disease (esca), in one of the world's most economically valuable fruit crops, grapevine. We found that drought totally inhibited esca leaf symptom expression. In order to understand the observed antagonism between drought and esca, we disentangled the plant physiological response to the two stresses by quantifying whole-plant water relations (i.e. water potential and stomatal conductance) and carbon balance (i.e. CO_2 assimilation, chlorophyll and non-structural carbohydrates, NSC). Our results highlight the distinct physiology behind these two stress responses, indicating that esca (and subsequent stomatal conductance decline) does not result from decreases in water potential, and generates different gas exchange and NSC seasonal dynamics compared to drought.

INTRODUCTION

For many plant pathogens it is still largely unknown if their interactions with abiotic stresses are synergistic, antagonistic, or neutral. These interactions are particularly crucial in the case of vascular diseases and drought (McDowell *et al*., 2008, Yadeta and Thomma, 2013, Oliva *et al*., 2014). Both affect the same plant tissue, the xylem vascular network, which is responsible for the movement of water and nutrients throughout the plant. A strong synergy when combining drought and vascular disease could accelerate plant death (McDowell *et al*., 2008, Oliva *et al*., 2014), and has strong implications in the context of climate change where a global increase of drought and associated plant mortality is expected (Allen *et al*., 2010).

Grapevine, one of the most economically valuable crops in the world (Alston and Sambucci, 2019), is being threatened by future climate change scenarios (Morales-Castilla *et al*., 2020). Since the early 2000s old world vineyards have exhibited increasing yield losses, and although the causes are not completely understood, an increased incidence of trunk diseases has been identified as one of the main contributors (Mondello *et al*., 2019, Claverie *et al*., 2020). One of the most prominent of these diseases is esca, a vascular disease associated with a loss in fruit quality and quantity, and increased vine mortality (Bertsch *et al*., 2013, Fischer and Ashnaei, 2019). Drought events also cause yield decline, and when severe and/or too long, grapevine mortality (Chaves *et al*. 2010, van Leeuven and Darriet, 2016). Due to their climatic and edaphic environment, most of the world's wine regions are exposed to a high risk of drought, as irrigation is not a sustainable long-term solution and rainfall is often not sufficient to supply grapevine evapotranspiration (e.g. in the mediterranean area, Fraga *et al*., 2013, Costa *et al*., 2016). Because both drought and esca are associated with xylem hydraulic failure (Gambetta *et al*. 2020, Bortolami *et al*. 2019, 2020), and theoretically, with non-structural carbohydrates consumption (McDowell *et al*., 2008, Oliva *et al*. 2014, Claverie *et al*., 2020), these stresses could synergize and amplify the current vineyard decline. Therefore, there are real and urgent concerns regarding the outcome of the interaction between drought events and vascular pathogenesis in grapevine.

On many recorded parameters, plant responses to vascular disease and drought appear similar and include decreases in leaf gas exchange (Magnin-Robert *et al*., 2011, Castillo-Argaez *et al*., 2020, Knipfer *et al*., 2020), losses of hydraulic conductivity (Choat *et al*., 2012, Bortolami *et al*., 2020, Mensah *et al*., 2020), wilting (i.e. decreases in cell turgor) and scorching of leaves (Lecomte *et al*., 2012, Bartlett *et al*., 2016, Flajšman *et al*., 2017). Because they induce similar plant responses, it could be assumed that their interactions would be synergistic. However, we lack the detailed whole-plant physiology studies necessary to determine if this is true. This is probably because studying disease-drought interaction can be extremely challenging. Some vascular diseases, including esca, cannot be reproduced through the artificial inoculation of

plants. Thus studies rely on naturally-infected, field experimentation where the disease history of specific plants is largely unknown and applying well-controlled water deficits (as well as controlling other environmental factors) is either difficult or impossible.

The main objective of this study was to understand the interaction between esca and drought, finding which whole-plant physiological thresholds would trigger their synergism (or antagonism). We overcame the technical barriers by transplanting control and naturally infected plants with known disease histories from the field into pots, to precisely manipulate their watering regime and study the combined effect of esca and drought. We maintained half of the plants under a water deficit at a predawn water potential (Ψ_{PD}) ≈ -1MPa during three months in two consecutive seasons, which simulated a moderate to severe level of drought (Charrier *et al*., 2018). During these periods we quantified plant-water relations (water potential, whole-plant and leaf- stomatal conductance), carbon balance (CO_2 assimilation, chlorophyll fluorescence and non-structural carbohydrates NSC quantification in leaves and stems), and the development of esca symptoms. Our results showed that alone esca and drought induced distinct whole-plant physiological responses; once combined the two stresses strongly interact, antagonistically, opening new perspectives on the plant-pathogen-environment relationships impacting vineyard sustainability.

RESULTS

Drought inhibits the formation of esca leaf symptoms

During vascular diseases, water deficit conditions can amplify (Croisé *et al*., 2001, Silva-Lima *et al*., 2019), hinder (Pennypacker *et al*., 1991, Arango-Velez *et al*., 2016), or have no effect (Lopisso *et al*., 2017) on vascular pathogens. However, most of the studies examining the impact of water deficit on fungal infections cannot be easily interpreted because water potential values were rarely recorded, thus in these cases it is impossible to assess to what extent plants (and pathogens) were experiencing drought conditions. In this study, we uprooted mature (30 years-old) naturally infected plants from the field after a long term disease monitoring. We then divided plants by their symptom history record: plants that never expressed esca leaf symptoms (previously asymptomatic, pA) and plants that expressed esca leaf symptoms at least once since 2012 (previously symptomatic, pS). From July to October (2018 and 2019), we subjected half of the plants to water deficit, targeting a moderate to severe level of stress (Ψ_{PD} ≈ -1MPa), while the well-watered plants maintained high Ψ_{PD} (close to 0 MPa), independently of their disease status (Fig. 1a). The same plants were subjected to water deficit each year. In both years, we observed that ~30% (on average) of well-watered (WW) plants developed esca leaf symptoms while water deficit totally inhibited esca leaf symptom development as none of the droughted plants developed leaf symptoms in either year (Table 1). More specifically, in 2018

Table 1. Effect of the watering regime and past disease historical record on esca leaf symptom development in *Vitis vinifera* cv Sauvignon blanc.

Watering regime	Well-watered (WW)		Water deficit (WD)	
Historical esca record	**pA**	**pS**	**pA**	**pS**
Presence esca leaf symptoms in 2018	14 % (2/14)	50 % (6/12)	0 % (0/13)	0 % (0/12)
Presence esca leaf symptoms in 2019	33 % (4/12)	31 % (4/13)	0 % (0/13)	0 % (0/13)

Plants are grouped by their watering regime: well-watered plants (WW), weekly mean $\Psi_{PD} > -0.3$ MPa; water deficit plants (WD) weekly mean $\Psi_{PD} < -0.5$ MPa from July to October, and by their disease historical record: plants that never expressed symptoms since 2012 (previously asymptomatic, pA), and plants that have expressed at least once since 2012 (previously symptomatic, pS). Ratios present the number of symptomatic plants in each category over the total number of plants of the category in each of the two different years.

14% of the previously asymptomatic plants (WW-pA) and 50% of the previously symptomatic plants (WW-pS) expressed esca leaf symptoms (Table 1). In 2019, 33% of WW-pA and 31% of WW-pS plants expressed esca leaf symptoms. In contrast, the totality of plants subjected to water deficit (WD) remained asymptomatic during the two years, independently of the disease status during the previous seasons (pA or pS; Table 1). Given the observed frequencies of symptom development in the WW-pA and WW-pS plants over the two years the likelihood of having no plants express symptoms during the two years is less than 1 in 100 million. Thus, our confidence that the drought effect is real is extremely high. Moreover, esca symptom incidence found in WW plants are similar to field observations in the parcel from which the plants were transplanted. For the period 2013-2017 we found an average (± SE) esca incidence of 39.5 ± 7%; more specifically, 12.4 ± 3% for pA plants (i.e. plants that expressed esca for the first time each year) and 54.2 ± 10% for pS plants (plants that already expressed esca). To better understand how and why esca and drought express their antagonism, we explored how plant-water relations and carbon balance changed under drought or esca at the whole plant scale.

Water potential regulation during esca pathogenesis was similar to control well-watered conditions, not to drought

During vascular pathogenesis, it has been found that *Verticillium* infection caused a decrease in minimum water potential (Bowden *et al*., 1990), inducing a drought-like event. However, water potential regulation has never been investigated during esca leaf symptom development. Applying the theoretical hydraulic model in plant water movement (Tyree and Sperry, 1988), we hypothesized that the loss in hydraulic conductivity observed during esca (Bortolami *et*

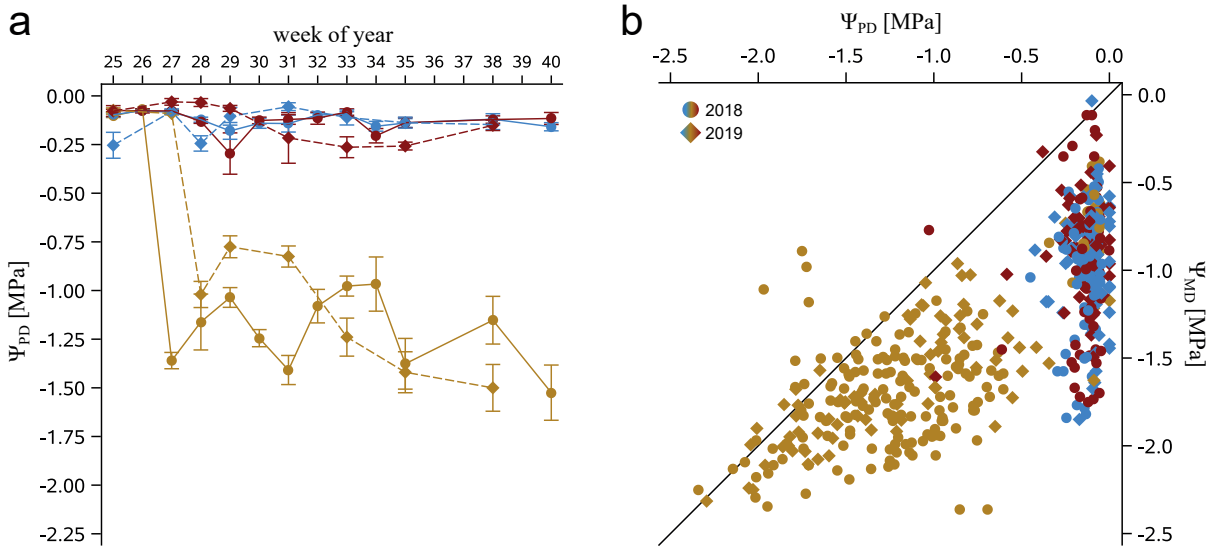

Figure 1. Leaf water potential (Ψ) monitoring in 2018 and 2019 in *Vitis vinifera* cv Sauvignon blanc. (**a**) Mean ± SE predawn water potential (Ψ_{PD}) values over the experimental periods, expressed in week of year from mid-June (week 25) to the beginning of October (week 40). Symbols and lines represent the year: circles and solid lines for 2018, diamonds and dashed lines for 2019. Colors represent the different stress applied: blue for control, red for esca symptomatic, and yellow for plants under water deficit (WD). (**b**) Relationship between Ψ_{PD} and midday water potential Ψ_{MD} over the two years, colors and symbols are the same as panel A. The black line indicates the 1:1 regression. A significant effect of the disease or water regime status was found for Ψ_{PD} ($F_{2,559}$=230.55, P<0.0001), and Ψ_{MD} ($F_{2,456}$=126.16, P<0.0001), using the same tests as in Supplementary Table 1.

al., 2019, 2020) would induce an increase in xylem tension (i.e. decrease in minimum water potential) in symptomatic plants, in order to maintain the same transpiration rate in leaves. Our results showed that midday leaf water potential (Ψ_{MD}) was not significantly different between well-watered control and esca symptomatic plants (Ψ were always measured in asymptomatic leaves) over two consecutive years (with average values of Ψ_{MD} = -0.98 ± 0.03 MPa and -0.94 ± 0.02 MPa respectively, Fig 1B), and was significantly lower after applying water deficit (Ψ_{MD} = -1.67 ± 0.02 MPa, on average, Fig 1B). This indicates that, contrary to what we expected, esca symptomatic plants were able to regulate their water potential similarly to controls, despite the presence of hydraulic dysfunctions in leaves and stems. However, in four out of 111 Ψ_{PD} measurements symptomatic plants presented Ψ_{PD} < -0.5 MPa, and in many cases when we measured Ψ in symptomatic leaves values were not reliable as gel, not water, was observed exuding from petioles. This suggests that in some (rare) cases the disease could lead to water transport impairment (i.e. the demand exceeded the supply). In these cases, we suspected that the occlusions inside xylem vessels induced a hydraulic disconnection between the soil (at field capacity) and the leaf. Given that esca has been shown to decrease leaf transpiration rates (Petit *et al*., 2006, Magnin-Robert *et al*., 2011), we hypothesized that changes in stomatal conductance and/or leaf canopy surface contribute to the maintenance of a sufficient water supply resulting in water potential values similar to control plants.

Drought and esca caused different dynamics in whole-plant and leaf gas exchange

During drought, stomatal closure results from decreases in xylem water potential and an accumulation of abscisic acid in leaves (McAdam and Brodribb, 2015). This mechanism prevents plants from excessive water loss and xylem embolism (Martin-StPaul *et al*., 2017). A decrease in leaf gas exchange has been observed also during vascular diseases (Magnin-Robert *et al*., 2011, Castillo-Argaez *et al*., 2020, among others), but the underlying mechanisms are still unknown. Currently, there are two prevailing hypotheses: (i) pathogen and/or plant derived vascular occlusions decrease hydraulic conductivity inducing stomatal closure (Bowden *et al*., 1990, Castillo-Argaez *et al*., 2020); or (ii) pathogen-derived toxins and/or elicitors cause cellular death, loss in photosynthetic efficiency, and a subsequent decrease in gas exchange (Sun *et al*., 2017, Fallon *et al*., 2020). To test how grapevines control their stomatal conductance and transpiration during esca leaf symptom development, and compare this with water deficit, we placed 20 plants in a mini-lysimeter greenhouse in order to continuously measure transpiration and determine whole-plant stomatal conductance (*Gs*, Fig. 2a, 2b). We also measured gas exchange (Fig. $2d_{i\text{-}iii}$), quantum yield of photosystem II (Fig. $2d_{iv}$), and chlorophyll content (Supplementary Fig. 1) at the leaf level.

For two consecutive years, we observed two distinct recurrent patterns of whole-plant *Gs* in stressed plants, one for plants under water-deficit, the other for plants presenting esca leaf symptoms (Fig. 2a, note that day 0 is specific for each plant and corresponds to the first day of water regime change during drought, or to the day in which the first symptomatic leaf appeared during esca pathogenesis). During each experimental period in the two years, control well-watered plants maintained an average *Gs* value of 141.18 mmol m^{-2} s^{-1} over the two years (Fig. 2a). The seasonal *Gs* dynamic in control plants is presented in Supplementary Fig. 2. We observed, as expected, that before imposing a different watering regime, plants presented *Gs* similar to controls (average value ± SE of 160.2 ± 2.7 mmol m^{-2} s^{-1}, Fig. 2a, *period I*). Once the watering regime changed until 12 days after, total *Gs* decreased, reaching a minimum average of 17.7 mmol m^{-2} s^{-1} (Fig. 2a, *period II*). After, *Gs* stabilized around the average value of 28.7 mmol m^{-2} s^{-1} (i.e. five times lower relative to control plants Fig. 2a, *period III*). In esca symptomatic plants, we observed that *Gs* followed (for every plant) the same pattern relative to the onset of symptom appearance. Before leaf symptom development (when the plant is apparently healthy and asymptomatic: *period I*), the level of *Gs* remained similar than in control plants (average value of 166.4 ± 1.4 mmol m^{-2} s^{-1}, Fig. 2a). Concomitantly with the onset of symptoms and until 12 days after, total *Gs* decreased (*period II*, Fig. 2a). Average *Gs* during *period II* for plants exhibiting symptoms was greater than water deficit plants, attaining a minimum daily average of 70.8 mmol m^{-2} s^{-1}. However, four out of ten plants reached *Gs* values similar to plants under water deficit (≈30 mmol m^{-2} s^{-1}, Fig. 2a). Later (i.e. after 13 days from the first leaf symptom appearance, *period III*), *Gs* recovered raising to an average value of 103.8 ± 2.2 mmol m^{-2} s^{-1}. Similarly to Gs dynamics, we found that whole-plant maximal transpiration

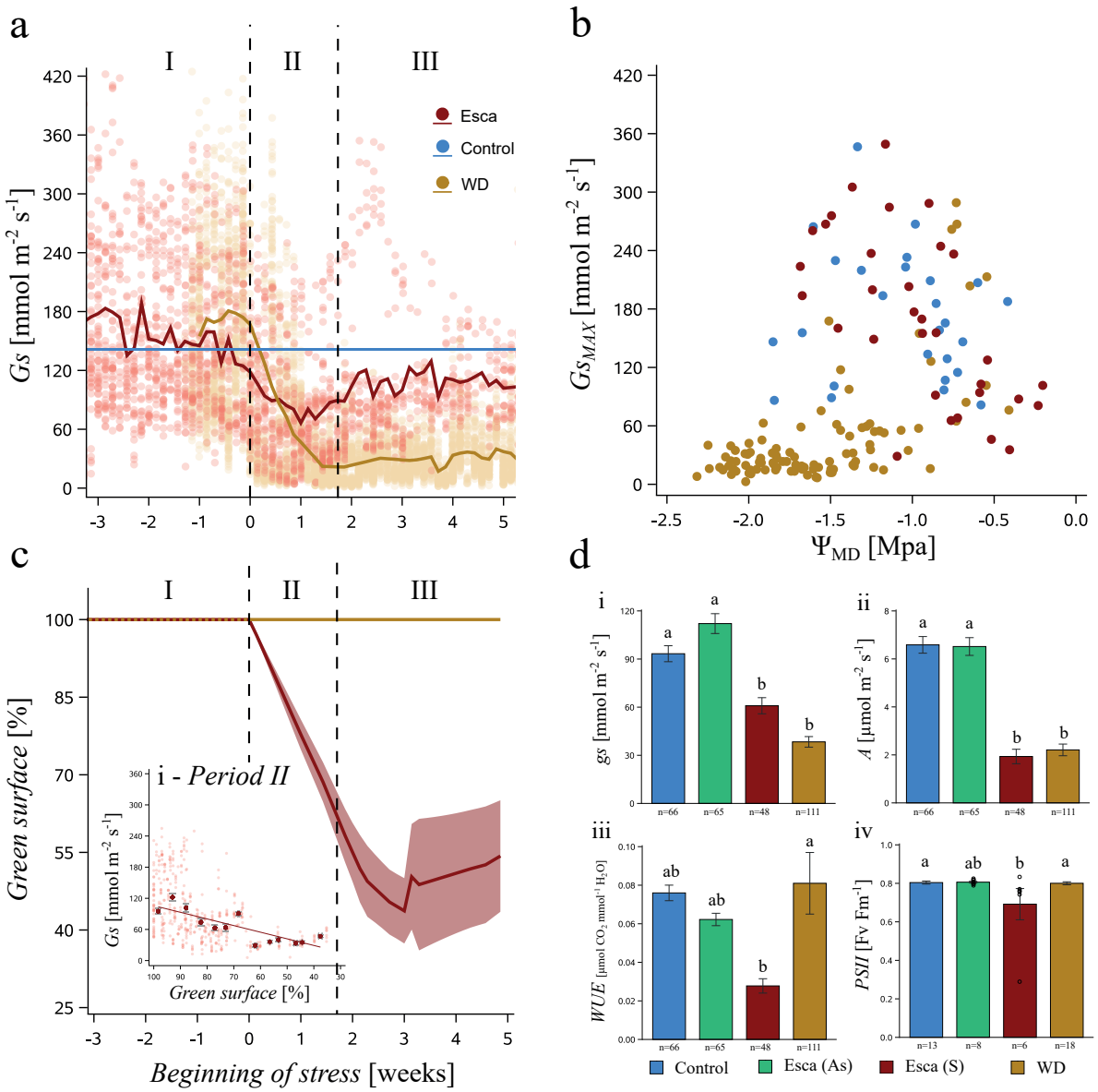

Figure 2. Whole-plant and leaf physiology during esca and water deficit in *Vitis vinifera* cv Sauvignon blanc: whole-plant stomatal conductance (**a-c**), leaf gas exchange and maximum quantum yield of photosystem II (**d**). (**a**) Evolution of the whole plant stomatal conductance *Gs* (mmol m^{-2} s^{-1}) relative to the beginning of stress in weeks (i.e. week 0 indicate the first apparition of leaf symptoms, or the day we changed the watering regime). Colors represent the different stress: blue for control, red for esca leaf symptoms and yellow for water deficit. The light blue line represents the average value of *Gs* in control plants over the two seasons. Dots represent hourly whole-plant *Gs* for each stressed plant, the thick (red and yellow) lines represent the five-day moving average of *Gs* values for symptomatic and water deficit plants. The vertical dotted lines separate three different time periods of esca symptom and water deficit development (see text for details). (**b**) Relationship between midday water potential (Ψ_{MD}) and the maximum hourly Gs recorded on the same day (Gs_{MAX}) for different stresses. Colors are the same as in Fig. 2A. (**c**) Evolution in the green canopy area relative to the beginning of stress during esca (red line) and water deficit (yellow line). Lines represent the average value, and the shaded band the standard error. (**c_i**) Relationship between *Gs* and green surface during *period II* for esca symptomatic plants. Dots represent hourly Gs, dark dots average Gs value in a 5% window of green surface (e.g. the first dark dot represents average *Gs* between 100% and 95% of green surface, the second between 95% and 90%). Red line represents the linear regression of average value. (**d_i**) Leaf stomatal conductance (*gs*, mmol m^{-2} s^{-1}). (**d_{ii}**) Net CO_2 leaf assimilation (*A*, µmol m^{-2} s^{-1}). (**d_{iii}**) Water Use Efficiency (*WUE=A/gs*, µmol $mmol^{-1}$). (**d_{iv}**) Maximum quantum yield of photosystem II (*PSII=Fv/Fm*) for control (blue), esca asymptomatic (both before and after symptoms, green), symptomatic (red), and water deficit (Ψ_{PD}< -0.5 MPa, yellow) leaves. Bars represent means, error bars SE, letters indicate statistical significance from independent mixed linear general models with Tukey post-hoc comparisons (Supplementary Table 1).

(E_{MAX}) were independent from VPD only in water deficit and esca symptomatic plants in *period II*, while the VPD sensibility for esca plants was similar to controls during *period I* and *III* (Supplementary Fig. 3).

During water deficit, we observed that the reduction of *Gs* in *periods II* and *III* corresponded to the decrease in soil water potential. Likewise, whole-plant Gs_{MAX} (i.e. hourly maximum *Gs* value of the day) decreased with decreases in Ψ_{MD} under water deficit ($P<0.0001$, $R^2=0.40$, Fig. 2b), especially below -1 MPa. However, esca exhibited the opposite response with Gs_{MAX} increasing with decreasing Ψ_{MD} (measured on asymptomatic leaves, $P<0.0001$, $R^2=0.41$, Fig. 2b). This result indicates that in well-watered esca plants, even when Ψ_{MD} reaches fairly negative values (i.e. -1 MPa and below), non-symptomatic leaves are receiving an ample water supply to sustain gas exchange and do not regulate their stomatal conductance.

During esca, the *Gs* drop in *period II* corresponded strongly with a decrease in the functional canopy (Fig. 2c, $2c_i$). We showed that during *period II*, the green canopy surface area decreased linearly over time (Fig. 2c), and this decrease was strongly correlated with the decrease in *Gs* ($P<0.0001$, $R^2=0.65$, Fig $2c_i$). The following *Gs* and VPD sensibility recovery (*period III*) was probably due to the growth (and activity) of new asymptomatic leaves at the top of symptomatic shoots (one example in Supplementary Fig. 4), as we observed an increase of green canopy (Fig. 2c), and total leaf surface (after day 230 in Supplementary Fig. 5).

At the leaf-level, asymptomatic leaves from esca plants (both before and after symptom appearance) and from control plants presented a significantly higher stomatal conductance (*gs*) (112.09 ± 6.2 mmol m^{-2} s^{-1} and 93.2 ± 4.5 mmol m^{-2} s^{-1}, on average ± SE, respectively), followed by esca symptomatic (60.9 ± 5 mmol m^{-2} s^{-1}), and water deficit (38.4 ± 3.3 mmol m^{-2} s^{-1}) leaves (Fig. $2d_i$, Supplementary Table 1). For net CO_2 assimilation *(A*, Fig. $2d_{ii}$, Supplementary Table 1), control leaves and asymptomatic leaves from esca plants presented similar values (6.6 ± 0.3, and 6.5 ± 0.4 µmol m^{-2} s^{-1} respectively), while *A* was significantly lower in symptomatic and water deficit leaves (1.93 ± 0.3, and 2.21 ± 0.2 µmol m^{-2} s^{-1}). Although *A* and *gs* were reduced during both esca leaf symptom development and water deficit, the quantity of assimilated CO_2 relative to the H_2O loss was different. Consequently, water use efficiency (*WUE*) during water deficit (0.08 ± 0.016 µmol $mmol^{-1}$) was similar to control, and esca asymptomatic, while significantly higher than symptomatic leaves (0.03 ± 0.004 µmol $mmol^{-1}$, Fig. $2d_{iii}$, Supplementary Table 1). The measurement of quantum yield of photosystem II (Fig. $2d_{iv}$, Supplementary Table 1) confirmed that esca symptomatic leaves are the only leaves with reduced photosynthetic activity. Specifically, all leaves presented *PSII* (*Fv*/*Fm*) values around 0.8 (the optimum value for healthy leaves, Schreiber *et al*., 1996), except for esca symptomatic leaves (0.69 ± 0.08, average ± SE, Fig. $2d_{iv}$). Finally, confirming that photosynthesis is more affected in esca symptomatic than in water deficit leaves, we observed that the total chlorophyll content, altogether with the ratio between chlorophyll a and b, was significantly lower in esca symptomatic leaves (Supplementary Fig. 1). Esca and water deficit both significantly affected whole-plant

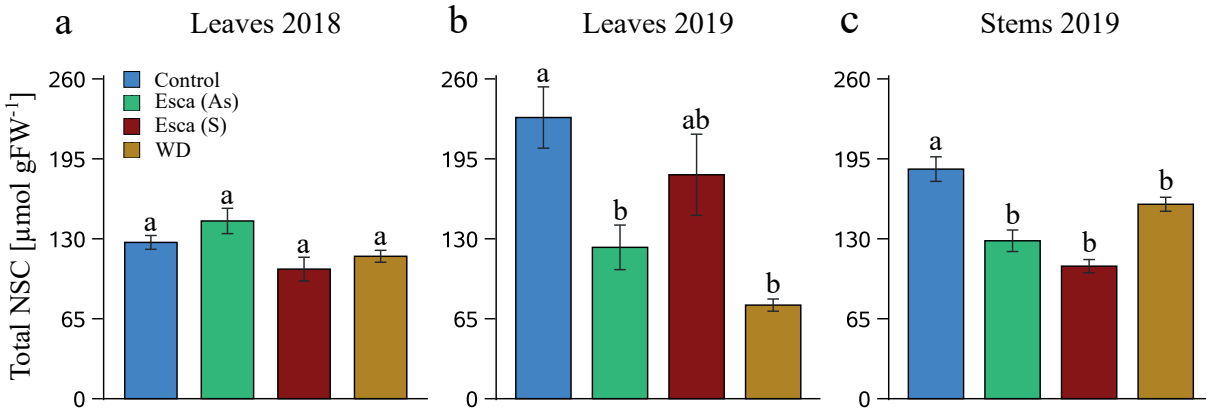

Figure 3. Total non-structural carbohydrates (NSC) content in µmol gFW^{-1} over the two years for control (blue), esca asymptomatic (both before and after symptoms, green), esca symptomatic (red), and water deficit (Ψ_{PD}<-0.5MPa, yellow) leaves and stems. (**a**) Mean NSC content in leaves in 2018. (**b**) Mean NSC content in leaves in 2019. (**c**) Mean NSC content in stems in 2019. Bars represent means and error bars standard error, letters indicate statistical significance from independent mixed linear general models with Tukey post-hoc comparisons (Supplementary Tables 2, 3).

Gs, but with very different seasonal dynamics, and gas exchange and photosynthetic activity at the leaf level. Given these differences, we explored the consequences on non-structural carbohydrate production and storage.

Non-structural carbohydrates (NSC) storage and balance during esca and water deficit

Pathogens and drought often cause imbalance in carbon status by variously affecting photosynthesis and growth (McDowell *et al*., 2008). Thus, at the start of the stress period or when stress is moderate, photosynthesis is usually less affected than growth, which leads to the accumulation of sugars (Muller *et al*., 2009). However, when the stress is prolonged or becomes severe, photosynthesis is in turn inhibited, eventually causing the depletion of stored non-structural carbohydrates (NSC), thereby accelerating plant decline. Also vascular pathogens could reduce the photosynthetic activity by causing cellular/leaf death, actively consume NSC for their survival, induce C-expensive plant defenses, and indirectly interfere with phloem transport when they generate xylem hydraulic failure (Oliva *et al*., 2014). In order to understand how esca and water deficit affect the carbon (im)balance, NSC were quantified in annual organs (leaves) during summer 2018 and 2019 and in perennial organs (stems) in winter and summer 2019 (Fig. 3, 4, Supplementary Fig. 6, 7, Tables 2, 3).

Strikingly, none of the treatments induced severe carbon depletion as the NSC levels were always relatively high. However, in these plants, clusters were removed right after bud-break, and their absence could have influenced the relative high NSC content in our samples. In 2018, we observed that all leaves (from control, symptomatic or water deficit plants) presented the same content of total NSC (around 130 µmol gFW^{-1}, Fig. 3a, Supplementary Table 2). Oppositely, in 2019 total NSC content in leaves was significantly affected by esca and water deficit (Fig. 3b, Supplementary Table 2). For esca, only asymptomatic leaves presented significantly

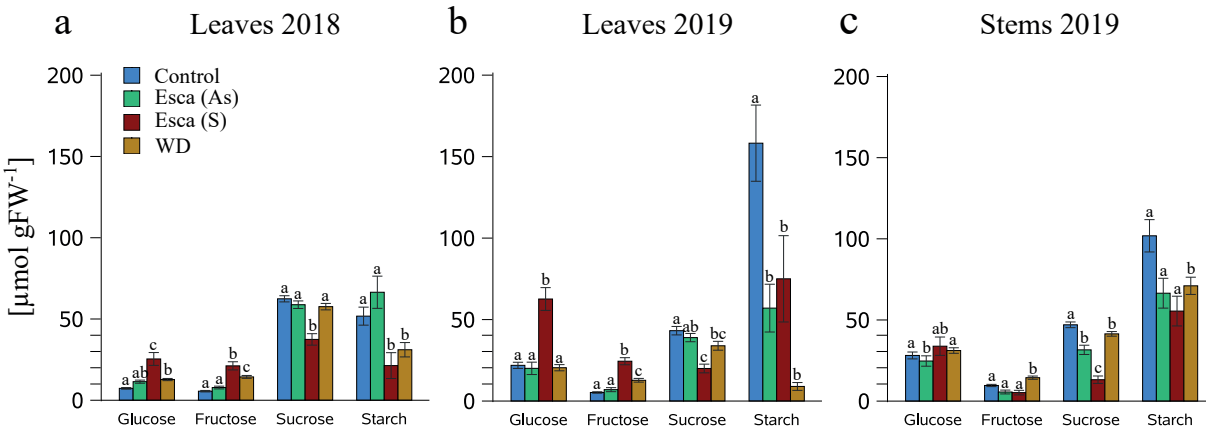

Figure 4. Content of different NSC (glucose, fructose, sucrose, and starch) in µmol gFW^{-1} over the two years for control (blue), esca asymptomatic (both before and after symptoms, green), esca symptomatic (red), and water deficit (Ψ_{PD}<-0.5MPa, yellow) leaves and stems. (**a**) Mean content in leaves in 2018. (**b**) Mean content in leaves in 2019. (**c**) Mean content in stems in 2019. Bars represent means and error bars standard error, letters indicate statistical significance from independent mixed linear general models with Tukey post-hoc comparisons. Different statistical tests were done for each different sugar (see Supplementary Tables 2, 3 for details).

lower NSC content compared to controls (Fig. 3b), while plants under the second year of water deficit presented leaves with the significantly lowest NSC content (0.3 times compared to controls on average, Fig. 3b). In 2019, control stems presented a significantly higher NSC content (186.6 ± 10 µmol gFW^{-1} on average), compared to the other stems (Fig. 3c, Supplementary Table 3). In 2019 we observed an opposite NSC distribution between leaves and stems (Fig. 3b, 3c) depending on the stress: control and esca symptomatic plants presented higher NSC content in leaves than in stems, while during water deficit (2nd year) NSC content was higher in stems than leaves. This result could indicate that esca and water deficit differently affect primary metabolism and carbohydrate storage dynamics.

Partitioning the different carbohydrates, we observed different dynamics for esca and water deficit (Fig. 4, Supplementary Fig. 6, 7, Tables 2, 3). During the experimental periods in each of the two years, the carbohydrate content in asymptomatic leaves from esca plants did not significantly differ from that of control leaves, except for starch in 2019 (Fig. 4a, 4b, Supplementary Table 2), confirming that asymptomatic leaves have a physiological functioning very close to control plants. Esca symptomatic and water deficit leaves accumulated high levels of glucose and fructose during both years (two to five times higher compared to controls, except for glucose during water deficit in 2019, Fig. 4a, 4b, Supplementary Table 2). The accumulation of hexoses and/or the increased ratio of hexoses to sucrose, often observed in plants infected with pathogens but also under drought, has been attributed to increased invertase activity, particularly the cell wall isoform (Berger *et al*. 2007; Medici *et al*., 2014). Sucrose content was significantly lower for esca symptomatic leaves (0.5 times compared to controls both years), while it was similar (or slightly lower) to control during water deficit (Fig. 4a, 4b), suggesting that phloem transport (sucrose is the mobile NSC form) was compromised only during esca, and not during water deficit. Starch was significantly lower during both stresses (0.5 times

lower on average); especially during the second year of water deficit (0.1 times compared to controls, corresponding to 9 ± 2.4 µmol gFW^{-1}), indicating that carbon reserves were consumed (or not produced) in response to stress. In stems, we observed differences in fructose content with significantly higher levels during water deficit (1.5 times relative to control, Fig. 4c, Supplementary Table 3), suggesting that the growth inhibition leads to hexose accumulation also in perennial organs. Sucrose was significantly lower in esca symptomatic stems (0.3 times relative to control, Fig. 4c), indicating that reduced phloem transport was also observed in stems. During esca and water deficit, stems exhibited glucose and starch contents similar (or slightly different) to controls, showing that reserve accumulation is still active during these stressing conditions (Fig. 4c). Finally, it is worth noting that in the NSC quantification during winter 2018-2019 dormancy (i.e. between the two experimental seasons) in stems, none of the quantified metabolites were significantly different compared to controls (Supplementary Fig. 7, Table 3).

The long-term esca leaf symptom history did not impact plant physiological response to drought

We observed that drought inhibits esca leaf symptom expression (Table 1). We then explored whether plant response to drought differed between plants with contrasting disease histories (pA-pS), and whether they presented different physiological profiles. As presented in Supplementary Table 4, we found that the disease's historical record had no significant effect on any of the recorded variables (water potential, whole-plant and leaf gas exchange, and NSC). This result suggests that esca do not alter long-term plant susceptibility to drought. Bortolami *et al* (2020) observed that plants with different disease histories presented similar hydraulic integrity; here we confirmed that esca leaf symptom development affects the plant physiology mainly during the year of expression and not over the long-term. These findings can partially explain why esca symptomatic plants can frequently appear asymptomatic during the successive seasons (as observed in field surveys, Guerin-Dubrana *et al*., 2013, Li *et al*., 2017).

DISCUSSION

Increasing plant mortality is one of the major issues threatening perennial forestry and agricultural ecosystems. The impact of biotic-abiotic stress interactions on plant physiology certainly plays a crucial role in the extent of this mortality. Here, we studied the interaction between drought and vascular disease and the subsequent physiological consequences in grapevine. Esca (a vascular disease) and drought are two stresses that frequently coexist in vineyards. Even though anecdotal importance has been ascribed to hot periods during esca leaf symptom

appearance (Marchi *et al*., 2006, Serra *et al*., 2018, Kraus *et al*., 2019), the underlying plant physiological status has still never been detailed during these events, leaving many doubts on how drought and esca interact.

We demonstrated that prolonged water deficit conditions (at $\Psi_{PD} \approx$ -1 MPa for three months) totally inhibited esca leaf symptom development. At the same time, plant disease history, i.e. esca leaf symptom expression over several years, had no impact on plant response to drought. Under the drought conditions applied plant transpiration was low while hydraulic integrity was preserved (Supplementary Fig. 3, 8), and we could speculate that transpiration is the key mechanism driving esca leaf symptom expression. The most prominent hypothesis of leaf symptom formation states that toxins (or elicitors) are transported from pathogens in the trunk up to the leaves by the transpiration stream (Claverie *et al*., 2020). Our findings tend to support the hypothesis where a decreased transpiration might result in decreased toxin transport. However, water deficit conditions also trigger other systemic responses that could interfere with pathogenicity and/or enhance plant defenses (e.g. accumulation in soluble sugars and phenolic compounds).

The clear antagonism between esca and drought strengthen the importance of integrative studies (i.e. monitoring plant physiology under multiple stresses) to understand the role of climate in perennial plant decline. We underlay the necessity of finding the physiological thresholds triggering different plant responses to stress if we are to understand the impact of climate change in viticulture. Interpreting our results, we could expect that future climate change could lead either to a decrease in esca incidence if Ψ_{PD} reaches low values (around -1 Mpa), or an increase in esca incidence if the VPD increases but the soil remains at field capacity resulting in high transpiration. Moreover, other practices, such as irrigation, that can temporarily mitigate water deficit, could accelerate vine decline given by esca. In this context, improving cultural practices in the absence of a complete understanding of biotic-abiotic interactions and the different physiological thresholds aiming to plant death could lead to unforeseen outcomes.

Esca and drought primarily affect the same plant tissue: the xylem vasculature. This simple fact, coupled with other similarities between the phenology of these stresses, have led many authors to hypothesize that vascular pathogens and water deficit induce the same mechanisms prior to plant death (Bowden *et al*., 1990, Yadeta and Thomma, 2013). Our results largely reject this hypothesis, finding that the two stresses induced distinct physiological responses. We demonstrated in previous work that esca pathogenesis is associated with hydraulic failure caused by vascular occlusion (Bortolami *et al*., 2019, 2020), which contrasts with the cavitation-induced hydraulic failure during drought (Tyree and Sperry, 1989). Here we showed that esca never caused any significant drop in water potential during our two-year study. This result can be explained by the observation of whole-plant stomatal conductance. *Gs* decreased during esca leaf symptoms (as during water deficit in *period II*, Fig. 2a) but it was directly correlated with the percentage of symptomatic leaves (% of the total plant canopy), not by a change in

soil (i.e. predawn) water potential as during drought. Consequently, as stomatal conductance decreased linearly with esca leaf symptom development, the remaining functional (i.e. non-occluded) xylem vessels sustain sufficient water transport to non-symptomatic leaves which function similar to controls. Interestingly, we observed that 2-3 weeks after the first apparition of leaf symptoms, on the top of symptomatic shoots, new asymptomatic shoots grew, and that *Gs* recovered to level close to control plants. Confirming this trend, we evidenced that at the whole-plant scale, transpiration sensibility to VPD was similar to water deficit conditions only during esca leaf symptom formation (i.e. in period II, Supplementary Fig. 3), and that asymptomatic regrowth can restore normal whole-plant transpiration rates in *period III*. In vineyards, grapevines are often continuously trimmed during summer to control canopy size thus only one study reported asymptomatic regrowth in the field after extreme esca leaf symptom development (Kraus *et al*., 2019). In the future new attention should be given on how the apparition of new asymptomatic leaves could restore (or mitigate) the negative effects of esca symptoms on berry quality and reserve synthesis. For example, our study showed that esca did not influence stem starch content in winter (Supplementary Fig. 7, contrasting from Petit *et al*., 2006), this could be due to the presence of new asymptomatic leaves that helped maintain starch reserves as in control plants.

Measurements at the leaf level showed that the photosynthetic apparatus is more compromised during esca than during drought. This result supports the hypothesis that during esca a more generalized cellular death (and not a direct stomatal control as during water deficit) reduces gas exchange and photosynthetic performance in leaves. However, these differences in photosynthesis did not result in a reduced total NSC content in symptomatic leaves, which was strongly affected only during the second year of water deficit. Esca symptomatic leaves and stems consistently exhibited lower sucrose concentrations (the main sugar transport form) suggesting that carbohydrate efflux from leaves would be reduced during esca. The presence of occluded xylem vessels in esca symptomatic plants, leading to hydraulic failure (Bortolami *et al*., 2019, 2020), could affect the phloem transport. In water deficit stems, we did not observe any hydraulic failure during our water deficit experimentation (Supplementary Fig. 8), Ψ_{PD} never reached a critical threshold leading to cavitation (Charrier *et al*., 2018, Dayer *et al*., 2020), and sucrose concentration was less impacted. Finally, regardless of the differences at the leaf level highlighted above both esca and two seasons of water deficit resulted in decreased total NSC content in stems.

In this context, even if esca and drought were antagonistic when applied simultaneously and if esca had no long-term impact on drought susceptibility, both stresses negatively impacted perennial organs and plant physiological functioning (although in distinct ways). Consequently, drought and vascular disease could act synergistically over the longer term, contributing together to plant decline.

MATERIALS AND METHODS

Plant material and esca symptom notation

Vitis vinifera cv. Sauvignon blanc, grafted onto 101-14 MGt, were planted in 1992 at INRAE Bordeaux-Nouvelle Aquitaine (44°47'24.8"N, 0°34'35.1"W). Following the protocol from Bortolami *et al*. (2019), plants (n=51) were uprooted in winter 2018 and transferred into 20-l pots, allowing environmental and physiological monitoring. In a subsample (n=10) of these plants the vascular pathogens related to esca were detected inside their trunk (Bortolami *et al*., 2020). During the two experimental seasons (2018 and 2019) fruits and secondary shoots were removed just after bud break. In the greenhouse, plants were irrigated with nutritive solution (0.1 mM $NH_4H_2PO_4$, 0.187 mM NH_4NO_3, 0.255 mM KNO_3, 0.025 mM $MgSO_4$, 0.002 mM Fe, and oligo-elements [B, Zn, Mn, Cu, and Mo]); climatic conditions were monitored every 15' using temperature and humidity probes (S-THB-M002, Onset, Bourne MA, USA) and global radiation sensors (S-LIx-M003, Onset, Bourne MA, USA) connected to a data logger (U300-NRC, Onset, Bourne MA, USA). From 2012, the development of esca leaf symptoms for all plants was monitored in the vineyard (2012-2017) and in the greenhouse (2018-2019) following Lecomte *et al*. (2012) to classify the plants as asymptomatic or esca-symptomatic every year. Before the experiment started (May 2018), each plant was classified by its disease historical record: plants that never expressed symptoms since 2012 (previously asymptomatic, pA), and plants that expressed symptoms at least once since 2012 (previously symptomatic, pS). During the two years of experimentation, the appearance of leaf symptom was checked twice a week (from June 2018 to October 2019) on every plant. Consequently each sample (leaf or stem) was classified by both a general disease status of the whole plant and the specific collected organ: samples from control plants (i.e. asymptomatic from June to October), asymptomatic samples from symptomatic plants (both before and after symptom appearance), and symptomatic (presenting tiger-stripe leaves) samples. One example of esca symptom appearance and evolution is presented in Supplementary Fig. 4.

Balance data analysis

From mid-June to October (in 2018 and 2019), a subset of plants (n=20) was placed in a mini-lysimeter greenhouse phenotyping platform (Bord'O platform, INRAE Bordeaux) where pots were continuously weighed on individual scales (CH15R11, OHAUS type CHAMP, Nänikon, Switzerland). The pots were placed into dark plastic bags, well fixed around the trunk, to prevent water loss by soil evaporation. The whole plant transpiration E [mmol s^{-1} m^{-2}] was calculated as follow:

$$E = (\Delta w/A_L) / 18000$$

Where: Δw corresponds to the weight changes during every hour [g s^{-1}], A_L to the total leaf area of the plant [m²], and 18000 to the molecular weight of water [g $mmol^{-1}$]. Δw was considered only when not aberrant (i.e. between 0 and -0.5 kg $hour^{-1}$). Moreover, to avoid rarely recorded Δw, extreme outliers values (i.e. values three times lower than the lower quartile, or three times higher than the highest quartile) were removed for each day and plant. Total leaf area (A_L) was estimated through the relationship obtained between the leaf midrib length and the leaf surface (measured with a leaf area meter, LI-3000, LI-COR, Lincoln, NE, USA) for ≈150 leaves. Leaf midribs were measured on all the leaves of each plant every week in 2018 and every-other week in 2019 and, in case of esca symptom presence, every leaf was noted as asymptomatic, esca-symptomatic, or from asymptomatic regrowth. In the majority of symptomatic plants, five to fifteen days after leaf symptoms appeared, new green shoots grew from the secondary buds: they were noted as "asymptomatic regrowth" (e.g. Supplementary Fig. 3). In order to obtain a daily constant change in leaf area, a linear increase (or decrease) was interpolated between each measure of leaf area. Likewise, a constant change in the percentage of symptomatic leaves was interpolated between each measure. The whole plant stomatal conductance *Gs* [mmol s^{-1} m^{-2}] was calculated as follow:

$$Gs = K_G(T) \times (E/D)$$

Where: $K_G(T)$ correspond to the conductance coefficient (Ewers *et al*. 2001, kPa m^3 kg^{-1}), *E* to the transpiration, and *D* to the vapor pressure deficit [kPa] calculated using hr [%] and T [°C] from climatic records (Jones 2013). To avoid errors in *Gs* estimations, values were used for analysis only when *D* was >0.6 kPa (Ewers and Oren 2000) and light conditions were saturating for photosynthesis (>700 µmol m^{-2} s^{-1} photosynthetic photon flux density, PPFD).

Water deficit treatment and maintenance

At the beginning of the two seasons, every plant was watered at its maximum capacity and left to drain water excess for half a day. The resulting weight was taken as field capacity, and well-watered plants were irrigated to this weight every-other day. The average watering volume from the plants on the scales was used to water the remaining plants that were not on the balances. Water deficit was induced on 25 (over 51) plants for two consecutive seasons (the same plants were subjected to water deficit in 2018 and 2019 from July to October) and the other 26 plants were kept under well-watered conditions. At the beginning of the experimentation in 2018, half of the water deficit plants had never expressed esca leaf symptoms since 2012 (pA), while the other half expressed symptoms at least once in the past (pS). Similarly 14 out of the 26 plants under the well-watered regime were previously asymptomatic (Table 1). Water deficit plants were maintained for a period of three months (from July to October 2018 and 2019) at a target weekly average Ψ_{PD} between -0.6 and -1.7 MPa, with outliers below or above these thresholds representing 20% of the values (Supplementary Fig. 9). These condi-

tions are sufficient to reduce plant transpiration without decreasing stem hydraulic conductivity in grapevine (Charrier *et al*., 2018). On the 1st of July 2018 and 2019, we stopped watering the plants. We then checked predawn water potential (Ψ_{PD}) with a Scholander pressure chamber (Precis 2000, Gradignan, France) on three up to five plants every-other day, and every day on two plants with stem psychrometers (ICT International, Armidale, NSW, Australia). Placed in a central internode of a stem of the current year, the psychrometers record the stem water potential (Ψ_{Stem}) every 30'. Once Ψ_{PD} reached an average of -1 MPa, we noted the exact weight for the 10 plants placed on the scales (see above). These plants were then watered with nutritive solution every three days (and at necessity when Ψ_{PD} dropped below -1.5 Mpa) at this weight until the end of the experiment (beginning of October). The average watering volume from these plants was used to water the remaining 15 plants that were not on the balances. During the whole experiment we watered water-stressed plants with 0.1 to 0.6 l every three days in pots with a pot capacity between 6 and 8 l (i.e. approximately from 1 to 10% of the field capacity).

Hydraulic integrity and water potential analysis

To check the effect of water deficit on the hydraulic integrity of the perennial organs, in 2019 we measured stem specific hydraulic conductivity (k_s) and stem theoretical hydraulic conductivity (k_{th}) in 73 different stems (39 control and 34 from water deficit plants) over 9 sampling dates as explained in Bortolami *et al*., 2020 (Supplementary Fig. 8). Water potential was monitored in at least 25 plants per date (every week in 2018 and every-other week in 2019), from June to October in 2018 and 2019. We measured Ψ (both Ψ_{PD} and Ψ_{MD}) on 26 different dates, corresponding to 632 measures for control (asymptomatic well-watered) plants, 213 in esca symptomatic, and 650 for water deficit. Every water potential measurement was done on mature leaves with a Scholander pressure chamber. Ψ_{PD} was measured between 04:00 and 06:00 a.m., Ψ_{MD} on well-exposed leaves between 01:00 and 03:00 p.m. Regarding esca symptomatic plants, water potentials were measured only on asymptomatic (green) leaves. The presence of gel and tyloses in the xylem vessels of symptomatic leaves (demonstrated by Bortolami *et al*. 2019) made the detection of water potential with the pressure chamber difficult (and sometimes impossible). Sometimes gel (and not water) was rapidly exuded from the petioles at high Ψ (≈0 MPa), sometimes it appeared at low Ψ (between -1 and -3 MPa), or did not appear at all (<-7 MPa). However, in asymptomatic leaves gel was not detected during Ψ measurements, therefore the values should reflect the water status of the plant.

Gas exchange analysis

Once a week from June to October 2019, maximal leaf gas exchange measurements were registered between 9:00 a.m. and 12:00 p.m. on mature well-exposed leaves using the TARGAS-1 portable photosynthesis system (PP-systems, Amesbury, MA, USA). Optimal conditions of

photosynthetic active radiation (PAR) were set in the cuvette [1500 µmol m^{-2} s^{-1}]. The following parameters were recorded on each leaf: stomatal conductance, *gs* [mmol s^{-1} m^{-2}]; CO_2 assimilation, *A* [µmol s^{-1} m^{-2}]; water use efficiency, *WUE* (= *A/gs*) [µmol CO_2 $mmol^{-1}$ H_2O]. In some cases the level of CO_2 absorbed (*A*) by the leaf was negative. In these cases *A* was close to 0 (between 0 and -1 µmol s^{-1} m^{-2}, n=24, 16 water deficit and 8 esca symptomatic), or too negative (between -2 and -20 µmol s^{-1} m^{-2}, n=20 esca symptomatic). We considered the first group of measures as a possible (but not quantifiable) leaf respiration, and the very low *A* values as artifacts given by the advanced leaf destruction during symptoms. Consequently, we manually changed all records in *A*=0 and *WUE*=0. However, other studies should confirmed the possible high respiration (i.e. CO_2 rejection) rates during esca leaf symptoms. Measurements were performed on 50 plants, on 12 different dates, for a total of 290 measures (66 measures on control leaves, 65 on asymptomatic leaves on esca plants, 48 on esca symptomatic leaves, and 111 on water deficit leaves). For symptomatic leaves, gas exchanges were measured on their green part. Plants under water deficit were considered for analysis only when $\Psi_{PD} < -0.5$ MPa, as plants with $\Psi_{PD} > -0.3$ Mpa (i.e. when every plant was still under well-watered conditions) presented values similar to control plants ($F_{1,13}$=0.25, *P*=0.62 for *A*, $F_{1,13}$=1.98, *P*=0.18 for *gs*).

Chlorophyll fluorescence measurements

Maximum quantum yield of photosystem II (Fv Fm^{-1}) was measured in early morning (between 9:00 and 11:00 a.m.) using a portable chlorophyll fluorometer (PAM2100, Walz, Germany). Measurements were carried out on two different dates in 2018 in 45 leaves (13 control, 8 esca asymptomatic, 6 esca symptomatic, and 18 water deficit). Disk shaped clips were attached on leaves the evening before the measurement in order to adapt the leaf to dark conditions. The minimal fluorescence at dark conditions (*Fo*) was recorded, then the maximal fluorescence (*Fm*) was measured at saturated light. Maximum quantum yield of photosystem II (*PSII*) was then calculated as:

$$PSII = Fv/Fm = (Fo-Fm)/Fm$$

Non-structural carbohydrates (NSC) and chlorophylls quantification

To quantify NSC over the course of the experimentation, leaves were sampled every week in 2018 on 24 random plants (half well-watered and half water deficit), on the same day and plants we measured Ψ_{PD} and Ψ_{MD}. In 2019, leaves and stems were sampled every-other week on 12 random plants (half well-watered and half water deficit). Thus, resulting in 25 sampling dates on 51 plants for a total of 509 samples, specifically, in 2018: 94 leaves from control plants, 66 esca asymptomatic, 26 esca symptomatic, and 132 water deficit; in 2019: 31 leaves and 32 stems from control plants, 20 leaves and 10 esca asymptomatic stems, 11 leaves and 6

esca symptomatic stems, and 33 leaves and 30 water deficit stems. All samples (stems or leaf blades) were collected in the early morning (between 07:00 and 10:00 a.m.) to avoid effects of NSC diel fluctuations, directly put in liquid nitrogen, and stored at -80 °C until analysis. For stems, one internode (including wood and bark) was sampled. For leaves, the whole blade (including green and scorched areas for symptomatic leaves) was sampled. Frozen samples were ground with ball tissue lyser (GenoGrinder 2010, Spex Sample Prep, Rickmansworth, England at 30Hz for 45" for leaves, and Tissuelyser II, Qiagen, Germantown, MD, USA, for stems). 20 ± 2 mg of powder were weighted into 1.1 mL-micronic tubes (MP32033L, Micronic, Lelystad, Netherlands), adding approximately the same volume of polyvinylpolypyrrolidone (77627, Sigma Aldrich, Darmstadt, Germany), to precipitate polyphenols and avoid interaction with the enzymes used to measure NSC. Samples were randomized into 96-micronic racks (MPW-51001BC, Micronic, Lelystad, Netherlands). Every rack contained: a maximum of 84 samples, six empty tubes (for extraction blank), and six tubes with a biological standard (obtained by mixing the powder from different samples). Assays were performed as described in Biais *et al*. (2014) using Starlet pipetting robot (Hamilton). After an ethanolic extraction, we divided (from every tube) the supernatant from the pellet. Determination of chlorophylls content was adapted from Arnon (1949). Immediately after extraction, 50 µL of supernatant was mixed with 120 µL 98% ethanol and the absorbance was read at 645 and 665 nm in a microplate reader (SAFAS MP96, Monaco). Chlorophylls content, expressed as mg gFW^{-1}, was calculated using the empirical formulas:

$$Chlorophyll\ a = 5.21 \times A_{665} - 2.07 \times A_{645}$$

$$Chlorophyll\ b = 9.29 \times A_{645} - 2.74 \times A_{665}$$

which has been obtained by using commercial chlorophyll, and A_{645} and A_{665} corresponds to the two absorbances. Glucose, fructose, and sucrose, expressed as µmol gFW^{-1}, were quantified in 5 µl of ethanolic supernatant, and the absorbance read at 340 nm in MP96 microplate readers (Stitt *et al*. 1989). For the determination of starch, expressed as µmol gFW^{-1}, the pellet was suspended in 0.1M NaOH and heated at 95°C for 20 min, neutralised with HCl and starch was then quantified from 5µl of supernatant and the absorbance read at 340 nm in MP96 microplate readers as in Hendriks *et al*. (2003).

Statistical analysis

The effect of esca leaf symptoms and water deficit was tested on water potential (Ψ_{PD} and Ψ_{MD}), leaf gas exchange (*gs*, *A*, *WUE*), the maximum quantum yield of photosystem II (*PSII*), chlorophyll content (a+b, and a/b), and NSC (glucose, fructose, sucrose, starch, and total NSC) content in leaves and stems, using independent mixed linear general models (one per each response variable, organ and experimental year). The treatment (control, esca asymptomatic, esca symptomatic and water deficit leaves) and the sampling date were entered as fixed effects

(covariables) and the plant was treated as a random effect since different leaves were sometimes analyzed from the same plant in proc GLIMMIX (SAS 9.4; SAS Institute), and logarithmic transformation were done when appropriate. Specific treatments were compared using Tukey post-hoc tests adjusted for multiple comparisons. The relationships between Ψ_{MD} on Gs_{MAX} during water deficit and esca, and between the green surface (using 5% interval average values) and *Gs* were calculated using linear regression models in proc REG (SAS 9.4; SAS Institute).

ACKNOWLEDGMENTS

We thank the experimental teams of UMR SAVE, UMR BFP, and UMR EGFV (Bord'O platform, INRAE, Bordeaux, France) for providing the materials and logistics. We thank Isabelle Demeaux (UMR SAVE) for providing technical knowledge and support. We thank all the people (from internships to professors) that help with the leaf surface measurements. This work was supported by the French Ministry of Agriculture, Agrifood, and Forestry (FranceAgriMer and CNIV) within the PHYSIOPATH project (program Plan National Dépérissement du Vignoble, 22001150-1506).

Supporting information for:

Grapevines under Drought Do Not Express Esca Leaf Symptoms: the Physiology behind Drought and Vascular Pathogen Antagonism

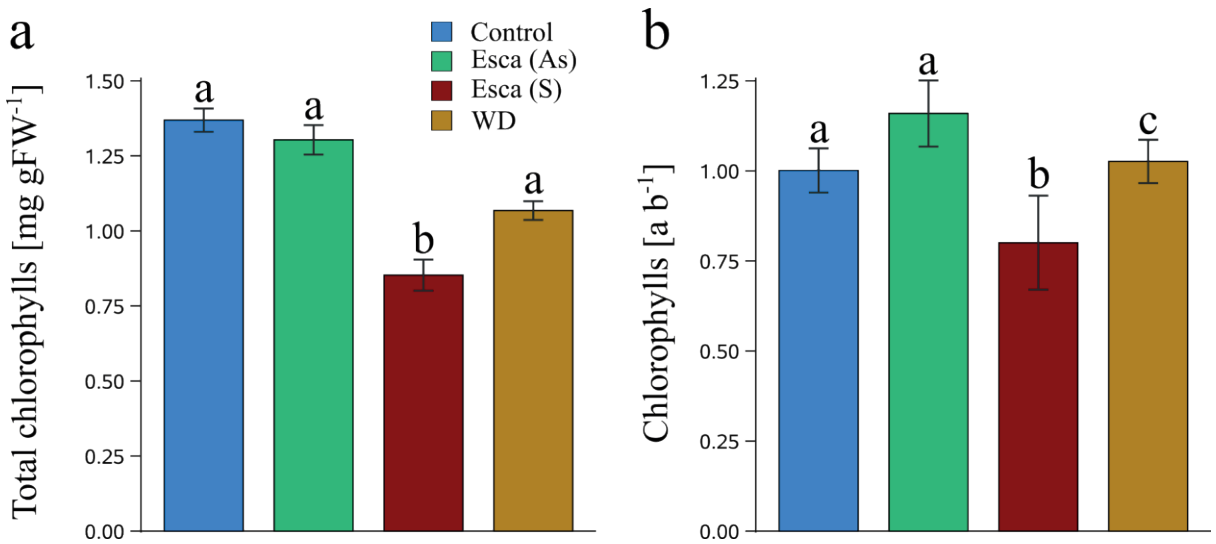

Supplementary Figure 1. Chlorophyll content over the two years for control (blue), esca asymptomatic (green), esca symptomatic (red), and water stress (yellow) leaves over the two years. n=413. (**a**) Total chlorophylls (a+b, mg gFW^{-1}), $F_{3,357}$=4.58, P=0.0037. (**b**) Ratios between chlorophyll a and chlorophyll b. $F_{3,357}$=17.47, P<0.0001. Bars represent means and error bars standard error, letters indicate statistical significance from independent mixed linear general models with Tukey post-hoc comparisons. In statistical tests, sampling date was treated as a fixed effect, plant as a random effect, and values from total chlorophylls were log transformed.

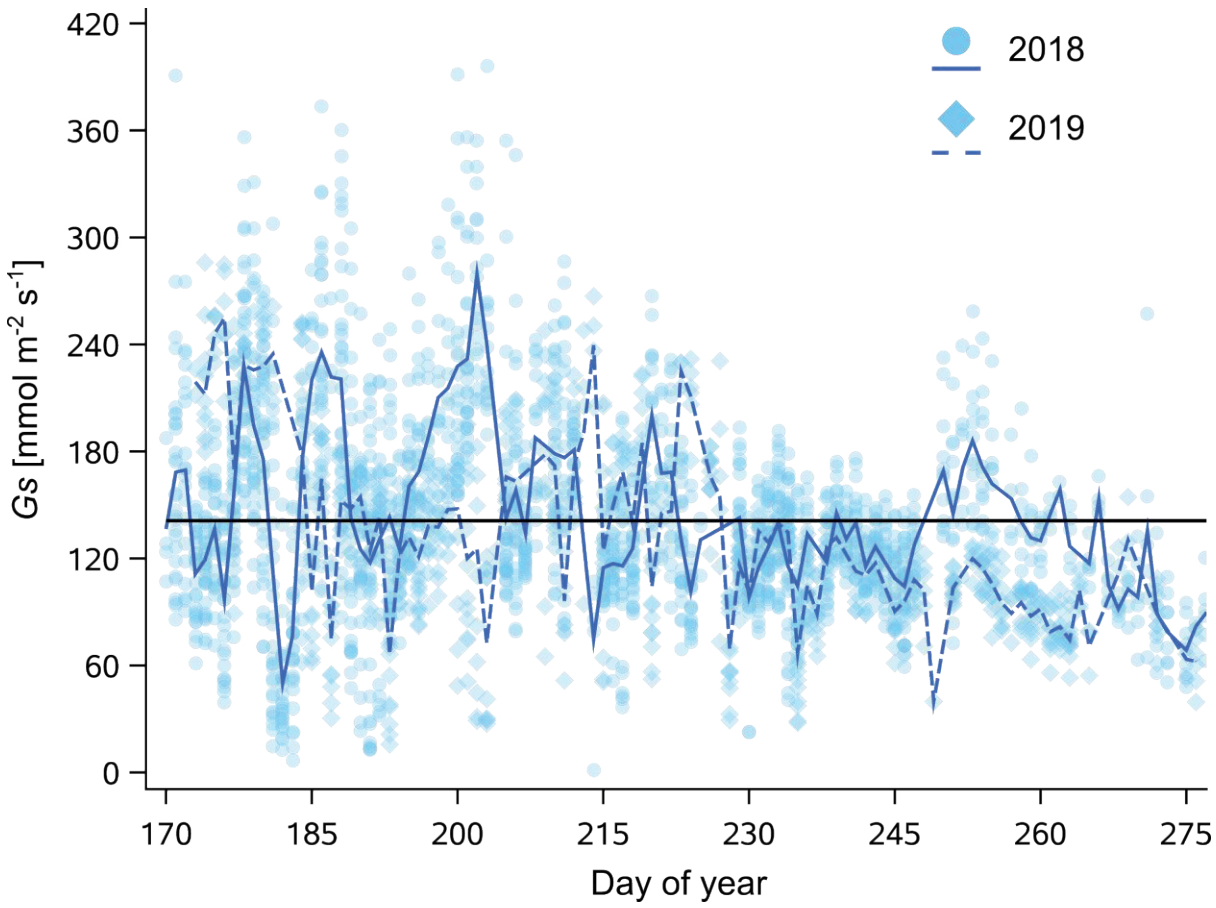

Supplementary Figure 2. Whole-plant *Gs* over the experimental seasons for control plants. Symbols represent hourly *Gs*, lines average daily *Gs*. Dots and solid line represent *Gs* in 2018, diamonds and dashed line *Gs* in 2019. The black horizontal band represents the average value over the two years (i.e. correspondent to blue horizontal band in Fig. 2A). We can observe that at the end of the season (late September), *Gs* values tend to decrease, probably due to the onset of the winter senescence process.

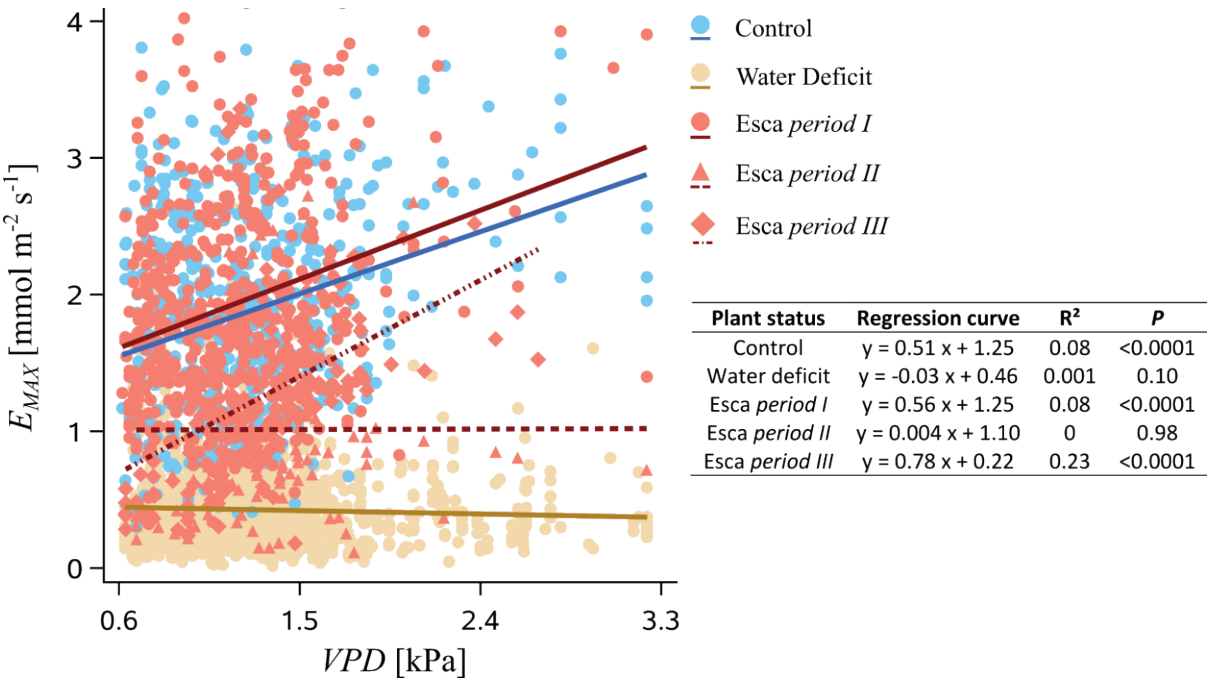

Plant status	Regression curve	R^2	*P*
Control	y = 0.51 x + 1.25	0.08	<0.0001
Water deficit	y = -0.03 x + 0.46	0.001	0.10
Esca *period I*	y = 0.56 x + 1.25	0.08	<0.0001
Esca *period II*	y = 0.004 x + 1.10	0	0.98
Esca *period III*	y = 0.78 x + 0.22	0.23	<0.0001

Supplementary Figure 3. Relationships between *VPD* [kPa] and E_{MAX} [mmol m^{-2} s^{-1}] in water deficit and esca leaf symptomatic plants during the two years of experiment. Blue circles and line correspond to control plants, yellow circle and line to water deficit plants (after changing the watering regime), red circles and solid line to esca symptomatic plants in *period I* (before leaf symptom appearance), red triangles and dashed line to esca symptomatic plants in *period II* (during esca leaf symptom formation), and red diamonds and dash-dotted line to esca symptomatic plants in *period III* (during asymptomatic regrowth formation). The corresponding regression curves are presented.

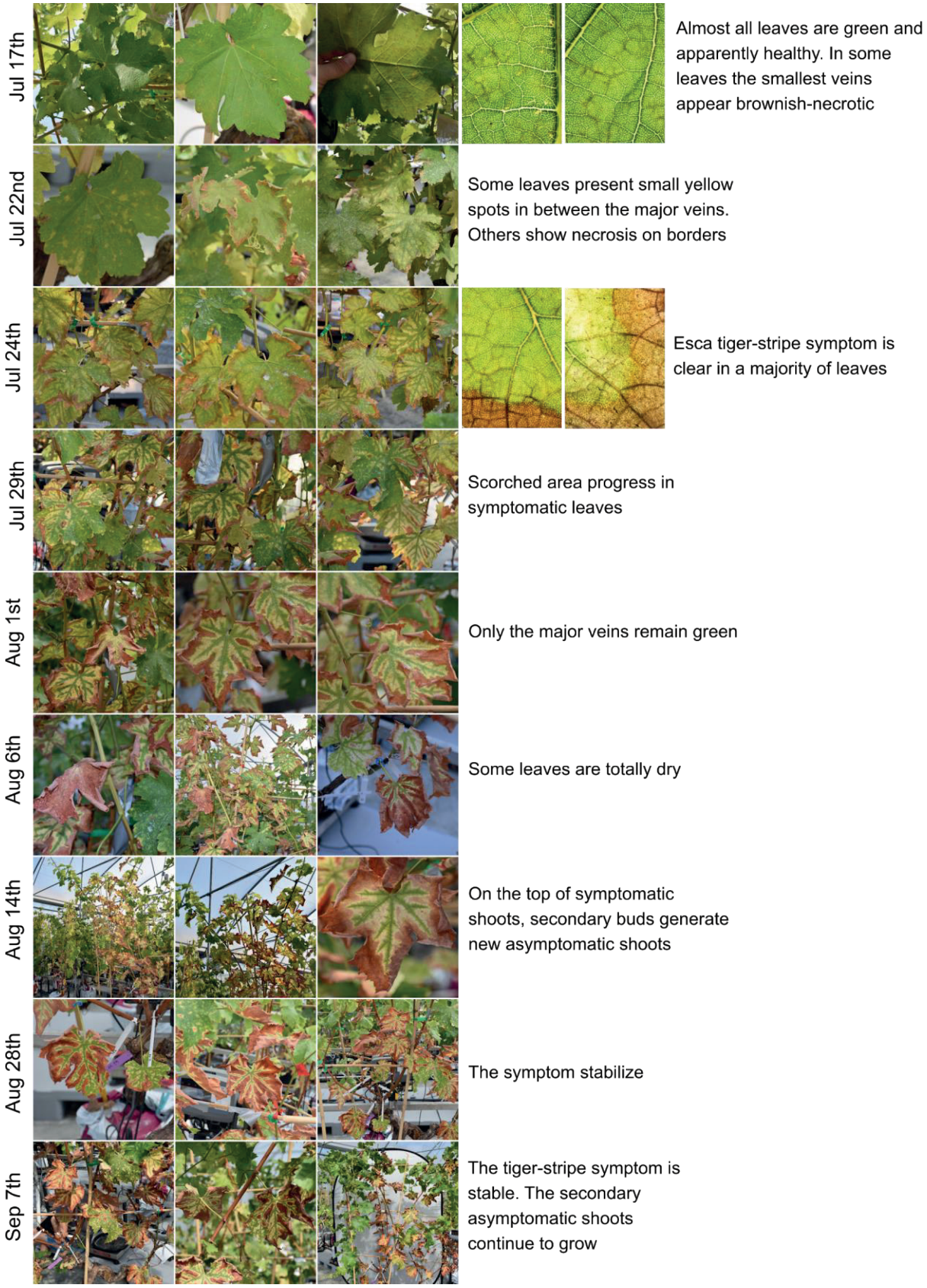

Supplementary Figure 4. Esca leaf symptom evolution in one plant of *V. vinifera* cv Sauvignon blanc

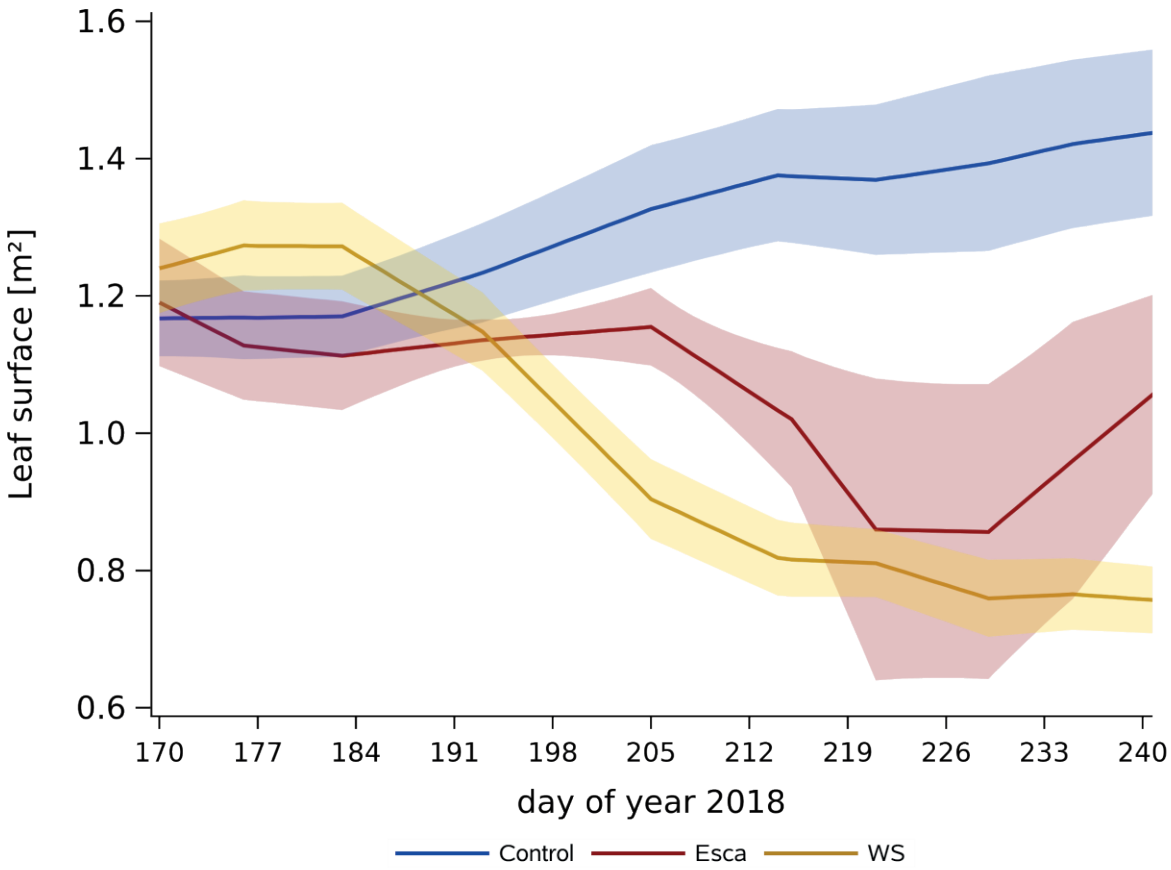

Supplementary Figure 5. Example of leaf surface evolution for control (blue), esca symptomatic (red), and water stressed (yellow) plants in 2018. Lines represent mean values, while band the SE during the season. Leaf surface was measured every week, a model interpolated a linear increase (or decrease) of leaf surface between two successive measures. Control plants increase their leaf surface during the season, leaf surface on WS plants decreased after the imposition of water deficit (day 180), regarding esca symptomatic plants we can observe a decrease during symptom appearance (between day 210 and 225), and a regrowth after day 230.

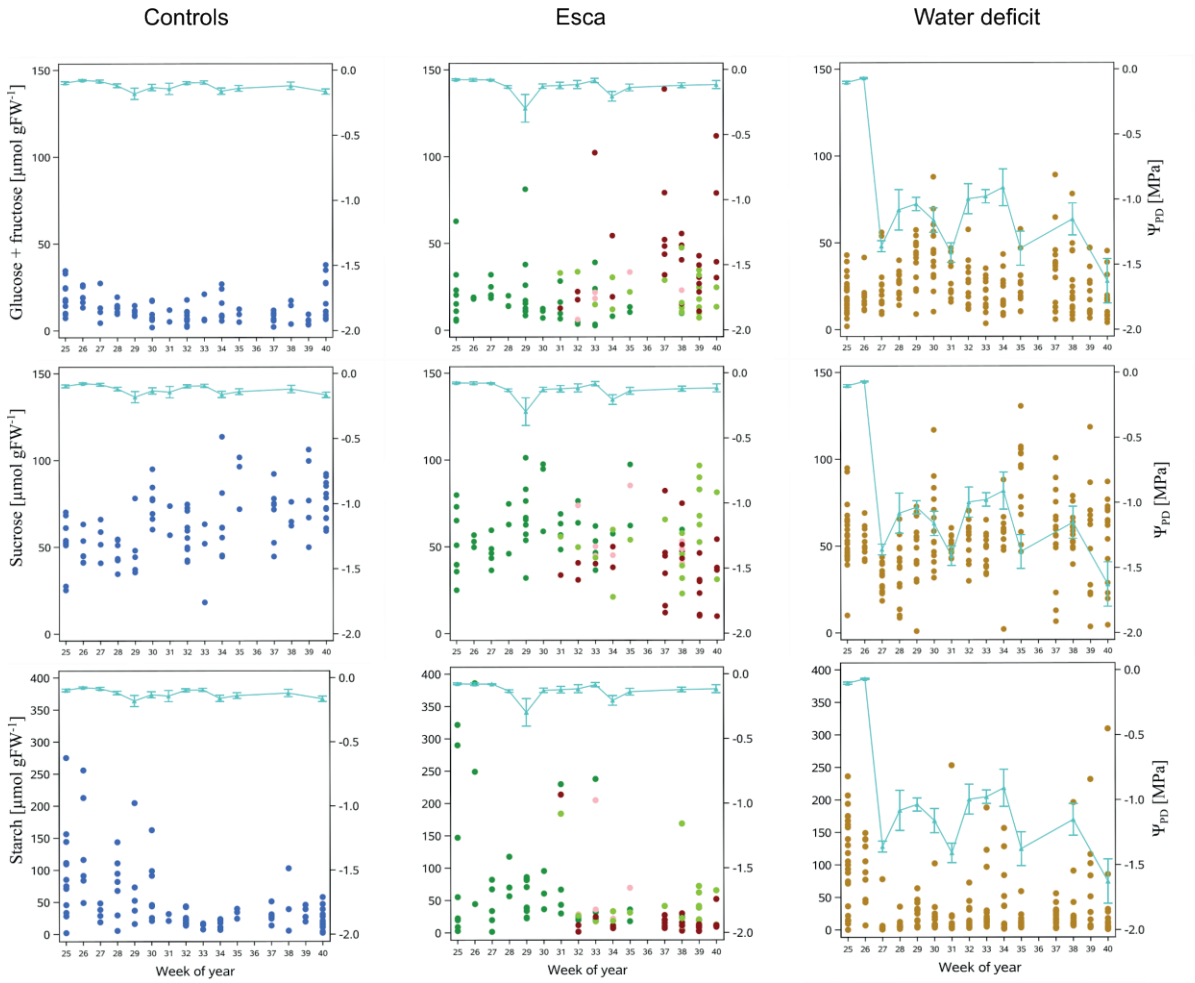

Supplementary Figure 6. Seasonal dynamic for the different NSC in leaves in 2018, compared to Ψ_{PD} values measured on the same plants at the same date. Panels are organized by stress conditions: control plants (dark blue dots), esca symptomatic plants (dark green dots for asymptomatic leaves before symptom appearance, light green dots for asymptomatic leaves in symptomatic plants, and red dots for esca symptomatic leaves), and water deficit plants (yellow dots). Dots represent single metabolite quantification, and triangles (light blue), mean Ψ_{PD} of the day ± SE.

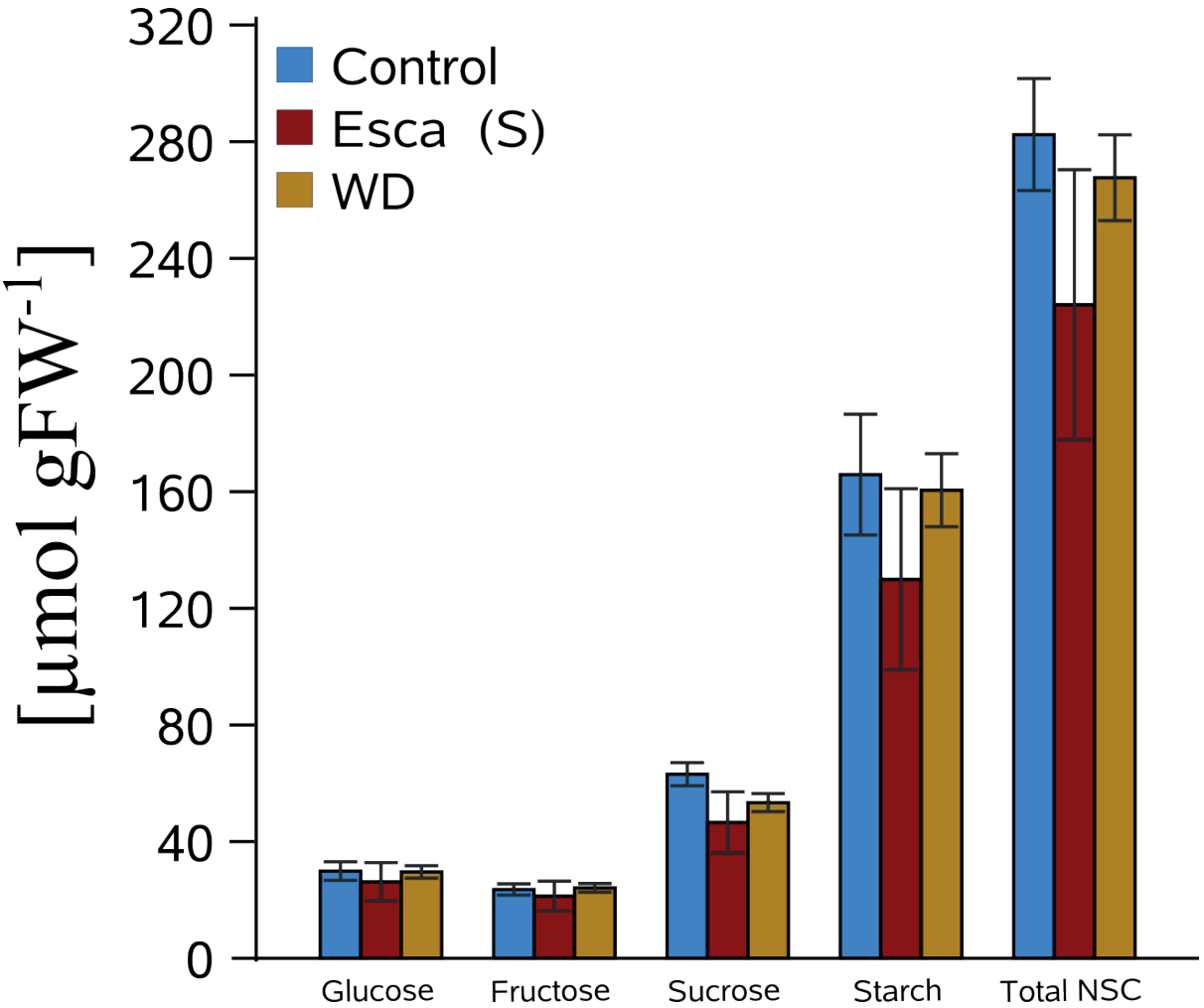

Supplementary Figure 7. NSC in µmol gFW^{-1} content in stems in winter 2018-2019, for control (blue, n=12), esca symptomatic (red, n=6), and plants after one year under water stress (yellow, n=25). Bars represent means and error bars SE. We used general linear mixed models to compare stressed and control plants and no statistical differences were found within any metabolite (Supplementary Table 3).

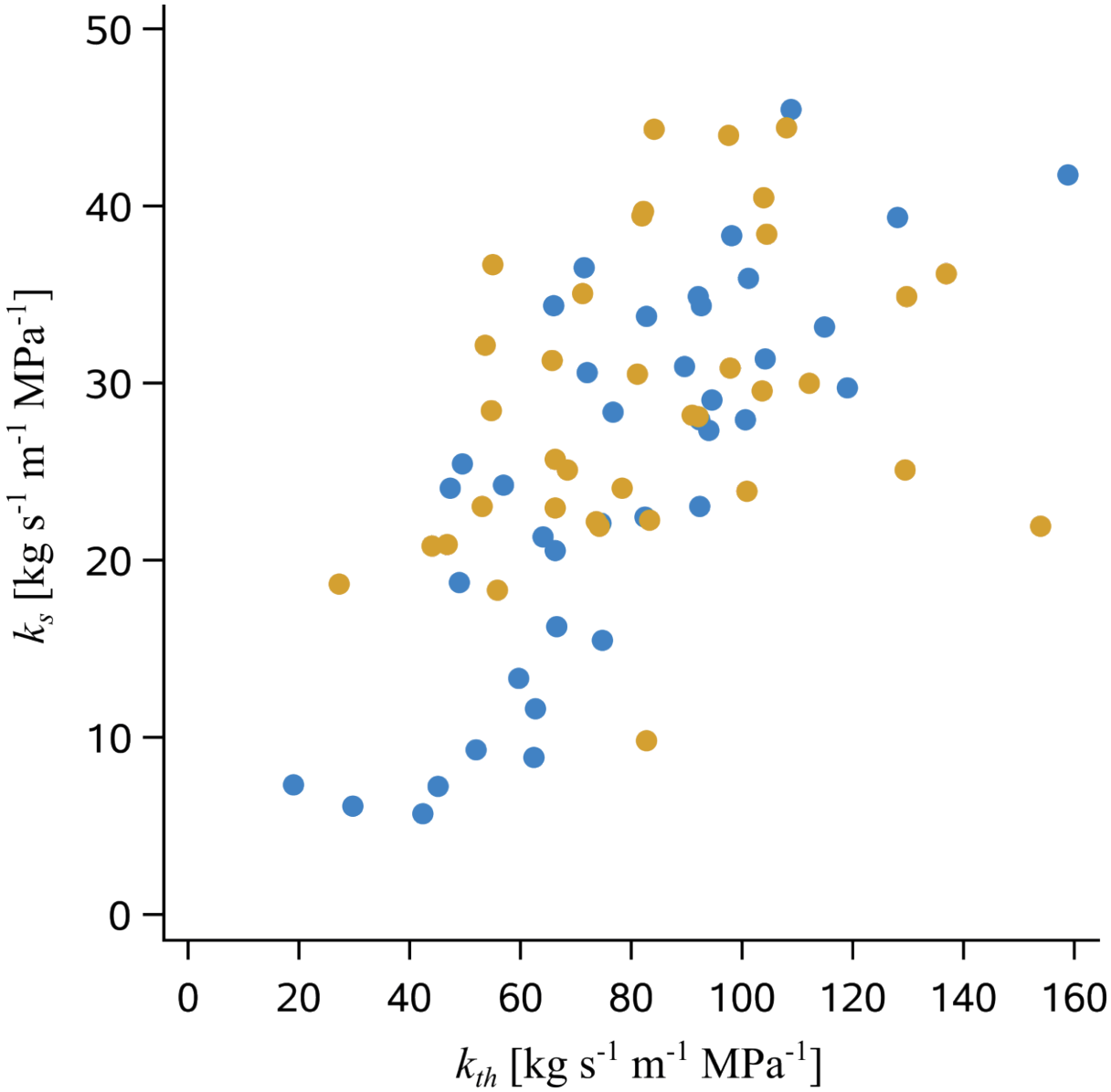

Supplementary Figure 8. Relationship between direct measurements of specific stem hydraulic conductivity (k_s) and theoretical stem hydraulic conductivity (k_{th}). Symbols represent values for control (blue) and water stressed (yellow) stems.

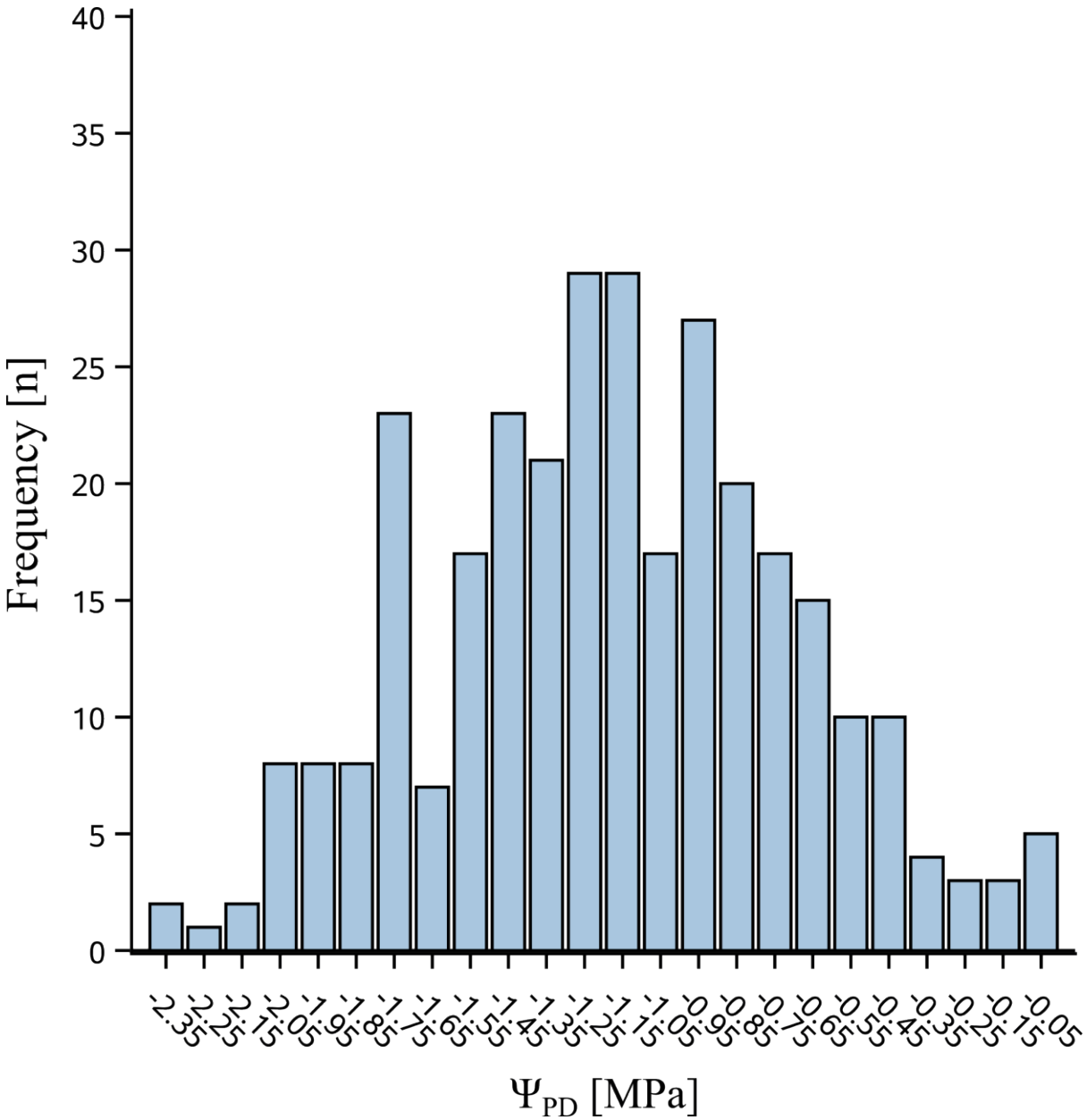

Supplementary Figure 9. Frequency of the recorded spectrum of Ψ_{PD} [MPa] over the two seasons in plants under water deficit (after changing the watering regime).

Supplementary Table 1. Effect of esca leaf symptoms and water deficit on leaf gas exchange and maximum quantum yield of photosystem II. We used independent mixed linear general models fitting a normal distribution. The treatment (control, esca asymptomatic, esca symptomatic and water deficit leaves) and the sampling date were entered as fixed effects (covariables) and the plant was treated as a random effect since different leaves were sometimes analyzed from the same plant. Statistical differences between specific treatments (Tukey comparisons) are presented in Fig. 2D.

Response variable	**Stress treatment**			**Sampling date**		
	DoF	**F**	***P***	**DoF**	**F**	***P***
gs	3,238	23.59	**<0.0001**	3,238	29.29	**<0.0001**
A	3,238	50.39	**<0.0001**	3,238	53.51	**<0.0001**
WUE	3,238	3.00	**0.03**	3,238	0.06	0.81
Psi II	3,17	3.86	**0.02**	Measured during the same week		

Supplementary Table 2. Effect of esca leaf symptom and water deficit on NSC content in leaves. We used independent mixed linear general models fitting a normal distribution. The treatment (control, esca asymptomatic, esca symptomatic and water deficit leaves) and the sampling date were entered as fixed effects (covariables), and the plant was treated as a random effect since different leaves were sometimes analyzed from the same plant. Only starch content in 2018 was log transformed prior to statistical test to fit a normal distribution. Statistical differences between specific treatments (Tukey comparisons) are presented in Fig. 3, 4, and 2018 weekly variation is presented in Supplementary Fig. 6.

year	Response variable	Stress treatment			Sampling date		
		DoF	**F**	***P***	**DoF**	**F**	***P***
2018	Glucose	3,271	26.5	**<0.0001**	3,268	9.63	**0.002**
	Fructose	3,271	23.07	**<0.0001**	3,268	1.15	0.60
	Sucrose	3,271	12.64	**<0.0001**	3,268	10.44	0.001
	Starch	3,271	9.51	**<0.0001**	3,268	13.80	**0.0002**
	Total NSC	3,271	1.41	0.24	3,268	15.52	**0.0001**
2019	Glucose	3,49	22.29	**<0.0001**	3,49	14.89	**0.0003**
	Fructose	3,49	38.51	**<0.0001**	3,49	1.20	0.27
	Sucrose	3,49	8.29	**0.0001**	3,49	61.61	**<0.0001**
	Starch	3,49	12.51	**<0.0001**	3,49	0.45	0.5
	Total NSC	3,49	11.02	**<0.0001**	3,49	1.21	0.28

Supplementary Table 3. Effect of esca leaf symptom and water deficit on NSC content in stems. We used independent mixed linear general models fitting a normal distribution. The treatment (control, esca asymptomatic, esca symptomatic and water deficit leaves) and the sampling date were entered as fixed effects (covariables), and the plant was treated as a random effect since different leaves were sometimes analyzed from the same plant. Statistical differences between specific treatments (Tukey comparisons) are presented in Fig. 3, 4, and Supplementary Fig. 7.

year	Response variable	Stress treatment			Sampling date		
		DoF	F	*P*	DoF	F	*P*
Winter 2018/2019	Glucose	2,40	0.23	0.79	Samples in winter were collected from all plants at the same date, the 22nd of January 2019. In correspondence with winter pruning.		
	Fructose	2,40	0.23	0.75			
	Sucrose	2,40	2.29	0.11			
	Starch	2,40	0.63	0.54			
	Total NSC	2,40	1.14	0.33			
Summer 2019	Glucose	3,31	8.32	**0.0003**	3,31	109.24	**<0.0001**
	Fructose	3,31	10.53	**<0.0001**	3,31	7.88	**0.0086**
	Sucrose	3,31	28.34	**<0.0001**	3,31	41.34	**<0.0001**
	Starch	3,31	16.35	**<0.0001**	3,31	195.08	**<0.0001**
	Total NSC	3,31	13.26	**<0.0001**	3,31	146.21	**<0.0001**

Supplementary Table 4. Effect of plant historical record (previously asymptomatic, pA, and previously symptomatic, pS) and its interaction with the sampling date on all recorded variables for plants under water deficit. We used independent mixed linear general models fitting a normal distribution. The historical record, the sampling date, and their interaction were entered as fixed effects (covariables) and the plant was treated as a random effect since different leaves were sometimes analyzed from the same plant. For whole-plant *Gs*, the day of year was treated

as a random effect as different hourly *Gs* could be recorded during the same day. For the metabolites in leaves (glucose, fructose, sucrose, starch, total NSC, and chlorophylls), the two sampling years were pooled together and the year of sampling treated as a fixed effect. The effect of the sampling date on the response variables is presented in Supplementary Tables 1, 2, 3.

Response variable	**Historical record (pA, pS)**			**Historical record and Sampling date interaction**		
	DoF	**F**	***P***	**DoF**	**F**	***P***
Gs	1,7972	1.77	0.18	1,7972	1.75	0.19
gs	1,84	0.01	0.93	1,84	0.02	0.90
A	1,84	0.32	0.58	1,84	0.41	0.52
WUE	1,84	0.18	0.67	1,84	0.18	0.67
PSII	1,4	1.06	0.36	Measured on one single week		
Glucose in leaves	1,222	0.23	0.63	1,222	0.18	0.67
Fructose in leaves	1,222	0.18	0.67	1,222	0.15	0.70
Sucrose in leaves	1,222	2.13	0.15	1,222	2.47	0.12
Starch in leaves	1,222	0.00	0.97	1,222	0.07	0.80
Total NSC in leaves	1,222	0.36	0.55	1,222	0.18	0.67
Chlorophylls (a+b)	1,222	0.02	0.90	1,222	0.04	0.85
Chlorophylls (a/b)	1,222	0.92	0.34	1,222	1.10	0.29
Glucose in stems	1,40	0.24	0.63	1,40	0.26	0.61
Fructose in stems	1,40	0.01	0.96	1,40	0.09	0.77
Sucrose in stems	1,40	1.22	0.28	1,40	1.18	0.28
Starch in stems	1,40	0.01	0.98	1,40	0.02	0.90
Total NSC in stems	1,40	0.03	0.87	1,40	0.09	0.77

Results summary - Chapter 5

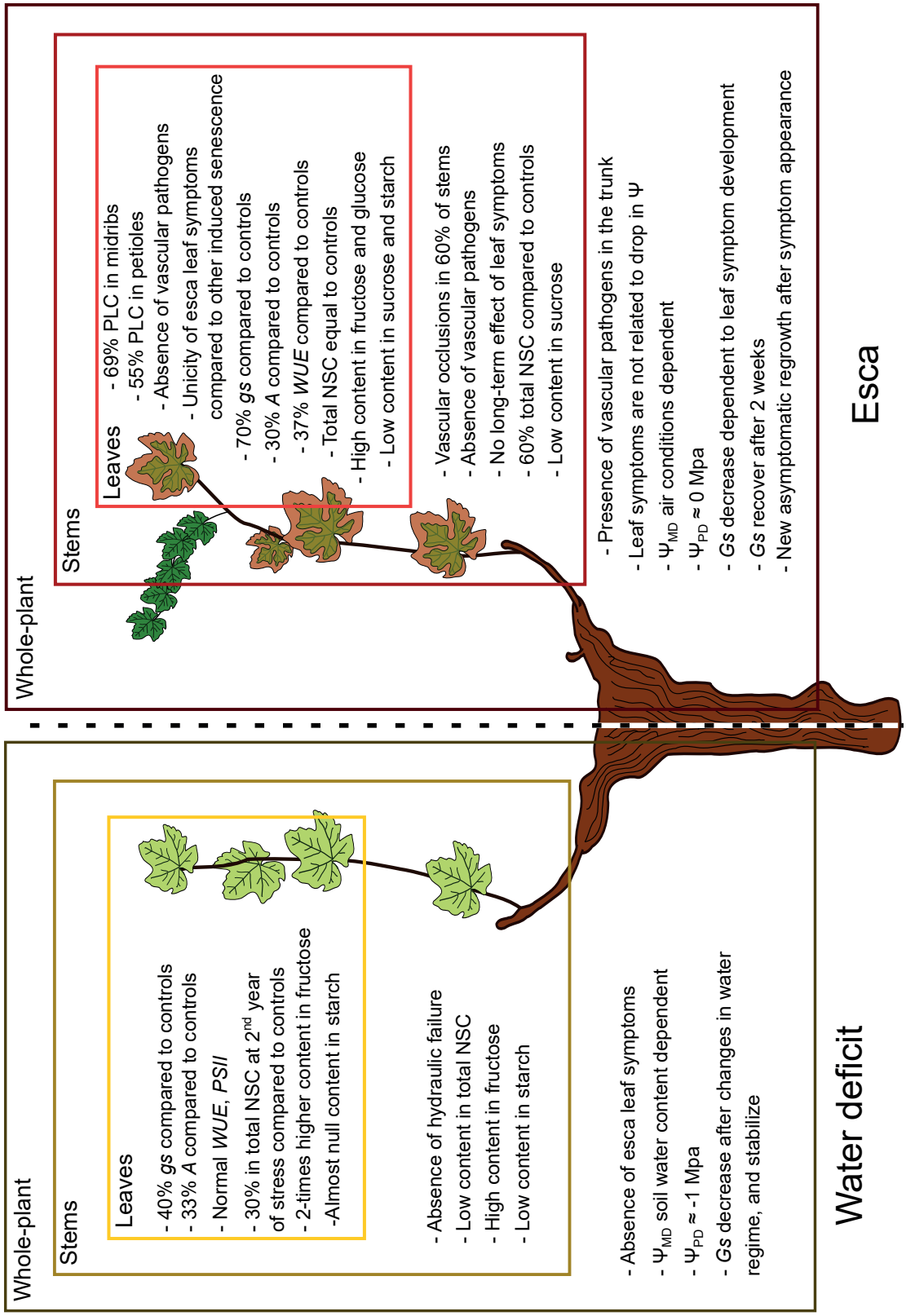

CHAPTER 6

Discussions, Conclusions, and Perspectives

Résumé: Durant cette thèse nous avons analysé les relations entre le fonctionnement hydraulique de la vigne, l'anatomie du xylème et la pathogenèse de l'esca. Cette étude a été animé par l'hypothèse que le fonctionnement hydraulique de la plante était au cœur du processus de dépérissement de la vigne, surtout lorsque l'esca et la sècheresse interagissent. Cependant des importantes lacunes empêchent la compréhension de l'esca. D'autant plus que même si l'esca est considérée comme une maladie vasculaire, ces effets sur le système vasculaire restent largement méconnus. Pour aborder ce défi scientifique, nous avons opté pour une approche intégrative. Nous avons commencé par les feuilles, en regardant à l'intérieur de leurs veines nous avons trouvé la présence (surprenante au début) d'occlusions dans les vaisseaux des feuilles symptomatiques (*Chapitre 2*). Nous avons comparé l'anatomie du xylème des feuilles symptomatiques d'esca avec d'autres processus de senescence et découvert l'unicité des occlusions vasculaires reliés à l'esca (*Chapitre 3*). Ensuite, nous avons quantifié l'effet de l'esca sur l'intégrité hydraulique des tiges sur le court et le long terme, trouvant que l'esca affecte les organes pérennes (les tiges) seulement saisonnièrement (*Chapitre 4*). Finalement, nous avons soumis la moitié des plantes à une contrainte hydrique en regardant les interactions entre la sécheresse et l'esca (*Chapitre 5*). Après l'observation (encore une fois avec surprise) que les plantes en sècheresse n'expriment jamais de symptômes foliaires d'esca, nous avons surveillé les relations hydriques et carbonées à l'échelle de la plante entière, trouvant que l'esca (et son conséquent décline de la conductance stomatique) ne résultent pas d'une chute du potentiel hydrique. Nous avons aussi découvert que, comparé à la sécheresse, l'esca génère différentes dynamiques saisonnières des échanges gazeux et des carbohydrates non-structuraux. Dans l'ensemble, ces résultats ouvrent nombreuses perspectives dans différents champs de recherche.

In this thesis, we analyzed the relationships between grapevine hydraulic functioning, xylem anatomy, and esca pathogenesis. This study was driven by the hypothesis that the plant hydraulic functioning is at the core of grapevine dieback, especially when drought and vascular diseases interact. However, important knowledge gaps are impeding the understanding of esca, considering that during this vascular disease the impacts of esca on the vascular system remained (almost) unknown. To address this scientific challenge, we used an integrative study. We started from the leaves, looking inside their vasculature, providing the evidence (surprising at first) of the presence of vascular occlusion, and their formation in functional vessels of esca symptomatic leaves (*Chapter 2*). We compared the xylem anatomy of esca symptomatic leaf midribs and other induced senescence process and discovered the uniqueness of vascular occlusions in esca leaf symptoms (*Chapter 3*). We then quantified the effect of esca on stem hydraulic integrity on the short and long term, finding that esca affects grapevine perennial organs (i.e. stems) only seasonally (*Chapter 4*). Finally, we submitted half of the plants to drought, investigating the interaction between drought and esca (*Chapter 5*). After the observation (once again with surprise) that plants under drought never showed esca leaf symptoms, we monitored the whole-plant water relations and carbon economy, finding that esca (and subsequent stomatal conductance decline) does not result from decreases in water potential, and generates different gas exchange and NSC seasonal dynamics compared to drought. Altogether, these results open many perspectives in different research fields.

6.1. Vascular occlusions, defining xylem hydraulic failure by nongaseous embolism

Classically, when studies have referred to hydraulic failure, they have considered air-induced embolism, produced during drought (Tyree and Sperry, 1989) or frost (Sevanto *et al*., 2012) events. Vascular occlusions have been associated with a multitude of processes (De Micco *et al*., 2016), but their presence has never been directly represented quantitatively as a loss of hydraulic conductivity, although many studies correlated occlusions with k_s decrease (Guerard *et al*., 2000, Sallé *et al*., 2008, Beier *et al*., 2017, Mensah *et al*., 2020). During vascular diseases, a role of hydraulic failure was suspected but never confirmed (Fradin and Thomma, 2006, Yadeta and Thomma, 2013). During esca, the suspicion of hydraulic failure was mainly given by the strict relationship found between the winter pruning and bad grafting practices on symptom incidence (Gramaje *et al*., 2018, Lecomte *et al*., 2018), leading to the hypothesis that artificial modifications in xylem pathways would increase the plant sensibility to hydraulic failure. In this context, even if still hypothetical, esca-related hydraulic failure was thought as air-related (i.e. cavitation and air embolism), and this conjecture founded the basis on the hypothetical synergy between drought and esca. However, the presence and nature (i.e. air, vascular occlusions, or obstruction by pathogens) of hydraulic failure were still unconfirmed. In this thesis, we observed occlusions primarily by tyloses and not by air inside the xylem vessels from esca symptomatic plants. We quantified their presence by different techniques, including X-ray microCT, optical visualization of leaf embolism, direct (k_s) and indirect (k_{th}) hydraulic

conductivity measurements, and light microscopy.

These occlusions, formed by tyloses and gels, impede a normal water flow in the plant confirmed by the use of contrasting agent iohexol during X-ray scans, where we observed that tyloses are formed in functional vessels, and they are not a mere consequence following air cavitation. The occlusions were related to a decrease in plant hydraulic conductivity. By X-ray microCT we found that vascular occlusions caused (on average) a PLC of 69% in leaf midribs, 55% in petioles, and 27% in stems. Comparing stem k_s to its theoretical analog (k_{th}) comparisons, we found that 60% of stems presented loss of hydraulic conductivity given by vascular occlusions. Finally, by the optical vulnerability (OV) technique, we found that 80% of leaves presented xylem functionality in less than half of the lamina surface.

These results support the conclusion that esca is related to hydraulic failure given by vascular occlusions. We define this failure as nongaseous embolism, as it decreases the hydraulic conductivity of the considered organ, but it is not formed by air (as previously hypothesized). In plant biology, no other authors used the term "nongaseous embolism" (webofknowledge.com consulted the 25th of January 2021); however, we stressed here the importance that this phenomenon could have on plant physiology, especially during biotic stresses, during which relationships with the plant hydraulic system are largely unknown.

During esca, the intensity of hydraulic failure is more related to the considered organ than to symptom severity. Indeed, we found relative high variability in the loss of hydraulic conductivity, as the standard error shift from the average occlusion PLC from 11% (in midribs) to 30% (in stems), and leaf lamina showed the highest variability at 38% around the average in OV (*Chapter 2* Fig. 3, *Chapter 3* Fig. 4, and *Chapter 4* Fig. 2). This variability was found within the same plants (i.e. different leaves or stems from the same plants presented variable PLC) and even within the same organ (see how sectorial dysfunctions can affect just half section of stems in *Chapter 4* Fig. 2j-l or a side of a leaf in *Chapter 3* Fig. 4G). Despite this variability, the fact that esca lead to hydraulic failure caused by vascular occlusions is now undeniable. We also observed that the level of hydraulic failure is decreasing from distal to basal organs: from the more to the less affected we observed leaf lamina > midribs > petioles > stems.

6.2. Hydraulic failure during esca, hypotheses on its formation

By which mechanisms the formation of vascular occlusion occurred, is now an open question. We found that appearance of esca leaf symptom is not related to a decrease in water potential (*Chapter 5*). Consequently, we can definitely exclude the intervention of air embolism (as during drought) prior to vascular occlusion formation. Moreover, this result reinforces the hypothesis that esca and drought induce different processes and plant responses, and the loss of hydraulic conductivity has different underlying origins.

Surely, we need to first consider the biotic agents as being responsible. Because *Pmin* and *Pch* develop in the xylem vessels (Pouzoulet *et al*., 2014) and are frequently found in esca symptomatic plants (Morales-Cruz *et al*., 2018), they have been suggested as the best candidates as

potential causal agents. However, their absence where the occlusions were observed (*Chapters 2* and *4*) are still delaying this interpretation. In this context, three major hypotheses could trigger the formation of nongaseous embolism and the subsequent hydraulic failure: (i) other (non-studied here) biotic agents, (ii) pathogen-derived or (iii) plant-derived molecules that move through the vasculature.

In the first hypothesis, our attention should focus on distinct group of pathogens: fungi and bacteria. Among fungi, Botryosphaeriaceae could play a major role in esca pathogenesis because they are related to grapevine trunk diseases (Bertsch *et al*., 2013, Fontaine *et al*., 2016), they are isolated in the brown necrosis in the external vasculature in the trunk (altogether with *Pch*, Kuntzman *et al*., 2010), and they were recently observed inside the xylem vessels (Khattab *et al*., 2021). From the Basidiomycota phylum, the *Fomitiporia* spp. which is associated with white rot (Fischer, 2006, Bruez *et al*., 2020) the most recurrent necrosis in symptomatic vines (Maher *et al*., 2012). Finally, bacteria can also cause vascular diseases in a large group of plants (Agrios, 2005), and their presence has been suggested as important in GTD development (Bruez *et al*., 2015, 2020, Haidar *et al*., 2015).

The second hypothesis, which predicts that the vascular pathogens produce toxins (or other elicitors) that would stimulate the nongaseous embolism, could explain the pattern of (distal organs or most affected decreasing basally) hydraulic failure during esca. Indeed, if we imagine a molecule flow in the xylem, we would expect that these molecules would be quickly transported to the leaves, and start to accumulate inside the leaf lamina. Once inside the leaves, these molecules would start their toxic action, creating necrosis in the interveinal zone, where the stomata are present in high number, and the water flow ends. Consequently, the toxic molecules would less affect the major veins as they accumulate in lower quantity. The same process would be then produced in all the part of the plant and be related to the quantity of toxins that are locally present. In this hypothesis, the functional xylem that is physically closer to the pathogens would be the least affected by toxic activities as the water flow is still active and is able to dilute and transport the molecules far away from the pathogens.

A third hypothesis on the formation of nongaseous embolism predicts that the plant, not pathogens, produces the triggering molecules. For example, the plant hormone ethylene stimulates the formation of vascular occlusions during *Xylella* infection (Perez-Donoso *et al*., 2006), and wound response (Sun *et al*., 2007) in grapevine. However, our preliminary results on ethylene quantification are suggesting that this hormone is not participating in esca senescence process (see Box 1 “preliminary results on ethylene quantifications during esca”).

Box 1. Preliminary results of the ethylene quantification during esca

Introduction

Ethylene is one of the main phytohormones regulating leaf senescence (Buchanan-Wollaston, 1997). It has been associated with tylose development after wounding (Sun et al., 2007, Che-Husin *et al*., 2018) or *Xylella fastidiosa* development (Perez-Donoso *et al*., 2006). Moreover, it has been detected after parasitic plant wounding (Texeira-Costa and Ceccantini, 2015), flooding (Hunt *et al*., 1981), and vascular fungi development (Fukuda *et al*., 1994), which are all related with vascular occlusions. As we demonstrated the existence of vascular occlusions during esca leaf symptom development (see *Chapters 2* to *4*), we hypothesized that a production of ethylene in symptomatic leaves could trigger tylose production.

Material and methods

Intact single leaves from control, esca symptomatic, and plants under water deficit (still attached to the plant) were inserted in plastic boxes, sealed with tape at the borders and with adhesive paste (Terostast-IX, Henkel, Dusseldorf, Germany) at the petiole level (as in Fig. B1.1). Sample sizes are detailed in Table B1.1. To avoid leaf burning the boxes were then covered with aluminum foils. The sampling has been realized in four different campaigns (between the 22th of July 2019 and the 20th of August 2019), leaves were left inside the boxes for 5 to 7 hours (from the morning to early afternoon) during the first three campaigns, and 24 hours for the last campaign. Using a syringe equipped with a very thin needle, we removed 1 ml from GC-MS tubes (2mm amber glass vials, locked with silicone/PTFE caps, Interchim, Montluçon, France), and substitute with 1 ml of air sampled in boxes. The tubes were then sent to ENSAT (Toulouse) facilities and the headspace in each tube was analyzed the following day with a gas chromatograph using a 2m x 3mm 80/100 alumina column, an injector at 110 °C, N_2 as vector gas in an isocratic oven temperature at 70 °C, and a FID detector at 250 °C (Chen *et al*., 2020). To prepare the blank samples, the air was sampled for every campaign in two places of the greenhouse and one outside the greenhouse; the maximum ethylene concentration of the air was used as blank. The ethylene production (ppb min^{-1} l^{-1}) was calculated as following:

Fig. B1.1. Experimental set-up for ethylene sampling during esca leaf symptom expression.

$$(E_L - E_0) / (t \times v)$$

Where: E_L corresponds to the ethylene quantified in the sample (ppb), E_0 corresponds to the maximum ethylene (out of the three blank samples) sampled in the air (ppb), t is the time between the sealing of the box and the sampling moment (min), and v correspond to the volume inside each box (l).

Results and discussion

All leaves presented very low values of ethylene production. Only control plants presented average values above ethylene concentration in the air (Table B1.1). This result suggest that ethylene is not produced in leaves during esca leaf symptom expression. We discarded the possibility of experimental bias (e.g. ethylene loss during transport or from boxes) as another experiment in the same greenhouse, in the same period, and using the same methodology, showed significant level of ethylene production in different species and stressing conditions (R. Burlett, personal communication). However, ethylene could appear and stimulate vascular occlusion in very short periods during esca pathogenesis, or ethylene could be effective at quantities below the limit of detection. Therefore, more research should be conducted to definitely discard ethylene intervention in esca leaf symptom formation. For example, we could imagine directly treating plants with ethylene, or applying chemicals in order to affect the ethylene perception by the plant.

Table B1.1. Ethylene production during esca leaf symptom expression. Plants are divided in control (asymptomatic) plants, plants under water deficit, plants presenting esca leaf symptoms, and plants asymptomatic during the sampling dates that will express esca leaf symptoms before the end of the season. The sample size of leaves and plants is indicated in parenthesis for each category. Values (ppb min^{-1} l^{-1}) correspond to mean ± SE ethylene production.

Control plants	Water Deficit plants	Esca symptomatic plants			Plants before esca leaf symptom appearance
		Asymptomatic leaves	Pre-symptomatic leaves	Tiger-stripe leaves	
(13 leaves from 7 plants)	(13 leaves from 10 plants)	(19 leaves from 7 plants)	(12 leaves from 9 plants)	(41 leaves from 10 plants)	(11 leaves from 3 plants)
0.010 ± 0.01	-0.018 ± 0.007	-0.004 ± 0.006	-0.009 ± 0.007	-0.003 ± 0.005	-0.006 ± 0.006

Acknowledgments

We strongly thank Christian Chervin from ENSAT (Toulouse) for his patience, the numerous email exchanges and calls, and for quantifying the ethylene in our samples. We thank Régis Burlett, Camille Parise, and Anne-Isabelle Gravel from UMR BIOGECO (INRAE) for their technical help in experimental set-up and provide the very thin needle for air sampling.

6.3. The link between nongaseous embolism and esca leaf symptom

In *Chapter 5*, we evidenced that esca leaf symptoms are not associated with a decrease in water potential. This result stresses the different physiology behind drought and esca. We could reasonably conclude that, opposite to drought-induced air embolism, the nongaseous embolism (found in *Chapters 3* to *4*) would not be caused by a decrease in water potential. This consideration, could be the starting point of a crucial scientific question: if the underlying mechanisms behind nongaseous and gaseous embolism are different, can we consider that they have the same consequences on the plant survival?

During drought, once P_{50} (or P_{88} depending on the species) is reached plants are not able to recover, even if in some species the long-term survival after P_{50} is still questioned (Adams *et al*., 2017). During esca, we still do not know the lethal thresholds of nongaseous embolism because our hydraulic measurements were destructives (the stems were cut off the plants) and we were not able to associate the loss of hydraulic conductivity to recovery or a subsequent mortality outcome. Moreover, some results in this thesis could even question the effective importance of nongaseous embolism in plant physiology.

The first observation that could question the consequences of nongaseous embolism is the presence of asymptomatic regrowth right after the appearance of leaf symptoms. Indeed, the observation that after symptom appearance (on average two weeks after) the plant was able to produce new asymptomatic tissues and to restore normal level of transpiration, suggest us that nongaseous embolism (and esca leaf symptom in general) cannot affect plant growth. In this context, we could hypothesize that the xylem tissue is "overbuilt" in grapevine (as found in many species, Brodersen *et al*., 2019), and the functionality loss of high proportion of vessels do not significantly affect plant functioning. However, we must remember that asymptomatic regrowth was not equally observed in all symptomatic plants and a correlation between level of nongaseous embolism in stems and symptom severity (as capacity of produce and maintain new stems) could exist.

The second observation that could question the role of nongaseous embolism in leaf symptom appearance and subsequent leaf mortality is the gas exchange dynamic. In *Chapter 5* (Fig. 2d), we evidenced that *WUE* and *PSII* at the leaf level are low in esca symptomatic leaves but not under drought, suggesting that during esca the photosynthetic apparatus is more affected during esca compared to drought. We could then conclude that loss in *gs* (and whole-plant *Gs*) decrease would be associated to a general leaf senescence, not to a decrease in water supply by loss in hydraulic conductivity. However, whole-plant *Gs* and percentage of symptomatic leaves were strongly correlated (*Chapter 5*, Fig. 2c), and we know that nongaseous embolism appear simultaneously (or right after) the onset of leaf symptoms (*Chapters 2* to *4*). Consequently, at present time it is impossible to dissociate the leaf senescence to nongaseous embolism formation, and conclude whether the decrease in gas exchange is caused by a decrease in xylem hydraulic conductivity or whether a more general senescence process induce leaf death and subsequent decrease in gas exchange and vascular occlusion.

However, these considerations are still hypothetical. In this thesis, we show that the water transport is compromised during esca, and in many cases, the xylem functionality is null or very low (independently from the organ analyzed). We correlated the presence of nongaseous embolism with symptom severity, as the totality of apoplectic stems presented vascular occlusions (*Chapter 4*). Moreover, hydraulic failure is the trait that distinguished the majority of esca symptomatic leaves and stems (*Chapters 2* to *4*); even from other induced-senescence process (*Chapter 3*). Together these results suggest that, even if not at the base of plant death during esca, hydraulic failure plays an important role during the disease process.

In this context, we could hypothesize two main processes during esca leaf symptom formation. The first, hypothesize that transport of toxins (or other molecules) directly cause the leaf symptoms and that hydraulic failure would be the mere consequences of an induced senescence process, where a portion of the canopy do not need water supply. In the second hypothesis, the leaf symptom would appear because different zone of the canopy are not well irrigated by hydraulic failure. We should stress that these two processes are not necessarily exclusive. From a third point of view, leaf senescence and nongaseous embolism form (almost) simultaneously. In that case, vascular occlusions would appear because leaves are dying, and leaves would start their senescence process because vessels are occluded. Finally, we still need to understand how nongaseous embolism affect vines over the long-term and if it affects plant susceptibility to drought (i.e. air embolism formation), which could be the real concern of this particular hydraulic failure mechanism.

6.4. Esca leaf symptoms and hydraulic failure, a spatial and temporal limited phenomenon

Our results presented in *Chapters 4* and *5*, suggest that esca leaf symptoms negatively affect grapevines only during the year of expression. The difference in the symptom history record (pA/pS plants) did not influence the stem hydraulic properties in control stems (*Chapter 4* Table 3), nor the response to water deficit (*Chapter 5* Suppl. Table 4). This result suggests that the pathogens can influence the functional part of the plants only in specific periods and conditions. In our study, esca leaf symptom presence did not even influence the winter reserves (*Chapter 5* Suppl. Fig. 6). However, we should take into account the conditions that mainly differentiate our greenhouse experiment from the field conditions; especially the absence of fruits, the irrigation with nutritive solution, and the presence of asymptomatic regrowth on the top of symptomatic stems. The absence of fruit (and a reduced crop load) in grapevine is known to increase whole-plant biomass and total NSC content (Dayer *et al*., 2013, Vaillant-Gaveau *et al*., 2014). Nutritive solution could also change plant physiology, surely because it contains all the minerals that are not always available in the field, and because a foliar treatment with mineral nutrients showed to reduce esca leaf symptom incidence (Calzarano *et al*., 2014), suggesting an enhanced defense response. Finally, the presence of asymptomatic regrowth (which is usually trimmed in vineyards) could have change the source/sink relationships in disease process as

described below. Indeed, even if the asymptomatic regrowth has not been reported in esca field surveys, its presence in our experimental design is raising interesting hypotheses on the disease process and on how the vines could escape or avoid pathogen activities.

The asymptomatic regrowth suggests that the newly formed xylem was not affected by the pathogens. In many cases, we observed a sectoring of the disease: when the vascular occlusions are observed in just a part of the stem (*Chapter 4* Fig. 2), or when we look at the brown necrosis along the vasculature (Lecomte *et al*., 2012, and *Annex 1* of this thesis). This dysfunctional sectoring reflects the xylem organization in grapevine, as it has been shown that xylem vessels are only partially interconnected, and that specific roots are only and directly connected to specific part of the canopy (McElrone *et al*., 2021). Consequently, we could hypothesize that the newly formed xylem is able to connect the new asymptomatic regrowth avoiding the pathogen-influenced zone in the trunk. This asymptomatic regrowth could also help the plant to create new sources of energy to fight against pathogens. In this context, we could imagine that vines should efficiently combat vascular pathogen infections in no (or minimal) pruning training systems. They could isolate the pathogens by creating an efficient restriction zone (as in CODIT model, see *Theoretical framework* in *Chapter 1*), and then isolate the necrosis by just simply growing around it. Minimal pruning is a training system developed in Australia (Possingham, 1996), and in the US (Reynolds and Wardle, 2001). However, this practice remains only experimental in Europe (Schultz *et al*., 2000) because its effect on fruit quality remain uncertain or negative (Weyand and Shcultz, 2006), even if its use could decrease GTD incidence (Travadon *et al*., 2016). In vineyards, vines are pruned in winter, and constantly trimmed in summer. This situation could help pathogen develop in pruning wounds after winter, and decrease vine defenses during summer. It has been shown that GTD incidence increased with intensive pruning (Gramaje *et al*., 2018, Lecomte *et al*., 2018). Because pruning is a common practice in perennial crops, intense pruning could explain why these pathogens are less descripted in forestry ecosystems (Table 1), and when they are detected in forests, they frequently do not induce symptoms (i.e. they are classified as endophytes, Table 1).

6.5. The hypothetical underlying mechanisms behind drought and esca antagonism

As presented in *Chapter 5*, grapevines never expressed esca leaf symptoms when submitted to a prolonged water deficit of $\Psi_{PD} \approx$ -1MPa. This water deficit was intense enough to induced stomatal closure but not hydraulic failure. Consequently, we could hypothesize different mechanisms underlying the antagonism between esca and drought. (i) Drought could induce the formation of smaller xylem vessels, more resistant to pathogen development. (ii) Drought, by inducing a decrease in transpiration rates, could reduce the transport of toxic metabolites. (iii) Drought could induce a more efficient defense response in the trunk and/or in leaves. (iv) Drought could induce a shift in microbial population composition in grapevines and/or a shift in pathogen aggressiveness.

We are almost able to discard the (i) hypothesis, as we did not observed vessel size distribution

or k_{th} changes in stems from plant under drought (*Chapter 5*, Suppl. Fig. 7). Moreover, the drought was applied on the 1st of July once the stems have already grown in well-watered conditions during spring. Consequently, even if the information on how water deficit would affect the xylem anatomy in trunks is still lacking, we can hypothesize that the majority of vessels (formed in spring) were similar in all the plants.

The (ii) hypothesis is in line with the more general "toxin hypothesis" on esca leaf symptom formation. Indeed, if we hypothesize that a pathogen-derived molecule is causing the leaf symptoms, this molecule would arrive in lower amount when the transpiration is reduced (i.e. during moderate drought events). The role of transpiration on esca leaf symptoms was explored during a preliminary experiment in this thesis (see Box 2 "The magic bag").

The (iii) hypothesis could also explain the drought-esca interaction. Drought is known to stimulate the formation of antioxidant compounds (Gambetta *et al*., 2020), and in controlled conditions polyphenols reduce esca-related pathogen growth (del Rio et al., 2004, Gomez et al., 2016). Consequently, these compounds could have enhanced plant response to pathogen activities. Moreover, we observed an accumulation in hexoses in leaves and stems during water deficit (*Chapter 5* Fig. 5), this accumulation could imply that a faster synthesis of defense compounds (as hexoses are the primary molecules of the secondary metabolism (Morkunas and Ratajczak, 2014).

The (iv) hypothesis needs deeper studies on microbial population equilibrium in asymptomatic and symptomatic plants (se Bruez *et al*., 2020). Considering that perennial plant dieback could frequently result from a change in microbial (or microbiome) community (Bettenfeld *et al*., 2020), the role of the microbial population equilibrium is more than a simple hypothesis. Drought is known to influence soil and root fungal (Rasmussen *et al*., 2019) and bacterial (Naylor and Coleman-Derr, 2018) populations, and interact with pathogens during dieback in forestry (Desprez-Loustau *et al*., 2006). In our case study, it could be possible that microorganisms that contrast the esca-related pathogens can easily develop during drought, or taking advantage of the decreased virulence of pathogens. We explored this hypothesis on the trunk ascomycete fungal community in a preliminary study using metagenomics (see *Annex 1* "Preliminary results on trunk necrosis extension and Ascomycota communities in grapevines under water deficit and esca").

Finally, it is worth noting that all the hypotheses (i to iv) are not necessarily exclusives and could contribute together to the drought-esca antagonism.

Box 2. The magic bag

Introduction

We demonstrated that grapevines under drought never showed esca leaf symptoms (Ch. 5). One of the main hypotheses on the underlying mechanisms behind esca and drought antagonism states that the reduced transpiration rate could reduce the transport of plant derived toxins (responsible for the visual symptoms). To test this hypothesis we randomly inserted intact leaves inside humid plastic bag at the beginning of the season (June) to reduce the transpiration rate on single leaves.

Material and methods

At the beginning of the season (mid-June) we randomly inserted intact leaves (still attached to the plants) inside transparent plastic bag with humid paper towel. Among all the plants in this experiment (n=20) only one expressed esca leaf symptoms (first symptom notation on 19th of August).

Results and discussion

On the 20th of August we opened the one bag left on the plant for three months. With great surprise, we noted that in the whole plant it was the only leaf completely green and without any sign of discoloration (Fig. B3.1). We hypothesized that the main affected parameter in the bagged leaf was the transpiration rate. We could then speculate that toxins, or any causal molecules, did not reach the leaves as they follow primarily the transpiration stream. This result open new perspectives on the role of transpiration during esca leaf symptom expression.

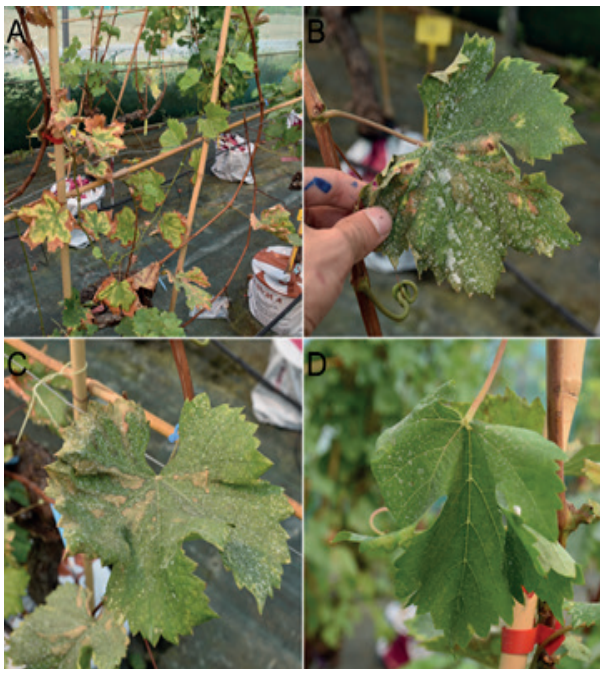

Figure B2.1. (**A**) Entire plant, tiger-stripe symptoms are well visible. (**B**, **C**) Two symptomatic leaves on the same stem on which we installed the bag. (**D**) The asymptomatic leaf that passed three months inside the humid bag. Picture A was taken the 30th of August, while B, C, and D the 20th of August.

Acknowledgments

I personally dedicate this experience to the entire greenhouse team, this is a small result but it was very intense to live! Thanks to Nathalie, Chloé, and Elena, who supported me in this experiment, I know it was disgusting to look at the molded bags. Thank you for leaving them there! I also thank my lab who stood my enthusiasm that day.

6.6. Drought and esca, which role could play the observed antagonism in vineyards?

During field surveys, esca leaf symptoms are usually associated with hot and rainy periods (Marchi *et al*., 2006, Serra *et al*., 2018, Kraus *et al*., 2019). However, plant physiological thresholds (i.e. water potential or stomatal conductance) were not monitored along with the field studies on esca incidence (Mugnai *et al*., 1999, Surico *et al*., 2000, Redondo *et al*., 2001, Marchi *et al*., 2006, di Marco *et al*., 2011, Guerin-Dubrana *et al*., 2013, Li *et al*., 2017, Serra *et al*. 2018, Lecomte *et al*., 2018, Calzarano *et al*., 2018, Kraus *et al*., 2019), making interpretations on environmental impact on disease expression impossible. Here we demonstrated that a specific drought level resulted in a total absence of esca leaf symptoms. This tendency should ideally be confirmed in the field by measuring midday and predawn water potential and obtain essential information on the vine water status in vineyards over multiple years of varying esca incidence. In addition, a study comparing esca leaf symptom presence and incidence among different climatic regions is still missing and would be essential to understand the role of specific environmental conditions. On our side, we can observe that esca leaf symptoms surveys are mostly done in France, Germany and northern Italy vineyards, which could be considered as ones of the most humid viticulture regions in the world.

In the thesis, we stressed plants at a specific target drought intensity of $\Psi_{PD} \approx$ -1MPa; consequently, the impact of other drought levels (lower or higher target Ψ_{PD}) is still unknown. In the case of a more intense drought (i.e. Ψ_{PD} below -1MPa), we could speculate that the pathogen and drought interaction would lead to an accelerated mortality as during pine wilt disease, where the plants defenses (enhanced during moderate drought) seems to be erased during intense drought (compare Salle *et al*., 2008 to Gao *et al*., 2017). However, we did not observe any long-term effect of the history of esca symptoms on the plant response to drought, indicating that drought always prevail on pathogens. Consequently, we could hypothesize that plants would equally die by drought, independently from the pathogen inoculum (or trunk necrosis extension). In contrast, the presence of vascular occlusions could suggest a possible synergy between drought and esca if intense drought is applied after formation of nongaseous embolism. This is a realistic scenario given that esca leaf symptoms (in France) appear generally between June and July (Lecomte *et al*., 2012) and the most intense drought events in vineyards are observed in August (Choné *et al*., 2001, van Leeuwen *et al*., 2009). Intuitively, if a symptomatic stem presents an average of 30% PLC, it would reach 88% PLC (i.e. mortality, Urli *et al*., 2013) at higher Ψ compared to control stems. In leaves, we showed that the majority of symptomatic leaves presented hydraulic dysfunctions in more than half of the hydraulic system (*Chapter 2* for midribs and petioles and *Chapter 3* for leaf lamina). In studies on grapevine drought resistance, the leaves that reach these losses of hydraulic conductivity are not able to recover (i.e. they are already dead, Dayer *et al*., 2020b).

If drought induces Ψ_{PD} above -1MPa we could imagine that the infected plants, at certain drought intensities, will start to express leaf symptoms. However, grapevine drought response

is also likely dependent on the variety and rootstock, especially in stomatal response to moderate drought intensity or VPD changes (Schultz, 2003, Charrier *et al*., 2018, Dayer *et al*., 2020b), while xylem embolism in stems seems to be uniform in a wide range of varieties (Charrier *et al*., 2018). Consequently, our comprehension on esca leaf symptom phenomenon should pass through the study of varietal-dependent responses as we only studied Sauvignon blanc in this thesis. For example, if the role of transpiration during esca highlighted here is confirmed in different varieties, we could predict leaf symptom expression depending on susceptibility to stomatal closure, which is known to be varietal-dependent (Levin *et al*., 2019).

CONCLUSIONS

In *Chapter 5*, we analyzed how drought and esca could affect the plant-water relations and carbon balance. We stressed the importance in finding the physiological thresholds that determine the impact of one or more stresses. As physiological thresholds, we are referring to both the applied stress intensities and the monitoring of the physiological consequences of these stresses. On one hand, the intensities were quantified recording Ψ_{PD} and esca leaf symptom severity. On the other hand, the consequences were quantified measuring the temporal sequence of physiological events.

We evidenced that esca is a water flow-driven process. The hydraulic failure incidence (by nongaseous embolism) decreased from distal to basal organs in esca symptomatic plants (*Chapters 2* to *4*), as well as the general induced senescence process. At the same time, we demonstrated that esca (i.e. leaf symptom and related hydraulic failure) is not related to a decrease in water potential. The results on NSC quantification confirmed the tendencies from previous works (Petit *et al*., 2006, Valtaud *et al*., 2011), suggesting a local response to pathogen activities in leaves and more general consequences given by the presence of hydraulic failure. The comparative study between esca and drought, demonstrated that the initial transpiration decrease during esca leaf symptoms appeared similarly to drought but resulted from different underlying mechanisms, evidenced by differences in the photosynthetic performance, in the water potential gradient, and the presence of nongaseous embolism during esca. The accumulation of hexoses was similar between esca and drought, but the influence on starch and sucrose contents suggested a different metabolic behavior. Sucrose (which is the mobile NSC form) is affected during esca, probably because nongaseous embolism affect phloem transport, and starch is almost absent in leaves at the second year of water deficit, suggesting a cumulative effect on repeated drought events on NSC consumption.

Evidencing that esca is a water flow-driven process could suggest how we could identify the physiological thresholds during symptom expression. Coupling our results with the field symptom surveys, we would expect an increased symptom incidence when the VPD is high and the soil water is high enough to support maximal transpiration. If the central role of transpiration during this process is confirmed, by comparing different varieties in different climatic conditions, we could forecast esca leaf symptom expression by coupling the probability of

re-expressing symptoms year after year (Guerin-Dubrana *et al*., 2013), with Ψ_{PD}, air VPD conditions, and the transpiration rates.

Studying the NSC balance in plants under stress could help us to understand the long-term consequences of drought and esca. First, there was a surprising (almost total) absence of starch in leaves during the second year under drought. This result could suggest that when drought is long and repeated over several seasons, the carbon balance in the plant is drastically modified and might cause death by carbon starvation over the long-term (as hypothesized by McDowell *et al*., 2008), which still was not the observed in this study. Second, we observed a reduced total NSC content in perennial organs (stems), suggesting a reduced amount of reserves for bud growth in the next season. Of course, many other studies are needed to explore the NSC content in other sink organs (especially roots) to confirm this trend. However, this result is even more important when we think that new healthy xylem is fundamental for generate asymptomatic stems and leaves and compartmentalize the pathogens in the trunk.

In this thesis we evidenced (as expected) that both stresses have a general negative influence on plant physiology. The observed antagonism between esca and drought does not rule out that the two stresses could synergistically contribute to plant decline. Drought could have strong long-term influence (as suggested by total NSC reduction, and hydraulic failure when drought is severe), and even if esca seems to negatively impact plant physiology only seasonally, all symptomatic plants presented high percentages of necrotic tissue inside their trunks (*Annex 1*), variable level of PLC in stems, and potentially high content of pathogen inoculum. Moreover, we need to consider that grapevines could be more sensible than recorded here. Simply because grapevines are cultivated to carry the grapes, and leaf mortality (or inefficiency) could be sufficient to severely decrease yield quality and quantity, even when plant mortality is not questioned. Esca is known to decrease berry quality (Calzarano *et al*., 2004, Lorrain *et al*., 2012), as well as too intense and prolonged drought (van Leeuwen and Darriet, 2016). Consequently, other studies are needed to record the impact of our findings in field conditions, where grapevines are also subjected to many other stress factors.

PERSPECTIVES

In this thesis, our results opened many research perspectives, resumed in Fig. 1. First, other studies should investigate the open questions in esca pathogenesis presented in this discussion. Regarding the role that pathogen-derived molecules could have; the long-term consequences of extensive nongaseous embolism; and the exact sequence and nature of events behind the leaf (and trunk) esca symptoms. Second, field studies should confirm the trends highlighted here, in different climates and varieties. Once the main findings are confirmed and more deeply explored (mostly the role in transpiration and the esca/drought antagonism), our comprehension of the general dieback process could greatly advance. Finally, the detection of the precise physiological thresholds inducing an interaction between the environmental conditions and esca,

as well as the long-term consequence of nongaseous embolism and its relations with pruning practices would help vineyard sustainability.

Table 1. Description of the two esca-related vascular pathogens (by genus) in non-*Vitis* hosts. Two different researches by keyword were done in webofknoledge.com (*Phaeomoniella*, NOT *Vitis*, NOT grapevine; and *Phaeoacremonium*, NOT *Vitis*, NOT grapevine).

Pathogen genus	Publication	Host genus	Crop/forestry	Symptom
Phaeomoniella	Di Marco *et al*., 2003	*Actinidia*	Crop	Endophyte
Phaeomoniella	Damm *et al*., 2010	*Prunus*	Crop	Wood necrosis
Phaeomoniella	Alonso *et al*., 2011	*Pinus*	Forestry	Endophyte
Phaeomoniella	Sanz-Ros *et al*., 2015	*Pinus*	Forestry	Endophyte
Phaeomoniella	Schulz *et al*., 2018	*Pinus*	Forestry	Wood necrosis
Phaeoacremonium	Di Marco *et al*., 2004	*Actinidia*	Crop	Wood decay
Phaeoacremonium	Carlucci *et al*., 2013	*Olea*	Crop	Wood decay
Phaeoacremonium	Lynch *et al*., 2013	*Quercus*	Crop	Trunk disease
Phaeoacremonium	Premalatha *et al*., 2013	*Aquilaria*	Forestry	Endophyte
Phaeoacremonium	Olmo *et al*., 2014	*Prunus*	Crop	Wood decay
Phaeoacremonium	Marin-Terrazas *et al*., 2014	*Prunus*	Crop	Branch dieback
Phaeoacremonium	Spies *et al*., 2018	*29 woody hosts*	Forestry/crop	Various
Phaeoacremonium	Panahandeh *et al*., 2019	*Synzygium*	Crop	Trunk disease
Phaeoacremonium	Bartnik *et al*., 2020	*Rosalia*	Forestry	Beetle association
Phaeoacremonium	Biedermann *et al*., 2020	*Saccharum*	Crop	Beetle association
Phaeoacremonium	Espargham *et al*., 2020	*Citrus*	Crop	Trunk disease
Phaeoacremonium	Lopez-Moral *et al*., 2020	*Pistacia*	Crop	Branch dieback
Phaeoacremonium	Scortichini *et al*., 2020	*Olea*	Crop	Quick decline

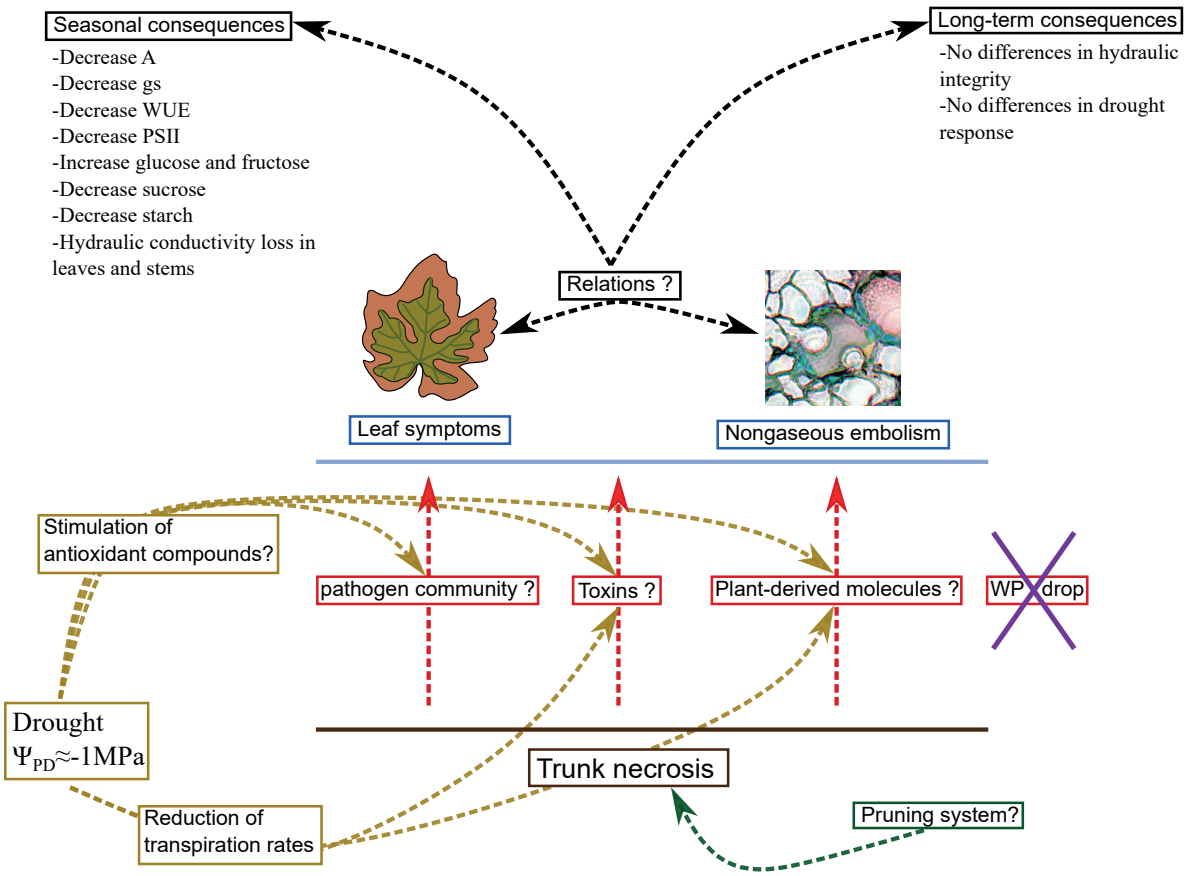

Figure 1. Schematic representation of hypothetical (dashed arrows) processes during esca and drought interaction based on the major findings of this thesis. Trunk necrosis (brown) is at the base of the esca pathogenesis, and different pruning systems (green lines), discussed in *Paragraph 6.4.*, could influence the necrosis extension and negative effects. From trunk necrosis to the leaf symptoms and the formation of nongaseous embolism, we hypothesized three different processes (red lines, discussed in *Paragraph 6.2.*): the intervention of different pathogen communities (explored in *Annex 1*), the transport via the transpiration stream of toxins and plat-derived molecules (briefly explored in *Boxes 1* and *2*), and we excluded (based on our findings) a drop in water potential. Leaf symptoms and nongaseous embolism (in blue, discussed in *Paragraph 6.1.*), could present different relationships (discussed in *Paragraph 6.3.*) resulting in seasonal and long-term consequences (in black, discussed in *Paragraphs 6.2.* and *6.4.*). Drought (in yellow), which consequences on grapevine dieback are discussed in *Paragraph 6.6.*, could influence the induction of esca leaf symptoms by (see *Paragraph 6.5.*) stimulating the production of antioxidant compounds by the plant (against other pathogens or molecules) or by reducing the transpiration rates (which could mostly influence the transport of toxins or other molecules).

Annex 1

Preliminary Results on Necrosis Extension and Ascomycota Communities in Plants under Water Deficit and Expressing Esca Leaf Symptoms

Authors

G. Bortolami, J. Vallance, N. Ferrer, G.A. Gambetta, C.E.L. Delmas

Author contribution

G.B., J.V., G.A.G., C.E.L.D. planned the experiment

G.B. and N.F. sampled the tissues and grounded the samples

N.F. carried out the DNA extraction

J.V. compiled the OTU table from DNA sequences and wrote the corresponding methodological section

G.B. analyzed the data

Introduction

As reviewed in Bettenfeld *et al*. (2020), woody perennial species can be considered as a holobiont, as they host many different microorganisms (such as viruses, bacteria, and fungi) interacting neutrally, positively, or negatively with the plant. In Grapevine Trunk Diseases (GTD) a shift in microbial communities could set the starting point for accelerated mortality (Bertsch *et al*., 2013, Bruez *et al*., 2020). During esca pathogenesis many doubts remain on (i) which pathogens are responsible for the different disease symptoms (in perennial and annual organs) and the final plant death, and on (ii) which environmental changes could trigger a critical (or restoring) shift in microbial community. Indeed, changes in microbial community could induce the development of symptoms and/or the production of apparently healthy leaves and stems during the asymptomatic seasons.

In this study, we used the same uprooted plants as in the other parts of this manuscript. We sampled different organs from 41 plants with different disease histories. In each sample, we analyzed the Ascomycota communities by high-throughput sequencing (MiSeq technology). This

result being very preliminary, we will simply present some relative abundance data by genus for three different scientific questions: (1) What is the long-term impact of esca leaf symptoms on Ascomycota community in the grapevine trunk of asymptomatic plants? (2) What is the impact of seasonal drought or esca leaf symptoms on Ascomycota community in the trunk? (3) What are the main Ascomycota genera colonizing the brown stripe necrosis along the trunk?

Material and methods

Plant material and replicates

The sampling was done between the 7th of October and the 14th of October 2019, in a subset of plants (n=41 *V. vinifera* cv. Sauvignon blanc) used in *Chapter 5*. Based on the treatments presented in *Chapter 5*, the plants could belong to three different groups with two possible treatments in each group: 1) the watering regime in 2018 and 2019: WW (well-watered for two years), and WD (water-deficit, presenting $\Psi_{PD} \approx$ -1MPa from July to October in 2018 and 2019). 2) The symptom history record from 2012 to 2019: pA (had never expressed esca leaf symptoms since 2012, previously asymptomatic), and pS (had expressed at least once esca leaf symptoms since 2012, previously symptomatic). 3) Esca leaf symptom expression in 2019: Control (asymptomatic), and Esca (expressing tiger-stripe symptoms).

As WD plants never expressed esca leaf symptoms (see *Chapter 5*), we sampled four different types of plant: WD (n=10, water-deficit, previously symptomatic); Esca (n=9, well-watered, previously symptomatic, and expressing tiger-stripe symptoms in 2019); Control-pS (n=11, well-watered, previously symptomatic, and asymptomatic in 2019); Control-pA (n=10, well-watered, asymptomatic since 2012).

In these plants, we sampled four different organs for DNA extraction and sequencing: petioles (as a pool of different petioles), stems of the current year (one debarked internode from the middle of the stem), stems of the previous year (cane, one debarked internode), and trunks. For esca plants we differentiated asymptomatic and tiger-stripe petioles and stems of the current year.

In trunks, we sampled a 2-cm high cross section at around 15 cm from the top of the trunk. We photographed the cross-sections (quantified the percentage surface of each type of necrosis as described below) and separated the tissues by their necrotic status: apparently healthy wood (healthy), black necrotic wood (black necrosis), white rot, and brown stripe. For white rot, if the necrotic tissues was insufficient for pathogen detections, we sampled white rot tissues from the neighbor trunk tissues. For brown stripe, we debarked the trunk and sampled the brown stripe (when present) at different height of the trunk.

We obtained a total of 234 samples composed of: 45 petioles, 43 stems (of the current year), 36 canes, 110 from trunks (Table A1).

Table A1. Sample size of different treatment and tissues sampled for Ascomycota community analysis.

	Water Deficit pS	Control pA	Control pS	Esca pS
Petioles	n = 10	n = 9	n = 10	Sympto n = 7 Asympto n = 9
Stem of the current year	n = 10	n = 9	n = 11	Sympto n = 9 Asympto n = 4
Cane of the previous season	n = 9	n = 9	n = 10	n = 8
Trunk	Apparently healthy n = 10 Black necrosis n = 10 White rot n = 5	Apparently healthy n = 10 Black necrosis n = 6 White rot n = 6	Apparently healthy n = 11 Black necrosis n = 10 White rot n = 8	Apparently healthy n = 9 Black necrosis n = 8 White rot n = 8 Brown stripe n = 7

Trunk necrosis analysis

Before tissue sampling, trunk cross sections were photographed (as in Fig. A1A). Using Imagej software (*Schneider* et al., 2012), we separated three different (necrotic) tissues: apparently healthy, black necrosis, and white rot. We measured the area of each different tissue (in mm^2) relative to the entire cross section.

DNA extraction and sequencing

All the samples were collected in sterile environment using sterile shears. For trunk samples, we cut with a sterile handsaw a 2 cm cross-section at 15 cm from the top of the trunk. With sterile shears, we removed the bark and separated the different necrosis in each cross-section. Each sample (petiole, stem, cane, or trunk) were directly put in liquid nitrogen and stored at -80 °C. Samples were ground in liquid nitrogen with a one-ball mill (TissueLyser II, Qiagen). Genomic DNA was extracted from 60-mg aliquots of wood tissues using the Indvisorb Spin Plant mini Kit (Orgentec, France) following the manufacturer's instructions. Empty tubes, *i.e.* with

nothing but extraction reagents, were included as negative control samples for DNA extraction. DNA extracts were then quantified with a spectrophotometer (DeNovix DS-11, CliniSciences) and homogenized at a concentration of 15 ng.μl^{-1}.

The ITS2 region of the nuclear ribosomal repeat unit was then amplified using the pair of primers GTAAf/GTTAr (Morales-Cruz *et al*., 2018), specifically optimized/designed to profile pathogenic ascomycete fungal communities associated with GTD. DNA was amplified by PCR in an Epgradient Mastercycler (Eppendorf) in a reaction mixture (25 µl final volume) consisting of 1 µl of DNA template (15 ng.μl^{-1}), 10 µl of 2X Platinum Hot Start PCR Master Mix (Invitrogen), 0.5 µl of each primer (10 µM), 1.25 µl of 20X Bovine Serum Albumin (New England BioLabs), and 11.75 µl of DNAse/RNAse free sterile water. The cycling parameters were as follow: enzyme activation at 95°C for 2 min; 35 cycles of denaturation at 95°C for 45 s, 60°C for 1 min, 72°C for 1 min 30 sec; and a final extension at 72°C for 10 min. Empty wells on PCR plates, *i.e.* mix without any DNA template, were used as negative PCR control samples. The PCR products were visualized using a 2% TBE gel electrophoresis (≈350bp) before being sent to the PGTB sequencing facility (Genome Transcriptome Facility of Bordeaux, Pierroton, France) for sequencing on an Illumina MiSeq platform (v3 chemistry, 2x300 bp). PCR products purification, multiplex identifiers and sequencing adapters addition, library sequencing and sequence demultiplexing (with exact index search) were carried out by the sequencing service.

Sequence analysis and OTU table construction

The FROGS pipeline (Find Rapidly OUT with Galaxy Solution) implemented on a galaxy instance (https://vm-galaxy-prod.toulouse.inra.fr/galaxy/) was used for data processing (Escudié *et al*., 2018). In brief, paired reads were merged using FLASH (Magoč and Salzberg, 2011) with a maximum of 5% mismatch in the overlapped region. After denoising (*i.e.* reads with no expected length, between 280 and 400bp, and containing ambiguous bases, N, were discarded) and primer/adapters removal with CUTADAPT (Martin, 2011), the clustering was done using SWARM (Mahé *et al*., 2014) with an aggregation distance d = 3. SWARM is a robust and fast clustering method for amplicon-based studies without global threshold and independent of sequence order (Mahé *et al*., 2014). Chimeras were then removed using VSEARCH (Rognes *et al*., 2016) and low abundance sequences were filtered at 0.00005% (*i.e.* keep OTUs with at least 0.00005% of all sequences, adapted from Bokulich *et al*., 2013), discarding singletons from the datasets. The ITS2 region was extracted using ITSx (Bengtsson-Palme *et al.*, 2013) before performing the taxonomic affiliation of the fungal OTUs using BLAST tools against the databases UNITE (v8.2_20200204 implemented in FROGS), trunkdiseaseID.org (http://www.grapeipm.org/) and NCBI (nr/nt) nucleotide collection (https://blast.ncbi.nlm.nih.gov/Blast.cgi). Finally, the maximum number of sequences of each OTU present in the negative controls (DNA extraction and PCRs) were subtracted from the sequence abundance of that OTU in the

experimental samples (Nguyen *et al*., 2015). The final OTU table had 257 samples and 275 non-chimeric, non-singleton fungal OTUs, representing 4,811,621 quality sequences.

Note that this preliminary view of the results concern the trunk samples only. The statistical analyses have not been realized yet.

Results

(1) Trunk necrosis extension in plants expressing esca leaf symptoms or subjected to water deficit

Trunk necrosis area (%) was measured on single trunk cross sections placed at 15 cm from the top of the trunk (i.e. the same used for Ascomycota metagenomic analysis). In control plants, we observed the same ratio between necrotic and apparently healthy tissues, independently from their symptom history (Fig. A1B). More specifically, apparently asymptomatic tissues represented (on average ± SE) 59.5 ± 5% and 56.2 ± 5% in control-pA and control-pS plants respectively, while black necrosis was present at 18.2 ±7% in control-pA and 23.0 ± 5% in control-pS cross sections, and white rot represented 22.3 ± 6% in control-pA, and 20.9 ± 5% in control-pS. In presence of esca leaf symptoms (Esca-pS, Fig. A1B), the three tissues presented (almost) equal ratios in trunk cross sections: 34.2 ± 6% for apparently healthy, 33.5 ± 5% for black necrosis, and 32.3 ± 6% for white rot. Under water deficit the % of cross sections for the apparently healthy tissue (49.7 ± 5%, Fig A1B) was similar to the % of black necrosis (38.0 ± 5%), while the white rot was present in significantly lower percentages (12.2 ± 5%).

Preliminary observations: The expression of esca leaf symptoms during the previous year seems (once again in this thesis) to have no effect on the percentage of necrotic tissue inside the trunk. It seems clear that both the expression of leaf symptoms during the year of sampling and the applied water deficit have influenced the extent (or the progression) of the necrosis. Necrosis surely has increased its area during the expression of leaf symptoms, while water deficit seems to influence the ratio between black necrosis and white rot. Indeed, if the percentage of apparently healthy tissue is similar between control plants and plants under water deficit, black necrosis has a higher ratio compared to white rot. If we exclude that water deficit has reduced the percentage of white rot (the conversion from white rot to healthy tissue should be considered science fiction), we could imagine that water deficit conditions affect the expansion of white rot, while they did not affect the expansion of black necrosis. This preliminary observation could enhance the link between white rot and esca leaf symptoms expression previously observed (Maher *et al*., 2012).

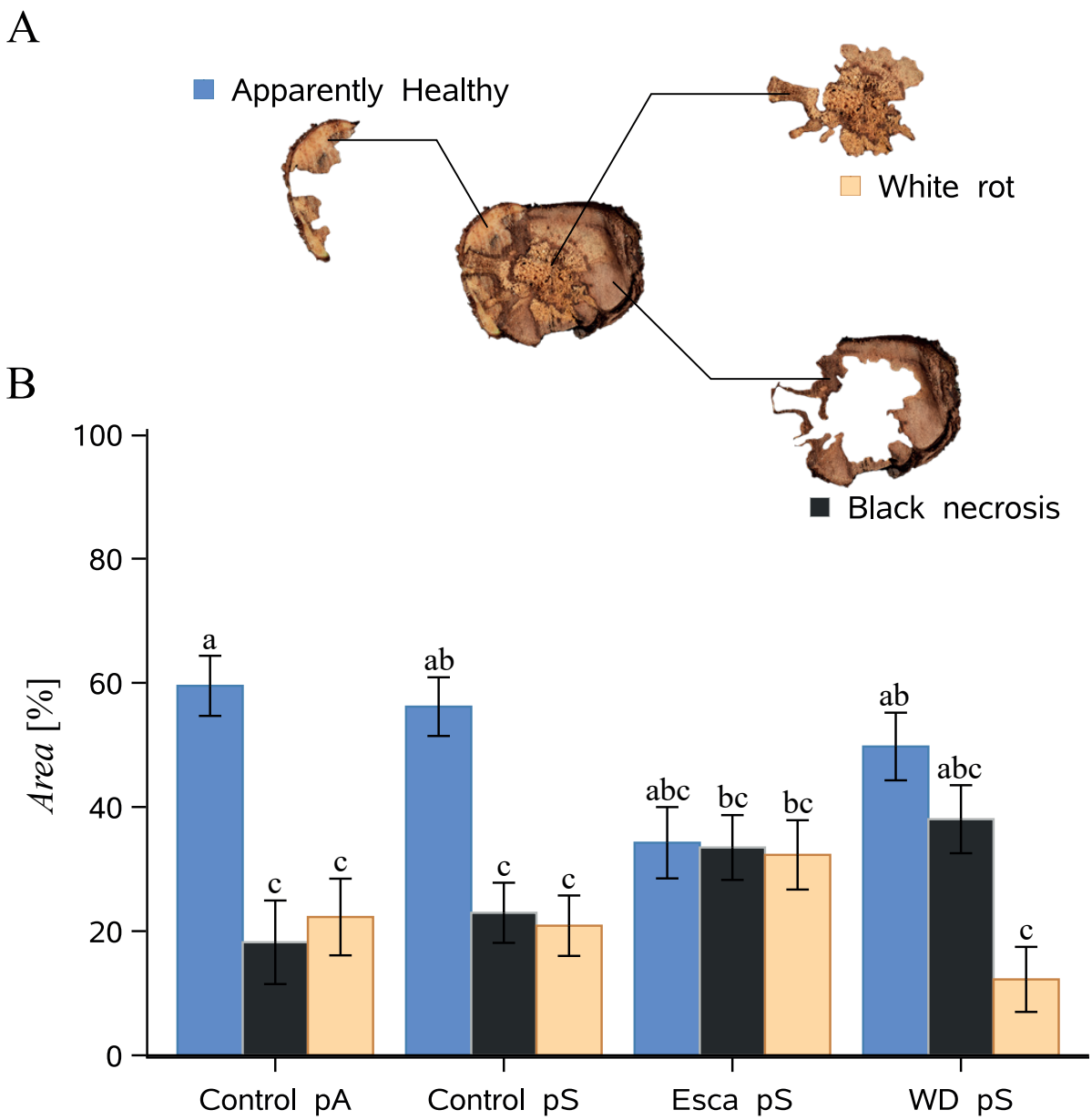

Figure A1. Analysis of trunk necrosis extension in cross sections from the plants used for Ascomycota metagenomic analysis. (**A**) Example of segmentation (by Imagej software) of the different tissues quantified (apparently healthy, black necrosis, and white rot). (**B**) Quantification of relative area (%) for each tissue in the considered cross-sections. Colors correspond to the kind of (necrotic) tissue: blue for apparently healthy, black for black necrosis, and cream for white rot. Bars are grouped by esca-water regime status: Control-pA, asymptomatic plants since 2012; Control-pS, plants that did not express esca leaf symptoms in 2019 (year of sampling) but expressed esca symptoms at least once since 2012; Esca-pS, plants that expressed esca leaf symptoms at least once before and in 2019; WD-pS, plants under water deficit for two years and that expressed at least once esca leaf symptoms between 2012 and 2017. Bars represent means and error bars standard error, letters indicate statistical significance from independent linear general models with Tukey post-hoc comparisons, $F_{11,114} = 7.78$, $P<0.0001$.

(2) What is the long-term impact of esca leaf symptoms expression on the Ascomycota community in the trunk?

To answer to this question, we sampled plants that did not express esca leaf symptoms during the sampling seasons ("Controls", n=21). We divided these plants by their previous esca symptoms record: pA = plants that never expressed esca leaf symptoms from 2012 to 2019 (n=10); pS = plants that expressed esca leaf symptoms at least once between 2012 and 2018 (n=11). To better distinguish the Ascomycota populations within the trunk of these plants, we analyzed separately black necrosis and apparently healthy wood (Fig. A2).

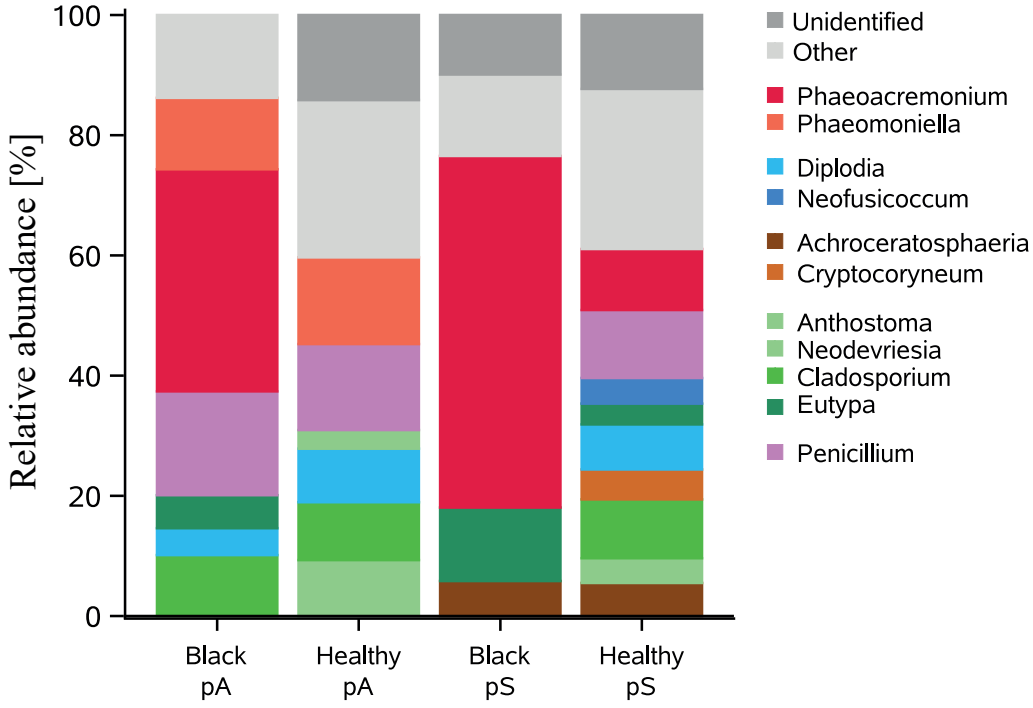

Figure A2. Ascomycota community composition characterized to the genus level (top 13 taxa) in grapevine trunk from control plants expressing (pS) or not (pA) esca leaf symptoms between 2012 and 2018. Samples are categorized by their symptom history record (pA, pS), and by the wood health status (Black for necrotized wood, Healthy for apparently healthy wood). Ascomycota genera are categorized by their function: dark grey for unidentified OTUs; light grey for genera with relative abundances <3%; red to orange for vascular pathogens; blue shades for Botryosphaeriaceae; brown for secondary pathogens (i.e. colonizing dead wood); green for other pathogenic fungi; and pink for fungi that might positively affect grapevine functions.

Preliminary observations: vascular pathogens such as *Phaeoacremonium* sp. appeared more present in necrotic black wood than in healthy wood; genera having small relative abundances were more frequent in apparently healthy wood; pS plants presented higher relative abundances of secondary pathogens and pA plants a higher relative abundance of *Penicillium* spp.

(3) What is the impact of a seasonal drought or esca leaf symptoms on the Ascomycota community in the trunk?

To answer this question, we sampled plants that expressed esca leaf symptoms at least once between 2012 and 2018 (pS) and categorized them by their water regime and current health status in 2019. WD = plants that were under water deficit from July to October and did not express esca leaf symptoms, n=10; Control = well-watered plants asymptomatic in 2019 (n=11); Esca = well-watered plants esca symptomatic in 2019 (n=10). We categorized the trunk tissues by the necrosis presence: Black = black necrosis; Healthy = apparently healthy wood; brown stripe = Brown stripe along the vasculature observed in symptomatic plants only (Fig. A3).

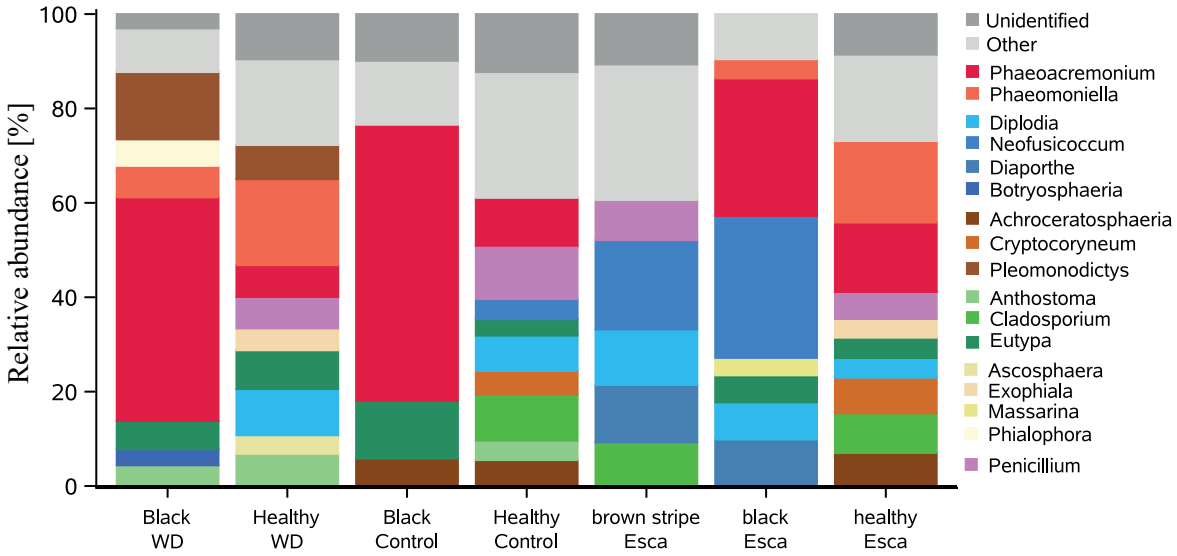

Figure A3. Ascomycota community composition characterized to the genus level (top 19 taxa) in grapevine wood of plants having expressed or not esca-leaf symptoms between and/or subjected to a water deficit. Samples are categorized by the submitted stress and wood health status. Ascomycota genera are categorized by their function: dark grey for unidentified OTUs; light grey for genera with relative abundances <3%; red to orange for vascular pathogens; blue shades for *Botryosphaeriaceae*; brown for secondary pathogens (i.e. colonizing dead wood); green for other pathogenic fungi; white cream shades for endophytic fungi; and pink for fungi that might positively affect grapevine functions.

Preliminary observations: vascular pathogens (with a general majority of *Phaeoacremonium* spp.) appeared more abundant in the black necrotic wood. In plants under water deficit, higher ratios of secondary pathogens were observed compared to WW plants. Plants expressing esca leaf symptoms were highly colonized by *Botryosphaeriaceae* spp. (mostly found in the necrotic wood). A higher diversity (number of observed genera) was obtained in healthy wood samples, independently of the submitted stress.

(4) What are the main Ascomycota genera colonizing the brown stripe necrosis along the trunk?

Esca leaf symptoms were frequently associated with a particular necrosis along the trunk. This necrosis, which is visible once we debarked the trunk, is a brown-orange stripe along the xylem vasculature that seems to connect the most basal part of the trunk with the leaf symptoms.

To answer to the question (3), we sampled the brown stripe necrosis from seven different plants (Fig. A4).

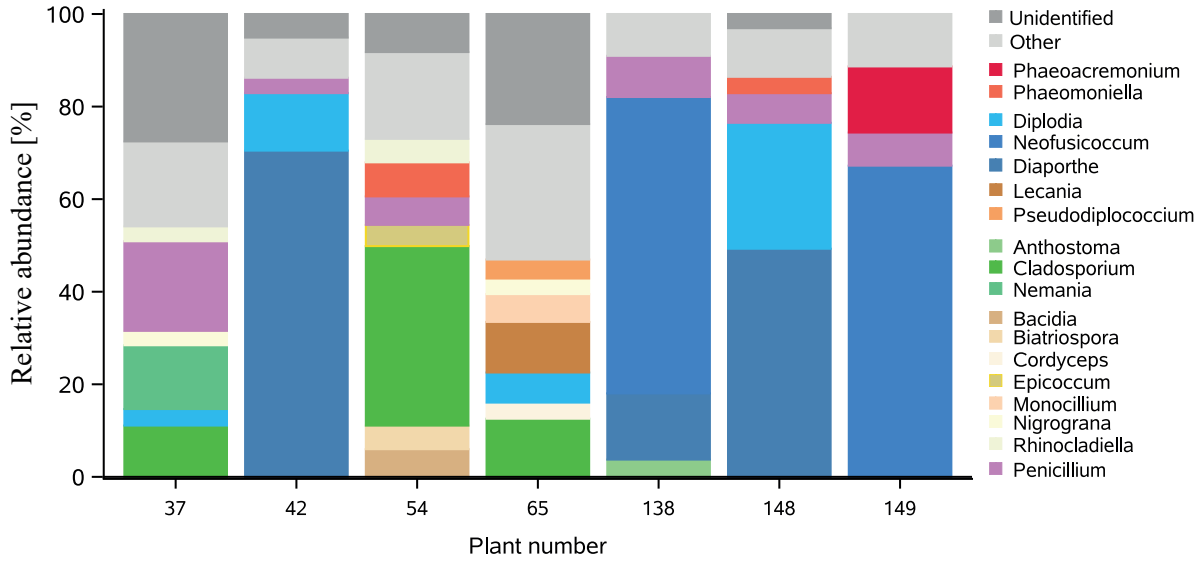

Figure A4. Ascomycota populations characterized to the genus level (top 20 taxa) in seven different brown stripe samples. Samples are categorized by plant number. Ascomycota genera are divided by their function: dark grey for unidentified OTUs; light grey for genera with relative abundances <3%; red to orange for vascular pathogens; blue shades for *Botryosphaeriaceae*; brown for secondary pathogens (i.e. colonizing dead wood); green for other pathogenic fungi; white cream shades for endophytic fungi; pink for fungi that might positively affect grapevine functions.

Preliminary observations: In four samples, the brown stripe was highly colonized (around 80% relative abundance) by *Botryosphaeriaceae* species. In the other samples, the relative abundance of *Cladosporium* spp. (a pathogen normally encountered in external green tissues) was high.

Conclusions and perspectives

These results, even if preliminary, open many research perspectives. From a first look on the plotted results, we can observe that vascular pathogens are more associated with black necrosis in the trunk than with esca leaf symptom expression of the year. In a second look we can observe that esca leaf symptoms seem to be associated to a strong presence of *Botryosphaeriace-*

ae species. We did not report here the results on the white rot as this type of necrosis is mostly caused by Basidiomycota fungal species (*i.e. Fomitiporia mediterranea*, not studied here). However, it could be interesting to study Ascomycota associations in this necrosis. Moreover, the other tissues not presented in this part, could reveal interesting results. Ascomycota changes in annual organs (petioles and stems), as well as the population changes between trunks and one-year old canes could reveal which species are able to colonize which tissues, and if some genera are more associated to specific necrosis or organs. Diversity analyses will be undertaken to confirm the visual differences discussed in this part of the manuscript.

Table A2. References for most abundant Ascomycota Genera found in grapevine trunk tissues.

Genus	Function	Reference
Phialophora	endophyte	Andrade-Linares and Philipp, 2013
Massarina	endophyte	Aptroot, 1998
Exophiala	endophyte	Maciá-Vincente et al., 2016
Rhinocladiella	endophyte	Teixeira et al., 2017
Nigrograna	endophyte	Kolarik, 2018
Biatriospora	endophyte	Kolarik et al., 2017
Penicillium	enhance plant resistance	Srinivasan et al., 2020
Neodevriesia	pathogen	Meng-Wang et al., 2017
Cladosporium	pathogen	Ogorek et al., 2012
Anthostoma	pathogen	Mirabolfathy et al., 2018
Nemania	pathogen	Edwards et al., 2003
Eutypa	pathogen	Larignon and Dubos, 1997
Neofusicoccum	pathogen (*Botryosphaeraiceae*)	Phillips et al., 2013
Diplodia	pathogen (*Botryosphaeraiceae*)	Phillips et al., 2013
Diaporthe	pathogen (*Botryosphaeraiceae*)	Phillips et al., 2013
Botryosphaeria	pathogen (*Botryosphaeraiceae*)	Phillips et al., 2013
Phaeomoniella	pathogen (vascular)	Pouzoulet et al., 2013
Phaeoacremonium	pathogen (vascular)	Pouzoulet et al., 2013
Pleomonodictys	secondary pathogen	Gams et al., 2018
Cryptocoryneum	secondary pathogen	Hashimoto et al., 2016
Achroceratosphaeria	secondary pathogen	Réblova et al., 2010
Pseudodiplococcium	secondary pathogen	Hernandez-Restrepo et al., 2017
Monocillium	secondary pathogen	Ashrafi et al., 2017
Lecania	secondary pathogen	Reesenaesborg et al., 2007
Bacidia	secondary pathogen	Llop et al., 2007
Ascosphaera	unknown	
Cordyceps	unknown	

Cited Literature

Abou-Mansour, E., Couché, E. and Tabacchi, R. (2004) 'Do fungal naphthalenones have a role in the development of esca symptoms?', *Phytopathologia Mediterranea*, 43(1), pp. 75–82. doi: http://dx.doi.org/10.14601/Phytopathol_Mediterr-1728.

Adams, H. D. *et al.* (2017) 'A multi-species synthesis of physiological mechanisms in drought-induced tree mortality', *Nature Ecology & Evolution*, 1(9), pp. 1285–1291. doi: 10.1038/s41559-017-0248-x.

Agrios, G. N. (2005) *Plant pathology*. 5th ed. Amsterdam ; Boston: Elsevier Academic Press.

Akpaninyang, F. E. and Opara, E. U. (2017) 'The Influence of Toxins in Disease Symptom Initiation in Plants: A Review', *Journal of Agriculture and Sustainability*, 10(1), pp. 29–52.

Aleemullah, M. and Walsh, K. B. (1996) 'Australian papaya dieback: evidence against the calcium deficiency hypothesis and observations on the significance of laticifer autofluorescence', *Australian Journal of Agricultural Research*, 47(3), pp. 371–385. doi: 10.1071/AR9960371.

Allen, C. D. *et al.* (2010) 'A global overview of drought and heat-induced tree mortality reveals emerging climate change risks for forests', *Forest Ecology and Management*, 259(4), pp. 660–684. doi: 10.1016/j.foreco.2009.09.001.

Alonso, R., Tiscornia, S. and Bettucci, L. (2011) 'Fungal endophytes of needles and twigs from *Pinus taeda* and *Pinus elliotti* in Uruguay', *Sydowia*, 63(2), pp. 141–153.

Alston, J. M., Sambucci, O. (2019) 'Grapes in the world economy'. In: Cantu D, Walker MA, eds. The grape genome. Cham: Springer, 1–24.

Alvindia, D. G. and Gallema, F. L. M. (2017) ' *Lasiodiplodia theobromae* causes vascular streak dieback (VSD)–like symptoms of cacao in Davao Region, Philippines', *Australasian Plant Disease Notes*, 12(1). doi: 10.1007/s13314-017-0279-9.

Ameglio, T. *et al.* (1999) 'Significance and limits in the use of predawn leaf water potential for tree irrigation', *Plant and Soil*, 207, pp. 155-167.

Anderegg, W. R. L. *et al.* (2012) 'The roles of hydraulic and carbon stress in a widespread climate-induced forest die-off', *Proceedings of the National Academy of Sciences*, 109(1), pp. 233–237. doi: 10.1073/pnas.1107891109.

Anderegg, W. R. L. *et al.* (2016) 'Meta-analysis reveals that hydraulic traits explain cross-species patterns of drought-induced tree mortality across the globe', *Proceedings of the National Academy of Sciences*, 113(18), pp. 5024–5029. doi: 10.1073/pnas.1525678113.

Andolfi, A. *et al.* (2011) 'Phytotoxins Produced by Fungi Associated with Grapevine Trunk Diseases', *Toxins*, 3(12), pp. 1569–1605. doi: 10.3390/toxins3121569.

Andrade-Linares, D. R. and Franken, P. (2013) 'Fungal Endophytes in Plant Roots: Taxonomy, Colonization Patterns, and Functions', in Aroca, R. (ed.) *Symbiotic Endophytes*. Berlin, Heidelberg: Springer Berlin Heidelberg (Soil Biology), pp. 311–334. doi: 10.1007/978-3-642-39317-4_16.

Andreini, L., Viti, R. and Scalabrelli, G. (2011) 'Preliminary histological observations on grapevine affected by esca disease', *Open Life Sciences*, 6(2). doi: 10.2478/s11535-011-0001-4.

Aptroot, A. (1998) 'A world revision of Massarina (Ascomycota)', *Nova Hedwigia*, 66(1–2), pp. 89–162. doi: 10.1127/nova.hedwigia/66/1998/89.

Arango-Velez, A. *et al.* (2016) 'Differences in defence responses of *Pinus contorta* and *Pinus banksiana* to the mountain pine beetle fungal associate *Grosmannia clavigera* are affected by

water deficit: Co-evolved and naïve pine response to *G. clavigera*', *Plant, Cell & Environment*, 39(4), pp. 726–744. doi: 10.1111/pce.12615.

Arnon, D. I. (1949) 'Copper enzymes in isolated chloroplasts. Polyphenoloxidase in *Beta Vulgaris*', *Plant Physiology*, 24(1), pp. 1–15. doi: 10.1104/pp.24.1.1.

Ashrafi, S. *et al.* (2017) '*Monocillium gamsii* sp. nov. and *Monocillium bulbillosum*: two nematode-associated fungi parasitising the eggs of *Heterodera filipjevi*', *MycoKeys*, 27, pp. 21–38. doi: 10.3897/mycokeys.27.21254.

Assmann, S. M. (2003) 'OPEN STOMATA1 opens the door to ABA signaling in Arabidopsis guard cells', *Trends in Plant Science*, 8(4), pp. 151–153. doi: 10.1016/S1360-1385(03)00052-9.

Attiwill, P. M. and Adams, M. A. (1993) 'Nutrient cycling in forests', *New Phytologist*, 124, pp. 561–582.

Bartlett, M. K. *et al.* (2016) 'The correlations and sequence of plant stomatal, hydraulic, and wilting responses to drought', *Proceedings of the National Academy of Sciences*, 113(46), pp. 13098–13103. doi: 10.1073/pnas.1604088113.

Bartnik, C. *et al.* (2020) 'Mycobiota of Dead *Ulmus glabra* Wood as Breeding Material for the Endangered *Rosalia alpina* (Coleoptera: Cerambycidae)', *Polish Journal of Ecology*, 68(1), p. 13. doi: 10.3161/15052249PJE2020.68.1.002.

Beier, G. L. *et al.* (2017) 'American elm cultivars: Variation in compartmentalization of infection by *Ophiostoma novo-ulmi* and its effects on hydraulic conductivity', *Forest Pathology*, 47(6), pp. 1–11. doi: 10.1111/efp.12369.

Bengtsson-Palme, J. *et al.* (2013) 'Improved software detection and extraction of ITS1 and ITS2 from ribosomal ITS sequences of fungi and other eukaryotes for analysis of environmental sequencing data', *Methods in Ecology and Evolution*. Edited by M. Bunce, p. n/a-n/a. doi: 10.1111/2041-210X.12073.

Bertsch, C. *et al.* (2013) 'Grapevine trunk diseases: complex and still poorly understood.', *Plant Pathology*, 62(2), pp. 243–265. doi: 10.1111/j.1365-3059.2012.02674.x.

Bettenfeld, P. *et al.* (2020) 'Woody Plant Declines. What's Wrong with the Microbiome?', *Trends in Plant Science*, 25(4), pp. 381–394. doi: 10.1016/j.tplants.2019.12.024.

Biais, B. *et al.* (2014) 'Remarkable Reproducibility of Enzyme Activity Profiles in Tomato Fruits Grown under Contrasting Environments Provides a Roadmap for Studies of Fruit Metabolism', *Plant Physiology*, 164(3), pp. 1204–1221. doi: 10.1104/pp.113.231241.

Biedermann, P. H. W. (2020) 'Cooperative Breeding in the Ambrosia Beetle Xyleborus affinis and Management of Its Fungal Symbionts', *Frontiers in Ecology and Evolution*, 8, p. 12.

Bokulich, N. A. *et al.* (2013) 'Quality-filtering vastly improves diversity estimates from Illumina amplicon sequencing', *Nature Methods*, 10(1), pp. 57–59. doi: 10.1038/nmeth.2276.

Bonsen, K. J. M. and Kučera, L. J. (1990) 'Vessel Occlusions in Plants: Morphological, Functional and Evolutionary Aspects', *IAWA Journal*, 11(4), pp. 393–399. doi: 10.1163/22941932-90000528.

Bortolami, G. *et al.* (2019) 'Exploring the Hydraulic Failure Hypothesis of Esca Leaf Symptom Formation', *Plant Physiology*, 181, pp. 1163–1174.

Bortolami, G. *et al.* (2020) 'Seasonal and long-term consequences of esca on grapevine stem xylem integrity'. preprint. Plant Biology. doi: 10.1101/2020.09.07.282582.

Bowden, R. L., Rouse, D. I. and Sharkey, T. D. (1990) 'Mechanism of Photosynthesis Decrease by *Verticillium dahliae* in Potato', *Plant Physiology*, 94(3), pp. 1048–1055. doi: 10.1104/pp.94.3.1048.

Brodersen, C. R. *et al.* (2013) 'In Vivo Visualizations of Drought-Induced Embolism Spread in Vitis vinifera', *Plant Physiology*, 161(4), pp. 1820–1829.

Brodersen, C. R. *et al.* (2019) 'Functional Status of Xylem Through Time', *Annual review of Plant Biology*, 70, pp. 407-433.

Brodribb, T. J. *et al.* (2010) 'Xylem function and growth rate interact to determine recovery rates after exposure to extreme water deficit', *New Phytologist*, 188(2), pp. 533–542. doi: 10.1111/j.1469-8137.2010.03393.x.

Brodribb, T. J. *et al.* (2016) 'Visual quantification of embolism reveals leaf vulnerability to hydraulic failure', *New Phytologist*, 209, pp. 1403–1409.

Brodribb, T. J. *et al.* (2020) 'Hanging by a thread? Forests and drought', *Science*, 368(6488), pp. 261–266. doi: 10.1126/science.aat7631.

Brodribb, T. J. and Holbrook, N. M. (2003) 'Stomatal Closure during Leaf Dehydration, Correlation with Other Leaf Physiological Traits', *Plant Physiology*, 132(4), pp. 2166–2173. doi: 10.1104/pp.103.023879.

Brown, A. A., Lawrence, D. P. and Baumgartner, K. (2020) 'Role of basidiomycete fungi in the grapevine trunk disease esca', *Plant Pathology*, 69(2), pp. 205–220. doi: 10.1111/ppa.13116.

Bruez, E. *et al.* (2014) 'Analyses of the Temporal Dynamics of Fungal Communities Colonizing the Healthy Wood Tissues of Esca Leaf-Symptomatic and Asymptomatic Vines', *PLoS ONE*. Edited by B. A. Vinatzer, 9(5). doi: 10.1371/journal.pone.0095928.

Bruez, E. *et al.* (2015) 'Bacteria in a wood fungal disease: characterization of bacterial communities in wood tissues of esca-foliar symptomatic and asymptomatic grapevines', *Frontiers in Microbiology*, 6. doi: 10.3389/fmicb.2015.01137.

Bruez, E. *et al.* (2016) 'Various fungal communities colonise the functional wood tissues of old grapevines externally free from grapevine trunk disease symptoms: Fungal microflora of GTD-free old vines', *Australian Journal of Grape and Wine Research*, 22(2), pp. 288–295. doi: 10.1111/ajgw.12209.

Bruez, E. *et al.* (2020) 'Major changes in grapevine wood microbiota are associated with the onset of esca, a devastating trunk disease', *Environmental Microbiology*, pp. 1462-2920.15180. doi: 10.1111/1462-2920.15180.

Bruno, G. and Sparapano, L. (2006) 'Effects of three esca-associated fungi on Vitis vinifera L.: III. Enzymes produced by the pathogens and their role in fungus-to-plant or in fungus-to-fungus interactions', *Physiological and Molecular Plant Pathology*, 69(4–6), pp. 182–194. doi: 10.1016/j.pmpp.2007.04.006.

Bruno, G., Sparapano, L. and Graniti, A. (2007) 'Effects of three esca-associated fungi on Vitis vinifera L.: IV. Diffusion through the xylem of metabolites produced by two tracheiphilous fungi in the woody tissue of grapevine leads to esca-like symptoms on leaves and berries', *Physiological and Molecular Plant Pathology*, 71(1–3), pp. 106–124. doi: 10.1016/j.pmpp.2007.12.004.

Buchanan-Wollaston, V. (1997) 'The molecular biology of leaf senescence', *Journal of Experimental Botany*, 48(2), pp. 181–199. doi: 10.1093/jxb/48.2.181.

Butault, J.-P. *et al.* (2011) 'L'utilisation des pesticides en France : état des lieux et perspectives

de réduction', *Notes et études socio-économiques*, 35, p. 7-26.

Cailleret, M. *et al.* (2017) 'A synthesis of radial growth patterns preceding tree mortality', *Global Change Biology*, 23(4), pp. 1675–1690. doi: 10.1111/gcb.13535.

Calzarano, F. *et al.* (2004) 'Effect of Esca on the Quality of Berries, Musts and Wines', *Phytopathologia Mediterranea*, 43(1), pp. 125–135.

Calzarano, F. *et al.* (2014) 'Grapevine leaf stripe disease symptoms (esca complex) are reduced by a nutrients and seaweed mixture', *Phytopathologia Mediterranea*, (3). doi: 10.14601/Phytopathol_Mediterr-15253.

Calzarano, F. *et al.* (2016) 'Patterns of phytoalexins in the grapevine leaf stripe disease (esca complex)/grapevine pathosystem', *Phytopathologia Mediterranea*, 55(3), pp. 410–426.

Canny, M. (1997) 'Tyloses and the Maintenance of Transpiration', *Annals of Botany*, 80(4), pp. 565–570. doi: 10.1006/anbo.1997.0475.

Carbonneau A. *et al*. (2015) 'Traité de la vigne: Physiologie, Terroir, Culture', *Dunod/ La vigne, Pratiques vitivinicoles.*

Carlucci, A. *et al.* (2013) '*Pleurostomophora richardsiae*, *Neofusicoccum parvum* and *Phaeoacremonium aleophilum* associated with a decline of olives in southern Italy', *Phytopathologia Mediterranea*, 52(3). doi: 10.14601/Phytopathol_Mediterr-13526.

Carminati, A. and Javaux, M. (2020) 'Soil Rather Than Xylem Vulnerability Controls Stomatal Response to Drought', *Trends in Plant Science*, 25(9), pp. 868–880. doi: 10.1016/j.tplants.2020.04.003.

Castillo-Argaez, R. *et al.* (2020) 'Leaf gas exchange and stable carbon isotope composition of redbay and avocado trees in response to laurel wilt or drought stress', *Environmental and Experimental Botany*, 171, p. 103948. doi: 10.1016/j.envexpbot.2019.103948.

Chaffey, N. J. and Pearson, J. A. (1985) 'Presence of Tyloses at the Blade/Sheath Junction in Senescing Leaves of Lolium temulentum L.', p. 10.

Charrier, G. *et al.* (2016) 'Evidence for Hydraulic Vulnerability Segmentation and Lack of Xylem Refilling under Tension', *Plant Physiology*, 172(3), pp. 1657–1668. doi: 10.1104/pp.16.01079.

Charrier, G. *et al.* (2018) 'Drought will not leave your glass empty: Low risk of hydraulic failure revealed by long-term drought observations in world's top wine regions', *Science Advances*, 4(1). doi: 10.1126/sciadv.aao6969.

Chattaway, M. (1949) 'The Development of Tyloses and Secretion of Gum in Heartwood Formation', *Australian Journal of Biological Sciences*, 2(3), p. 227. doi: 10.1071/BI9490227.

Chattaway, M. (1953) 'The occurrence of heartwood crystals in certain timbers', *Australian Journal of Botany*, 1(1), p. 27. doi: 10.1071/BT9530027.

Chaves, M. M. *et al.* (2010) 'Grapevine under deficit irrigation: hints from physiological and molecular data', *Annals of Botany*, 105(5), pp. 661–676. doi: 10.1093/aob/mcq030.

Che-Husin, N.-M., Joyce, D. C. and Irving, D. E. (2018) 'Gel xylem occlusions decrease hydraulic conductance of cut *Acacia holosericea* foliage stems', *Postharvest Biology and Technology*, 135, pp. 27–37. doi: 10.1016/j.postharvbio.2017.08.015.

Choat, B. *et al.* (2009) 'The effects of Pierce's disease on leaf and petiole hydraulic conductance in *Vitis vinifera* cv. Chardonnay', *Physiologia Plantarum*, 136(4), pp. 384–394. doi: 10.1111/j.1399-3054.2009.01231.x.

Choat, B. *et al.* (2012) 'Global convergence in the vulnerability of forests to drought', *Nature*, 491, pp. 752-756. doi: 10.1038/nature11688.

Choat, B., Cobb, A. R. and Jansen, S. (2008) 'Structure and function of bordered pits: new discoveries and impacts on whole-plant hydraulic function', *New Phytologist*, 177(3), pp. 608–626. doi: 10.1111/j.1469-8137.2007.02317.x.

Choné, X. (2001) 'Stem Water Potential is a Sensitive Indicator of Grapevine Water Status', *Annals of Botany*, 87(4), pp. 477–483. doi: 10.1006/anbo.2000.1361.

Claverie, M. *et al.* (2020) 'Current knowledge on Grapevine Trunk Diseases with complex etiology: a systemic approach', *Phytopathologia Mediterranea*, 59, pp. 29–53. doi: https://doi.org/10.14601/Phyto-11150.

Clérivet, A. *et al.* (2000) 'Tyloses and gels associated with cellulose accumulation in vessels are responses of plane tree seedlings (*Platanus* × *acerifolia*) to the vascular fungus *Ceratocystis fimbriata* f. sp platani', *Trees*, 15(1), pp. 25–31. doi: 10.1007/s004680000063.

Cloete, M. *et al.* (2015) 'Pathogenicity of South African Hymenochaetales taxa isolated from esca-infected grapevines', *Phytopathologia Mediterranea*, 54(2), pp. 368–379. doi: 10.14601/Phytopathol_Mediterr-16237.

Cochard, H. (2002) 'A technique for measuring xylem hydraulic conductance under high negative pressures: Xylem conductance measured under negative pressure', *Plant, Cell & Environment*, 25(6), pp. 815–819. doi: 10.1046/j.1365-3040.2002.00863.x.

Collins, B. R. *et al.* (2009) 'The effects of Phytophthora ramorum infection on hydraulic conductivity and tylosis formation in tanoak sapwood', *Canadian Journal of Forest Research*, 39(9), pp. 1766–1776. doi: 10.1139/X09-097.

Corrêa, T. R. *et al.* (2017) 'Phenotypic markers in early selection for tolerance to dieback in Eucalyptus', *Industrial Crops and Products*, 107, pp. 130–138. doi: 10.1016/j.indcrop.2017.05.032.

Costa, J. M. (2016) 'Modern viticulture in southern Europe: Vulnerabilities and strategies for adaptation to water scarcity', *Agricultural Water Management*, p. 14.

Costanza, R. *et al*. (1997) 'The value of the world's ecosystem', *Nature*, 387 p. 253-260.

Crang, R., Lyons-Sobaski, S. and Wise, R. (2018) *Plant Anatomy: A Concept-Based Approach to the Structure of Seed Plants*. Cham: Springer International Publishing. doi: 10.1007/978-3-319-77315-5.

Croise, L. *et al.* (2001) 'Effects of drought stress and high density stem inoculations with Leptographium wingfieldii on hydraulic properties of young Scots pine trees', *Tree Physiology*, 21(7), pp. 427–436. doi: 10.1093/treephys/21.7.427.

Czemmel, S. *et al.* (2015) 'Genes Expressed in Grapevine Leaves Reveal Latent Wood Infection by the Fungal Pathogen Neofusicoccum parvum', *PLOS ONE*. Edited by H. Gerós, 10(3), p. e0121828. doi: 10.1371/journal.pone.0121828.

Damm, U., Fourie, P. H. and Crous, P. W. (2010) '*Coniochaeta* (*Lecythophora*), *Collophora* gen. nov. and *Phaeomoniella* species associated with wood necroses of *Prunus* trees', *Persoonia - Molecular Phylogeny and Evolution of Fungi*, 24(1), pp. 60–80. doi: 10.3767/003158510X500705.

Davison, E. M. (2014) 'Resolving confusions about jarrah dieback - don't forget the plants', *Australasian Plant Pathology*, 43(6), pp. 691–701. doi: 10.1007/s13313-014-0302-y.

Davison, E. M. and Tay, F. C. S. (1985) 'The effect of waterlogging on seedlings of *Eucalyptus marginata*', *New Phytologist*, 101(4), pp. 743–753. doi: 10.1111/j.1469-8137.1985.tb02879.x.

Dayer, S. *et al.* (2013) 'Carbohydrate reserve status of Malbec grapevines after several years of regulated deficit irrigation and crop load regulation: Irrigation and crop load effects on carbohydrates', *Australian Journal of Grape and Wine Research*, 19(3), pp. 422–430. doi: 10.1111/ajgw.12044.

Dayer, S. *et al.* (2016) 'Leaf carbohydrate metabolism in Malbec grapevines: combined effects of regulated deficit irrigation and crop load: Leaf carbohydrate metabolism in Malbec', *Australian Journal of Grape and Wine Research*, 22(1), pp. 115–123. doi: 10.1111/ajgw.12180.

Dayer, S. *et al.* (2020)a 'Nighttime transpiration represents a negligible part of water loss and does not increase the risk of water stress in grapevine', *Plant, Cell & Environment*, p. pce.13923. doi: 10.1111/pce.13923.

Dayer, S. *et al.* (2020)b 'The sequence and thresholds of leaf hydraulic traits underlying grapevine varietal differences in drought tolerance', *Journal of Experimental Botany*, 71(14), pp. 4333–4344. doi: 10.1093/jxb/eraa186.

De Micco, V. *et al.* (2016) 'Tyloses and gums: a review of structure, function and occurrence of vessel occlusions', *IAWA Journal*, 37(2), pp. 186–205. doi: 10.1163/22941932-20160130.

Del Rio, J. A. *et al.* (2001) 'Tylose formation and changes in phenolic compounds of grape roots infected with *Phaeomoniella chlamydospora* and *Phaeoacremonium species*', *Phytopathologia Mediterranea*, 40, pp. S394–S399. doi: http://dx.doi.org/10.14601/Phytopathol_Mediterr-1644.

Delzon, S. and Cochard, H. (2014) 'Recent advances in tree hydraulics highlight the ecological significance of the hydraulic safety margin', *New Phytologist*, 203(2), pp. 355–358. doi: 10.1111/nph.12798.

Desprez-Loustau, M.-L. *et al.* (2006) 'Interactive effects of drought and pathogens in forest trees', *Annals of Forest Science*, 63(6), pp. 597–612. doi: 10.1051/forest:2006040.

Deyett, E. *et al.* (2019) 'Assessment of Pierce's disease susceptibility in *Vitis vinifera* cultivars with different pedigrees', *Plant Pathology*, 68(6), pp. 1079–1087. doi: 10.1111/ppa.13027.

Di Marco, S. (2003) 'The wood decay of kiwifruit and first control measures', *Acta horticulturae,* 610, pp. 291-294.

Di Marco, S. *et al*. (2011) 'First studies on the potential of a copper formulation for the control of leaf stripe disease within esca complex in grapevine', *Phytopathologia mediterranea*, 50, S300-S309.

Dixon, H. H. and Joly, J. (1895) 'On the Ascent of Sap', *Philosophical Transactions of the Royal Society of London*, 186, pp. 563-576.

Edwards (2003) 'The Xylariaceae as phytopathogens', *Recent development in plant sciences*, 1, pp. 1-19.

Elgersma, D. M. (1970) 'Length and diameter of xylem vessels as factors in resistance of elms to Ceratocystis ulmi', *Netherlands Journal of Plant Pathology*, 76(3), pp. 179–182. doi: 10.1007/BF01974328.

Elmer, W. H. *et al.* (2013) 'Sudden Vegetation Dieback in Atlantic and Gulf Coast Salt Marshes', *Plant Disease*, 97(4), pp. 436–445. doi: 10.1094/PDIS-09-12-0871-FE.

Escudié, F. *et al.* (2018) 'FROGS: Find, Rapidly, OTUs with Galaxy Solution', *Bioinformatics*., 34(8), pp. 1287–1294. doi: 10.1093/bioinformatics/btx791.

Eskalen, A. *et al.* (2013) 'Host Range of Fusarium Dieback and Its Ambrosia Beetle (Cole-

optera: Scolytinae) Vector in Southern California', *Plant Disease*, 97(7), pp. 938–951. doi: 10.1094/PDIS-11-12-1026-RE.

Espargham, N., Mohammadi, H. and Gramaje, D. (2020) 'A Survey of Trunk Disease Pathogens within Citrus Trees in Iran', *Plants*, p. 20.

Et-Touil, A. *et al.* (2005) 'External symptoms and histopathological changes following inoculation of elms putatively resistant to Dutch elm disease with genetically close strains of Ophiostoma', *Canadian Journal of Botany*, 83, pp. 656–667.

Ewel, J. J. (1999) 'Natural systems as models for the design of sustainable systems of land use', *Agroforestry Systems*, p. 21.

Facelli, E. *et al.* (2009) 'Location of *Xanthomonas translucens* in pistachio trees', *Australasian Plant Pathology*, 38(6), p. 584. doi: 10.1071/AP09044.

Fallon, B. *et al.* (2020) 'Spectral differentiation of oak wilt from foliar fungal disease and drought is correlated with physiological changes', *Tree Physiology*, 40(3), pp. 377–390. doi: 10.1093/treephys/tpaa005.

Felician, A. J., Eskalen, A. and Gubler, W. D. (2004) 'Differential susceptibility of three grapevine cultivars to *Phaeoacremonium aleophilum* and *Phaeomoniella chlamydospora* in California', *Phytopathologia Mediterranea*, 43(1), p. 4.

Fischer, M. (2002) 'A new wood-decaying basidiomycete species associated with esca of grapevine: *Fomitiporia mediterranea* (*Hymenochaetales*)', *Mycological Progress*, 1(3), pp. 315–324.

Fischer, M. (2006) 'Biodiversity and geographic distribution of basidiomycetes causing esca-associated white rot in grapevine' *Phytopathologia Mediterranea*, 45, pp. S30-S42.

Fischer, M. and Ashnaei, S. P. (2019) 'Grapevine, esca complex, and environment: the disease triangle', *Phytopathologia Mediterranea*, p. 22.

Flajšman, M., Radišek, S. and Javornik, B. (2017) 'Pathogenicity Assay of Verticillium nonalfalfae on Hop Plants', *Bio-protocol*, 7(6). doi: 10.21769/BioProtoc.2171.

Fleurat-Lessard, P. *et al.* (2013) 'Differential occurrence of suberized sheaths in canes of grapevines suffering from black dead arm, esca or Eutypa dieback', *Trees*, 27(4), pp. 1087–1100. doi: 10.1007/s00468-013-0859-z.

Fontaine, F. *et al.* (2016) 'The effects of grapevine trunk diseases (GTDs) on vine physiology', *European Journal of Plant Pathology*, 144(4), pp. 707–721. doi: 10.1007/s10658-015-0770-0.

Fradin, E. F. and Thomma, B. P. H. J. (2006) 'Physiology and molecular aspects of Verticillium wilt diseases caused by V. dahliae and V. albo-atrum', *Molecular Plant Pathology*, 7(2), pp. 71–86. doi: 10.1111/j.1364-3703.2006.00323.x.

Fraga, H. *et al.* (2013) 'Future scenarios for viticultural zoning in Europe: ensemble projections and uncertainties', *International Journal of Biometeorology*, 57(6), pp. 909–925. doi: 10.1007/s00484-012-0617-8.

Franceschi, V. R. and Nakata, P. A. (2005) 'Calcium oxalate in plants: Formation and Function', p. 33.

Franklin, J. F., Shugart, H. H. and Harmon, M. E. (1987) 'Tree Death as an Ecological Process', *BioScience*, 37(8), pp. 550–556. doi: 10.2307/1310665.

Fritschi, F. B., Lin, H. and Walker, M. A. (2008) 'Scanning Electron Microscopy Reveals Different Response Pattern of Four *Vitis* Genotypes to *Xylella fastidiosa* Infection', *Plant Disease*,

92(2), pp. 276–286. doi: 10.1094/PDIS-92-2-0276.

Fukuda, K., Hogetsu, T. and Suzuki, K. (1994) 'Ethylene production during symptom development of pine-wilt disease', *Forest Pathology*, 24(4), pp. 193–202. doi: 10.1111/j.1439-0329.1994.tb00985.x.

Gambetta, G. A. *et al.* (2007) 'Leaf scorch symptoms are not correlated with bacterial populations during Pierce's disease', *Journal of Experimental Botany*, 58(15–16), pp. 4037–4046. doi: 10.1093/jxb/erm260.

Gambetta, G. A. *et al.* (2020) 'The physiology of drought stress in grapevine: towards an integrative definition of drought tolerance', *Journal of Experimental Botany*, 16, pp. 4658–4676. doi: 10.1093/jxb/eraa245.

Gams, W. *et al.* (2019) 'The ascomycete genus *Niesslia* and associated monocillium-like anamorphs', *Mycological Progress*, 18(1–2), pp. 5–76. doi: 10.1007/s11557-018-1459-5.

Gao, X. *et al.* (2017) 'Influence of severe drought on the resistance of *Pinus yunnanensis* to a bark beetle-associated fungus', *Forest Pathology*. 47(4). doi: 10.1111/efp.12345.

Gärtner, H., Lucchinetti, S. and Schweingruber, F. H. (2014) 'New perspectives for wood anatomical analysis in dendrosciences: The GSL1-microtome', *Dendrochronologia*, 32(1), pp. 47–51. doi: 10.1016/j.dendro.2013.07.002.

Gersony, J. T. *et al.* (2020) 'Leaf Carbon Export and Nonstructural Carbohydrates in Relation to Diurnal Water Dynamics in Mature Oak Trees', *Plant Physiology*, 183(4), pp. 1612–1621. doi: 10.1104/pp.20.00426.

Goberville, E. *et al.* (2016) 'Climate change and the ash dieback crisis', *Scientific Reports*, 6(1). doi: 10.1038/srep35303.

Gómez, P. *et al.* (2016) 'Grapevine xylem response to fungi involved in trunk diseases: Grapevine vascular defence', *Annals of Applied Biology*, 169(1), pp. 116–124. doi: 10.1111/aab.12285.

Goufo, P. and Cortez, I. (2020) 'A Lipidomic Analysis of Leaves of Esca-Affected Grapevine Suggests a Role for Galactolipids in the Defense Response and Appearance of Foliar Symptoms', *Biology*, 9(9), p. 268. doi: 10.3390/biology9090268.

Goufo, P., Marques, A. C. and Cortez, I. (2019) 'Exhibition of Local but Not Systemic Induced Phenolic Defenses in *Vitis vinifera* L. Affected by Brown Wood Streaking, Grapevine Leaf Stripe, and Apoplexy (Esca Complex)', *Plants*, 8(10), p. 412. doi: 10.3390/plants8100412.

Gramaje, D. *et al.* (2015) '*Phaeoacremonium*: From esca disease to phaeohyphomycosis', *Fungal biology*, 119, pp. 759-783.

Gramaje, D., Úrbez-Torres, J. R. and Sosnowski, M. R. (2018) 'Managing Grapevine Trunk Diseases With Respect to Etiology and Epidemiology: Current Strategies and Future Prospects', *Plant Disease*, 102(1), pp. 12–39. doi: 10.1094/PDIS-04-17-0512-FE.

Guérard, N. *et al.* (2007) 'Do trees use reserve or newly assimilated carbon for their defense reactions? A 13C labeling approach with young Scots pines inoculated with a bark-beetle-associated fungus (*Ophiostoma brunneo ciliatum*)', *Annals of Forest Science*, 64(6), pp. 601–608. doi: 10.1051/forest:2007038.

Guerin-Dubrana, L. *et al.* (2013) 'statistical analysis of grapevine mortality associated with esca or Eutypa dieback foliar expression', *Phytopathologia Mediterranea*, 52(2), pp. 276–288.

Hacke, U. G. and Sperry, J. S. (2001) 'Functional and ecological xylem anatomy', *Perspectives in Plant Ecology, Evolution and Systematics*, 4(2), 97-115.

Häffner, E., Konietzki, S. and Diederichsen, E. (2015) 'Keeping Control: The Role of Senescence and Development in Plant Pathogenesis and Defense', *Plants*, 4(3), pp. 449–488. doi: 10.3390/plants4030449.

Hagedorn, F. *et al.* (2016) 'Recovery of trees from drought depends on belowground sink control', *Nature Plants*, 2(8), p. 16111. doi: 10.1038/nplants.2016.111.

Haidar, R. *et al.* (2016) 'Screening and modes of action of antagonistic bacteria to control the fungal pathogen *Phaeomoniella chlamydospora* involved in grapevine trunk diseases', *Microbiological Research*, 192, pp. 172–184. doi: 10.1016/j.micres.2016.07.003.

Hartmann, H. (2015) 'Carbon starvation during drought-induced tree', *Journal of Plant Hydraulics*, 2, p. 5.

Hayslett, M., Juzwik, J. and Moltzan, B. (2008) 'Three *Colopterus* Beetle Species Carry the Oak Wilt Fungus to Fresh Wounds on Red Oak in Missouri', *Plant Disease*, 92(2), pp. 270–275. doi: 10.1094/PDIS-92-2-0270.

Hendriks, J. H. M. *et al.* (2003) 'ADP-Glucose Pyrophosphorylase Is Activated by Posttranslational Redox-Modification in Response to Light and to Sugars in Leaves of *Arabidopsis* and Other Plant Species', *Plant Physiology*, 133(2), pp. 838–849. doi: 10.1104/pp.103.024513.

Hernández-Restrepo, M. *et al.* (2017) 'Phylogeny of saprobic microfungi from Southern Europe', *Studies in Mycology*, 86, pp. 53–97. doi: 10.1016/j.simyco.2017.05.002.

Hoch, G., Richter, A. and Körner, Ch. (2003) 'Non-structural carbon compounds in temperate forest trees: Non-structural carbon compounds in temperate forest trees', *Plant, Cell & Environment*, 26(7), pp. 1067–1081. doi: 10.1046/j.0016-8025.2003.01032.x.

Hochberg, U. *et al.* (2015) 'The variability in the xylem architecture of grapevine petiole and its contribution to hydraulic differences', *Functional Plant Biology*, 42(4), p. 357. doi: 10.1071/FP14167.

Hochberg, U. *et al.* (2016) 'Grapevine petioles are more sensitive to drought induced embolism than stems: evidence from *in vivo* MRI and microcomputed tomography observations of hydraulic vulnerability segmentation: Hydraulic vulnerability segmentation in grapevine', *Plant, Cell & Environment*, 39(9), pp. 1886–1894. doi: 10.1111/pce.12688.

Hochberg, U. *et al.* (2017) 'Stomatal Closure, Basal Leaf Embolism, and Shedding Protect the Hydraulic Integrity of Grape Stems', *Plant Physiology*, 174(2), pp. 764–775. doi: 10.1104/pp.16.01816.

Holbrook, N. M. *et al.* (2001) 'In Vivo Observation of Cavitation and Embolism Repair Using Magnetic Resonance Imaging', *Plant physiology* 126, p. 27-31.

Hunt, P. G. *et al.* (1981) 'Flooding-induced soil and plant ethylene accumulation and water status response of field-grown tobacco', *Plant and Soil*, 59(3), pp. 427–439. doi: 10.1007/BF02184547.

Jacobi, W. R. and MacDonald, W. L. (1980) 'colonization of resistant and suceptible oaks by Ceratocystis fagacearum', *Phytopathology*, 70(7), pp. 618–623.

Jacobsen, A. L. *et al.* (2012) 'Dieback and mortality of South African fynbos shrubs is likely driven by a novel pathogen and pathogen-induced hydraulic failure: Pathogen-induced fynbos shrub mortality', *Austral Ecology*, 37(2), pp. 227–235. doi: 10.1111/j.1442-9993.2011.02268.x.

Jauregui-Zuniga *et al.* (2003) 'Crystallochemical characterization of calcium oxalate crystals isolated from seed coats of Phaseolus vulgaris and leaves of *Vitis vinifera*', *Journal of plant physiology*, 170, pp. 239-245.

Jones, H. G. (2013) *Plants and Microclimate: A Quantitative Approach to Environmental Plant Physiology*. 3rd edn. Cambridge: Cambridge University Press. doi: 10.1017/CBO9780511845727.

Kaplan, J. *et al.* (2016) 'Identifying economic hurdles to early adoption of preventative practices. The case of trunk diseases in California winegrape vineyards', *Wine Economics and Policy*, 5, p. 127-141.

Khattab, I. M. *et al.* (2021) 'Ancestral chemotypes of cultivated grapevine with resistance to Botryosphaeriaceae-related dieback allocate metabolism towards bioactive stilbenes', *New Phytologist*, 229(2), pp. 1133–1146. doi: 10.1111/nph.16919.

King, A. *et al.* (2016) 'Tomography and imaging at the PSICHE beam line of the SOLEIL synchrotron', *Review of Scientific Instruments*, 87(9), p. 093704. doi: 10.1063/1.4961365.

Klosterman, S. J. *et al.* (2009) 'Diversity, Pathogenicity, and Management of Verticillium Species', *Annual Review of Phytopathology*, 47(1), pp. 39–62. doi: 10.1146/annurev-phyto-080508-081748.

Knipfer, T. *et al.* (2015) 'Water Transport Properties of the Grape Pedicel during Fruit Development: Insights into Xylem Anatomy and Function Using Microtomography', *Plant Physiology*, 168(4), pp. 1590–1602. doi: 10.1104/pp.15.00031.

Knipfer, T. *et al.* (2020) 'Predicting Stomatal Closure and Turgor Loss in Woody Plants Using Predawn and Midday Water Potential', *Plant Physiology*, 184(2), pp. 881–894. doi: 10.1104/pp.20.00500.

Kolařík (2017) 'Biatriospora (Ascomycota: Pleosporales) is an ecologically diverse genus including facultative marine fungi and endophytes with biotechnological potential'.

Kolařík, M. (2018) 'New taxonomic combinations in endophytic representatives of the genus *Nigrograna* .', *Czech Mycology*, 70(2), pp. 123–126. doi: 10.33585/cmy.70202.

Kraus, C., Voegele, R. T. and Fischer, M. (2019) 'The Esca complex in German vineyards: does the training system influence occurrence of GLSD symptoms?', *European Journal of Plant Pathology*, 155(1), pp. 265–279. doi: 10.1007/s10658-019-01769-0.

Kreuzwieser, J. and Rennenberg, H. (2014) 'Molecular and physiological responses of trees to waterlogging stress: Responses of tree to waterlogging', *Plant, Cell & Environment*, 37, 2245–2259. doi: 10.1111/pce.12310.

Kuntzmann, P. *et al.* (2010) 'Esca, BDA, and eutypiosis: foliar symptoms, trunk lesions, and fungi observed in diseased vinestocks in two vineyards in Alsace', *Vitis*, 49(2), pp. 71–76.

Kuroda, K. (2012) 'Monitoring of xylem embolism and dysfunction by the acoustic emission technique in *Pinus thunbergii* inoculated with the pine wood nematode *Bursaphelenchus xylophilus*', *Journal of Forest Research*, 17(1), pp. 58–64. doi: 10.1007/s10310-010-0246-1.

Lachenbruch, B. and Zhao, J.-P. (2019) 'Effects of phloem on canopy dieback, tested with manipulations and a canker pathogen in the *Corylus avellana*/*Anisogramma anomala* host/pathogen system', *Tree Physiology*, 39(7), pp. 1086–1098. doi: 10.1093/treephys/tpz027.

Larignon, P. and Dubos, B. (1997) 'Fungi associated with esca disease in grapevine', *European Journal of Plant Pathology*, 103(2), pp. 147–157. doi: 10.1023/A:1008638409410.

Larignon, P. and Gramaje, D. (2015) 'Abstracts of oral and poster presentation given at the first COST Action FA 1303 workshop on Grapevine Trunk Diseases, Cognac, France, 23-24 June 2015', *Phytopathologia Mediterranea*, 54(2). doi: 10.14601/Phytopathol_Mediterr-16495.

Lecomte, P. *et al.* (2012) 'New Insights into Esca of Grapevine: The Development of Foliar

Symptoms and Their Association with Xylem Discoloration', *Plant Disease*, 96(7), pp. 924–934. doi: 10.1094/PDIS-09-11-0776-RE.

Lecomte, P. *et al.* (2018) 'Esca of grapevine and training practices in France: results of a 10-year survey', *Phytopathologia Mediterranea*, 57(3). doi: 10.14601/Phytopathol_Mediterr-22025.

Lee, E. F. *et al.* (2013) 'Analysis of HRCT-derived xylem network reveals reverse flow in some vessels', *Journal of Theoretical Biology*, 333, pp. 146–155. doi: 10.1016/j.jtbi.2013.05.021.

Letousey, P. *et al.* (2010) 'Early Events Prior to Visual Symptoms in the Apoplectic Form of Grapevine Esca Disease', *Phytopathology*, 100(5), pp. 424–431. doi: 10.1094/PHYTO-100-5-0424.

Levin, A. D., Williams, L. E. and Matthews, M. A. (2019) 'A continuum of stomatal responses to water deficits among 17 wine grape cultivars (*Vitis vinifera*)', *Functional Plant Biology*, 47(1), pp. 11-25. doi: 10.1071/FP19073.

Li, S. *et al.* (2017) 'Spatial and Temporal Pattern Analyses of Esca Grapevine Disease in Vineyards in France', *Phytopathology*, 107(1), pp. 59–69. doi: 10.1094/PHYTO-07-15-0154-R.

Lim, P. O., Kim, H. J. and Gil Nam, H. (2007) 'Leaf Senescence', *Annual Review of Plant Biology*, 58(1), pp. 115–136. doi: 10.1146/annurev.arplant.57.032905.105316.

Llop, E., Ekman, S. and Hladun, N. L. (2007) '*Bacidia thyrrenica* (Ramalinaceae, lichenized Ascomycota), a new species from the Mediterranean region, and a comparison of European members of the Bacidia rubella group', *Nova Hedwigia*, 85(3–4), pp. 445–455. doi: 10.1127/0029-5035/2007/0085-0445.

López-Moral, A. *et al.* (2020) 'Aetiology of branch dieback, panicle and shoot blight of pistachio associated with fungal trunk pathogens in southern Spain', *Plant Pathology*, 69:1237–1269. DOI: 10.1111/ppa.13209

Lopisso, D. T. *et al.* (2017) 'The Vascular Pathogen *Verticillium longisporum* Does Not Affect Water Relations and Plant Responses to Drought Stress of Its Host, *Brassica napus*', *Phytopathology*, 107(4), pp. 444–454. doi: 10.1094/PHYTO-07-16-0280-R.

Lorrain, B. *et al.* (2012) 'Effect of Esca disease on the phenolic and sensory attributes of Cabernet Sauvignon grapes, musts and wines: Esca effect on grapes and wines composition', *Australian Journal of Grape and Wine Research*, 18(1), pp. 64–72. doi: 10.1111/j.1755-0238.2011.00172.x.

Luini, E. *et al.* (2010) 'Inhibitory effects of polypeptides secreted by the grapevine pathogens *Phaeomoniella chlamydospora* and *Phaeoacremonium aleophilum* on plant cell activities', *Physiological and Molecular Plant Pathology*, 74(5–6), pp. 403–411. doi: 10.1016/j.pmpp.2010.06.007.

Lynch, S. C., Wang, H. and Eskalen, A. (2013) 'Identification of New Fungal Pathogens of Coast Live Oak in California', *Plant Disease*, 97, pp. 1025-1036.

Maciá-Vicente, J. G., Glynou, K. and Piepenbring, M. (2016) 'A new species of *Exophiala* associated with roots', *Mycological Progress*, 15(2), p. 18. doi: 10.1007/s11557-016-1161-4.

Magnin-Robert, M. *et al.* (2011) 'Leaf stripe form of esca induces alteration of photosynthesis and defence reactions in presymptomatic leaves', *Functional Plant Biology*, 38(11). doi: 10.1071/FP11083.

Magnin-Robert, M. *et al.* (2016) 'Changes in Plant Metabolism and Accumulation of Fungal Metabolites in Response to Esca Proper and Apoplexy Expression in the Whole Grapevine', *Phytopathology*, 106(6), pp. 541–553. doi: 10.1094/PHYTO-09-15-0207-R.

Magoc, T. and Salzberg, S. L. (2011) 'FLASH: fast length adjustment of short reads to improve genome assemblies', *Bioinformatics*, 27(21), pp. 2957–2963. doi: 10.1093/bioinformatics/btr507.

Mahé, F. *et al.* (2014) 'Swarm: robust and fast clustering method for amplicon-based studies', *PeerJ*, 2. doi: 10.7717/peerj.593.

Maher, N. *et al.* (2012) 'Wood necrosis in esca-affected vines: types, relationships and possible links with foliar symptom expression', *OENO One*, 46(1). doi: 10.20870/oeno-one.2012.46.1.1507.

Malézieux, E. *et al.* (2009) 'Mixing plant species in cropping systems: concepts, tools and models. A review', *Agron. Sustain. Dev*, 29, pp. 43-72.

Marchi, G. *et al.* (2006) 'Some observations on the relationship of manifest and hidden esca to rainfall', *Phytopathologia Mediterranea*, 45, pp. S117–S126.

Marín-Terrazas, M. *et al.* (2016) 'First report of Phaeoacremonium minimum causing wood decay in nursery plants of almond in Spain', *Plant Disease*, p. 3.

Martín, L. *et al.* (2019) 'Specific profile of Tempranillo grapevines related to Esca-leaf symptoms and climate conditions', *Plant Physiology and Biochemistry*, 135, pp. 575–587. doi: 10.1016/j.plaphy.2018.10.040.

Martin, M. (2011) 'Cutadapt removes adapter sequences from high-throighput sequencing reads', *EMBnet.journal*, 17.1.

Martin, N. *et al.* (2009) 'Phaeomoniella chlamydospora infection induces changes in phenolic compounds content in Vitis vinifera', *Phytopathologia Mediterranea*, 48(1), pp. 101–116. doi: http://dx.doi.org/10.14601/Phytopathol_Mediterr-2879.

Martin-StPaul, N., Delzon, S. and Cochard, H. (2017) 'Plant resistance to drought depends on timely stomatal closure', *Ecology Letters*. Edited by H. Maherali, 20(11), pp. 1437–1447. doi: 10.1111/ele.12851.

Masi, M. *et al.* (2018) 'Advances on Fungal Phytotoxins and Their Role in Grapevine Trunk Diseases', *Journal of Agricultural and Food Chemistry*, 66(24), pp. 5948–5958. doi: 10.1021/acs.jafc.8b00773.

Massonnet, M. *et al.* (2017) '*Neofusicoccum parvum* Colonization of the Grapevine Woody Stem Triggers Asynchronous Host Responses at the Site of Infection and in the Leaves', *Frontiers in Plant Science*, 8. doi: 10.3389/fpls.2017.01117.

McAdam, S. A. M. and Brodribb, T. J. (2015) 'The Evolution of Mechanisms Driving the Stomatal Response to Vapor Pressure Deficit', *Plant Physiology*, 167(3), pp. 833–843. doi: 10.1104/pp.114.252940.

McCully, M. *et al.* (2014) 'Some properties of the walls of metaxylem vessels of maize roots, including tests of the wettability of their lumenal wall surfaces', *Annals of Botany*, 113(6), pp. 977–989. doi: 10.1093/aob/mcu020.

McDowell, N. *et al.* (2008) 'Mechanisms of plant survival and mortality during drought: why do some plants survive while others succumb to drought?', *New Phytologist*, 178(4), pp. 719–739. doi: 10.1111/j.1469-8137.2008.02436.x.

McElrone, A. J., Jackson, S. and Habdas, P. (2008) 'Hydraulic disruption and passive migration by a bacterial pathogen in oak tree xylem', *Journal of Experimental Botany*, 59(10), pp. 2649–2657. doi: 10.1093/jxb/ern124.

McElrone, A. J., Grant, J. A. and Kluepfel, D. A. (2010) 'The role of tyloses in crown hydrau-

lic failure of mature walnut trees afflicted by apoplexy disorder', *Tree Physiology*, 30(6), pp. 761–772. doi: 10.1093/treephys/tpq026.

McElrone, A. J. *et al.* (2021) 'Functional hydraulic sectoring in grapevines as evidenced by sap flow, dye infusion, leaf removal, and microCT', *Annals of Botany*.

McNabb, H. S., Heybroek, H. M. and Macdonald, W. L. (1970) 'Anatomical factors in resistance to Dutch elm disease', *Netherlands Journal of Plant Pathology*, 76(3), pp. 196–205. doi: 10.1007/BF01974331.

Mensah, J. K. *et al.* (2020) 'Physiological response of *Pinus taeda* L. trees to stem inoculation with Leptographium terebrantis', *Trees*. doi: 10.1007/s00468-020-01965-0.

Méthot, P.-O. and Alizon, S. (2014) 'What is a pathogen? Toward a process view of host-parasite interactions', *Virulence*, 5(8), pp. 775–785. doi: 10.4161/21505594.2014.960726.

Miller, H. J. and Hiemstra, J. A. (1987) 'The ash wilt disease: A preliminary investigation of wood anatomy', *Netherlands Journal of Plant Pathology*, 93(6), pp. 253–260. doi: 10.1007/BF01998200.

Mirabolfathy, M., Javadi, A. and Peighami Ashnaei, S. (2018) 'The occurrence of *Anthostoma decipiens* , the causal agent of ' *Carpinus betulus* decline', in northern Iran', *New Disease Reports*, 37, p. 20. doi: 10.5197/j.2044-0588.2018.037.020.

Mirone, A. *et al.* (2014) 'The PyHST2 hybrid distributed code for high speed tomographic reconstruction with iterative reconstruction and a priori knowledge capabilities', *Nuclear Instruments and Methods in Physics Research Section B: Beam Interactions with Materials and Atoms*, 324, pp. 41–48. doi: 10.1016/j.nimb.2013.09.030.

Mondello, V. *et al.* (2018) 'Grapevine Trunk Diseases: A Review of Fifteen Years of Trials for Their Control with Chemicals and Biocontrol Agents', *Plant Disease*, 102(7), pp. 1189–1217. doi: 10.1094/PDIS-08-17-1181-FE.

Montagnini, F. and Nair, P. K. R. (2004) 'Carbon sequestration: An underexploited environmental benefit of agroforestry systems', *Agroforestry Systems*, 61, pp. 281–295.

Morales-Castilla, I. *et al.* (2020) 'Diversity buffers winegrowing regions from climate change losses', *Proceedings of the National Academy of Sciences*, 117(6), pp. 2864–2869. doi: 10.1073/pnas.1906731117.

Morales-Cruz, A. *et al.* (2018) 'Closed-reference metatranscriptomics enables *in planta* profiling of putative virulence activities in the grapevine trunk disease complex: Transcriptomics of pathogen communities', *Molecular Plant Pathology*, 19(2), pp. 490–503. doi: 10.1111/mpp.12544.

Moyo, P. *et al.* (2014) 'Arthropods Vector Grapevine Trunk Disease Pathogens', *Phytopathoogy,* 104, pp.1063-1069.

Mugnai, L., Graniti, A. and Surico, G. (1999) 'Esca (Black Measles) and Brown Wood-Streaking: Two Old and Elusive Diseases of Grapevines', *Plant Disease*, 83(5), pp. 404–418. doi: 10.1094/PDIS.1999.83.5.404.

Muller, B. *et al.* (2011) 'Water deficits uncouple growth from photosynthesis, increase C content, and modify the relationships between C and growth in sink organs', *Journal of Experimental Botany*, 62(6), pp. 1715–1729. doi: 10.1093/jxb/erq438.

Naylor, D. and Coleman-Derr, D. (2018) 'Drought Stress and Root-Associated Bacterial Communities', *Frontiers in Plant Science*, 8. doi: 10.3389/fpls.2017.02223.

Neghliz, H. *et al.* (2016) 'Ear Rachis Xylem Occlusion and Associated Loss in Hydraulic Con-

ductance Coincide with the End of Grain Filling for Wheat', *Frontiers in Plant Science*, 7. doi: 10.3389/fpls.2016.00920.

Newbanks, D. (1983) 'Evidence for Xylem Dysfunction by Embolization in Dutch Elm Disease', *Phytopathology*, 73(7). doi: 10.1094/Phyto-73-1060.

Nguyen, N. H. *et al.* (2015) 'Parsing ecological signal from noise in next generation amplicon sequencing', *New Phytologist*, 205(4), pp. 1389–1393. doi: 10.1111/nph.12923.

O'Brien, M. J. *et al.* (2017) 'A synthesis of tree functional traits related to drought-induced mortality in forests across climatic zones', *Journal of Applied Ecology*. Edited by J. Firn, 54(6), pp. 1669–1686. doi: 10.1111/1365-2664.12874.

Ogórek, R. *et al.* (2012) 'Characteristics and taxonomy of Cladosporium fungi', *Mikologia Lekarska*, 19 (2), pp. 80-85.

Oliva, J., Stenlid, J. and Martínez-Vilalta, J. (2014) 'The effect of fungal pathogens on the water and carbon economy of trees: implications for drought-induced mortality', *New Phytologist*, 203(4), pp. 1028–1035. doi: 10.1111/nph.12857.

Olmo, M. D. *et al.* (2014) 'First report of *Phaeoacremonium venezuelense* associated with wood decay of apricot trees in Spain.', *Plant Disease*.

Oses, R. *et al.* (2008) 'Fungal endophytes in xylem of healthy Chilean trees and their possible role in early wood decay', *Fungal Diversity*, 33, pp. 77–86.

Ouadi, L. *et al.* (2019) 'Ecophysiological impacts of Esca, a devastating grapevine trunk disease, on Vitis vinifera L.', *PLOS ONE*, 14(9), pp. 1–20. doi: 10.1371/journal.pone.0222586.

Ouellette, G. B. *et al.* (1999) 'Ultrastructural and cytochemical study of colonization of xylem vessel elements of susceptible and resistant *Dianthus caryophyllus* by *Fusarium oxysporum* f.sp. dianthi', *Can. J. Bot.*, 77, pp. 644–663.

Paganin, D. *et al.* (2002) 'Simultaneous phase and amplitude extraction from a single defocused image of a homogeneous object', *Journal of Microscopy*, 206(1), pp. 33–40. doi: 10.1046/j.1365-2818.2002.01010.x.

Panahandeh, S., Mohammadi, H. and Gramaje, D. (2019) 'Trunk Disease Fungi Associated with *Syzygium cumini* in Iran', *Plant Disease*, 103(4), pp. 711–720. doi: 10.1094/PDIS-06-18-0923-RE.

Pandey, S. *et al.* (2019) '*Fusarium equiseti* is associated with the wilt and dieback of *Aquilaria malaccensis* in Northeast India', *Forest Pathology*, 49(2), p. e12489. doi: 10.1111/efp.12489.

Park, J.-H. and Juzwik, J. (2014) '*Ceratocystis smalleyi* colonization of bitternut hickory and host responses in the xylem', *Forest Pathology*, 44(4), pp. 282–292. doi: 10.1111/efp.12098.

Parke, J. L. *et al.* (2007) '*Phytophthora ramorum* Colonizes Tanoak Xylem and Is Associated with Reduced Stem Water Transport', *Phytopathology*, 97(12), pp. 1558–1567. doi: 10.1094/PHYTO-97-12-1558.

Pearce, R. B. (1996) 'Antimicrobial defences in the wood of living trees', *New Phytologist*, 132(2), pp. 203–233. doi: 10.1111/j.1469-8137.1996.tb01842.x.

Pellizzari, E. *et al.* (2016) 'Wood anatomy and carbon-isotope discrimination support long-term hydraulic deterioration as a major cause of drought-induced dieback', *Global Change Biology*, 22(6), pp. 2125–2137. doi: 10.1111/gcb.13227.

Pennypacker, B. W., Leath, K. T. and Hill, R. R. (1991) 'Impact of droght stress on the expression of resistance to *Verticillium albo-atrum* in alfalfa', *Phytopathology*, 81, pp. 1014–1024.

Perez-Donoso, A. G. *et al.* (2006) '*Xylella fastidiosa* Infection and Ethylene Exposure Result in Xylem and Water Movement Disruption in Grapevine Shoots', *Plant Physiology*, 143(2), pp. 1024–1036. doi: 10.1104/pp.106.087023.

Pérez-Donoso, A. G. *et al.* (2016) 'Vessel embolism and tyloses in early stages of Pierce's disease: Embolism and tyloses in Pierce's disease', *Australian Journal of Grape and Wine Research*, 22(1), pp. 81–86. doi: 10.1111/ajgw.12178.

Petit, A.-N. *et al.* (2006) 'Alteration of Photosynthesis in Grapevines Affected by Esca', *Phytopathology*, 96(10), pp. 1060–1066. doi: 10.1094/PHYTO-96-1060.

Phillips, A. J. L. *et al.* (2013) 'The Botryosphaeriaceae: genera and species known from culture', *Studies in Mycology*, 76, pp. 51–167. doi: 10.3114/sim0021.

Pietro, A. D. *et al.* (2003) '*Fusarium oxysporum* : exploring the molecular arsenal of a vascular wilt fungus: The molecular arsenal of *F. oxysporum*', *Molecular Plant Pathology*, 4(5), pp. 315–325. doi: 10.1046/j.1364-3703.2003.00180.x.

Pita, P. *et al.* (2018) 'Further insights into the components of resistance to *Ophiostoma novo-ulmi* in *Ulmus minor*: hydraulic conductance, stomatal sensitivity and bark dehydration', *Tree Physiology*, 38(2), pp. 252–262. doi: 10.1093/treephys/tpx123.

Pouzoulet, J. *et al.* (2013) 'A method to detect and quantify *Phaeomoniella chlamydospora* and *Phaeoacremonium aleophilum* DNA in grapevine-wood samples', *Applied Microbiology and Biotechnology*, 97(23), pp. 10163–10175. doi: 10.1007/s00253-013-5299-6.

Pouzoulet, J. *et al.* (2014) 'Can vessel dimension explain tolerance toward fungal vascular wilt diseases in woody plants? Lessons from Dutch elm disease and esca disease in grapevine', *Frontiers in Plant Science*, 5. doi: 10.3389/fpls.2014.00253.

Pouzoulet, J. *et al.* (2017) 'Xylem Vessel Diameter Affects the Compartmentalization of the Vascular Pathogen Phaeomoniella chlamydospora in Grapevine', *Frontiers in Plant Science*, 8, pp. 1–13. doi: 10.3389/fpls.2017.01442.

Pouzoulet, J. *et al.* (2019) 'Modeling of xylem vessel occlusion in grapevine', *Tree Physiology*, 39(8), pp. 1438–1445. doi: 10.1093/treephys/tpz036.

Pouzoulet, J. *et al.* (2020) 'Behind the curtain of the compartmentalization process: Exploring how xylem vessel diameter impacts vascular pathogen resistance', *Plant, Cell & Environment*. doi: 10.1111/pce.13848.

Pratt, R. B. and Jacobsen, A. L. (2018) 'Identifying which conduits are moving water in woody plants: a new HRCT-based method', *Tree Physiology*. Edited by F. Meinzer, 38(8), pp. 1200–1212. doi: 10.1093/treephys/tpy034.

Premalatha, K. (2013) 'Molecular phylogenetic identification of endophytic fungi isolated from resinous and healthy wood of Aquilaria malaccensis, a red listed and highly exploited medicinal tree', *Fungal Ecology*, 6, pp. 205-211.

Qi, F., Jing, T. and Zhan, Y. (2012) 'Characterization of Endophytic Fungi from Acer ginnala Maxim. in an Artificial Plantation: Media Effect and Tissue-Dependent Variation', *PLoS ONE*, 7(10), p. e46785. doi: 10.1371/journal.pone.0046785.

Raimondo, F. *et al.* (2010) 'A tracheomycosis as a tool for studying the impact of stem xylem dysfunction on leaf water status and gas exchange in Citrus aurantium L.', *Trees*, 24(2), pp. 327–333. doi: 10.1007/s00468-009-0402-4.

Rasmussen, P. U., Bennett, A. E. and Tack, A. J. M. (2020) 'The impact of elevated temperature and drought on the ecology and evolution of plant–soil microbe interactions', *Journal of*

Ecology, 108(1), pp. 337–352. doi: 10.1111/1365-2745.13292.

Réblová, M., Fournier, J. and Hyde, K. D. (2010) '*Achroceratosphaeria*, a new ascomycete genus in the Sordariomycetes, and re-evaluation of *Ceratosphaeria incolorata*', *Fungal Diversity*, 43(1), pp. 75–84. doi: 10.1007/s13225-010-0032-6.

Redondo, C. *et al.* (2001) 'Spatial distribution of symptomatic grapevines with esca disease in the Madrid region (Spain)', *Phytopathologia mediterranea*, 40, pp. S439-S442.

Reese Næsborg, R., Ekman, S. and Tibell, L. (2007) 'Molecular phylogeny of the genus Lecania (Ramalinaceae, lichenized Ascomycota)', *Mycological Research*, 111(5), pp. 581–591. doi: 10.1016/j.mycres.2007.03.001.

Reis, P. *et al.* (2016) 'Reproducing Botryosphaeria Dieback Foliar Symptoms in a Simple Model System', *Plant Disease*, 100(6), pp. 1071–1079. doi: 10.1094/PDIS-10-15-1194-RE.

Renaud, J. P. and Mauffette, Y. (1991) 'The relationships of crown dieback with carbohydrate content and growth of sugar maple (Acer saccharum)', *Canadian Journal of Forest Research*, 21, pp. 1111–1118.

Reusche, M. *et al.* (2012) 'Verticillium Infection Triggers VASCULAR-RELATED NAC DOMAIN7-Dependent de Novo Xylem Formation and Enhances Drought Tolerance in Arabidopsis', *The Plant Cell*, 24(9), pp. 3823–3837. doi: 10.1105/tpc.112.103374.

Reynolds, A. G. and Wardle, D. A. (2001) 'Evaluation of Minimal Pruning upon Vine Performance and Berry Composition of Chancellor', *American Journal of Enology and Viticulture*, 52(1).

Riou, C. *et al.* (2016) 'Action plan against declining vineyards: An innovative approach', *BIO Web of Conferences*, 7. doi: 10.1051/bioconf/20160701040.

Rioux, D. *et al.* (1998) 'Immunocytochemical Evidence that Secretion of Pectin Occurs During Gel (Gum) and Tylosis Formation in Trees', *Phytopathology*, 88(6), pp. 494–505. doi: 10.1094/PHYTO.1998.88.6.494.

Rioux, D. *et al.* (2018) 'First Extensive Microscopic Study of Butternut Defense Mechanisms Following Inoculation with the Canker Pathogen *Ophiognomonia clavigignenti-juglandacearum* Reveals Compartmentalization of Tissue Damage', *Phytopathology*, 108(11), pp. 1237–1252. doi: 10.1094/PHYTO-03-18-0076-R.

Rodrigues, M. *et al.* (1993) 'Osmotic Adjustment in Water Stressed Grapevine Leaves in Relation to Carbon Assimilation', *Functional Plant Biology*, 20(3), p. 309. doi: 10.1071/PP9930309.

Rodríguez-Calcerrada, J. *et al.* (2020) 'Stem metabolism under drought stress – a paradox of increasing respiratory substrates and decreasing respiratory rates', *Physiologia Plantarum*, 1, pp. 1-14. doi: 10.1111/ppl.13145.

Rogiers, S. Y. *et al.* (2020) 'Potassium and Magnesium Mediate the Light and CO2 Photosynthetic Responses of Grapevines', *Biology*, 9(7). doi: 10.3390/biology9070144.

Rognes, T. *et al.* (2016) 'VSEARCH: a versatile open source tool for metagenomics', *PeerJ*, 4. doi: 10.7717/peerj.2584.

Roland R.Dute, R. R., Duncan, K. M. and Duke, B. (1999) 'Tyloses in Abscission Scars of Loblolly Pinel', *IAWA Journal*, 20(1), pp. 67–74. doi: 10.1163/22941932-90001549.

Romanazzi, G. *et al.* (2009) 'Esca in young and mature vineyards, and molecular diagnosis of the associated fungi', *European Journal of Plant Pathology*, 125(2), pp. 277–290. doi: 10.1007/s10658-009-9481-8.

Rossi, R. E. *et al.* (2020) 'The role of multiple stressors in a dwarf red mangrove (*Rhizophora mangle*) dieback', *Estuarine, Coastal and Shelf Science*, 237. doi: 10.1016/j.ecss.2020.106660.

Šafránková, I., Holková, L. and Kmoch, M. (2013) 'Leaf spot and dieback of Buxus caused by *Cylindrocladium buxicola*', *Plant Protection Science*, 49(4), pp. 165–168. doi: 10.17221/82/2012-PPS.

Sala, A., Piper, F. and Hoch, G. (2010) 'Physiological mechanisms of drought-induced tree mortality are far from being resolved: Letters', *New Phytologist*, 186(2), pp. 274–281. doi: 10.1111/j.1469-8137.2009.03167.x.

Sala, A., Woodruff, D. R. and Meinzer, F. C. (2012) 'Carbon dynamics in trees: feast or famine?', *Tree Physiology*, 32(6), pp. 764–775. doi: 10.1093/treephys/tpr143.

Salle, A. *et al.* (2008) 'Seasonal water stress and the resistance of *Pinus yunnanensis* to a bark-beetle-associated fungus', *Tree Physiology*, 28(5), pp. 679–687. doi: 10.1093/treephys/28.5.679.

Salleo, S. *et al.* (2002) 'Changes in stem and leaf hydraulics preceding leaf shedding in Castanea sativa L.', *Biologia plantarum*, 45(2), pp. 227–234. doi: https://doi.org/10.1023/A:1015192522354.

Sanz-Ros, A. V. *et al.* (2015) 'Fungal endophytic communities on twigs of fast and slow growing Scots pine (Pinus sylvestris L.) in northern Spain', *Fungal Biology*, 119(10), pp. 870–883. doi: 10.1016/j.funbio.2015.06.008.

Savage, J. A. *et al.* (2017) 'Maintenance of carbohydrate transport in tall trees', *Nature Plants*, 3(12), pp. 965–972. doi: 10.1038/s41477-017-0064-y.

Savi, T. *et al.* (2019)a 'Drought-induced dieback of *Pinus nigra*: a tale of hydraulic failure and carbon starvation', *Conservation Physiology*, 7. doi: 10.1093/conphys/coz012.

Savi, T. *et al*. (2019)b 'Gas exchange, biomass and non-structural carbohydrates dynamics in vines under combined drought and biotic stress', BMC Plant Biology, 19. https://doi.org/10.1186/s12870-019-2017-2

Schippers, J. H. M. *et al.* (2015) 'Living to Die and Dying to Live: The Survival Strategy behind Leaf Senescence', *Plant Physiology*, 169(2), pp. 914–930. doi: 10.1104/pp.15.00498.

Schneider, C. A., Rasband, W. S. and Eliceiri, K. W. (2012) 'NIH Image to ImageJ: 25 years of image analysis', *Nature Methods*, 9(7), pp. 671–675. doi: 10.1038/nmeth.2089.

Schultz, H. R. *et al.* (2000) 'Adaptation and Utilization of Minimal Pruning Systems for Quality Production in Cool Climates', *American Journal of Enology and* Viticulture, 51(5).

Schultz, H. R. (2003) 'Differences in hydraulic architecture account for near-isohydric and anisohydric behaviour of two field-grown *Vitis vinifera* L. cultivars during drought', *Plant, Cell and Environment*, 26(8), pp. 1393–1405. doi: 10.1046/j.1365-3040.2003.01064.x.

Schulz, A. N. *et al.* (2018) 'Association of *Caliciopsis pinea* Peck and Matsucoccus macrocicatrices Richards with eastern white pine (*Pinus strobus* L.) seedling dieback', *Forest Ecology and Management*, 423, pp. 70–83. doi: 10.1016/j.foreco.2018.03.013.

Scoffoni, C. *et al.* (2017) 'Outside-Xylem Vulnerability, Not Xylem Embolism, Controls Leaf Hydraulic Decline during Dehydration', *Plant Physiology*, 173(2), pp. 1197–1210. doi: 10.1104/pp.16.01643.

Scortichini, M. (2020) 'Predisposing Factors for "Olive Quick Decline Syndrome" in Salento (Apulia, Italy)', *Agronomy*, 10, pp. 1445-1460.

Seker, S. S., Akbulut, M. K. and Senel, G. (2016) 'Calcium oxalate crystal (CaOx) composition at different growth stages of petiole in *Vitis vinifera* (Vitaceae)', *Advanced Studies in Biology*, 8, pp. 1–8. doi: 10.12988/asb.2016.51146.

Serra, S. *et al.* (2018) 'Expression of grapevine leaf stripe disease foliar symptoms in four cultivars in relation to grapevine phenology and climatic conditions', *Phytopathologia Mediterranea*, 57(3). doi: 10.14601/Phytopathol_Mediterr-24088.

Sevanto, S., Holbrook, N. M. and Ball, M. C. (2012) 'Freeze/Thaw-Induced Embolism: Probability of Critical Bubble Formation Depends on Speed of Ice Formation', *Frontiers in Plant Science*, 3. doi: 10.3389/fpls.2012.00107.

Shigo, A. L. (1984) 'Compartmentalization: a conceptual framework for understanding how trees grow and defend themselves', *Annual Review of Phytopathology*, 22, pp. 189–214.

Silva Lima, L. K. S. *et al.* (2019) 'Water deficit increases the susceptibility of yellow passion fruit seedlings to Fusarium wilt in controlled conditions', *Scientia Horticulturae*, 243, pp. 609–621. doi: 10.1016/j.scienta.2018.09.017.

Solla, A. and Gil, L. (2002) 'Xylem vessel diameter as a factor in resistance of *Ulmus minor* to Ophiostoma novo-ulmi', *Forest Pathology*, 32(2), pp. 123–134. doi: 10.1046/j.1439-0329.2002.00274.x.

Somavilla, N. S., Kolb, R. M. and Rossatto, D. R. (2014) 'Leaf anatomical traits corroborate the leaf economic spectrum: a case study with deciduous forest tree species', *Brazilian Journal of Botany*, 37(1), pp. 69–82. doi: 10.1007/s40415-013-0038-x.

Songy, A. *et al.* (2019) 'Grapevine trunk diseases under thermal and water stresses', *Planta*, 249(6), pp. 1655–1679. doi: 10.1007/s00425-019-03111-8.

Sorek, Y. *et al.* (2020) 'An increase in xylem embolism resistance of grapevine leaves during the growing season is coordinated with stomatal regulation, turgor loss point and intervessel pit membranes', *New Phytologist*.

Souza, A. G. C. *et al.* (2013) 'First Report on the Association Between *Ceratocystis fimbriata* , an Agent of Mango Wilt, *Xyleborus affinis* , and the Sawdust Produced During Beetle Colonization in Brazil', *Plant Disease*, 97(8), pp. 1116–1116. doi: 10.1094/PDIS-12-12-1204-PDN.

Sperry, J. S., Donnelly, J. R. and Tyree, M. T. (1988) 'A method for measuring hydraulic conductivity and embolism in xylem', *Plant, Cell and Environment*, 11(1), pp. 35–40. doi: 10.1111/j.1365-3040.1988.tb01774.x.

Spies, C. F. J. *et al.* (2018) '*Phaeoacremonium* species diversity on woody hosts in the Western Cape Province of South Africa', *Persoonia - Molecular Phylogeny and Evolution of Fungi*, 40(1), pp. 26–62. doi: 10.3767/persoonia.2018.40.02.

Srinivasan, R. *et al.* (2020) 'Penicillium', in *Beneficial Microbes in Agro-Ecology*. Elsevier, pp. 651–667. doi: 10.1016/B978-0-12-823414-3.00032-0.

Steudle, E. (2001) 'Water uptake by plant roots: an integration of views', in Gašparíková, O. et al. (eds) *Recent Advances of Plant Root Structure and Function*. Dordrecht: Springer Netherlands, pp. 71–82. doi: 10.1007/978-94-017-2858-4_9.

Stitt (1989) 'Metabolite Levels in Specific Cells and Subcellular Compartments of Plant Leaves'. *Methods in enzymatology*, 174. doi: https://doi.org/10.1016/0076-6879(89)74035-0.

Sun, Q. *et al.* (2007) 'Ethylene and Not Embolism Is Required for Wound-Induced Tylose Development in Stems of Grapevines', *Plant Physiology*, 145(4), pp. 1629–1636. doi: 10.1104/pp.107.100537.

Sun, Q., Rost, T. L. and Matthews, M. A. (2008) 'Wound-induced vascular occlusions in Vitis vinifera (Vitaceae): Tyloses in summer and gels in winter1', *American Journal of Botany*, 95(12), pp. 1498–1505. doi: 10.3732/ajb.0800061.

Sun, Q. *et al.* (2013) 'Vascular Occlusions in Grapevines with Pierce's Disease Make Disease Symptom Development Worse', *Plant Physiology*, 161(3), pp. 1529–1541. doi: 10.1104/pp.112.208157.

Sun, Y. *et al.* (2017) 'Wilted cucumber plants infected by Fusarium oxysporum f. sp. cucumerinum do not suffer from water shortage', *Annals of Botany*, 120(3), pp. 427–436. doi: 10.1093/aob/mcx065.

Surico, G. *et al.* (2000) 'Analysis of the spatial spread of esca in some Tuscan vineyards (Italy)', *Phytopathologia Mediterranea*, 39, pp. 211–224.

Surico, G., Mugnai, L. and Marchi, G. (2006) 'Older and more recent observations on esca: a critical overview', *Phytopathologia Mediterranea*, 45, pp. S68–S86. doi: http://dx.doi.org/10.14601/Phytopathol_Mediterr-1847.

Taiz, T. and Zeiger (2003) *Plant physiology. 3rd edition*.

Talboys, P. W. (1972) 'Resistance to Vascular Wilt Fungi', *Proceedings of the Royal Society of London. Series B, Biological Sciences*, 181(1064,), pp. 319–332.

Teixeira, M. M. *et al.* (2017) 'Exploring the genomic diversity of black yeasts and relatives (Chaetothyriales, Ascomycota)', *Studies in Mycology*, 86, pp. 1–28. doi: 10.1016/j.simyco.2017.01.001.

Teixeira-Costa, L. and Ceccantini, G. (2015) 'Embolism increase and anatomical modifications caused by a parasitic plant: *Phoradendron* crassifolium (Santalaceae) on *Tapirira* guianensis (Anacardiaceae), *IAWA Journal*, 36(2), pp. 138–151. doi: 10.1163/22941932-00000091.

Tixier, A. *et al.* (2018) 'Diurnal Variation in Nonstructural Carbohydrate Storage in Trees: Remobilization and Vertical Mixing', *Plant Physiology*, 178(4), pp. 1602–1613. doi: 10.1104/pp.18.00923.

Tixier, A. *et al.* (2020) 'Comparison of phenological traits, growth patterns, and seasonal dynamics of non-structural carbohydrate in Mediterranean tree crop species', *Scientific Reports*, 10(1), p. 347. doi: 10.1038/s41598-019-57016-3.

Tomasella, M. *et al.* (2017) 'Post-drought hydraulic recovery is accompanied by non-structural carbohydrate depletion in the stem wood of Norway spruce saplings', *Scientific Reports*, 7(1). doi: 10.1038/s41598-017-14645-w.

Torres-Ruiz, J. M. *et al.* (2015) 'Direct X-Ray Microtomography Observation Confirms the Induction of Embolism upon Xylem Cutting under Tension', *Plant Physiology*, 167(1), pp. 40–43. doi: 10.1104/pp.114.249706.

Torres-Ruiz, J. M., Sperry, J. S. and Fernández, J. E. (2012) 'Improving xylem hydraulic conductivity measurements by correcting the error caused by passive water uptake', *Physiologia Plantarum*, 146(2), pp. 129–135. doi: 10.1111/j.1399-3054.2012.01619.x.

Tränkner, M. *et al.* (2016) 'Magnesium deficiency decreases biomass water-use efficiency and increases leaf water-use efficiency and oxidative stress in barley plants', *Plant and Soil*, 406(1–2), pp. 409–423. doi: 10.1007/s11104-016-2886-1.

Travadon, R. (2016) 'Grapevine pruning systems and cultivars influence the diversity of wood-colonizing fungi', *Fungal Ecology*, 24, pp. 82-93.

Tulik, M., Yaman, B. and Köse, N. (2018) 'Comparative tree-ring anatomy of Fraxinus excel-

sior with Chalara dieback', *Journal of Forestry Research*. doi: 10.1007/s11676-017-0586-1.

Tyree, M. T. and Ewers, F. W. (1991) 'The hydraulic architecture of trees and other woody plants', *New Phytologist*, 119(3), pp. 345–360. doi: 10.1111/j.1469-8137.1991.tb00035.x.

Tyree, M. T. and Sperry, J. S. (1988) 'Do Woody Plants Operate Near the Point of Catastrophic Xylem Dysfunction Caused by Dynamic Water Stress? : Answers from a Model', *Plant Physiology*, 88(3), pp. 574–580. doi: 10.1104/pp.88.3.574.

Tyree, M. T. and Sperry, J. S. (1989) 'Vulnerability of Xylem to Cavitation and Embolism', *Annu. Rev. Plant. Physiol. Plant. Mol. Biol.*, 40, pp. 19-38.

Tyree, M. T. and Zimmermann M. H. (2002) 'Xylem structure and the ascent of sap', *Springer series in Wood science*.

Umebayashi, T. *et al.* (2011) 'The Developmental Process of Xylem Embolisms in Pine Wilt Disease Monitored by Multipoint Imaging Using Compact Magnetic Resonance Imaging', *Plant Physiology*, 156(2), pp. 943–951. doi: 10.1104/pp.110.170282.

Úrbez-Torres, J. R. *et al.* (2013) 'Olive Twig and Branch Dieback: Etiology, Incidence, and Distribution in California', *Plant Disease*, 97(2), pp. 231–244. doi: 10.1094/PDIS-04-12-0390-RE.

Urli, M. *et al.* (2013) 'Xylem embolism threshold for catastrophic hydraulic failure in angiosperm trees', *Tree Physiology*, 33(7), pp. 672–683. doi: 10.1093/treephys/tpt030.

Vaillant-Gaveau, N. *et al.* (2014) 'Relationships between carbohydrates and reproductive development in chardonnay grapevine: impact of defoliation and fruit removal treatments during four successive growing seasons', *OENO One*, 48(4), p. 219. doi: 10.20870/oeno-one.2014.48.4.1694.

Valtaud, C. *et al.* (2009) 'Developmental and ultrastructural Features of *Phaeomoniella chlamydospora* and *Phaeoacremonium aleophilum* in Relation to Xylem Degradation in Esca Disease of the Grapevine', *Journal of Plant Pathology*, 91, pp. 37–51. doi: http://dx.doi.org/10.4454/jpp.v91i1.622.

Valtaud, C. *et al.* (2009) 'Systemic effects on leaf glutathione metabolism and defence protein expression caused by esca infection in grapevines', *Functional Plant Biology*, 36(3), p. 260. doi: 10.1071/FP08293.

Valtaud, C. *et al.* (2011) 'Systemic damage in leaf metabolism caused by esca infection in grapevines: Starch and soluble sugars in esca-infected Vitis leaves', *Australian Journal of Grape and Wine Research*, 17(1), pp. 101–110. doi: 10.1111/j.1755-0238.2010.00122.x.

Van Alfen, N. K. (1989) 'Reassessment of Plant Wilt Toxins', *Annual Review of Phytopathology*, 27, pp. 533–550.

van Leeuwen, C. and Seguin, G. (2006) 'The concept of terroir in viticulture', *Journal of Wine Research*, 17(1), pp. 1–10. doi: 10.1080/09571260600633135.

van Leeuwen, C. *et al.* (2009) 'Vine water status is a key factor in grape ripening and vintage quality for red Bordeaux wine. How can it be assessed for vineyard management purposes?', *OENO One*, 43(3), p. 121. doi: 10.20870/oeno-one.2009.43.3.798.

van Leeuwen, C. and Darriet, P. (2016) 'The Impact of Climate Change on Viticulture and Wine Quality', *Journal of Wine Economics*, 11(1), pp. 150–167

van Leeuwen *et al.* (2019) 'An Update on the Impact of Climate Change in Viticulture and Potential Adaptations', *Agronomy*, 9(9), p. 514. doi: 10.3390/agronomy9090514.

VanderMolen, G. E., Beckman, C. H. and Rodehorst, E. (1987) 'The ultrastructure of tylose formation in resistant banana following inoculation with *Fusarium oxysporum* f.sp. *cubense*', *Physiological and Molecular Plant Pathology*, 31(2), pp. 185–200. doi: 10.1016/0885-5765(87)90063-4.

Venturas, M. *et al.* (2014) 'Heritability of *Ulmus minor* resistance to Dutch elm disease and its relationship to vessel size, but not to xylem vulnerability to drought', *Plant Pathology*, 63(3), pp. 500–509. doi: 10.1111/ppa.12115.

Viala, P. (1926). 'Recherches sur les maladies de la vigne: esca', *Ann. Epiphyties* 12:1-108.

Wang, M. M. (2017) Molecular phylogeny of *Neodevriesia*, with two new species and several new combinations, *Mycologia*, 109(6), pp. 965-974.

Webber, J. F. (2004) 'Experimental studies on factors influencing the transmission of Dutch elm disease', *Invest Agrar: Sist Recur For* 13 (1), 197-205.

Weyand, K. M. and Schultz, H. R. (2006) 'Regulating yield and wine quality of minimal pruning systems through the application of gibberellic acid', *Journal International des Sciences de la Vigne et du Vin*, 40, 151-163.

Wheeler, J. K. *et al.* (2013) 'Cutting xylem under tension or supersaturated with gas can generate PLC and the appearance of rapid recovery from embolism: Sampling induced embolism', *Plant, Cell & Environment*. doi: 10.1111/pce.12139.

White, C. L., Halleen, F. and Mostert, L. (2011) 'Symptoms and fungi associated with esca in South African vineyards', *Phytopathologia Mediterranea*, 50, pp. S236–S246.

Worrall, J. J. (2009) 'Dieback and Mortality of *Alnus* in the Southern Rocky Mountains, USA', *Plant Disease*, 93(3), pp. 293–298. doi: 10.1094/PDIS-93-3-0293.

Yadeta, K. A. and J. Thomma, B. P. H. (2013) 'The xylem as battleground for plant hosts and vascular wilt pathogens', *Frontiers in Plant Science*, 4. doi: 10.3389/fpls.2013.00097.

Yazaki, K. *et al.* (2018) 'Pine wilt disease causes cavitation around the resin canals and irrecoverable xylem conduit dysfunction', *Journal of Experimental Botany*, 69(3), pp. 589–602. doi: 10.1093/jxb/erx417.

Zimmermann, M. H. (1978) 'Vessel ends and the disruption of water flow in plants', *the American Phytopathological Society* 3340.

Zimmermann, M. H. (1979) 'The Discovery of Tylose Formation by a Viennese lady in 1845', *IAWA Bulletin*, (2), pp. 51–56.